Functional analysis of the SseK family of *Salmonella* SPI-2 type III secretion system effectors

Regina Agnes Günster

MRC Centre for Molecular Bacteriology and Infection
Department of Medicine

Imperial College London

Submitted for the degree of
Doctor of Philosophy

Supervised by Prof. David W. Holden

London, November 2017

ABSTRACT

In humans, serovars of *Salmonella enterica* cause diseases ranging from gastroenteritis to systemic typhoid fever. *Salmonella* encodes numerous translocated virulence (effector) proteins that enable the bacterium's complex intracellular lifestyle. Three poorly characterised *Salmonella* effectors are the SseK proteins: SseK1, SseK2 and SseK3. This work showed that all three effectors are translocated by the SPI-2 type III secretion system into macrophages. Despite high amino acid similarity between the proteins, SseK1 is cytosolic and SseK2 and SseK3 associate with the Golgi network. When ectopically expressed in mammalian cells, SseK1, SseK2 and SseK3 suppressed NF-κB pathway activation. This inhibition was specific for TNFα-induced signaling but not TLR4-, or interleukin-induced NF-κB pathway activation. After physiological delivery of the effectors into macrophages during *Salmonella* infection, SseK1 and SseK3 inhibited NF-κB activity in an additive manner and suppressed TNFα-induced necroptotic host cell death. Despite stable interaction between SseK3 and the E3-ubiquitin ligase TRIM32 in macrophages, SseK3-mediated inhibition of NF-κB activation and host cell death did not require TRIM32. In addition, bacterial burden in *Trim32*$^{-/-}$ mice were indistinguishable from wild-type mice after short-term infection with *Salmonella.* Catalytic activity of the SseK effectors required a DxD motif, which in SseK1 and SseK3 is essential for arginine-*N*-acetylglucosamine (GlcNAc)-ylation of target proteins. In infected macrophages, SseK1 and SseK3 caused arginine-GlcNAcylation of a diverse range of distinct bacterial and host proteins, including auto-GlcNAcylation of SseK1 and SseK3. Both SseK1 and SseK3 induced arginine-GlcNAcylation of TRADD, which is most likely the cause of the effector's inhibitory effect on both NF-κB activation and host cell death. In addition, a large number of Golgi network associated proteins were identified as potential SseK3 GlcNAcylation targets. This suggests additional, yet-to-be validated functions of the effectors during *Salmonella* infection besides inhibition of NF-κB signalling and necroptosis in macrophages.

ACKNOWLEDGEMENTS

I would like to thank my supervisor Prof. David Holden for the opportunity to work and learn in his group. Your simultaneous guidance, support and freedom offered during my PhD has allowed me to grow as a scientist.

My special thanks to Teresa Thurston for mentoring me during my thesis. I can't express how grateful I am for all your support, the discussions, encouragement and help. Thanks for believing in me!

Sophie Matthews, thank you for your amazing support when the project needed it the most. I'm grateful for your experimental help but even more so for you friendship.

Thanks to all past and present members of the Holden lab – Megan Winterbotham, Elliott Jennings, Nathalie Rolhion, Grzegorz Grabe, Ethel Bayer Santos, Mei Liu, Luciano Rigano, Eric Alix, Xiujun Yu, Alan O'Neill, Camilla Godlee, Ondrej Cerny and Xin Li - who were always willing to answer my questions and offered their advice.

My bench neighbors, Julian Rycroft and Charlotte Durkin. Together with Robbie Fisher, Sina Krokowski, Alex Willis, Daphne Staples and Damián Lobato-Márquez you made my PhD much more fun with your laughter and endless moral support. Thanks for all the coffee breaks and late lab hours with encouragement and helpful discussions, both scientific and otherwise.

I'd also like to thank Diego Esposito and Katrin Rittinger for solving the crystal structure of SseK3 and Jasio Debski for processing my mass spectrometry samples and helpful discussion.

My parents, Ursula and Wilhelm Günster. Without your support, encouragement and love this PhD would have been impossible. Danke!

DECLARATION OF ORIGINALITY

I hereby declare that the work presented in this thesis is my own original work. Any contribution to this thesis by others, published or otherwise, is acknowledged throughout the text with all references listed in the bibliography.

This thesis contains material, including figures and intellectual content, which is published in:

Günster, R.A., Matthews, S.A., Holden, D.W., Thurston, T.L.M., 2017**. SseK1 and SseK3 T3SS effectors inhibit NF-κB signalling and necroptotic cell death in *Salmonella*-infected macrophages.** Infect. Immun. 85, e00010-17. https://doi.org/10.1128/IAI.00010-17.

COPYRIGHT DECLARATION

CONTENTS

LIST OF FIGURES

LIST OF TABLES

ABBREVIATIONS

aa	Amino acid
AB^R	Antibiotic resistance
ADP	Adenosine 5’-diphosphate
Arg	Arginine
ASC	Apoptosis-associated speck-like protein containing CARD
BB	B-box
BBS	Bardet–Biedl syndrome
bp	Base pairs
BSA	Bovine serum albumin
C. rodentium	*Citrobacter rodentium*
casp	Caspase
CC	Coiled-coil
CFU	Colony forming units
CHX	Cycloheximide
CI	Competitive index
cIAP	Cellular inhibitor of apoptosis protein
DAMP	Damage associated molecular pattern molecule
DAPI	4',6-diamidino-2-phenylindole
DC	Dendritic cell
DD	Death domain
DISC	Death-inducing signalling complex
DNA	Deoxyribonucleic acid
dsRNA	Double-stranded RNA
DxD	Aspartic acid-X-aspartic acid
E. coli	*Escherichia coli*
EHEC	Enterohemorrhagic *E. coli*
EPEC	Enteropathogenic *E. coli*
ER	Endoplasmic reticulum
ERK	Extracellular signal-regulated kinase
ETs	Extracellular traps
FADD	FAS-associated death domain protein
FASL	FAS ligand
FASR	FAS receptor
FCS	Fetal calf serum
FSB	Final sample buffer
GFP	Green fluorescent protein

GlcNAc	*N*-acetyl-D-glucosamine
GST	Glutathione S-transferase
GT	Glycosyltransferase
h.p.u.	Hours post uptake
HA	Hemagglutinin
HMW	High molecular weight
HRP	Horseradish peroxidase
IFN	Interferon
IκB	NF-κb inhibitor
IKK	Iκb kinase complex
IL	Interleukin
iNTS	Invasive non-typhoidal salmonellosis
IRF	Interferon regulatory factor
ISRE	IFN-stimulated response element
JAK	Janus kinase
JNK	Jun N-terminal kinase
LB	Lennox broth
LDH	Lactate dehydrogenase
LGMD2H	Limb-girdle muscular dystrophy 2H
LPS	Lipopolysaccharide
M cells	Microfold cells
MAPK	Mitogen-activated protein kinase
MBP	Maltose-binding protein
MDA5	Melanoma differentiation-associated protein 5
MHCII	Major histocompatibility complex II
MKK	Mitogen-activated protein kinase kinase
MLKL	Mixed-lineage kinase domain-like
MOI	Multiplicity of infection
MS	Mass spectrometry
n.s.	Non-significant
NEL	Novel E3 ligase domain
NF-κB	Nuclear factor-kappab
NIK	NF-κb-inducing kinase
NleB	Non-LEE encoded effector protein B
NLR	NOD-like receptors
NLRP	NACHT, LRR and PYD domains-containing protein
NOD	Nucleotide-binding oligomerisation domain
NRAMP-1	Natural resistance-associated macrophage protein-1

NTS	Non-typhoidal *Salmonella*
OGA	Protein *O*-GlcNAcase
OGT	*O*-GlcNAc transferase subunit p110
PAMP	Pathogen associated molecular pattern
PBS	Phosphate buffered saline
PCR	Polymerase chain reaction
pE	Empty vector
pH	Negative logarithmic value of the hydrogen ion (H+) concentration
PI	Propidium iodide
PIAS	Protein inhibitor of activated STAT
poly(I:C)	Polyinosinic:polycytidylic acid
PRR	Pattern recognition receptor
PTM	Post translational modification
qPCR	Quantitative PCR
RIG-I	Retinoic acid-inducible gene
RING	Really interesting new gene
RIPK	Receptor-interacting protein kinase
RLR	RIG-I-like receptor
RNA	Ribonucleic acid
ROS	Reactive oxygen species
rpm	Rounds per minute
S. Enteritidis	*Salmonella enterica* subsp. *Enterica* serovar Enteritidis
S. Paratyphi	*Salmonella enterica* subsp. *Enterica* serovar Paratyphi
S. Typhi	*Salmonella enterica* subsp. *Enterica* serovar Typhi
S. Typhimurium	*Salmonella enterica* subsp. *Enterica* serovar Typhimurium
SCV	*Salmonella*-containing vacuole
SDS-PAGE	Sodium dodecyl sulfate polyacrylamide gel electrophoresis
SEM	Standard error of the mean
Ser	Serine
Sif	*Salmonella*-induced filament
Sop	*Salmonella* outer protein
SPI	*Salmonella* pathogenicity island
Spv	*Salmonella* plasmid virulence
Sse	Secretion system effector
Ssp	*Salmonella* secreted protein
ssRNA	Single-stranded RNA
STAT	Signal transducer and activator of transcription
Ste	*Salmonella* translocated effector

T3SS	Type III secretion systems
TBK1	TANK-binding kinase 1
TLR	Toll-like receptor
TNFα	Tumor necrosis factor alpha
TNFR	TNFα receptor
TRADD	TNFR1- associated death domain protein
TRAF	TNF receptor-associated factor
TRAIL	TNF-related apoptosis-inducing ligand
TRAILR	TRAIL receptor
TRIM	Tripartite motif-containing protein
UI	Uninfected
Ub	Ubiquitin
WT	Wild-type

1 INTRODUCTION

1.1 *Salmonella* pathogenesis

Recently the World Health Organisation identified twelve bacteria for which new antibiotics are urgently needed, listing *Salmonellae* species among the pathogens with high priority for research and development (WHO, 2017). With multi-drug resistant *Salmonella* strains as an increasing and significant global problem, intensive research to understand the fundamental mechanisms of *Salmonella* infection and subsequent rational treatment and vaccine development is of great importance.

Salmonella species are Gram-negative, flagellated, rod-shaped, facultative anaerobic, ubiquitous human and animal pathogens from the Enterobacteriaceae family. Using a combination of molecular and serotyping techniques *Salmonella* can be further classified into two species, *Salmonella bongori* and *Salmonella enterica*, and several *Salmonella enterica* subspecies: *enterica* (I), *salamae* (II), *arizonae* (IIIa), *diarizonae* (IIIb), *houtenae* (IV) and *indica* (VI) (Desai et al., 2013; Grimont and Weill, 2007; Malorny et al., 2011). Of the more than 2600 known *Salmonella* serological variants (serovars) only approximately 50 serovars account for over 80% of all clinical isolates of *Salmonella* from humans (CDC, 2016). In humans, *Salmonella* infection presents itself clinically in the form of acute gastroenteritis, invasive bacteremia or severe typhoid fever with the severity of disease depending on host factors and the serotype of *Salmonella*.

1.1.1 Human diseases caused by *Salmonella* species

S. enterica serovars Typhi and Paratyphi (*S*. Typhi and *S.* Paratyphi) are the cause of severe forms of invasive typhoid fever (enteric fever) which is life-threatening in many parts of the developing world. In 2010, there were an estimated 27 million typhoid fever episodes worldwide with a case-fatality rate of 1% with effective treatment (Buckle et al., 2012; Crump et al., 2004). Typhoidal *Salmonella* species are highly adapted and human-restricted pathogens (Spanò, 2016) and infection is caused by faeco-oral transmission. Following ingestion of contaminated food or water only a small proportion of the bacteria survive the passage of the acidic gastric environment and reach the small intestine. The inflammatory response in the ileum is mild and *S.* Typhi can subsequently invade enterocytes and microfold

cells (M cells) of Peyer's patches within the epithelium of the small intestinal mucosa to access the underlying immunological tissue. There, *Salmonella* multiplies within mononuclear phagocytes of the mesenteric lymph nodes and causes bacteraemia and systemic infection by spread to the liver, spleen, bone marrow, and gallbladder (Dougan and Baker, 2014). Clinical manifestation of (para-) typhoid *Salmonella* infection is non-specific with sustained fever and symptoms frequently including chills, abdominal pain, hepatosplenomegaly, rash, nausea, anorexia, diarrhoea or constipation (Azmatullah et al., 2015). The infections are generally resolved, but 2–5% of those who contract typhoid fever become chronic asymptomatic carriers who can unwittingly facilitate bacterial spread (Gonzalez-Escobedo et al., 2011; Levine et al., 1982).

Salmonella enterica ssp. *enterica* serovars Enteritidis and Typhimurium (*S*. Enteritidis and *S*. Typhimurium) are the main cause of food-born gastroenteritis worldwide with an estimated 93.8 million cases and approximately 155,000 deaths annually (Majowicz et al., 2010). Due to the broad host spectrum of non-typhoidal *Salmonella* (NTS) serovars, humans are commonly infected through the consumption of contaminated food of animal origin, mainly meat, poultry, eggs and milk. In contrast to typhoid fever, NTS cause acute inflammation of the intestinal mucosa and Peyer's patches manifesting in acute gastroenteritis and watery diarrhoea. In the majority of cases, non-typhoidal *Salmonella* do not proceed beyond the mesenteric lymph nodes and the disease is self-limiting, resolving within 4-7 days (Chen et al., 2013; Zhang et al., 2003).

However, non-typhoidal *Salmonella* can cause an extra-intestinal disease leading to invasive bacteraemia. Invasive non-typhoidal *Salmonella* (iNTS) disease closely resembles enteric fever in that patients can suffer from high fever, hepatosplenomegaly, pneumonia-mimicking respiratory complications, metastatic meningitis and osteomyelitis, with intestinal symptoms often being absent (Feasey et al., 2012). iNTS is most prevalent in sub-Saharan Africa and has a bimodal niche, predominantly affecting malarial and/or malnourished children or HIV-infected adults (Uche et al., 2017). With an estimated 3.4 million cases of iNTS globally each year (Ao et al., 2015) this disease is less frequent than typhoid fever but has a significantly higher case fatality rate of approximately 20% but can exceed 50% in HIV-infected patients (MacLennan and Levine, 2013; Uche et al., 2017).

1.1.2 Experimental models of *Salmonella* infection

Most of our current understanding of the complex mechanisms that lead to *Salmonella* infections in humans are derived from studies using various animal and tissue culture models. While no ideal animal model exists to accurately simulate human gastroenteritis and invasive disease, the mouse model has been successfully used to study a diverse range of bacterial and host factors contributing to salmonellosis.

As *S.* Typhi is an exclusive human pathogen, no suitable animal model (other than higher primates (Edsall et al., 1960)) is available to study typhoid fever. However, mice infected with *S*. Typhimurium lack intestinal inflammation but develop a systemic disease that closely resembles typhoid fever in humans (Zhang et al., 2003). Similar to *S.* Typhi in humans, *S.* Typhimurium crosses the murine intestinal mucosa, enters the underlying reticuloendothelial system and disseminates to the mesenteric lymph nodes, liver and spleen (Carter and Collins, 1974; Jones, 1994; Voedisch et al., 2009). Wild-type mice are able to contain bacterial loads at these systemic sites, do not develop severe acute typhoid disease and can therefore be used as a chronic infection model (Monack et al., 2004). In contrast, mice lacking the natural resistance-associated macrophage protein-1 (NRAMP-1, also Slc11a1) are unable to control bacterial loads and are highly susceptible to salmonellosis (Govoni et al., 1996; Nairz et al., 2009). Therefore, *Nramp-1*$^{-/-}$ mice lineages like BALB/c and C57BL/6 are commonly used as a model for acute typhoid fever.

Oral infection of primates and cattle with non-typhoidal *Salmonella* species are the best models of gastroenteritis in humans (Costa et al., 2012; Higginson et al., 2016; Kent et al., 1966). However, due to the ethical concerns, cost, and the inability for genetic manipulation of both model systems, the mouse model is the most commonly used *Salmonella*-induced colitis model. To mimic human gastroenteritis in the mouse, antibiotic pre-treatment (Streptomycin) of adult mice is required to reduce the intestinal microbiota. This allows *Salmonella* to efficiently colonise the cecum and colon and is characterised by overt intestinal inflammation similar to human enterocolitis (Barthel et al., 2003; Kaiser et al., 2012).

Many aspects of *Salmonella* pathogenesis can be studied in *in vitro* tissue culture systems in addition to animal models. Studies in disease-relevant cell types have contributed greatly to our understanding of the molecular mechanisms of *Salmonella* infection. Epithelial cell lines (e.g. HeLa, Caco2) are commonly used to investigate active bacterial invasion and intracellular

growth whilst intracellular replication and survival after phagocytosis is studied in murine and human macrophage-like cell lines (e.g. RAW 264.7, J774, U937), as well as primary bone marrow-derived macrophages.

1.1.3 *Salmonella* virulence determinants

Salmonella has a very complex lifestyle, including extracellular motility, host cell invasion, intracellular survival, replication and persistence. Fast adaptation to different environmental conditions during infection is tightly regulated and is mediated by virulence genes, many of which are present on horizontally-acquired genetic elements, such as prophages, plasmids and pathogenicity islands (Marcus et al., 2000).

During the initial stages of *Salmonella* infection, the bacterium traverses through the stomach and small intestine. In this extracellular environment chemotaxis and motility of the bacteria is dependent on flagella. Currently the precise contribution of flagella to human disease is not fully understood but studies in cultured cells and the calf ileal-loop model suggest flagella facilitate motility towards, and infection of, the intestinal mucosa (Haiko and Westerlund-Wikström, 2013; Schmitt et al., 2001). *Salmonella* fimbriae, hair-like structures on the bacterial surface, have been shown to be important for colonisation of intestinal epithelium by bringing the bacteria in close, direct contact with host cells (Humphries et al., 2001; van der Velden et al., 1998). This favours the active invasion of mucosal cells by *Salmonella*, leading to the intracellular stage of infection. *Salmonella enterica* species encode 21 *Salmonella* pathogenicity islands (SPI), dense clusters of virulence genes on the bacterial chromosome (Fookes et al., 2011). SPI-1 and SPI-2 are essential for *Salmonella* pathogenicity (Galán and Curtiss, 1989a; Hensel et al., 1995) and are present in all enteric serovars while many other SPIs confer host specificity to different serovars (Sabbagh et al., 2010). One important example is SPI-7, which is present in *S.* Typhi but absent from *S*. Typhimurium and encodes the Vi capsule polysaccharide that reduces the inflammatory responses provoked by *S.* Typhi in intestinal tissue (Seth-Smith, 2008; Tran et al., 2010).

SPI-1 and SPI-2 encode two type III secretion systems (T3SSs) which facilitate bacterial invasion (Zhou and Galán, 2001) and intracellular replication (Ochman et al., 1996), respectively. T3SSs are needle-like structures that span the bacterial cell envelope and deliver

effector proteins into mammalian cells through a translocon pore that is formed in the host cell membrane (Mueller et al., 2008). Following activation in the intestine of the infected host, the SPI-1 T3SS translocates effectors across the host plasma membrane (Galán, 2001) inducing bacterial uptake into epithelial cells, as well as inflammation of the gut epithelium (Patel and Galán, 2005). After uptake into host cells, *Salmonella* resides in the *Salmonella*-containing vacuole (SCV) where the SPI-2 T3SS is activated to facilitate intracellular replication of bacteria (Figueira and Holden, 2012; Jennings et al., 2017) (Figure 1.1). The SPI-2 T3SS translocates a range of bacterial effectors into the host cell that are encoded in various locations on the *Salmonella* genome as well as on the pSLT virulence plasmid which contains the *spv* (*Salmonella* plasmid virulence) operon in *S.* Typhimurium (e.g. Mazurkiewicz et al. 2008). Expression kinetics of the SPI-1 and SPI-2 secretion systems are tightly controlled by two-component regulatory systems that sense changes in environmental signals such as pH, osmolarity and antimicrobial peptides (Yoon et al., 2009). Of note are the PhoP/PhoQ, EnvZ/OmpR and SsrA/SsrB systems which are required for the repression of SPI-1 and flagella genes once the bacteria reside in the SCV and the upregulation of the SPI-2 T3SS genes (Bader et al., 2005; Lee et al., 2000). Deregulation/deletion of either of the two-component or type III secretion systems leads to severe attenuation of the mutant bacteria in mouse infections and therefore genes regulated or secreted by these systems are of special interest for studies of virulence (Cirillo et al., 1998; Dorman et al., 1989; Galán and Curtiss, 1989b; Miller et al., 1989).

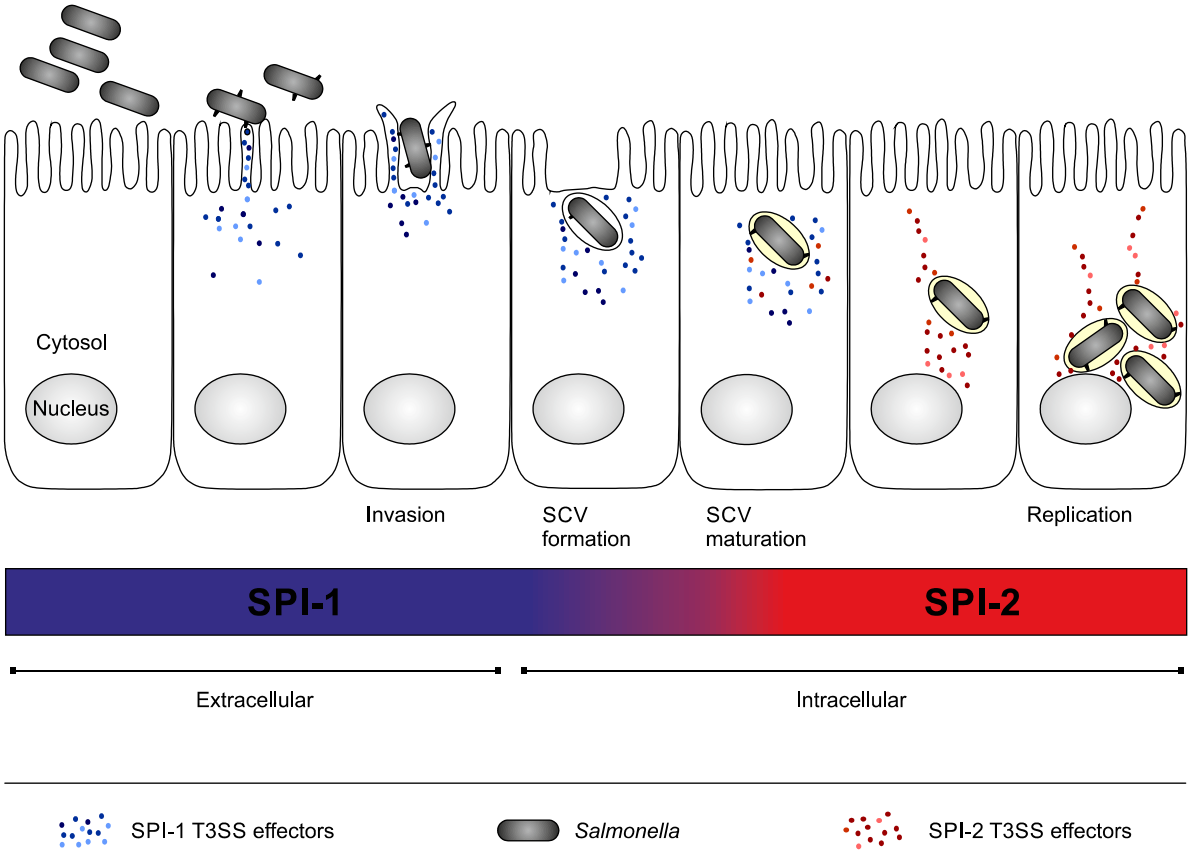

Figure 1.1. **Schematic illustration of an epithelial cell infection by *Salmonella* enterica**

Illustration of *Salmonella* host cell invasion and establishment of the *Salmonella*-containing vacuole (SCV) and bacterial replication, including temporal (from left to right) and spatial expression of the SPI-1 and SPI-2 type III secretion systems (T3SSs) (Adapted from. http://www.itqb.unl.pt/labs/infection-biology).

1.2 Innate host cell responses to *Salmonella* infection

The mammalian innate immune system is a rapid, non-specific defence system intrinsic to all (nucleated) cell types and essential for the control of bacterial infections. A large range of pattern recognition receptors (PRRs) including Toll-like receptors (TLRs), nucleotide-binding oligomerisation domain (NOD)-like receptors (NLRs), retinoic acid-inducible gene (RIG)-I like helicases (RLRs) and C-type lectin receptors mediate the recognition of pathogen associated molecular patterns (PAMPs) (Kawai and Akira, 2009). TLRs recognise bacterial lipopolysaccharide (LPS) (TLR4/CD14), flagellin (TLR5), lipoproteins (TLR1/2, TLR6/TLR2) as well as microbial RNA (TLR3, TLR7, TLR8) and DNA (TLR9) on the plasma membrane and in intracellular vesicles (Kaisho and Akira, 2006). In the host cell cytosol PRRs detect bacterial peptidoglycan (NOD1/2), toxins (NLRP1), flagella (NAIP5/6), LPS (caspase-11), RNA (RIG-1, MDA5) and DNA (cGas), to name the most well studied examples (Mogensen,

2009). PRR stimulation leads to the activation of various signalling pathways that ultimately result in the production of inflammatory cytokines and/or death of the infected cell. This in turn facilitates the infiltration of inflammatory immune cells to control and clear microbial infection (Medzhitov, 2007).

1.2.1 Inflammatory signalling

Innate inflammatory signalling leads to the transcriptional induction of genes encoding enzymes, chemokines and cytokines, to promote the recruitment and activation of leukocytes which are crucial for the elimination of pathogens and cellular debris (Mastroeni and Bryant, 2013). Three key inflammatory signalling pathways are activated by PRRs upon PAMP recognition; the nuclear factor κB (NF-κB), mitogen-activated protein kinase (MAPK) and interferon responsive factor (IRF) pathways which culminate in the activation of transcription factors required for pro-inflammatory cytokine expression (Figure 1.2). These pathways are essential for effective infection control and animals lacking components of these signalling cascades are highly susceptible to bacterial infection. It is important to note, that there is extensive cross-talk between the innate inflammatory signalling pathways described below which is beyond the scope of this introduction but is reviewed here (Kawai and Akira, 2011; Oeckinghaus et al., 2011).

1.2.1.1 The NF-κB pathway

During *Salmonella* infection NF-κB signalling is activated mainly by the engagement of TLR4 with bacterial LPS but also by secondary cytokine signalling via tumor necrosis factor α (TNFα) and interleukin-1 (IL-1) (see 1.2.1.4 below). Even though the initial events following receptor activation differ between stimuli, they activate a conserved signalling cascade of phosphorylation and ubiquitination events that culminate in the translocation of the NF-κB transcription factors into the host cell nucleus (Figure 1.2) (Napetschnig and Wu, 2013). Under normal physiological conditions, NF-κB/Rel transcription factors (including p65 (RelA), p50 and c-Rel) are bound and inhibited by cytoplasmic NF-κB inhibitor (IκB) proteins (Baeuerle and Baltimore, 1988; Tam and Sen, 2001). Activation of the classical (or canonical) NF-κB

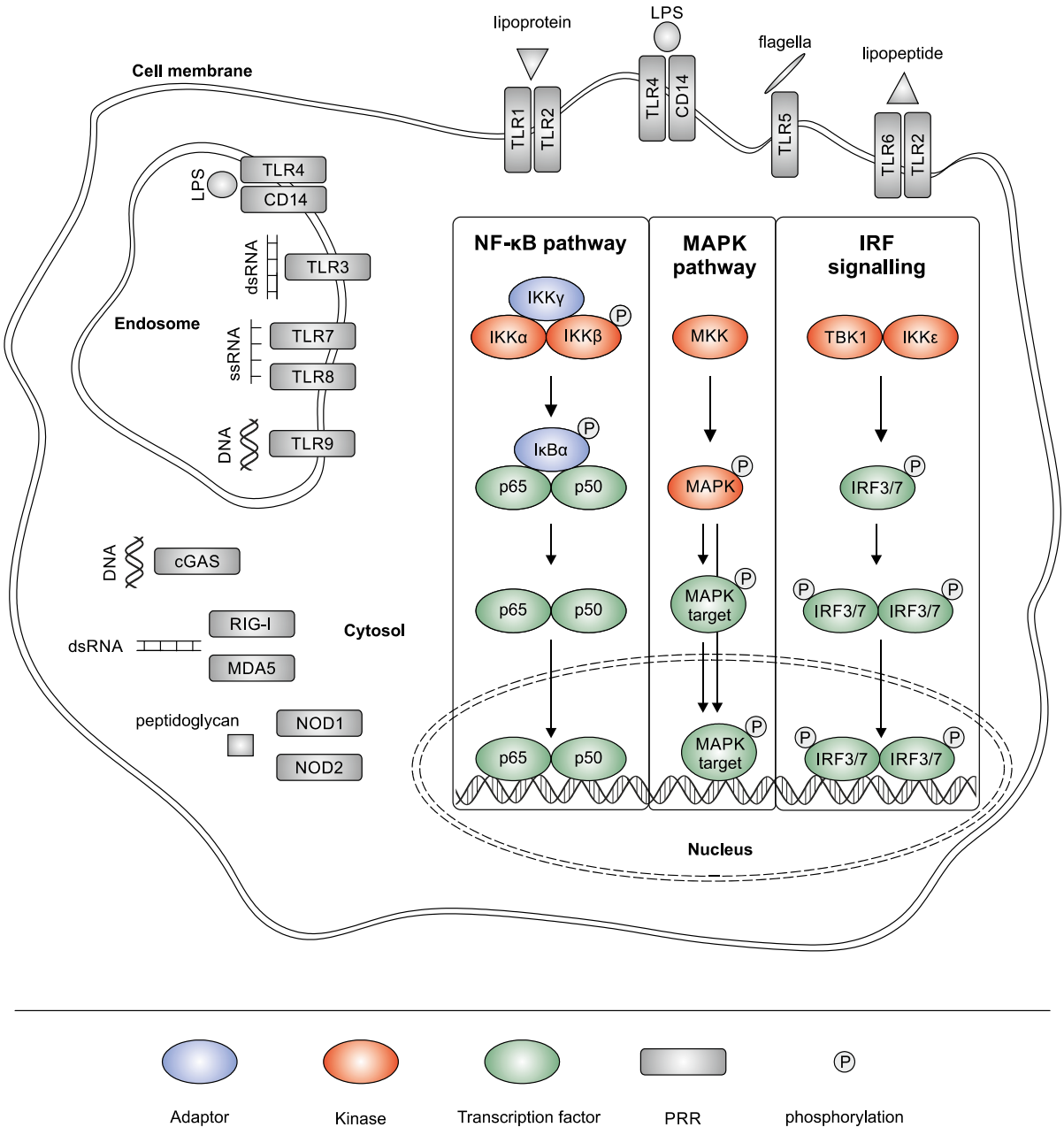

Figure 1.2. **Schematic representation of innate inflammatory signalling cascades upon bacterial infection**

During bacterial infection, pattern recognition receptors (PRRs) like the toll-like receptors (TLRs), nucleotide-binding and oligomerisation domain (NOD) proteins and RIG-I-like receptors recognise bacterial components including lipopolysaccharide (LPS), DNA, RNA, peptidoglycan and flagella to initiate an immune response. Initial events following receptor activation differ between stimuli but activate conserved signalling cascades, including the nuclear factor κB (NF-κB), mitogen-activated protein kinase (MAPK) and interferon responsive factor (IRF) signalling pathways. Each distinct signalling pathway is a conserved sequence of phosphorylation (and ubiquitination) events culminating in the translocation of active transcription factors to the nucleus to initiate pro-inflammatory gene expression. Due to space limitations, this schematic only includes well-studied ligands, receptors and core signalling components directly upstream of the key transcription factors of the NF-κB, MAPK and IRF signalling pathways.

signalling pathway by different agonists leads to the activation of the IκB kinase complex (IKKβ, IKKα, and IKKγ), which phosphorylates IκBα (Zandi et al., 1997). This subsequently leads to ubiquitination and degradation of IκBα (Chen et al., 1995), freeing associated NF-κB dimers which in turn translocate to the nucleus and initiate transcription of pro-inflammatory genes (Oeckinghaus and Ghosh, 2009). Alternatively, NF-κB-inducing kinase (NIK) and IKKα can induce cleavage of p100 to p52 via the proteasome that ultimately forms a heterodimer with RelB, independent of the trimeric IKK complex (non-canonical or alternative NF-κB pathway) (Sun, 2011). The activation of the p52/RelB complexes leads to the prolonged transcription of an alternative subset of NF-κB responsive genes (Hoffmann et al., 2006, 2003).

1.2.1.2 The MAPK pathway

The mitogen-activated protein kinase cascades are central signalling pathways that regulate a wide variety of cellular processes during homeostasis and microbial infection (Figure 1.2) (Arthur and Ley, 2013). MAPK signalling is initiated by TLR activation and comprises a three-tier kinase module in which MAPKK kinase (MAPKKK) phosphorylates and activates MAPK kinases (MAPKK), which phosphorylate and activate downstream MAPKs. Well studied MAPKs include Jun N-terminal kinase 1, 2 or 3 (JNK1/2/3), p38 and extracellular signal-regulated kinase 1 or 2 (ERK1/2) (reviewed in (Bogoyevitch et al., 2010; Roskoski, 2012; Weston and Davis, 2002)). These MAPKs in turn phosphorylate serine and/or threonine residues in target proteins, mainly transcriptional factors of the AP-1 family like c-Fos, c-Jun, ATF-2 and c-myc (Plotnikov et al., 2011). This leads to the transcriptional upregulation of pro-inflammatory genes required for an effective inflammatory response.

1.2.1.3 IRF signalling

In contrast to the NF-κB and MAPK pathways, IRF signalling is mainly activated by PRRs that recognise bacterial DNA and RNA in the host cell cytoplasm but also by various TLRs including TLR3, TLR4, TLR7 and TLR9 (Figure 1.2) (Honda and Taniguchi, 2006). Despite diverse initial stimulation and signalling events, the pathways converge at the TBK1-IKKε complex (TBK1; TANK-binding kinase 1) (Kawai and Akira, 2009). Activation of TBK1 leads to the phosphorylation of IRF3 and IRF7, resulting in IRF3/7 homo-and hetero-dimerisation

(Fitzgerald et al., 2003; Sharma et al., 2003). These dimers subsequently translocate to the nucleus where they bind to IFN-stimulated response element (ISRE)-promoters and activate the transcription of type I interferon (IFN) genes (Grandvaux et al., 2002).

1.2.1.4 Secondary immune signalling

All three above described inflammatory pathways, NF-κB, MAPK and IRF signalling, lead to the transcriptional activation of chemokines and cytokines including IL-1α/β, IL-6, TNFα, IFN-α, β, γ (IFNα/β/γ), IL-8 and RANTES. These proteins in turn can activate the same signalling pathways in an auto- and paracrine manner, leading to a positive feedback-loop and recruitment of immune cells. In addition, interferons induce janus kinase (JAK) and two signal transducer and activator of transcription (STAT) signalling pathways. Type I interferons (IFNα/β) initiate the phosphorylation and hetero-dimerisation of STAT1 and STAT2, which in turn binds to IRF9 (ISGF3 complex) to activate ISRE-dependent gene expression. This leads to a dampening of TLR-induced immunity by repression of neutrophil chemotaxis, reduced IL-1 cytokine family activity and increased macrophage cytotoxicity, enabling bacterial dissemination (Perkins et al., 2015; Robinson et al., 2012). Type II interferon (IFNγ) initiates STAT1 homo-dimerisation and subsequent binding to GAS elements to initiate transcription (Platanias, 2005). In contrast to type I interferons, IFNγ is crucial for the control of *Salmonella* infection by activation of macrophages and induction of major histocompatibility complex II (MHCII) expression necessary for adaptive immunity (Bao et al., 2000; Steimle et al., 1994).

1.2.2 Host cell death

Host cell death is an effective mechanism by which mammalian cells eliminate the intracellular niche of pathogenic bacteria and expose the microbes to neutrophil-mediated killing. Recognition of infection by PRR leads to programmed cell death signalling pathways resulting in apoptosis, necroptosis or pyroptosis (see below and Figure 1.3) (Jorgensen et al., 2017). Additionally, host cell death is regulated by death domain (DD)-containing receptors that are activated by soluble TNFα or FAS ligand (FASL) and TNF-related apoptosis-inducing ligand (TRAIL) on cytotoxic T cells, natural killer cells and macrophages, respectively (Guicciardi and Gores, 2009).

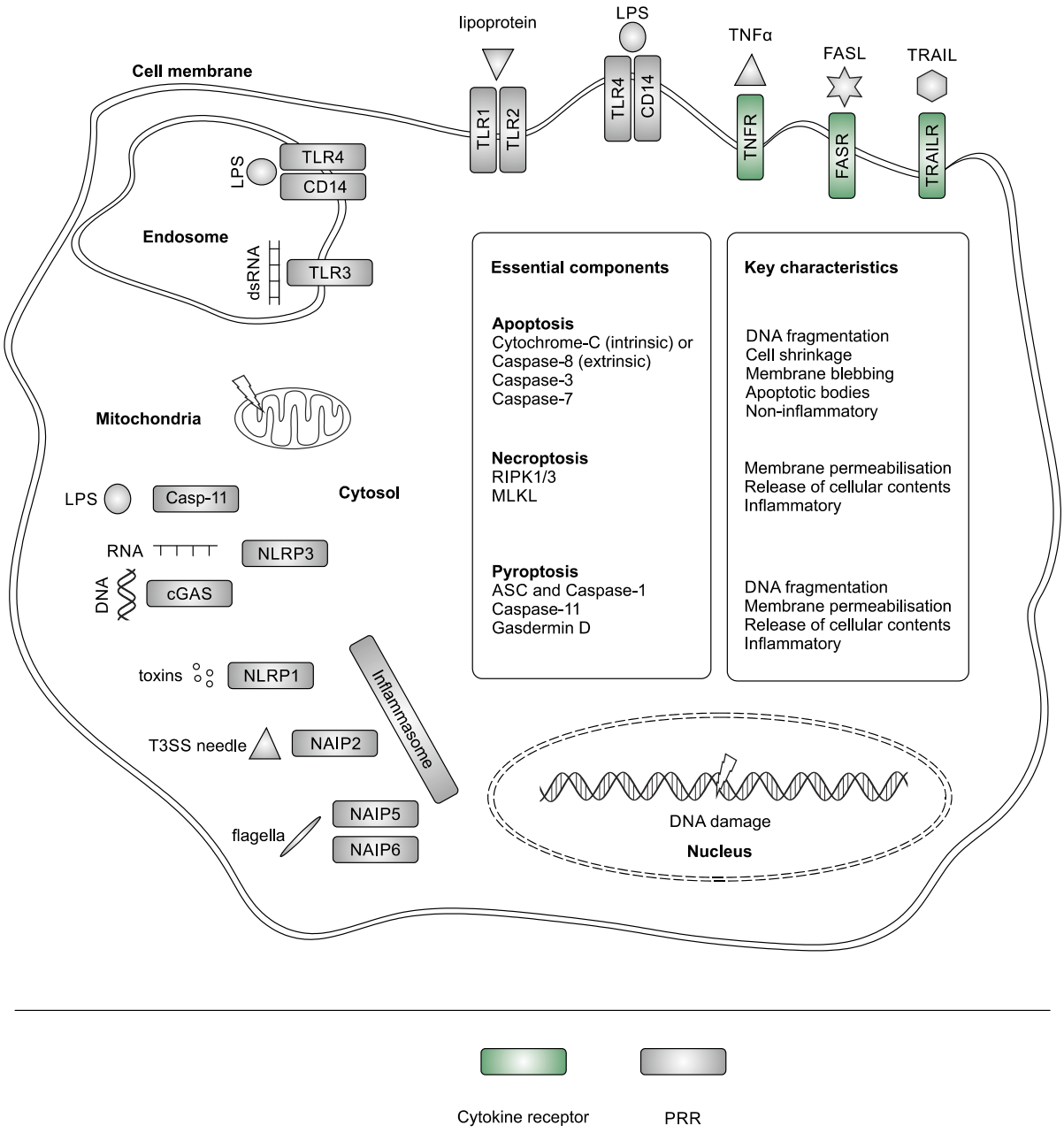

Figure 1.3. **Schematic representation of signalling receptors resulting in host cell death upon bacterial infection**

Engagement of pattern recognition receptors (PRRs) including toll-like receptors (TLRs), NOD-like receptors (NLRs) and caspase-11 by bacterial components like lipopolysaccharide (LPS), DNA, RNA flagella and toxins leads to the induction of programmed host cell death. In addition, activation of cytokine receptors like tumour necrosis factor α receptor 1 (TNFR1), TRAIL receptor (TRAILR) or FAS receptor (FASR) by their respective ligands induces cytotoxicity. Resulting apoptosis, necroptosis and/or pyroptosis differ in their molecular components and phenotypic characteristic, and in concert contribute to pathogen control. Due to space limitations, this schematic only includes well-studied ligands and receptors leading to apoptosis, necroptosis or pyroptosis as well as essential components and key characteristics of the cell death types.

1.2.2.1 Apoptosis

Apoptosis is a tightly controlled physiological form of programmed cell death required for homeostasis and innate immunity (Elmore, 2007). During bacterial infection apoptosis is mainly activated through external signals (extrinsic apoptosis) but can also be activated intrinsically by damage to mitochondria or DNA. Extrinsic apoptosis is largely initiated by engagement of death domain-containing receptors (TNFR, TRAILR and FASR) and TRIF mediated TLR signalling (Figure 1.3) (Ruckdeschel et al., 2004; Walczak, 2013). Activation of caspases, a group of specialised cysteine proteases, is an integral part of apoptosis common to all types of activation (McIlwain et al., 2015). Initiator caspases (e.g. casp-8) are activated upon different stimuli and cleave effector caspases (casp-3, casp-7) which then proteolytically degrade a large range of intracellular proteins to carry out the cell death programme. Apoptosis is morphologically characterised by cell shrinkage, gradual condensation and degradation of DNA, exposure of phospholipids on the cell surface and blebbing of the plasma membrane followed by fragmentation of the cell into small membrane-coated apoptotic bodies (Häcker, 2000). Apoptotic bodies are non-inflammatory but late apoptotic bodies can become inflammatory when not phagocytised by macrophages.

1.2.2.2 Necroptosis

Mainly activated by death-domain containing receptors (e.g. TNFR, TRAILR, FASR), necroptosis is a secondary, highly inflammatory form of cell death (Figure 1.3) (Pasparakis and Vandenabeele, 2015). Activation of these death domain receptors leads to the formation of the death-inducing signalling complex (DISC). This complex consists of FAS-associated death domain protein (FADD) and pro-caspase-8 but can additionally include TNFR1-associated death domain protein (TRADD) (see example for TNFR1 Figure 1.4). Unlike apoptosis, during necroptosis caspase-8 is not activated and instead RIPK1 (rip interacting protein kinase 1) and RIPK3 associate, auto- and transphosphorylate each other, and form a complex (necrosome) that phosphorylates the pseudokinase MLKL (mixed-lineage kinase domain-like) (Li et al., 2012; Sun et al., 2012; Zhang et al., 2009; Zhao et al., 2012). Phosphorylated MLKL localises to the plasma membrane where it is suggested to oligomerise and form pores that allow the influx of cations (Wang et al., 2014; Xia et al., 2016). This membrane permeabilisation leads

to membrane rupture and release of the cellular contents into the extracellular environment which is highly inflammatory, yet necroptosis does not directly kill intracellular bacteria (Jorgensen et al., 2016). Instead bacteria are released into the extracellular medium upon necroptosis and eliminated by attracted neutrophils.

1.2.2.3 Pyroptosis

Pyroptosis is another form of programmed lytic cell death in response to microbial infection (Jorgensen and Miao, 2015). Key molecular components of pyroptosis are inflammasomes composed of NLR proteins or AIM2-like receptor proteins that recognise cytosolic bacterial components like DNA (cGas), flagellin (NAIP5/6), toxins (NLRP1), the T3SS needle (NAIP1) and rod subunits (NAIP2) (Broz and Dixit, 2016). This leads to polymerisation of apoptosis-associated speck-like protein containing CARD (ASC) and to activation of caspase-1. This protease subsequently cleaves pro-IL-1β, pro-IL-18 and gasdermin D. Processed gasdermin D then associates with the cell membrane and oligomerises to form the pyroptotic pore (Ding et al., 2016; Liu et al., 2016). Alternatively, caspase-11 can recognise cytosolic LPS directly and induce cleavage of gasdermin D independently of caspase-1 (Shi et al. 2014; Aglietti et al. 2016). Due to the plasma membrane permeabilisation by gasdermin D, pyroptosis is phenotypically characterised by rapid cell swelling, membrane rupture and highly inflammatory release of damage associated molecular pattern molecules (DAMPs), including a large number of cytokines (IL-1α, IL-1β, IL-6, IL-18 and TNFα) (Bergsbaken et al., 2009). Similar to apoptosis, DNA fragmentation occurs during pyroptosis, however the underlying mechanism is distinct from apoptosis and currently not fully understood. Pyroptosis is insufficient to kill intracellular bacteria directly *in vivo*; instead bacteria are released into the extracellular space, taken by to neutrophils and killed by ROS (Jorgensen et al., 2016).

1.2.2.4 Alternative forms of cell death

ETosis is a specialised form of cell death utilised by specialised immune cells (e.g. neutrophils, eosinophiles and mast cells) to combat infections (Brinkmann et al., 2004; Remijsen et al., 2011). This form of regulated necrosis is characterised by chromatin

decondensation and the subsequent release of extracellular traps (ETs). These traps are composed of DNA, chromatin, and histones that immobilise and kill bacteria and fungi in the extracellular space.

In addition to these programmed forms of cell death it has been proposed that mammalian cells can be overwhelmed by bacterial replication and physically rupture due to a large bacterial burden.

1.2.3 TNF signalling – linking inflammatory signalling and cell death

TNFα is a pro-inflammatory cytokine that has important roles in cellular homeostasis and mammalian immunity (Kalliolias and Ivashkiv, 2015). TNFα binds to the TNF receptor 1 (TNFR1), which subsequently initiates the NF-κB and cell death pathways via its cytoplasmic death domain (Figure 1.4). Upon stimulation TNFR1 translocates to lipid rafts (Legler et al., 2003) and the cytoplasmic domain of the receptor undergoes a conformational change which allows the recruitment of TRADD and the formation of a large membrane-bound receptor complex. This, so called complex I, includes TRADD (Hsu et al., 1995), RIPK1 (Hsu et al., 1996a), TNF receptor-associated factor 2 (TRAF2) (Hsu et al., 1996b) and cellular inhibitor of apoptosis proteins (cIAPs) (Shu et al., 1996). Complex I in turn activates NF-κB and MAPK signalling via the TAB-TAK complex (Wang et al., 2001) but can also transition into the death-inducing signalling complex. This complex (IIA) is not receptor-associated and consists of TRADD, the FAS-associated death domain protein (FADD), and pro-caspase-8 (Figure 1.4) (Micheau and Tschopp, 2003). Activation of caspase-8 leads to the cleavage of the executer caspases (caspase-3/-7) and ultimately results in apoptotic cell death. Alternatively, if the levels of caspase-8 activity are low, RIPK1 and RIPK3 associate, auto- and trans-phosphorylate each other, and form complex IIB with MLKL (Figure 1.4), which is required for the induction of necroptosis (Li et al., 2012; Vercammen et al., 1998; Zhang et al., 2009; Zhao et al., 2012). Activation of the NF-κB signalling pathway by TNFα leads to the upregulation of pro-survival factors that counteract the simultaneous cell death activation. This results in a tightly controlled balance that can be tipped towards either survival or cell death by additional stimuli.

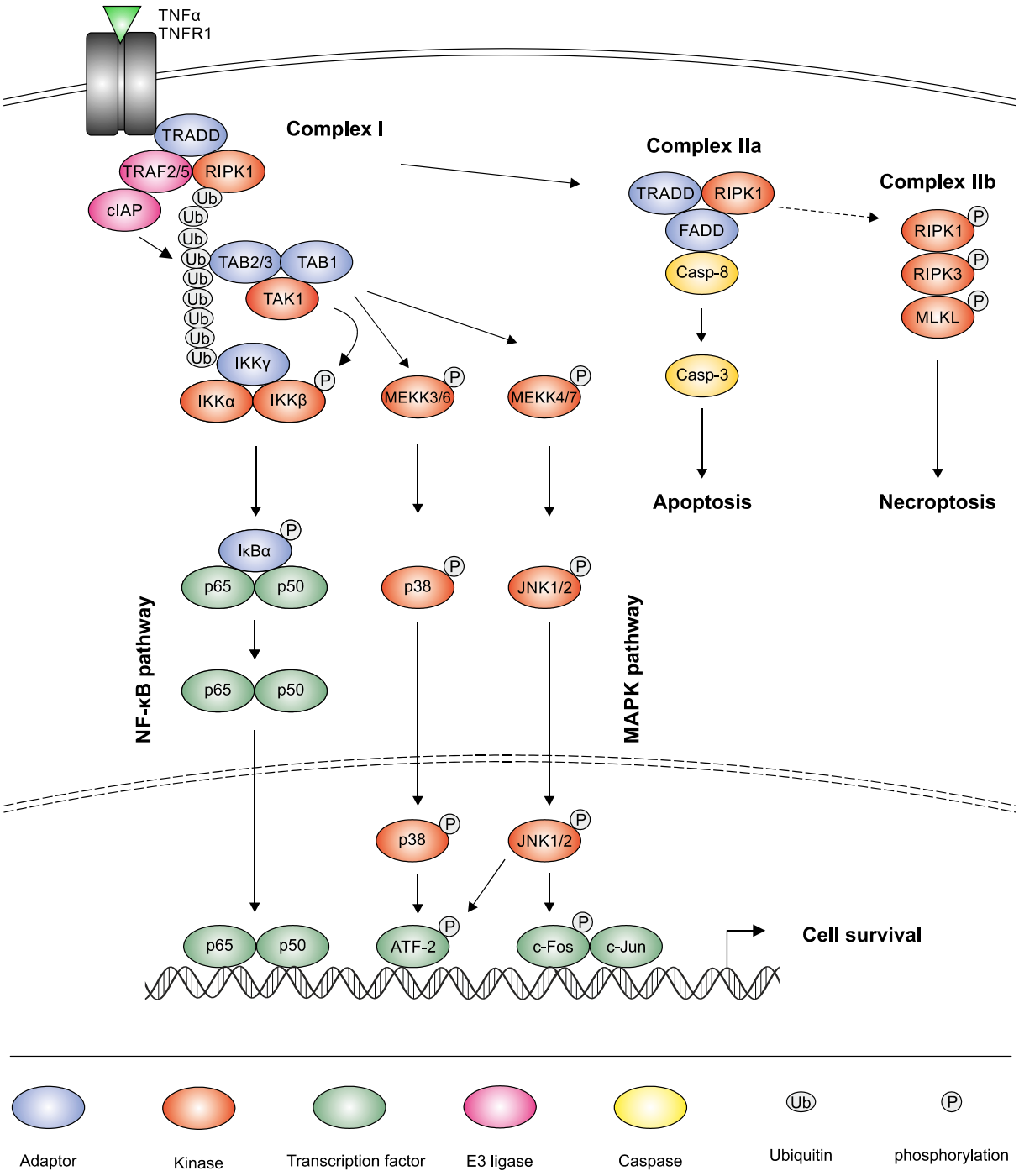

Figure 1.4. **Schematic representation of TNFR1 signalling**

Tumour necrosis factor α (TNFα) activation of the TNF receptor 1 (TNFR1) results in the recruitment of the TNFR1-associated death domain protein (TRADD), receptor-interacting serine/threonine-protein kinase 1 (RIPK1), TNF receptor-associated factor 2 (TRAF2) and cellular inhibitor of apoptosis proteins (c-IAP) (complex I). Complex I activates nuclear factor κB (NF-κB) and mitogen activated protein kinase (MAPK) signalling pathways via the TAB-TAK complex resulting in the expression of pro-survival genes. Additionally, complex I can transition into the death-inducing signalling complex (DISC, complex IIa). Complex IIa is not receptor-associated and consists of TRADD, the FAS-associated death domain protein (FADD), and pro-caspase-8. Activation of caspase-8 leads to the cleavage of the executer caspase (casp-3) and results in apoptotic cell death. Alternatively, if

caspase-8 activity is low, RIPK1 and RIPK3 associate with complex IIa and auto- and trans-phosphorylate each other to form complex IIB with the mixed-lineage kinase domain-like protein (MLKL) to induce necroptosis.

1.3 Manipulation of host cell processes by *Salmonella* effector proteins

In an evolutionary race, *Salmonella* has evolved remarkably sophisticated mechanisms to specifically and potently interfere with host cell functions and achieve favorable conditions for bacterial survival and replication. Many of these functions are carried out by effector proteins that are translocated into the host cell by T3SSs (Figueira and Holden, 2012; Jennings et al., 2017) (also see 1.1.3). *Salmonella* effectors mainly exert their function by enzymatic activity (e.g. AvrA, SteC,) but can also function as adaptors to facilitate or enhance the interaction and activity of host proteins (e.g. SseF, SteD). Often various bacterial proteins modulate the same biological process resulting in a complex interplay of cooperating (e.g. SseF/SseG) and opposing (e.g. SifA/SopD2) *Salmonella* effector function. In addition, effectors differ in the range of biological functions they modulate. Numerous effectors exert more than one function via multiple host cell targets (e.g. SipA, SopB) whereas others have very specific, even host cell type restricted function (e.g. SteD) (further detailed in 1.3.1 and 1.3.2)

Due to the frame of this thesis, the following section mainly focuses on the function of immune modulatory effectors translocated by the SPI-2 T3SS but will also provide an overview of other processes regulated by SPI-1 and SPI-2 T3SS effectors.

1.3.1 Functions of SPI-1 T3SS effectors

Invasion of intestinal cells including M cells and epithelial cells by *Salmonella*, is essential to establish infection. Active cell invasion is mediated by at least five effector proteins (SipA, SipC, SopB, SopE, and SopE2) that are translocated into the host cell by the SPI-1 T3SS. These effectors trigger intensive remodeling of the actin cytoskeleton, membrane ruffling and bacterial internalisation by macropinocytosis (Patel and Galán, 2005). This is achieved by direct effector interaction with actin (SipA (Zhou et al., 1999), SipC (Hayward and Koronakis, 1999)), as well as by activation of small GTPases required for the formation of actin networks (SopB, SopE, SopE2 (Patel and Galán, 2006)). Following complete *Salmonella* internalisation the host cell cytoskeleton returns back to its resting state. This is due to the

effector SptP, which reverses the activation of RAC1 and CDC42 by SopE, SopE2 and SopB (Fu and Galán, 1999), presenting a sophisticated example of opposing bacterial effector functions. *Salmonella* then establishes its intracellular niche, the *Salmonella* containing vacuole (SCV). SopB and SptP manipulate the host membrane phosphoinositide contents, regulate early endosome-SCV fusion and induce highly dynamic spacious vacuole-associated tubules that favour bacterial survival in the host cell (LaRock et al., 2015; Ramos-Morales, 2012). During the intermediate stage of SCV development in epithelial cells, it is moved to a juxtanuclear position by the activity of the SPI-1 T3SS effectors SipA and SopB and there tethered and further modified by various SPI-2 T3SS effectors (Ramos-Morales, 2012; Salcedo and Holden, 2003) (see 1.3.2).

SPI-1 T3SS effectors also trigger acute intestinal inflammation which is beneficial for the transmission of gastrointestinal serovars of *Salmonella* and typical for gastroenteritis (Byndloss et al., 2016). Of note are SopE, SopE2 and SopB which induce the MAPK and NF-κB pathways by activation of Rho GTPases leading to the production of pro-inflammatory cytokines and the recruitment of leukocytes to the intestinal mucosa (Bruno et al., 2009; Patel and Galán, 2006). The SPI-1 T3SS is also known to activate caspase-1-mediated pyroptotic cell death through secretion of flagellin, SipB and rod components in macrophages (Hersh et al., 1999; Miao et al., 2010, 2006). In addition, SopE activates caspase-1 in intestinal stromal cells to augment cell death and inflammation (Müller et al., 2009). Conversely, SptP and AvrA act to inhibit the action of the MAPK-dependent immune response and dampen host cell cytotoxicity (Jones et al., 2008; Lin et al., 2003) to maintain the intracellular niche by reducing clearance of the bacteria by the immune system.

1.3.2 Functions of SPI-2 T3SS effectors

The intracellular phase of *Salmonella* growth within epithelial cells and macrophages protects the bacteria from extracellular immunity and is essential for pathogenesis. To date, 28 effector proteins have been identified that are translocated by the SPI-2 T3SS system.

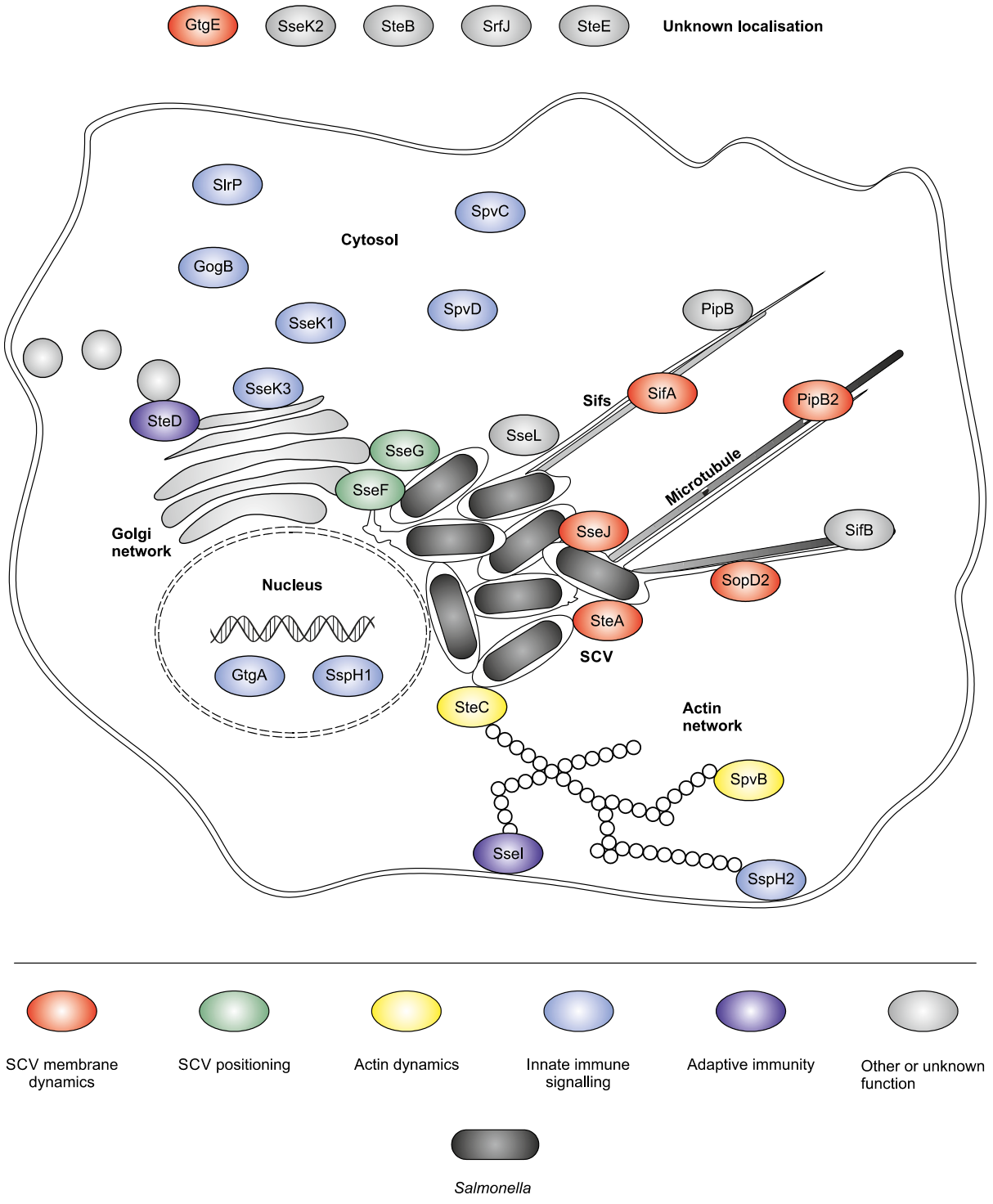

Figure 1.5. **Localisation and functions of *Salmonella* SPI-2 T3SS effector proteins in the host cell**

Many effectors are associated with tubules that emanate from the *Salmonella*-containing vacuole (SCV), including SifA, PipB2, SseJ, SopD2 and SteA. Other translocated effectors associate with the Golgi network (SseK2 and SseK3) or are integral membrane proteins (SteD, SseF, SseG). In contrast, SseK1, SpvC, SpvD, GogB and SlrP are mainly cytosolic whilst GtgA and SspH1 accumulate in the host nucleus (adapted from Figueira and Holden, 2012).

These proteins mediate functions including controlling SCV membrane dynamics and SCV positioning in the host cell, manipulating the host cytoskeleton and interfering with immune activation (summarised in Figure 1.5).

Once inside the host cell *Salmonella* faces two potentially harmful environments, the cytosol and/or the lysosome-vacuolar system. Upon SPI-1 T3SS-mediated invasion or passive phagocytosis, *Salmonella* resides in the SCV but can stochastically escape into the cytosol. Both the cytosol of epithelial cells as well as macrophages has been shown to limit bacterial replication by autophagy (Birmingham et al., 2006), cell extrusion (Knodler et al., 2010), pyroptotic cell death (Aachoui et al., 2013) and an additional unidentified mechanism of growth restriction (Thurston et al., 2016). To avoid this hostile environment various SPI-2 T3SS effectors function in a coordinated manner to regulate SCV membrane dynamics and maintain an intact vacuolar membrane. Integral to this process are SifA, PipB2, SopD2, SteA and SseJ which positively (SifA (Beuzón et al., 2000), PipB2 (Henry et al., 2006)) and negatively (SseJ (Ruiz-Albert et al., 2002), SopD2 (Schroeder et al., 2010)) affect SCV integrity as well as SCV partitioning (SteA (Domingues et al., 2014)). These effectors are also required for the formation of *Salmonella* induced filaments (Sifs) (Schroeder et al., 2011). Sifs are lysosomal glycoprotein-containing membrane tubules that extend centrifugally from SCVs along microtubules and have recently been suggested to enable nutrient acquisition for vacuolar bacteria (Liss et al., 2017) but their complete functional significance (if any) is not fully understood.

Bacteria-containing vacuoles frequently fuse with lysosomes leading to the exposure of the bacteria to degradative hydrolytic enzymes. SifA actively attenuates lysosome function by subverting retrograde trafficking of mannose-6-phosphate receptors required for the delivery of hydrolases to endosomes (McGourty et al., 2012). In addition, SopD2 and GtgE have been shown to interfere with endosome to lysosome trafficking (D'Costa et al., 2015; Spanò et al., 2016). Together, these SPI-2 T3SS effectors enable *Salmonella* replication in a less toxic SCV.

In epithelial cells, bacterial replication occurs in tight microcolonies, which are tethered to the Golgi network by the bacterial adaptors SseF and SseG's interaction with the Golgi protein ACBD3 (Salcedo and Holden, 2003; Yu et al., 2016). This is thought to enable the acquisition of membrane and nutrients by interactions with the dense vesicular tubular compartments of the Golgi network.

In various cell types these SCV clusters of replicating bacteria are surrounded by a dense F-actin meshwork (Méresse et al., 2001). This is dependent on the SPI-2 T3SS effector kinase SteC and leads to restrained bacterial growth in epithelial cells (Odendall et al., 2012; Poh et al., 2008). In contrast, SpvB, a *Salmonella* effector encoded on the *spv* operon of the *Salmonella* virulence plasmid, has been demonstrated to prevent F-actin polymerisation by adenosine 5'-diphosphate (ADP)-ribosylation of G-actin (Hochmann et al., 2006; Lesnick et al., 2001). Interestingly, deletion of *spvB* results in an increased actin network surrounding the SCV in epithelial cells (Miao et al., 2003), suggesting direct opposing effects of SteC and SpvB to tightly control bacterial replication. In addition, SpvB causes an apoptotic-like cell death during late stages of macrophage infection (Browne et al., 2008). This cytotoxicity requires SpvB catalytic activity and is characterised by actin cytoskeleton destabilisation and increased levels of caspase-3 activation (Browne et al., 2008), yet the precise molecular mechanism is not understood.

To date, half of the SPI-2 T3SS effectors with known functions are involved in the manipulation of the host innate and adaptive immune system (summarised in Table 1.1). Even though inflammation is beneficial for the transmission of gastrointestinal serovars of *Salmonella* (Byndloss et al., 2016), it can also result in pathogen clearance and is therefore a major target for bacterial intervention.

SpvC is a phosphothreonine lyase that irreversibly dephosphorylates active ERK, p38 and JNK MAPKs, thereby inhibiting transcription of pro-inflammatory cytokines and reducing inflammation of the gut mucosa (Haneda et al., 2012; Mazurkiewicz et al., 2008). Currently, SpvC is the only SPI-2 T2SS effector known to inhibit MAPK signaling during *Salmonella* infection.

In contrast, at least six SPI-2 T3SS effectors (SpvD, GtgA, SspH1, GogB, SseK1, SseK3) have been shown to inhibit various components of the NF-κB pathway. Of main interest to this work is the SseK family of effectors, SseK1, SseK2 and SseK3. SseK1 and SseK3 have previously been described to inhibit NF-κB reporter activity after ectopic expression (Li et al., 2013; Yang et al., 2015) and are discussed in detail in section 1.4.

SpvD binds to Exportin-2 (XPO2) in the host cell cytoplasm and thereby deregulates nuclear-cytoplasmic recycling of importins. This prevents efficient nuclear import of p65 which relys on importins to take it to the nucleus and thus leads to reduced activation of NF-κB responsive

genes (Rolhion et al., 2016). Based on biochemical analysis and the effectors crystal structure, SpvD is proposed to function as a cysteine hydrolase (Grabe et al., 2016). However, its only known host interaction partner, XPO2, does not appear to be modified by SpvD. Nevertheless, catalytic activity of SpvD is required for its inhibition of NF-κB activity (Grabe et al., 2016), suggesting that SpvD can function both as an adaptor and enzyme to inhibit NF-κB signaling.

GtgA, GogA and PipA are a family of zinc metalloproteases that specifically and redundantly target components of the NF-κB signaling pathway (Sun et al., 2016). All three proteases cleave the DNA-binding loop of the transcription factors p65 (RelA) and RelB, preventing transcriptional NF-κB activity (Sun et al., 2016). Despite high amino acid identity and functional redundancy of the effectors, to date only GtgA has been demonstrated to be translocated by the SPI-2 T3SS (Niemann et al., 2011), suggesting that the effectors have different translocation kinetics during *Salmonella* infection. By directly or indirectly targeting p65 - the final component of the NF-κB signaling pathway, both SpvD and the GgtA/GogA/PipA family effectors inhibit NF-κB-driven cytokine production, independent of the stimulus activating the pathway.

Tight regulation of ubiquitination and subsequent degradation of signaling components is essential for effective immunity and is targeted by different SPI-2 T3SS effectors. SspH1, SspH2 and SlrP are bacterial E3-ubiquitin ligases, which evolved independently from mammalian E3 enzymes and contain the catalytic site in a unique fold in the proteins C-terminal region (novel E3 ligase domain, NEL) (Quezada et al., 2009). Overexpression of SspH1 inhibits NF-κB pathway activity (Haraga and Miller, 2003), however this is independent of the effectors catalytic function (Keszei et al., 2014). Yet catalytic activity of the effector is required for the ubiquitination and proteasome-dependent degradation of PKN1 by SspH1, leading to attenuated androgen receptor responsiveness (Keszei et al., 2014). SspH2 modulates immune signaling by forming a trimeric complex with the NLR co-chaperone SGT1 and the receptor NOD1, and ubiquitination of both SGT1 and NOD1 (Bhavsar et al., 2013; Fiskin et al., 2016). This leads to significantly enhanced NOD1-mediated IL-8 secretion (Bhavsar et al., 2013), suggesting a pro-inflammatory function for SspH2 which is in direct contrast to other SPI-2 T3SS effectors. SlrP has been reported to interact with thioredoxin (TRX1) and the endoplasmic reticulum (ER) chaperone ERdj3 (Bernal-Bayard et al., 2010; Bernal-Bayard and Ramos-Morales, 2009). In addition, SlrP has recently been demonstrated to inhibit

inflammasome activation and prevent IL-1β-mediated anorexia (Rao et al., 2017). Whether this phenotype is linked to Slrp's published targets is currently unknown.

In addition to these E3 ubiquitin ligases, *Salmonella* also translocates SseL, a lysine 63-specific deubiquitinase (Rytkönen et al., 2007). SseL has been proposed to suppress pro-inflammatory NF-κB signaling by counteracting IκBα ubiquitination (Le Negrate et al., 2008), however two other studies found no effect of SseL on cytokine production (Mesquita et al., 2013; Rytkönen et al., 2007).

GogB also inhibits IκBα degradation and NF-κB activation in macrophages. This effector interacts with SKP1 and FBXO22 and thereby targets the SCF ubiquitin ligase complex to dampen the host inflammatory response in a not yet fully characterised manner (Pilar et al., 2012).

After oral ingestion, *Salmonella* encounters dendritic cells (DCs) in the epithelium and Peyer's patches of the small intestine (Farache et al., 2013). DCs are specialised antigen-presenting cells, that displaying antigenic (*Salmonella*) peptides on MHCII molecules to CD4+ T cells, leading to their activation, proliferation, and differentiation (Lipscomb and Masten, 2002). This is crucial for bacterial clearance and the establishment of an effective immunological memory. Two SPI-2 T3SS effectors stand out due to their inhibition of adaptive immunity. SseI (also called SrfH) inhibits normal cell migration of primary macrophages and dendritic cells (McLaughlin et al., 2009). This is dependent on the effectors interaction with IQGAP1, an important regulator of cell migration, and allows long-term chronic systemic *Salmonella* infection in mice (Lawley et al., 2006; McLaughlin et al., 2009). SteD functions as an adaptor between MHCII and the E3-ubiquitin ligase MARCH8, leading to increased ubiquitination and surface depletion of MHCII. This results in reduced T cell activation during *Salmonella* infection of mice (Bayer-Santos et al., 2016).

In combination, all the above-described effectors counteract the host's defense mechanisms during *Salmonella* infection by a diverse set of molecular functions and targets. Yet, despite intensive research, the physiological and/or biochemical function of many SPI-2 T3SS effectors is not, or only poorly, understood (e.g. PipB, SteA, SrfJ, SifB, SteB, SteE, SseK2, SseL) and therefore requires further investigation.

Table 1.1. **Summary of the biochemical activity, host cell interaction partners and physiological functions of immune modulatory SPI-2 T3SS effectors**

Effector	Biochemical Activity	Interaction Partner(s) / Substrate(s)	Function(s)	Reference(s)
GogB		SKP1, FBXO22	Inhibition of NF-κB signalling	(Pilar et al. 2012)
GtgA	Zinc metalloprotease	p65, RelB	Inhibition of NF-κB signalling	(Sun et al. 2016)
SlrP	E3 ubiquitin ligase	ERdj3, TRX1	Inhibition of IL-1β release	(Rao et al. 2017; Bernal-Bayard & Ramos-Morales 2009; Bernal-Bayard et al. 2010)
SpvC	Phosphothreonine lyase	ERK, p38, JNK	Inhibition of MAPK signalling	(Mazurkiewicz et al. 2008; Haneda et al. 2012)
SpvD	Cysteine hydrolase	XPO2	Inhibition of NF-κB signalling	(Rolhion et al. 2016; Grabe et al. 2016)
SseI	Cysteine hydrolase	IQGAP1	Inhibition of directional macrophages and DCs migration	(McLaughlin et al. 2009)
SseK1	Glycosyl transferase	TRADD	Inhibition of NF-κB signalling	(Li et al. 2013)
SseK3		TRIM32	Inhibition of NF-κB signalling	(Yang et al. 2015)
SspH1	E3 ubiquitin ligase	PKN1	Inhibition of NF-κB signalling and androgen steroid receptor signalling	(Haraga & Miller 2003; Keszei et al. 2014)
SspH2	E3 ubiquitin ligase	UbcH5-Ubiquitin, SGT1, NOD1	Activation of NOD1 signalling	(Bhavsar et al. 2013; Fiskin et al. 2016)
SteD		MHCII, MARCH8	Inhibition antigen presentation and T cell activation	(Bayer-Santos et al. 2016)

1.4 The SseK – NleB effector family

1.4.1 *Salmonella* SseK effectors

Prior to this study, three *Salmonella* effector proteins, SseK1, SseK2 and SseK3, represented an interesting and yet poorly characterised group of SPI-2 T3SS translocated proteins. SseK1 and SseK2 were identified in 2004 based on their homology to the enterohaemorrhagic *E. coli* protein Z4328 and the *Citrobacter rodentium* (*C. rodentium*) effector protein NleB (Kujat Choy et al., 2004). The genes encoding SseK1 (STM4157; SL1344_4096) and SseK2 (STM2137; SL1344_2113) are located outside the major SPIs in the *Salmonella* genome and are widely distributed amongst the known *Salmonella* serovars (Nuccio and Bäumler, 2014). The third, more recently discovered family member SseK3 (sb26; STM1344_1928), is encoded within the phage ST64B lysogen and only carried by some *Salmonella* subspecies that contain the phage (e.g. *S.* Typhimurium strains SL1344 and NTCC 12023) (Brown et al., 2011) (Figure 1.6).

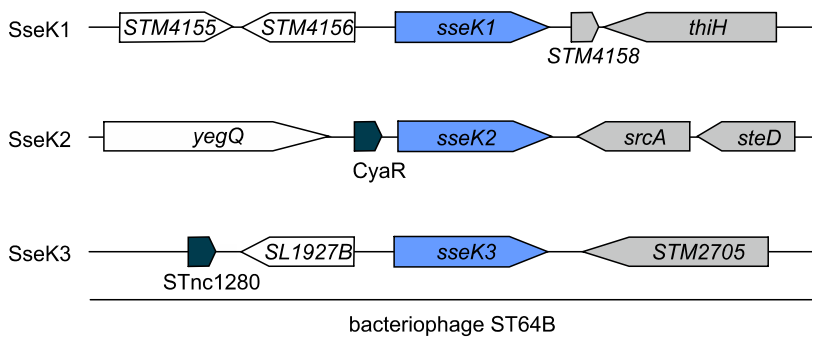

Figure 1.6. **Genomic location of the *S.* Typhimurium effector genes *sseK1, sseK2* and *sseK3***

Using *in vitro* growth techniques in SPI-1 or SPI-2 inducing media it was shown that all three SseK family members are translocated by one or both SPI T3SSs (Brown et al., 2011; Kujat Choy et al., 2004; Niemann et al., 2011). Selective use of different SPI deletion mutants revealed that SseK1 can be secreted and translocated by both the SPI-1 and SPI-2 T3SSs from as early as 4 hours post uptake (h.p.u.) in epithelial cells and 8 h.p.u. in macrophages (Baisón-Olmo et al., 2015; Kujat Choy et al., 2004). Both SseK2 and SseK3 have been shown to be translocated into HeLa cell at late infection time points (18 and 21 h.p.u., respectively) (Brown et al., 2011; Kujat Choy et al., 2004). However, in contrast to Ssek1, SseK2 and SseK3 are secreted exclusively by the SPI-2 T3SS *in vitro* and which T3SS facilitates translocation into

host cells has not yet been demonstrated (Brown et al., 2011; Kujat Choy et al., 2004). mRNA expression of all three SseK effectors is upregulated in SPI-2 inducing conditions *in vitro* as well as in macrophages (Kröger et al., 2013; Srikumar et al., 2015), however the underlying regulatory mechanisms have not been studied in detail. SseK1 expression in macrophages is dependent on the PhoP/Q two-component system (Baisón-Olmo et al., 2015) whilst *in vitro* studies suggest that the OmpR/EnvZ and SsrA/B regulatory systems are also required for the effectors optimal mRNA expression under SPI-2 inducing conditions (Colgan et al., 2016). mRNA expression of both SseK2 and SseK3 is completely abolished in mutants of the PhoP/Q, OmpR/EnvZ and SsrA/B two-component systems (Colgan et al., 2016) and SseK3 protein expression was absent during infection with an Δ*ssrB* mutant in HeLa cells (Brown et al., 2011).

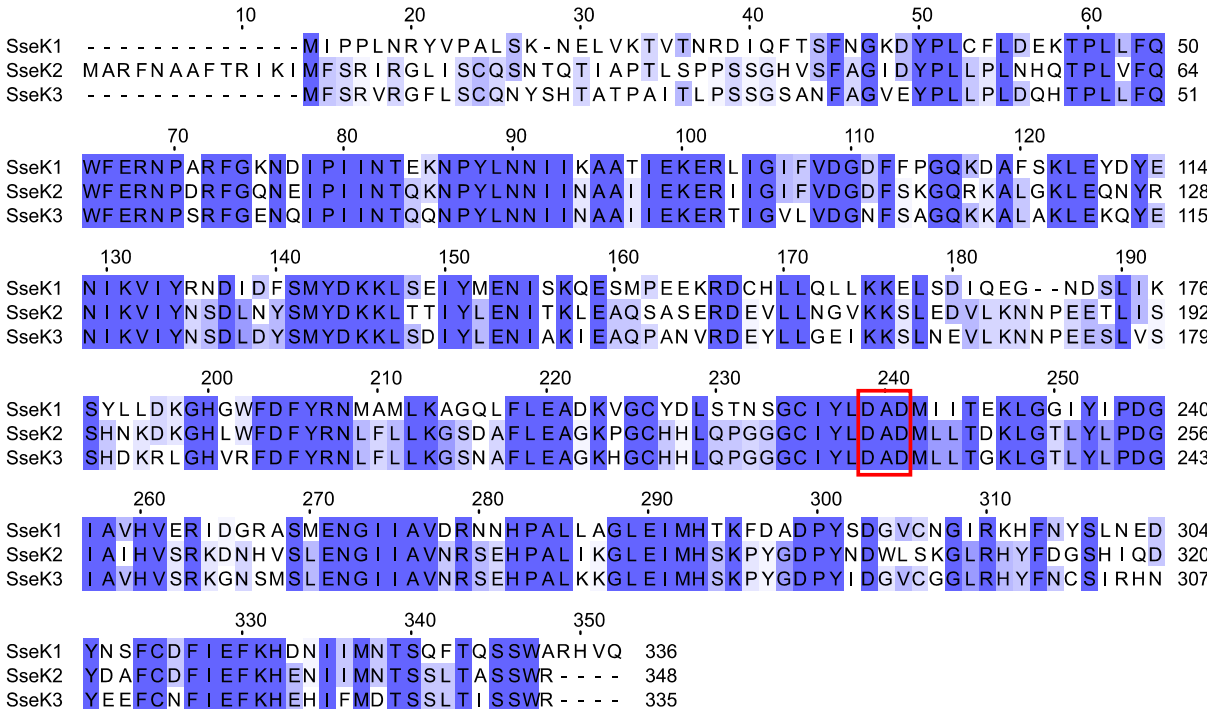

Figure 1.7. **Amino acid alignment of the SseK family members**

Amino acid sequence alignment of the *S.* Typhimurium NTCC 12023 SseK effectors produced with Jalview (Waterhouse et al., 2009). The conserved DxD motif is highlighted with the red box.

These expression and secretion data indicate that the translocation kinetics of the SseK effectors might be very diverse even though the proteins share a high protein sequence similarity (>60%, Figure 1.7). Interestingly, the N-terminal region (aa 1-32) of the proteins shows highest sequence diversity and in SseK1 is essential for protein translocation (Kujat

Choy et al., 2004). Variation in this region might therefore additionally contribute to different translocation kinetics and functions of the effectors.

The SseK effectors contain no known motifs or domains that might indicate the intracellular localisation of the proteins. So far it was shown that ectopically expressed or translocated SseK1 is distributed uniformly throughout the host cell cytosol with no specific localisation to the SCV or the actin cytoskeleton (Knodler et al., 2011; Kujat Choy et al., 2004). In contrast, localisation of translocated SseK3 to host membranes has been demonstrated and ectopically expressed GFP-SseK3 localises closely to the Golgi network (Brown et al., 2011; Yang et al., 2015). The localisation of SseK2 is unknown, as SseK2 expression levels were below the detection limit (Kujat Choy et al., 2004). The differential localisation of the SseK1 and SseK3 suggests that these proteins might have different host cell targets and functions.

When ectopically expressed, both SseK1 and SseK3 have been shown to inhibit TNFα-induced NF-κB signalling (Li et al., 2013; Yang et al., 2015). In addition, overexpressed SseK1 was reported to post-translationally modify TRADD by arginine-GlcNAcylation in the death domain, which is proposed to be the underlying mechanism of the effector's NF-κB phenotype (see 1.4.2) (Li et al., 2013). Independently, both our group and Yang et al. 2015 showed that ectopically expressed SseK3 can bind stably to tripartite motif containing protein 32 (TRIM32). However, no modification of TRIM32 by SseK3 has been reported and the physiological consequence of this interaction is unknown. Overall, the role of SseK1 and SseK3 during *Salmonella* infection is unknown and no function(s) have been reported for SseK2.

During *Salmonella* infection Δ*sseK1* and Δ*sseK2* mutants reside in intact SCVs and induce dynamic Sifs that are indistinguishable from wild-type infected cells, suggesting that they are not involved in SCV modulation (Rajashekar et al., 2014). Analysis of the intracellular bacterial growth of single (Δ*sseK1*, Δ*sseK2*, Δ*sseK3)*, double (Δ*sseK1/2*, Δ*sseK1/3)* and triple (Δ*sseK1/2/3*) deletion mutants in macrophages showed no significant reduction in replication (Figueira et al., 2013). In addition, *sseK* single deletion mutants were not significantly attenuated compared to wild-type bacteria in a competitive index experiment and the Δ*sseK1/2/3* mutant was indistinguishable from wild-type bacteria in its ability to disseminate and colonise the liver and spleen in short term mouse infections (Buckner et al., 2011; Kidwai et al., 2013). Interestingly, an Δ*sseK2* mutant was highly attenuated in long term infection (50

days) of mice, suggesting that SseK2 contributes to persistence of *S.* Typhimurium during systemic infection (Lawley et al., 2006).

1.4.2 NleB – a bacterial GlcNAc transferase

Escherichia coli (*E. coli*) and *S.* Typhimurium are both Gram-negative enterobacteria that share a large proportion of their genome, including some horizontally transferred pathogenicity determinants such as the T3SSs (Porwollik and McClelland, 2003). Even though the lifestyle and pathogenesis of both bacteria are vastly different, molecular mechanisms of effector function might still be shared by both species. NleB from enterohemorrhagic *E. coli* (EHEC), enteropathogenic *E. coli* (EPEC) and *C. rodentium* are the best studied homologues of the SseK effectors and share 57–76% amino acid identity and 80–92% similarity to the *Salmonella* proteins. In EHEC and EPEC NleB is involved in the regulation of the host inflammatory response (Nadler et al., 2010; Newton et al., 2010) while *C. rodentium* NleB is essential for colonisation and virulence in mice (Kelly et al., 2006). Two seminal studies have identified NleB as an arginine-specific *N*-acetyl-D-glucosamine (GlcNAc)-transferase able to inhibit death receptor signalling pathways by specifically modifying the death domain of proteins such as FADD and TRADD (Li et al., 2013; Pearson et al., 2013). This prevents the proteins dimerisation and thereby reduces the activation of death receptor signalling pathways. By targeting a protein family common to both the NF-κB and cell death signalling pathways (Figure 1.4) arginine-GlcNAcylation by NleB results in reduced host cell immune signalling and cytotoxicity during EPEC/EHEC infection (Li et al., 2013; Pearson et al., 2013). In addition to the modification of death domain proteins, NleB has also been proposed to disrupt GAPDH mediated poly-ubiquitination and activation of TRAF2 and TRAF3, resulting in NF-κB pathway inhibition (Gao et al., 2016, 2013).

1.4.3 Protein Glycosylation

Half of all human proteins are estimated to contain at least one glycan site, making protein glycosylation one of the most common post-translational modifications characterised to date (Apweiler et al., 1999; Hart and Copeland, 2010). Glycosylation is facilitated by specialised glycosyltransferases (GT) that are specific for both the sugar donor substrate and

the acceptor substrate. In eukaryotes protein glycosylation mainly involves the covalent attachment of glycans to serine, threonine, or asparagine residues, resulting in *N*- or *O*-glycosidic bonds between the carbohydrate and the polypeptide backbone protein (Hurtado-Guerrero and Davies, 2012). Both *O*-glycosylation and *N*-glycosylation can be the starting point for the formation of an extraordinary array of complex glycans found on extracellular glycoproteins (Moremen et al., 2014). In contrast, monosaccharide *O*-glycosylation of intracellular portions is not elongated or further modified and is characterised by the attachment of a single *N*-acetylglucosamine. The mammalian *O*-GlcNAc transferase (OGT) utilises UDP-*N*-acetylglucosamine derived from the hexosamine pathway to covalently attach the sugar to the hydroxyl moiety of serine or threonine residues in target proteins, which in turn can be actively removed by the *O*-GlcNAcylase (OGA) (Hart and Akimoto, 2009). This makes monosaccharide *O*-GlcNAcylation a transient form of post-translational modification, often thought to compete with protein phosphorylation, that is involved in diseases such as cancer (Slawson and Hart, 2011; Yi et al., 2013), diabetes (Ma and Hart, 2013; Yang et al., 2008) and Alzheimer's (Yuzwa et al., 2012; Zhu et al., 2014).

In contrast to OGT, NleB targets arginine residues for mono-glycosylation by transferring *N*-acetylgucosamine to the amino acids reactive amide group, making NleB a non-canonical *N*-GlcNAc transferase (Li et al., 2013; Pearson et al., 2013). Arginine-GlcNAcylation by NleB differs significantly from mammalian O-GlcNAcylation (Figure 1.8) and cannot be removed by mammalian O-GlcNAcylases, suggesting that it is irreversible (Li et al., 2013). NleB is classified as a GT-8 gylcosyltransferase, based on its predicted structural homology to known proteins of this family (Gao et al., 2013). These enzymes typically adopt a GT-A fold consisting of an α/β/α sandwich resembling a Rossmann fold and a Asp-X-Asp (DxD) catalytic motif (Lairson et al., 2008). The DxD motif is required for the coordination of a divalent cation (usually magnesium or manganese) and/or the sugar donor and mediates the sugar transfer to target proteins (Lairson et al., 2008).

Both the predicted GT-A fold and DxD motif of NleB are fully conserved in the *Salmonella* SseK effector family (Figure 1.7) suggesting that these proteins are glycosyltransferases with similar enzymatic activity to NleB. Indeed, SseK1 has been shown to GlcNAcylate TRADD when overexpressed ectopically (Li et al., 2013). However, even though SseK1 is therefore considered to be functionally identical to NleB the precise amino acid in TRADD that is

modified by SseK1 has not been determined. Mutation of the DxD motif in SseK3 abolished the proteins inhibitory effect on NF-κB signalling (Yang et al., 2015) however, direct evidence for catalytic activity of SseK3 is missing.

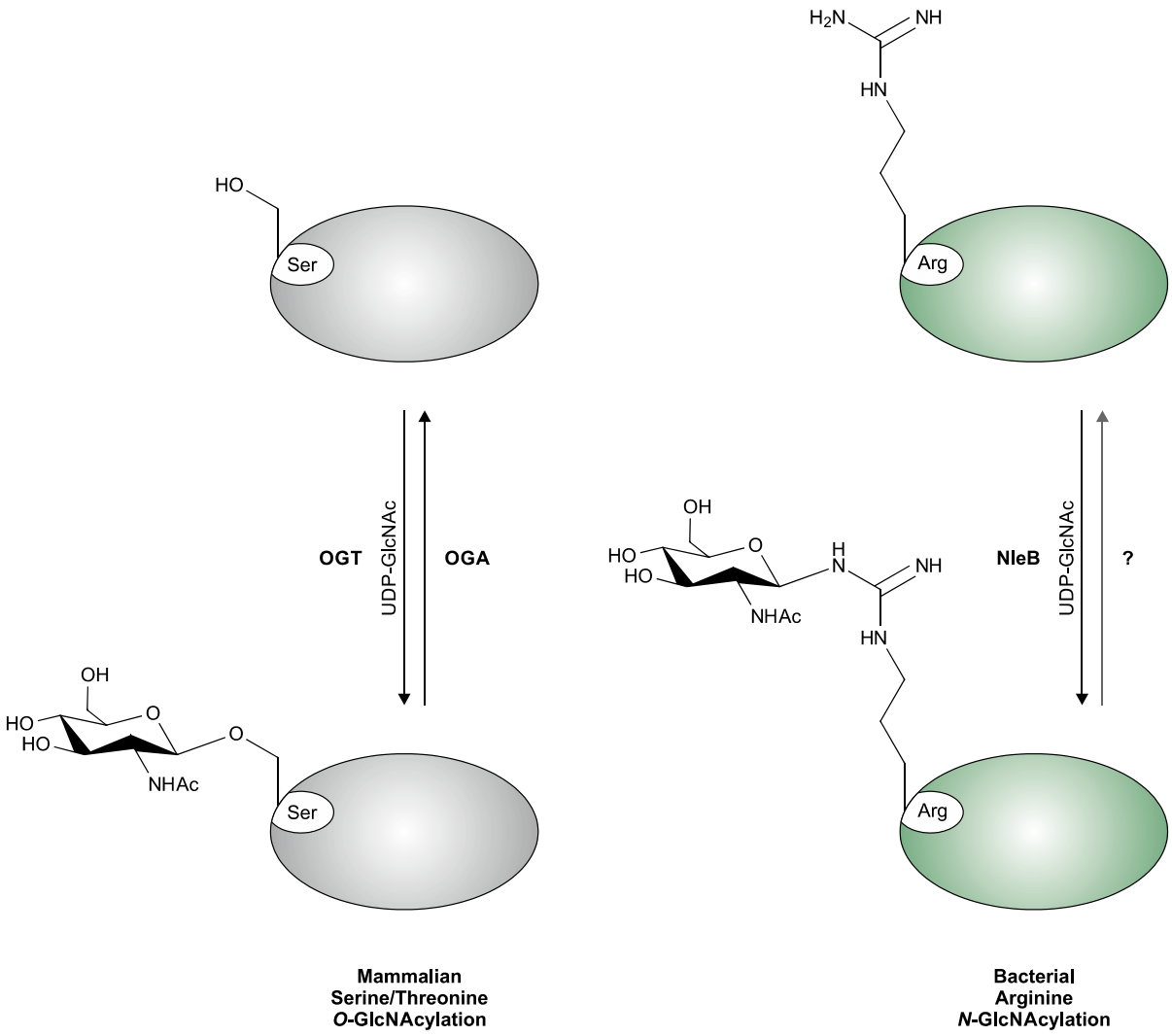

Figure 1.8. **Schematic representation of protein GlcNAcylation**

Mammalian protein *O*-GlcNAcylation on serine or threonine residues is controlled by two highly conserved enzymes, OGT and OGA. In contrast, NleB-mediated *N*-GlcNAcylation of death domain containing proteins occurs on arginine residues and is proposed to be irreversible. Ser, serine; Arg, arginine.

1.5 Tripartite motif proteins

1.5.1 TRIM proteins in innate immunity

Tripartite motif (TRIM) E3 ligases form a family of over 70 mammalian proteins involved in the regulation of a large spectrum of essential biological processes, including regulation of cell growth and differentiation, development, and immunity (Hatakeyama, 2011; McNab et al., 2011; Tocchini and Ciosk, 2015). All TRIM proteins share a conserved domain architecture consisting of an N-terminal Really Interesting New Gene (RING) domain, one or two B-box (BB) domains, a Coiled-Coil (CC) region and a variable C-terminal protein interaction domain (Borden, 1998; Meroni and Diez-Roux, 2005; Reymond et al., 2001). TRIM proteins mainly exert their biological functions by ubiquitination of specific substrates via their RING domain, which confers E3 ligase activity. This post-translational modification results in the covalent attachment of the ubiquitin peptide to target proteins and can, depending on the ubiquitin linkage, mediate different signals ranging from proteasome-mediated degradation to localisation and specific pathway activation (Komander and Rape, 2012). Additional functional diversity of the TRIM proteins results from differing C-terminal domains that are involved in a wide range of target protein interactions.

A large proportion of TRIM proteins have been reported to be involved in the regulation of innate immune signalling and anti-viral restriction (Rajsbaum et al., 2014a; Uchil et al., 2013; Versteeg et al., 2013). TRIM proteins positively (e.g. TRIM8 (Tomar et al., 2012), TRIM20 (Chae et al., 2008)) and negatively (e.g. TRIM9 (M. Shi et al., 2014), TRIM30α (Shi et al., 2008)) modulate the NF-κB pathway in a complex interplay between the TRIM E3 ligases and proteins at different steps in the NF-κB signalling cascade (Tomar and Singh, 2015). In addition, recognition of cytosolic DNA and subsequent IRF-mediated gene expression can also be activated (e.g. TRIM6 (Rajsbaum et al., 2014b), TRIM15 (Uchil et al., 2013)) and repressed (e.g. TRIM11 (Lee et al., 2013), TRIM28 (Liang et al., 2011)) by TRIM proteins, resulting in altered levels of type I and II interferons. Tight regulation of all these processes is required for efficient anti-viral and anti-microbial activities and dysregulation is often linked with auto-immunity and auto-inflammatory disease (Jefferies et al., 2011). Various TRIM proteins also restrict virus entry, replication and release (Uchil et al., 2008) with the best characterised example being TRIM5α. The c-terminal SPRY domain of TRIM5α directly binds to the retroviral capsid and promotes its disassembly before completion of reverse transcription of viral RNA.

Currently the precise mechanism involved in this process is not fully understood but functional TRIM5α is required for the control of human immunodeficiency virus in rhesus macaque or N-tropic murine leukemia viruses in humans (Grütter and Luban, 2012). Conversely, TRIM proteins required for efficient immune signalling are targeted by viral proteins, which is best understood for TRIM25. Following RNA recognition, RIG-I undergoes K63-linked ubiquitination by TRIM25, which is crucial for subsequent activation of MAVS (a key signalling adaptor protein) and therefore TRIM25 is required for IFNβ production and NF-κB promoter activation (Gack et al., 2007). This is inhibited by the Influenza NS1 protein which specifically interacts with the CC domain of TRIM25, preventing TRIM25 oligomerisation and thereby abolishing RIG-1 ubiquitination and downstream signalling (Gack et al., 2009).

In contrast to the well-studied role of TRIM E3 ligases as anti-viral proteins, little is known about their function during bacterial infection. Due to their role in immune signalling homeostasis and autophagy (Hatakeyama, 2017; Mandell et al., 2014), a large proportion of TRIM proteins are likely to be involved in anti-microbial recognition and restriction. Individual studies have addressed the effects of TRIM21, TRIM38, TRIM56 and TRIM65 on *Salmonella* infections (see below). However, to date no studies have been published that systematically address effects of TRIMs protein on bacterial invasion and replication. TRIM21 is a cytosolic antibody receptor that recognises antibody-coated pathogens including *Salmonella*, activating NF-κB signalling and cytokine production (McEwan et al., 2013; Rakebrandt et al., 2014). In addition, recognition of opsonised *Salmonella* by TRIM21 is proposed to restrict intracellular replication by targeting the bacteria for antibacterial autophagy (Rakebrandt et al., 2014). TRIM38 negatively regulates TLR3/4-mediated signalling and is required to dampen the innate immune response to *Salmonella*. As a consequence *Trim38*$^{-/-}$ mice are highly susceptible to *S*. Typhimurium–induced septic shock (Hu et al., 2015). Two independent studies reported recently that the *Salmonella* SPI-1 T3SS effector SopA can ubiquitinate TRIM56 and TRIM65 during bacterial infection. TRIM56 and TRIM65 are enhancers of RIG-1 and MDA-5 mediated signalling, respectively. However, the studies came to opposing conclusions on whether the SopA-TRIM56/65 interaction positively or negatively affects TRIM protein stability and therefore innate immunity (Fiskin et al., 2017; Kamanova et al., 2016). Overall these data suggest that TRIM proteins are important for the control of microbial infections and therefore plausible targets for bacterial effector proteins.

1.5.2 Tripartite motif protein 32

Tripartite motif protein 32 (TRIM32) features an N-terminal RING domain required for E3 ligase catalytic activity, a type 2 B-box domain, a Coiled-Coil domain necessary for dimerisation of the protein and 6 C-terminal domain NHL repeats (NHL domain) involved in target protein interaction (Koliopoulos et al., 2016) (Figure 1.9A). Dimerisation of TRIM32 is required for its E3 ligase activity and the protein is proposed to adopt a homo-tetrameric tertiary structure consisting of two anti-parallel dimers (Koliopoulos et al., 2016) (Figure 1.9B).

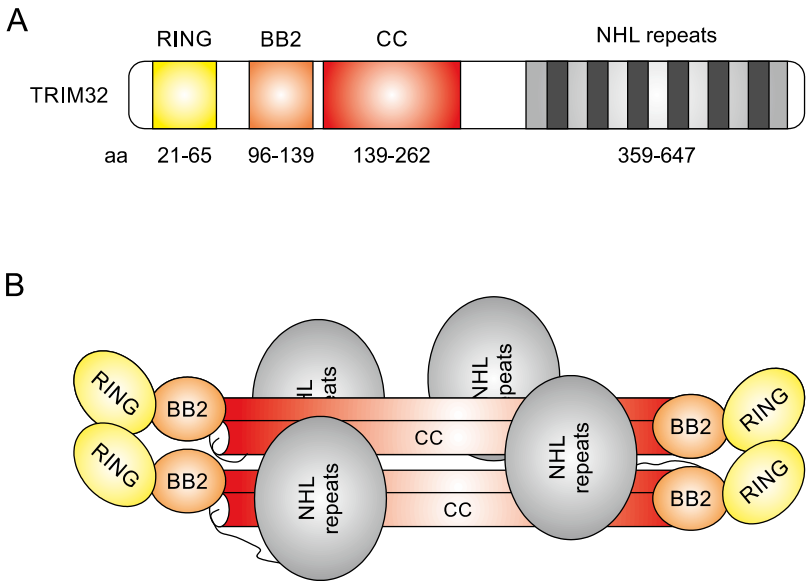

Figure 1.9. **Schematic representation of TRIM32 domain structure and proposed model of TRIM32 tetramerisation**

(A) TRIM32 domain structure consisting of an N-terminal E3 ligase domain (RING), B-box 2 (BB2), coiled-coil domain (CC) and c-terminal NHL-domain for target interaction. (B) Proposed model of TRIM32 tertiary structure based on (Koliopoulos et al., 2016).

TRIM32 mediates the majority of its functions via ubiquitination of itself (auto-ubiquitination) and target proteins, which requires the TRIM32 RING domain and interaction with different E2 ligases (Koliopoulos et al., 2016; Napolitano et al., 2011). TRIM32-mediated K48 ubiquitination is mainly implicated in proteasome-mediated target degradation (Fu et al., 2015; Mokhonova et al., 2015), whereas K63 ubiquitination is implicated in immune signalling (Zhang et al., 2012). Due to its wide spectrum of substrates TRIM32 is involved in the

regulation of different molecular processes including muscle physiology, neuronal differentiation, cancer and innate immunity (Figure 1.10).

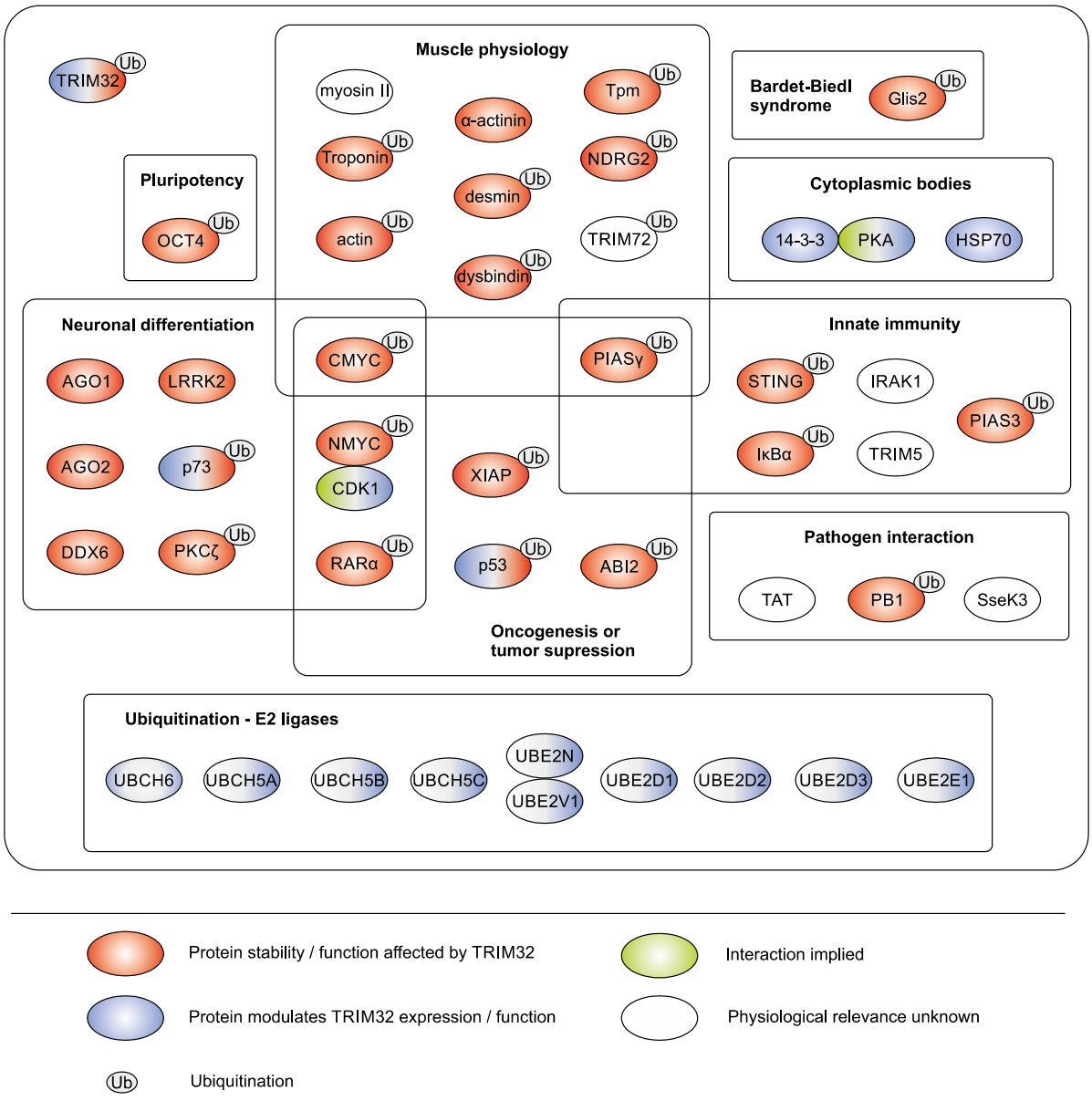

Figure 1.10. **Summary of TRIM32 interaction partners clustered into biological processes**

The information in this figure was compiled from references in the text and does not include unverified TRIM32 interaction partners identified in large-scale screens. Ub, ubiquitin.

Mutations in TRIM32 have been linked to two distinct diseases, Bardet–Biedl syndrome (BBS) and Limb Girdle Muscular Dystrophy type 2H (LGMD2H). BBS is a pleiotropic ciliopathic disorder caused by a mutation in the TRIM32 B-box (Chiang et al., 2006), whereas LGMD2H is

a mild form of autosomal recessive muscular dystrophy resulting from different disease-causing deletions and mutations in the TRIM32 NHL-domain (Borg et al., 2009; Cossée et al., 2009; Frosk et al., 2002; Nectoux et al., 2014; Neri et al., 2013; Saccone et al., 2008). To date it is not fully understood how mutation of TRIM32 leads to disease but TRIM32 has been shown to interact with (and ubiquitinate) different muscle-relevant proteins such as actin, α-actinin, desmin, tropomyosin and dysbindin (Cohen et al., 2012; Kudryashova et al., 2005; Locke et al., 2009). In addition, TRIM32 is involved in muscle regeneration by activation and differentiation, as well as reduced senescence of satellite cells (Kudryashova et al., 2012; Yonghua Liu et al., 2017; Mokhonova et al., 2015; Nicklas et al., 2012). Interesting, *Trim32*$^{-/-}$ mice show muscular dystrophy with both neurogenic and myogenic characteristics (Kudryashova et al., 2009). During neuronal development TRIM32 is necessary for the correct induction of neuronal differentiation by suppressing proliferation and inducing differentiation of neuronal stem cells (Gonzalez-Cano et al., 2013; Hillje et al., 2011; Nicklas et al., 2015; Sato et al., 2011; Schwamborn et al., 2009). In addition, altered expression levels of TRIM32 have been linked to Alzheimer's disease, autism, attention deficit hyperactivity disorder, anxiety, and obsessive compulsive disorder (Lionel et al., 2014, 2011; Ruan et al., 2014; Yokota et al., 2006).

TRIM32 expression is elevated in a large number of diverse cancer types (Horn et al., 2004; Kano et al., 2008; Liu et al., 2014) and has recently been proposed as a prognostic marker for gastric cancer (Ito et al., 2017). Interestingly, TRIM32 has been reported to have both oncogenic and tumour suppressive properties depending on the tumour type investigated. Through ubiquitionation and subsequent degradation of p53, ABl2 and PIASγ, TRIM32 supressess apoptosis whilst promoting cell growth, transforming activity and cell motility, suggesting oncogenic function of TRIM32 (Horn et al., 2004; Kano et al., 2008; Liu et al., 2014). On the other hand, TRIM32 can promote apoptosis by facilitating degradation of XIAP and enhances cell death in neuroblastomas (Izumi and Kaneko, 2014; Ryu et al., 2011).

Even though TRIM32 was originally identified due to its binding to lentiviral Tat proteins (Fridell et al., 1995) little is known about the role of TRIM32 in anti-viral and anti-microbial restriction. TRIM32 stably binds to Tat proteins in the host nucleus but it has not been established whether TRIM32 displays any effect on Tat function (Fridell et al., 1995). In large-scale screens, TRIM32 has been shown to suppress retroviral gene expression and lentiviral

particle release from the host cell (Uchil et al., 2008). However, the underlying mechanism has not been investigated. During influenza infection, TRIM32 mediates K48-linked ubiquitination of PB1, which results in augmented PB1 degradation and reduced viral polymerase activity (Fu et al., 2015), strengthening earlier findings that TRIM32 is an anti-viral protein. Interestingly, TRIM32 has been reported to hetero-dimerise with the anti-viral protein TRIM5 (Woodsmith et al., 2012), the relevance of this interaction has not been further addressed though. To date, nothing is known about the function of TRIM32 during bacterial infection. Unpublished work from our laboratory and a report from Yang and colleagues (Yang et al., 2015) showed that TRIM32 interacts stably with the *Salmonella* SPI-2 T3SS SseK3 when expressed ectopically. However, the physiological relevance of this interaction has not been addressed prior to this thesis. In addition, TRIM32 has been shown to regulate different innate immune signalling pathways and alter cytokine expression. Overexpression of TRIM32 increases basal levels of NF-κB and AP-1 reporter activity (Uchil et al., 2013). TRIM32-mediated activation of NF-κB signalling occurs prior to TAK1 activation (Uchil et al., 2013) and in keratinocytes this is dependent on TRIM32-mediated ubiquitionation and subsequent degradation of the NF-κB pathway inhibitor PIASγ (Albor et al., 2006). In contrast to these data, TRIM32 has also been shown to interact directly with and ubiquitinate IκBα (Ruelas et al., 2015); however to date this finding has not been confirmed by any other study. TRIM32 potently enhances STING-mediated activation of ISRE and IFN-promoters in response to viral infection (Zhang et al., 2012). Interestingly, which cytokines are regulated by TRIM32 overexpression or deficiency differs greatly between published reports, which is likely due to the different cell types and tissues analysed (Fu et al., 2017; Liu et al., 2010; Yuangang Liu et al., 2017; Zhang et al., 2012). Overall, these data show that TRIM32 has diverse functions in innate immune signalling and might therefore be a likely target for bacterial effector-mediated intervention with host cell immunity.

1.6 Aim of this work

The aim of this project is to investigate the functions of the SPI-2 T3SS SseK effector proteins. This includes identification of host processes targeted by the effectors as well as the mechanism(s) underlying their effects and their physiological relevance.

Specifically, the project aims were:

(i) Investigation of the SseK family members physiological functions during macrophage infection with focus on innate immune signalling and host cell death

(ii) Identification, validation and characterisation of SseK family interaction partners and/or enzymatic targets

(iii) Analysis of whether the identified SseK host interaction partners from aim (ii) are required for the observed phenotypes from aim (i)

2 MATERIALS AND METHODS

2.1 General buffers

LB broth - 2% Lennox L Broth Base (Invitrogen #12780-052), autoclaved

LB agar - LB broth, supplemented with 1.5% (w/v) agar (Thermo Fisher #LP0011B), autoclaved

SOC medium - 2% (w/v) tryptone (SLS #LP042B), 0.5% (w/v) yeast extract (SLS #LP021B), 0.5% (w/v) NaCl (Sigma #S7653), 10 mM $MgCl_2$ (Sigma #M8266), and 20 mM glucose (Sigma #G5767)

10x PBS - 1.37 M NaCl (Sigma# S7653), 27 mM KCl (Sigma #P9541), 100 mM Na_2HPO_4 (Sigma # S3264), 20 mM KH_2PO_4 (Sigma #P5379), adjusted pH to 7.4 with HCl (VWR # 20252.335)

10x TBS - 48.22 g Tris base (Sigma # T1503), 175.32 g NaCl (Sigma# S7653), adjusted to pH 7.4 with conc. HCl (VWR # 20252.335), H_2O to 2 l

1x TBST buffer - 1x TBS, 0.1% Tween-20 (Sigma # P2287)

FSB - 125 mM Tris-Cl pH 6.8 (Sigma # T1503), 4% SDS (VWR #442444H), 10% glycerol (Sigma #G5516), bromophenol blue (Sigma #B5525), H_2O

2.2 Bacterial cell culture

All bacterial strains detailed in Table 2.1 were cultured at 37°C on LB agar plates or in LB medium with agitation at 200 rpm. Cultures were inoculated from a single colony for overnight growth and when necessary supplemented with antibiotics as below:

Carbenicillin (Carb, Sigma #C1389)	100 µg/ml
Kanamycin (Kan, Sigma #K1377)	50 µg/ml

Table 2.1. **Bacterial strains**

Name	Description	Source or Reference
***S*. Typhimurium NCTC 12023 strains**		
wild-type	12023 *S.* Typhimurium wild-type	NTCC
Δ*ssaV*	Δ*ssaV*::km	(Deiwick et al., 1998)
Δ*sseL*	Δ*sseL*::km	(Rytkönen et al. 2007)
Δ*sseK1*	Δ*sseK1*::km	(Figueira et al. 2013)
Δ*sseK2*	Δ*sseK2*::km	(Figueira et al. 2013)
Δ*sseK3*	Δ*sseK3*::km	(Figueira et al. 2013)
Δ*sseK1/2*	Δ*sseK1*/Δ*sseK2*::km	(Figueira et al. 2013)
Δ*sseK1/3*	Δ*sseK1*/Δ*sseK3*::km	(Figueira et al. 2013)
Δ*sseK1/2/3*	Δ*sseK1*/Δ*sseK2*/Δ*sseK3*::km	(Figueira et al. 2013)
Δ*sifA*	Δ*sifA:*::mTn*5*	(Beuzón et al., 2000)
***E. coli* strains**		
BL21(DE3)	Protein expression strain	New England
DH5α	Cloning procedures	Thermo Scientific

2.3 Genetic techniques

2.3.1 Transformation of chemically competent *E. coli* cells

50 µl of chemically competent *E. coli* cells (DH5α or BL12) were mixed with 5-7.5 µl of ligation reaction and incubated on ice for 30 min. Bacteria were heat shocked at 42°C for 45 sec for DNA uptake and then returned on ice for two more minutes. Cells were recovered at 37°C for 1 h in 500 µl of SOC medium and plated on LB agar with appropriate antibiotics.

2.3.2 Preparation and transformation of electro-competent *S*. Typhimurium cells

S. Typhimurium cultures were inoculated (1:33 dilution) from overnight cultures in fresh LB medium and grown for 2.5 h at 37°C. Then the bacteria were collected, washed three times in ice-cold sterile water and once in ice-cold 10% glycerol (Sigma #G5516). The cells were resuspended in 100 µl of ice-cold 10% glycerol, mixed with 100 ng of the appropriate plasmid and electroporated at 2.5 kV, 200 Ω, 25 µF. Afterwards 500 µl of SOC medium was

added for cell recovery at 37°C. Transformed bacteria were selected on LB agar plates with appropriate antibiotics.

2.4 Nucleic acid techniques

Concentrations of nucleic acid solutions were determined by measurements using a NanoDrop Lite Spectrophotometer (Thermo Fisher).

2.4.1 DNA isolation

S. Typhimurium and *E.coli* genomic DNA was isolated using the Wizard Genomic DNA Purification Kit (Promega #A1120) according to the manufacturer's instructions.

Plasmid DNA was extracted from transformed DH5α cells using the GenElute Plasmid Miniprep Kit (Sigma Aldrich #PLN350) or the NucleoBond Xtra Midi Plus Kit (Macherey-Nagel #740412.10) following the manufacturer's recommendations.

2.4.2 Plasmid construction

All primers and plasmids used in this study are detailed in Table 2.2 and Table 2.3, respectively.

SseK1, *sseK2*, and *sseK3* and their upstream promoter regions (200 bp, 200 bp, and 1000 bp, respectively) were amplified from *S*. Typhimurium 12023 genomic DNA (see 2.4.1) by PCR. DNA fragments were purified (QIAquick PCR Purification Kit, Qiagen #28106) and digested with EcoRI (NEB #R0101) and BamHI (NEB #R0136S) for 2 h at 37°C. Subsequently genes were in-gel ligated (1.5% NuSieve GTG agarose, Lonza #50081; T4 ligase system, NEB #M0202T) into pWSK29-2HA (Pruneda et al., 2016) using EcoRI and BamHI restriction sites, which resulted in C-terminal hemagglutinin (HA)- tagged effectors.

For protein expression in mammalian cells, the open reading frames of SseK1, SseK2, and SseK3 were amplified from *S.* Typhimurium 12023 genomic DNA by PCR. N-terminal deletion mutants of SseK3 (ΔN13, ΔN31, ΔN44) were amplified from the m4pGFP-SseK3 plasmid and the neutral N-terminal SseK3 mutant (R4Q/R6Q/L9Q) was created by using a site specific

mutagenesis primer at the 5' end. All amino acid substitutions to alanine (e.g. $SseK_{AAA}$ constructs) were created by using overlap-PCR with site specific mutagenesis primers (Higuchi et al., 1988). SseK1-SseK3 chimeras were created using the same overlap-PCR technique. *NleB* was amplified from genomic DNA from the *E. coli* O157:H7 Sakai strain. Full-length *Fadd*, *Tradd*, *Trim2*, *Trim3* and *Trim32* were amplified from murine cDNA. Mutant $FADD_{R117A}$ and $TRADD_{R233A}$ were created by overlap-PCR. Human *XIAP* was digested from the plasmid m6pPAC-FLAG-XIAP (T. Thurston). Human *IRAK1* and *IRAK4* were digested from plasmids from F. Randow. Murine *Piasy* was amplified from the commercial plasmid pCMV6-PIASy (Origene). PCR template for human dominant negative (DN) *IκB* (S32A/S36A) was a gift from F. Randow. The *Renilla* luciferase gene was amplified from the plasmid pRLTK (Promega) and ligated into m6pPAC (NcoI-NotI) without a tag. After PCR amplification DNA fragments were purified (QIAquick PCR Purification Kit, Qiagen #28106) and digested with PciI (NEB #R0655) and NotI (NEB #R0189) for 2 h at 37°C. For genes containing internal PciI or NotI restriction sites, NcoI (NEB #R0193), BsaI (NEB #R0535S) or BsmBI (NEB #R0580) were used. The genes were ligated into the mammalian expression plasmid m4pGFP or m6pPAC-FLAG (both gifts from F. Randow). The ptCMV-GFP and ptCMV-FLAG plasmids (T. Thurston) are a derivative from the pEGFP-N1 plasmid (Clontech). PCR fragments were ligated into the mentioned plasmids that were digested with PciI and NotI restriction enzymes resulting in an N-terminal GFP or FLAG-tag, respectively.

For protein purification full-length s*seK1*, *nleB* and *Trim32* PCR fragments were ligated into petM30 or petM41 using the plasmids NcoI and NotI restriction sites in the multiple cloning site. This resulted in N-terminally tagged His- Glutathione S-transferase (GST) or His- maltose-binding protein (MBP) fusion proteins, respectively.

All plasmids were checked by sequencing (GATC).

Table 2.2. **Synthetic DNA oligonucleotides used for plasmid cloning and sequencing**

Internal ID	Use		Species	5’ to 3’ nucleotide sequence
Cloning primers				
Trx-299 F	200 bp-SseK1	FW	*S.* Typhimurium 12023	CGCGGGGAATTCAAATATGATGCCATTTCTGG
Trx-300 R	200 bp-SseK1	REV	*S.* Typhimurium 12023	CGCGGGGGATCCCTGCACATGCCTCGCCCATG
Trx-301 F	200 bp-SseK2	FW	*S.* Typhimurium 12023	CGCGGGGAATTCAATGGGCGCTTAGGTTTAGAG
Trx-302 R	200 bp-SseK2	REV	*S.* Typhimurium 12023	CGCGGGGGATCCCCTCCAAGAACTGGCAGTTA
Trx-339 F	1000 bp-SseK3	FW	*S.* Typhimurium 12023	CGCGGGGAATTCCACAGCAATTAATCTTCTGCCCG
Trx-304 R	1000 bp-SseK3	REV	*S.* Typhimurium 12023	CGCGGGGGATCCTCTCCAGGAGCTGATAGTCAAAC
Trx-187 F	SseK1	FW	*S.* Typhimurium 12023	CGCGGGACATGTCA ATGATCCCACCATTAAATAG
Trx-188 R	SseK1	REV	*S.* Typhimurium 12023	CGCGGGGCGGCCGCCTACTGCACATGCCTCGCCCATG
RGO-083 F	SseK1$_{AAA}$	FW	*S.* Typhimurium 12023	ATAGTGGGTGTATATATCTTGCTGCTGCTATGATTATCACGGAAAAACT
RGO-084 R	SseK1$_{AAA}$	REV	*S.* Typhimurium 12023	AGTTTTTCCGTGATAATCATAGCAGCAGCAAGATATATACACCCACTAT
Trx-189 F	SseK2	FW	*S.* Typhimurium 12023	CGCGGGACATGTCAATGGCACGTTTTAATGCCGC
Trx-190 R	SseK2	REV	*S.* Typhimurium 12023	CGCGGGGCGGCCGCTTACCTCCAAGAACTGGCAG
RGO-085 F	SseK2$_{AAA}$	FW	*S.* Typhimurium 12023	GCGGTGGGTGCATATATCTTGCTGCTGCTATGTTACTTACTGATAAACT
RGO-086 R	SseK2$_{AAA}$	REV	*S.* Typhimurium 12023	AGTTTATCAGTAAGTAACATAGCAGCAGCAAGATATATGCACCCACCGC
Trx-197 F	SseK3	FW	*S.* Typhimurium 12023	CGCGGGCCATGGCAATGTTTTCTCGAGTCAGAGGTTTTC
Trx-198 R	SseK3	REV	*S.* Typhimurium 12023	CGCGGG GCGGCCGCTTATCTCCAGGAGCTGATAGTC
Trx-355 F	SseK3$_{AAA}$	FW	*S.* Typhimurium 12023	GGTGGCTGCATATATCTTGCTGCTGCTATGTTACTTACAGGTAAAC
Trx-356 R	SseK3$_{AAA}$	REV	*S.* Typhimurium 12023	GTTTACCTGTAAGTAACATAGCAGCAGCAAGATATATGCAGCCACC

Internal ID	Use		Species	5’ to 3’ nucleotide sequence
Trx-391 F	SseK3$_{\Delta N13}$	FW	*S.* Typhimurium 12023	CGCGGGCCATGGCATATTCTCATACTGCAACTCC
Trx-392 F	SseK3$_{\Delta N31}$	FW	*S.* Typhimurium 12023	CGCGGGCCATGGCATTTGCCGGAGTTGAATATCC
Trx-383 F	SseK3$_{\Delta N44}$	FW	*S.* Typhimurium 12023	CGCGGGCCATGGCACACACCCCCCTACTTTTTCAA
Trx-381 F	SseK3$_{N44}$	FW	*S.* Typhimurium 12023	CGCGGGACATGTCAATGTTTTCTCGAGTCAGAGGTTTTC
Trx-382 R	SseK3$_{N44}$	REV	*S.* Typhimurium 12023	CGCGGG GCGGCCGCTTACTGATCTAATGGCAATAAAGG
RGO-023 F	SseK3$_{31\text{-}34AAA}$	FW	*S.* Typhimurium 12023	CTTCATCAGGTAGTGCAAACGCTGCCGCAGTTGAATATCCTTTATTGCC
RGO-024 R	SseK3$_{31\text{-}34AAA}$	REV	*S.* Typhimurium 12023	GGCAATAAAGGATATTCAACTGCGGCAGCGTTTGCACTACCTGATGAAG
RGO-025 F	SseK3$_{35\text{-}37AAA}$	FW	*S.* Typhimurium 12023	GTAGTGCAAACTTTGCCGGAGCTGCCGCACCTTTATTGCCATTAGATCA
RGO-026 R	SseK3$_{35\text{-}37AAA}$	REV	*S.* Typhimurium 12023	TGATCTAATGGCAATAAAGGTGCGGCAGCTCCGGCAAAGTTTGCACTAC
RGO-027 F	SseK3$_{38\text{-}41AAA}$	FW	*S.* Typhimurium 12023	ACTTTGCCGGAGTTGAATATGCTGCCGCAGCGTTAGATCAGCACACCCCCCT
RGO-028 R	SseK3$_{38\text{-}41AAA}$	REV	*S.* Typhimurium 12023	AGGGGGGTGTGCTGATCTAACGCTGCGGCAGCATATTCAACTCCGGCAAAGT
RGO-029 F	SseK3$_{42\text{-}44AAA}$	FW	*S.* Typhimurium 12023	TTGAATATCCTTTATTGCCAGCTGCCGCACACACCCCCCTACTTTTTCA
RGO-030 R	SseK3$_{42\text{-}44AAA}$	REV	*S.* Typhimurium 12023	TGAAAAAGTAGGGGGGTGTGTGCGGCAGCTGGCAATAAAGGATATTCAA
RGO-031 F	SseK3$_{N13}$:K1$_{\Delta N12}$	FW	*S.* Typhimurium 12023	GTTTTCTTTCATGCCAGAACAAAAATGAATTGGTTAAAAC
RGO-032 R	SseK3$_{N13}$:K1$_{\Delta N12}$	REV	*S.* Typhimurium 12023	GTTTTAACCAATTCATTTTTGTTCTGGCATGAAAGAAAAC
RGO-033 F	SseK3$_{N31}$:K1$_{\Delta N30}$	FW	*S.* Typhimurium 12023	CTTCATCAGGTAGTGCAAACTTTAATGGAAAAGATTATCC
RGO-034 R	SseK3$_{N31}$:K1$_{\Delta N30}$	REV	*S.* Typhimurium 12023	GGATAATCTTTTCCATTAAAGTTTGCACTACCTGATGAAG
RGO-035 F	SseK3$_{N44}$:K1$_{\Delta N43}$	FW	*S.* Typhimurium 12023	CTTTATTGCCATTAGATCAGAAAACCCCTCTTCTTTTCCA
RGO-036 R	SseK3$_{N44}$:K1$_{\Delta N43}$	REV	*S.* Typhimurium 12023	TGGAAAAGAAGAGGGGTTTTCTGATCTAATGGCAATAAAG

Internal ID	Use		Species	5’ to 3’ nucleotide sequence
RGO-255 F	$SseK3_{Neutral}$	FW	*S.* Typhimurium 12023	CCGCGGGCCATGGCAATGTTTTCTCAAGTCCAAGGTTTTCAATCATGC
Trx-353 F	NleB	FW	*E.coli* O157:H7 Sakai	CGCGGGACATGTCCATGTTATCTTCATTAAATGTC
Trx-354 R	NleB	REV	*E.coli* O157:H7 Sakai	CGCGGGGCGGCCGCTTACCATGAACTGCTGG
Trx-390* F	FADD	FW	*Mus musculus*	CGCGGGACATGTCCATGGACCCATTCCTGGTGCTG
Trx-254 R	FADD	REV	*Mus musculus*	CGCGGGGCGGCCGCTCAGGGTGTTTCTGAGGAAGAC
RGO-192 F	$FADD_{R117A}$	FW	*Mus musculus*	CTGGAAAAGACTGGCCGCCGAGCTGAAGGTGTC
RGO-193 R	$FADD_{R117A}$	REV	*Mus musculus*	GACACCTTCAGCTCGGCGGCCAGTCTTTTCCAG
RGO-108 F	TRADD	FW	*Mus musculus*	CGCGGGACATGTCCATGGCAGCCGGTCAGAATGG
RGO-155 R	TRADD	REV	*Mus musculus*	CGCGGGCGTCTCCGGCCGTTAGGCCAGGCCGCCATCCG
RGO-194 F	$TRADD_{R233A}$	FW	*Mus musculus*	CTCAAGTGGCGCAGGGTGGGGGCCTCGCTGCAGCGTAACTGTCG
RGO-195 R	$TRADD_{R233A}$	REV	*Mus musculus*	CGACAGTTACGCTGCAGCGAGGCCCCCACCCTGCGCCACTTGAG
Trx-321 F	TRIM2	FW	*Mus musculus*	CGCGGGACATGTCC ATGGCCAGTGAGGGCGCCAGCATC
Trx-322 R	TRIM2	REV	*Mus musculus*	CGCGGGGCGGCCGCTTACTGTAAGTACCGGTAGACC
Trx-323 F	TRIM3	FW	*Mus musculus*	CGCGGGACATGTCCATGGCAAAGAGGGAGGACAGCCC
Trx-324 R	TRIM3	REV	*Mus musculus*	CGCGGGGCGGCCGCCTACTGGAGGTATCGATAGGC
Trx-294 F	TRIM32	FW	*Mus musculus*	CGCGGGACATGTCCATGGCTGCGGCTGCAGCAGCTTC
Trx-295 R	TRIM32	REV	*Mus musculus*	CGCGGGGCGGCCGCTTAAGGGGTGGAATATCTTCTCAG
Trx-401	PIASγ	FW	*Mus musculus*	CGCGGGACATGTCCATGGCGGCAGAGCTGGTGGAG
Trx-402	PIASγ	REV	*Mus musculus*	CGCGGG GCGGCCGCTCAGCACGCGGGCACCAGGCC

Internal ID	Use		Species	5’ to 3’ nucleotide sequence
Trx-409	XIAP	FW	*Mus musculus*	CGCGGGACATGTCCATGACTTTTAACAGTTTTGAA
Trx-410	XIAP	REV	*Mus musculus*	CGCGGGGCGGCCGCCTAAGACATAAAAATTTTTTGC
RGO-186 F	DN IκBα	FW	*Homo sapiens*	CGCGGGACATGTCCATGTTCCAGGCGGCCGAGCGCCCCCAGGAGTGGGC
RGO-187 R	DN IκBα	REV	*Homo sapiens*	CGCGGGGCGGCCGCTCATAACGTCAGACGCTGGCCTCCAAACACACAGT
RGO-037 F	RLuc	FW		CGCGGGCCATGGCAATGACTTCGAAAGTTTATGA
RGO-038 R	RLuc	REV		CGCGGGGCGGCCGCTTATTGTTCATTTTTGAGAA
Seuencing				
M13F	pWSK29	FW		GTTTTCCCAGTCACGAC
M13R	pWSK29	REV		CAGGAAACAGCTATGAC
Trx-12	m4pGFP ptCMV-GFP	FW		TCAAGATCCGCCACAACATCG
Flx-211	m4pGFP	REV		CTGGTGATATTGTTGAGTCA
Trx-47	ptCMV-GFP ptCMV-FLAG	REV		GGTTCAGGGGGAGGTGTGGG
Trx-46	ptCMV-FLAG	FW		CAAATGGGCGGTAGGCGTG
Flx-190	m6pPAC-FLAG	FW		tagacggcatcgcagcttgga
Flx-561	m6pPAC-FLAG	REV		ACGCACACCGGCCTTATTCCA

Table 2.3. **Plasmids used in this study**

Internal ID	Trivial Name	Description	AB^R	Source or Reference
	pFPV25.1	*rpsM::gfpmut3a* promoter fusion in pFPV	Carb^R	(Valdivia and Falkow, 1996)
	pFCcGi	*rpsM::mCherry* and *PBAD::gfpmut3a* promoter fusions in pFPV25	Carb^R	(Helaine et al., 2010)
	pWSK29-SseL-2HA (pSseL)	pWSK29 containing C-terminal 2HA-tagged SseL with 300 bp endogenous promoter	Carb^R	(Pruneda et al., 2016)
pRG-29	pWSK29-Empty (pE)	pWSK29 empty control plasmid	Carb^R	(Wang and Kushner, 1991)
T-298.2	pWSK29-SseK1-HA (pSseK1)	pWSK29 containing C-terminal 2HA-tagged SseK1 with 200 bp	Carb^R	(Günster et al., 2017)
pRG-54.3	pWSK29-SseK1$_{AAA}$-HA (pSseK1AAA)	pWSK29 containing C-terminal 2HA-tagged SseK1 mutant DAD$_{223-225}$ mutated to AAA with 200 bp endogenous promoter	Carb^R	This study
T-299.1	pWSK29-SseK2-HA (pSseK2)	pWSK29 containing C-terminal 2HA-tagged SseK2 with 200bp endogenous promoter	Carb^R	(Günster et al., 2017)
pRG-56.3	pWSK29-SseK2$_{AAA}$-HA (pSseK2AAA)	pWSK29 containing C-terminal 2HA-tagged SseK2 mutant DAD$_{239-241}$ mutated to AAA with 200 bp endogenous promoter	Carb^R	This study
T-277.6	pWSK29-SseK3-HA (pSseK3)	pWSK29 containing C-terminal 2HA-tagged SseK3 with 1000 bp endogenous promoter	Carb^R	(Günster et al., 2017)
pRG-47.10	pWSK29-SseK3$_{AAA}$-HA (pSseK3AAA)	pWSK29 containing C-terminal 2HA-tagged SseK3 mutant DAD$_{226-228}$ mutated to AAA with 1000 bp endogenous promoter	Carb^R	This study
	pEGFP-N1	GFP control plasmid	Kan^R	Clontech
T-322	ptCMV-GFP-SseK1	SseK1 with N-terminal GFP-tag	Kan^R	(Günster et al., 2017)
pRG-79.1	ptCMV-GFP-SseK1$_{AAA}$	SseK1 mutant DAD$_{223-225}$ mutated to AAA with N-terminal GFP-tag	Kan^R	(Günster et al., 2017)

Internal ID	Trivial Name	Description	AB^R	Source or Reference
pRG-89.1	ptCMV-GFP-SseK2	SseK2 with N-terminal GFP-tag	Kan^R	(Günster et al., 2017)
pRG-82.1	ptCMV-GFP-SseK2$_{AAA}$	SseK2 mutant DAD$_{239-241}$ mutated to AAA with N-terminal GFP-tag	Kan^R	(Günster et al., 2017)
T-324	ptCMV-GFP-SseK3	SseK3 with N-terminal GFP-tag	Kan^R	(Günster et al., 2017)
T-325	ptCMV-GFP-SseK3$_{AAA}$	SseK3 mutant DAD$_{226-228}$ mutated to AAA with N-terminal GFP-tag	Kan^R	(Günster et al., 2017)
pRG-146.1	ptCMV-GFP-SseK3$_{\Delta N13}$	SseK3 truncation aa14-335 with N-terminal GFP-tag	Kan^R	This study
pRG-133.2	ptCMV-GFP-SseK3$_{\Delta N31}$	SseK3 truncation aa32-335 with N-terminal GFP-tag	Kan^R	This study
pRG-147.2	ptCMV-GFP-SseK3$_{\Delta N44}$	SseK3 truncation aa45-335 with N-terminal GFP-tag	Kan^R	This study
pRG-141.1	ptCMV-GFP-SseK3$_{Neutral}$	SseK3 mutant R4Q/R6Q/L9Q with N-terminal GFP-tag	Kan^R	This study
pRG-90.1	ptCMV-GFP-NleB	NleB with N-terminal GFP-tag	Kan^R	(Günster et al., 2017)
pRG-101.5	ptCMV-GFP-DN IκBα	Dominant negative human IκBα (S32A/ S36A) with N-terminal GFP-tag	Kan^R	(Günster et al., 2017)
T-282	ptCMV-FLAG-SseK3	SseK3 with N-terminal FLAG-tag	Kan^R	T. Thurston
T-281	ptCMV-FLAG-TRIM2	Murine TRIM2 with N-terminal FLAG-tag	Kan^R	T. Thurston
T-280	ptCMV-FLAG-TRIM3	Murine TRIM3 with N-terminal FLAG-tag	Kan^R	T. Thurston
T-263.3	ptCMV-FLAG-TRIM32	Murine TRIM32 with N-terminal FLAG-tag	Kan^R	T. Thurston
pRG-001	ptCMV-FLAG-DN IκBα	Dominant negative human IκBα (S32A/ S36A) with N-terminal FLAG-tag	Kan^R	This study
pRG-002	pRLTK	Constitutively active Renilla luciferase	Carb^R	F. Randow
T-295.2	p4κB:Luc	*luc* gene under control of NF-κB consensus promoter	Carb^R	F. Randow

Internal ID	Trivial Name	Description	AB^R	Source or Reference
T-294.2	pISRE	*luc* gene under control of ISRE consensus promoter	Carb^R	F. Randow
pRG-140.1	m3psinrevκB-*luc*	*luc* gene under control of NF-κB consensus promoter	Carb^R	F. Randow
pRG-015.5	m6pPAC-RLuc	Constitutively active Renilla luciferase for macrophage transduction	Carb^R	(Günster et al., 2017)
pRG-016.6	pEAKMMP-AU1-TLR4	Human TLR4 for NF-κB pathway activation	Carb^R	F. Randow
pRG-017.1	m4pGFP-SseK1	SseK1 with N-terminal GFP-tag	Carb^R	(Günster et al., 2017)
pRG-018.1	m4pGFP-SseK1$_{AAA}$	SseK1 mutant DAD$_{223-225}$ mutated to AAA with N-terminal GFP-tag	Carb^R	This study
pRG-019.8	m4pGFP-SseK2	SseK2 with N-terminal GFP-tag	Carb^R	T. Thurston
pRG-020.4	m4pGFP-SseK2$_{AAA}$	SseK2 mutant DAD$_{239-241}$ mutated to AAA with N-terminal GFP-tag	Carb^R	This study
pRG-021.6	m4pGFP-SseK3	SseK3 with N-terminal GFP-tag	Carb^R	(Günster et al., 2017)
T-263.3	m4pGFP-SseK3$_{AAA}$	SseK3 mutant DAD$_{226-228}$ mutated to AAA with N-terminal GFP-	Carb^R	This study
pRG-001	m4pGFP-SseK3$_{\Delta N13}$	SseK3 truncation aa14-335 with N-terminal GFP-tag	Carb^R	This study
pRG-002	m4pGFP-SseK3$_{\Delta N31}$	SseK3 truncation aa32-335 with N-terminal GFP-tag	Carb^R	This study
T-295.2	m4pGFP-SseK3$_{\Delta N44}$	SseK3 truncation aa45-335 with N-terminal GFP-tag	Carb^R	This study
T-294.2	m4pGFP-SseK3$_{N44}$	SseK3 truncation aa1-44 with N-terminal GFP-tag	Carb^R	This study
pRG-140.1	m4pGFP-SseK3$_{Neutral}$	SseK3 mutant R4Q/R6Q/L9Q with N-terminal GFP-tag	Carb^R	This study
pRG-015.5	m4pGFP-SseK3$_{32-34AAA}$	SseK3 mutant FAG$_{32-34}$ mutated to AAA with N-terminal GFP-tag	Carb^R	This study
pRG-016.6	m4pGFP-SseK3$_{35-37AAA}$	SseK3 mutant VEY$_{35-37}$ mutated to AAA with N-terminal GFP-tag	Carb^R	This study

Internal ID	Trivial Name	Description	AB^R	Source or Reference
pRG-017.1	m4pGFP-SseK3$_{38\text{-}41AAA}$	SseK3 mutant PLLP$_{38\text{-}41}$ mutated to AAA with N-terminal GFP-tag	Carb^R	This study
pRG-018.1	m4pGFP-SseK3$_{42\text{-}44AAA}$	SseK3 mutant LDQ$_{42\text{-}44}$ mutated to AAA with N-terminal GFP-tag	Carb^R	This study
pRG-019.8	m4pGFP-SseK3$_{N13}$:K1$_{\Delta N12}$	SseK3$_{1\text{-}13}$:SseK1$_{13\text{-}336}$ chimera with N-terminal GFP-tag	Carb^R	This study
pRG-020.4	m4pGFP-SseK3$_{N31}$:K1$_{\Delta N30}$	SseK3$_{1\text{-}31}$:SseK1$_{31\text{-}336}$ chimera with N-terminal GFP-tag	Carb^R	This study
pRG-021.6	m4pGFP-SseK3$_{N44}$:K1$_{\Delta N43}$	SseK3$_{1\text{-}44}$:SseK1$_{44\text{-}336}$ chimera with N-terminal GFP-tag	Carb^R	This study
T-264.12	m4pGFP-NleB	NleB with N-terminal GFP-tag	Carb^R	(Günster et al., 2017)
T-333	m4pGFP-FADD	Murine FADD with N-terminal GFP-tag	Carb^R	(Günster et al., 2017)
pRG-65.3	m4pGFP-TRADD	Murine TRADD with N-terminal GFP-tag	Carb^R	(Günster et al., 2017)
pRG-32.1	m4pGFP-IRAK1	Human IRAK1 with N-terminal GFP-tag	Carb^R	This study
pRG-26.3	m4pGFP-IRAK4	Human IRAK4 with N-terminal GFP-tag	Carb^R	This study
T-003	m4pGFP-STING	Human STING with N-terminal GFP-tag	Carb^R	T. Thurston
pRG-44.2	m4pGFP-PIASγ	Murine PIASγ with N-terminal GFP-tag	Carb^R	This study
pRG-25.1	m4pGFP-XIAP	Murine XIAP with N-terminal GFP-tag	Carb^R	This study
pRG-009	m4pGFP-TRIM2	Murine TRIM2 with N-terminal GFP-tag	Carb^R	This study
T-253	m4pGFP-TRIM32	Murine TRIM32 with N-terminal GFP-tag	Carb^R	T. Thurston
T-052	m6pPAC-FLAG-GFP	GFP control plasmid	Carb^R	(Günster et al., 2017)
T-334	m6pPAC-FLAG-FADD	Murine FADD with N-terminal FLAG-tag	Carb^R	(Günster et al., 2017)

Internal ID	Trivial Name	Description	AB^R	Source or Reference
pRG-110.9	m6pPAC-FLAG-FADD$_{R117A}$	Murine FADD with R_{117} mutated to A with N-terminal FLAG-tag	Carb^R	(Günster et al., 2017)
pRG-66.3	m6pPAC-FLAG-TRADD	Murine TRADD with N-terminal FLAG-tag	Carb^R	(Günster et al., 2017)
pRG-112.14	m6pPAC-FLAG-	Murine TRADD with R_{233} mutated to A with N-terminal FLAG-	Carb^R	(Günster et al., 2017)
T-258.4	m6pPAC-FLAG-TRIM2	Murine TRIM2 with N-terminal FLAG-tag	Carb^R	T. Thurston
T-244	m6pPAC-FLAG-TRIM32	Murine TRIM32 with N-terminal FLAG-tag	Carb^R	(Günster et al., 2017)
	pMW172-GST-3C	GST control plasmid	Kan^R	C. Durkin
T-272	petM30-GST-SseK1	SseK1 with N-terminal 6xHis-GST-tag	Kan^R	T. Thurston
T-273	petM30-GST-SseK3	SseK3 with N-terminal 6xHis-GST-tag	Kan^R	T. Thurston
T-271	petM41-MBP-TRIM32	Murine TRIM32 with N-terminal 6xHis-MBP-tag	Kan^R	T. Thurston

2.4.3 RNA isolation

Total RNA was isolated from ~1x 10^6 murine splenic CD11b positive cells using the RNeasy Mini Kit (Qiagen #74104) according to the manufacturer's recommendation. Afterwards RNA was either used immediately for cDNA synthesis or stored at -80°C.

2.4.4 Reverse transcription (cDNA synthesis)

400 ng of total RNA per sample was used to prepare cDNA using the QuantiTect Reverse Transcription Kit (Qiagen #205311). Importantly this procedure included a genomic DNA wipe-out step to avoid contamination of the cDNA by residual genomic DNA.

2.4.5 Quantitative PCR

Quantitative PCR (qPCR, SYBR Green PCR Master Mix, Life technologies #4309155) was performed using 0.5 µl cDNA and 0.2 µM gene-specific primers (Table 2.4). Primers were selected to generate an amplicon across different exons and their specificity was confirmed using Primer-BLAST (NCBI). A Rotor-Gene 3000 (Corbett Research) PCR cycler was used to acquire emission data and a significant cycle threshold (cT) value from the SYBR Green reporter dye. All samples were analysed in technical duplicates. Relative mRNA amounts were calculated from a titration curve of cDNA and were normalised to the expression of the Rps9 housekeeping gene.

Table 2.4. **Gene-specific qPCR primers**

Internal ID	Use		Species	5' to 3' nucleotide sequence
RGO-130 qF	*Il-6*	FW	*Mus musculus*	AGACAAAGCCAGAGTCCTTCAG
RGO-131 qR	*Il-6*	REV	*Mus musculus*	GGTCTTGGTCCTTAGCCACTC
RGO-132 qF	*Tnfα*	FW	*Mus musculus*	GATCGGTCCCCAAAGGGATG
RGO-133 qR	*Tnfα*	REV	*Mus musculus*	GTTTGCTACGACGTGGGCTA
RGO-134 qF	*Irf7*	FW	*Mus musculus*	AAGGTGTACGAACTTAGCCG
RGO-135 qR	*Irf7*	REV	*Mus musculus*	GGTTTGGAGCCCAGCATTTTC
Trx-395	*Ifnβ*	FW	*Mus musculus*	GCAGCTGAATGGAAAGATCA
Trx-396	*Ifnβ*	REV	*Mus musculus*	TGGCAAAGGCAGTGTAACTC
RGO-138 qF	*Rps9*	FW	*Mus musculus*	AACAAACGTGAGGTTTGGAGG
RGO-139 qR	*Rps9*	REV	*Mus musculus*	GTCCAGCACCCCAATGCGAA

2.5 Cell biology techniques

2.5.1 Cell culture and seeding

RAW 264.7 macrophages and HeLa cells were obtained from the European Collection of Animal and Cell Cultures (Salisbury, UK). 293ET cells were a gift from Felix Randow. Cells lines were cultured in Dulbecco's modified Eagle's medium (DMEM; Sigma #D5796) supplemented with 10% fetal calf serum (FCS; Sigma/Invitrogen) in 5% CO_2 at 37°C. Stably transduced RAW 264.7 cells and CRISPR generated TRIM32 knock-out cells (generated by T. Thuston (Günster et al., 2017)) were cultured and seeded as specified for wild-type RAW 264.7 macrophages.

24 hours prior to use (infection or transfection) cells were seeded at the following densities:

RAW 264.7 macrophages: 3 x 10^4 cells/well (96-well plate), 1 x 10^5 cells/well (24-well plate), 3 x 10^5 cells/well (12-well plate), 6 x10^5 cells/well (6-well plate) or 1 x 10^7 cells per 15 cm ∅ dish

293ET cells: 5 x 10^4 cells/well (24-well plate), 4 x10^5 cells/well (6-well plate)

HeLa cells: 5 x 10^4 cells/well (24-well plate), 3 x 10^5 cells/well (6-well plate)

2.5.2 *In vitro* infection of mammalian cells

For the infection of phagocytic RAW 264.7 macrophages stationary-phase *Salmonella* cultures were opsonised in DMEM with 10% mouse serum for 20 min. Infection was carried out with an approximate multiplicity of infection (MOI) of 10:1 and was synchronised by centrifugation for 5 min at 110 x g followed by incubation for 25 min at 37°C. As centrifugation of macrophages infected in 15 cm ∅ dishes was not possible, cells were instead infected with un-opsonised stationary-phase *Salmonella* cultures at an approximate MOI of 30:1 for 30 min at 37°C. For SPI-1-mediated invasion of cells, stationary-phase *Salmonella* cultures were subcultured (1:33) for 3.5 h at 37°C. HeLa cells (6-well plate) were infected with 25 µl of subculture for 15 min. After the intended time of infection cells were washed three times in sterile PBS and extracellular bacteria were killed in medium containing 100 µg/ml gentamicin (Sigma #G9516) for 1 h. Subsequently, the medium was replaced with fresh medium containing 20 µg/ml gentamicin for the remainder of the infection.

2.5.3 Colony forming units assay

To assay bacteria replication by colony forming unit (CFU) assay triplicate wells of RAW 264.7 macrophages were infected for 2, 16 or 20 hours with different *Salmonella* strains in 24-well plates (see 2.5.2). After the indicated time point cells were washed twice with cold PBS and then lysed in 1 ml 0.1% triton X-100 in PBS for 5 min at room temperature. Subsequently, serial dilutions of the released bacteria were plated in technical duplicates on LB agar plates to determine colony forming units.

2.5.4 Generation of stable cell lines

Stable RAW 264.7 macrophage cell lines were created by retroviral transduction as described in (Randow and Sale, 2006). In short, virus containing the m4pGFP plasmid was generated in 293ET cells after transfection with VSVg, pol/gag and proviral plasmids and used to transduce RAW 264.7 cells. To achieve optimal transduction efficiency (approximately 30%) a titration of virus was used. Successfully transduced macrophages were isolated by flow cytometry cell sorting to obtain a homogenous population of GFP-tagged protein expressing cells. NF-κB reporter macrophages were created by simultaneous transduction with retroviruses containing the m3psinrevκB-*luc* or m6pPAC-RLuc plasmid. Subsequently, cells were selected with 1.5 µg/ml puromycin for up to 10 days (Sigma #P8833).

2.5.5 Drug treatment of cells

To inhibit NF-κB signalling in RAW 264.7 macrophages, cells were pre-treated with 1, 5 or 10 µM PS-1145 (Sigma #P6624) or an equal volume of DMSO for 1 h. Subsequently, cells were infected with the indicated *Salmonella* strains (see 2.5.2) for 30 min and maintained in 30 µg/ml gentamicin containing medium for the duration of the experiment (20 h).

To inhibit TNF-α stimulation of cells, RAW 264.7 macrophages were pre-exposed to 10 or 50 µg/ml Etanercept (Enbrel; Pfizer) for 30 min and subsequently infected with the indicated *Salmonella* strains (see 2.5.2). Treatment with the IL1 receptor antagonist Anakinra (Kineret; Sobi) at a concentration of 10 or 50 µg/ml served as a negative control. Exposure of cells to Enbrel and Anakinra was maintained throughout the full duration of the experiments.

2.5.6 Transfection of mammalian cells

293ET and HeLa cells were transfected with Lipofectamine 2000 (Invitrogen #11668019) according to the manufacturer's recommendations. If not stated otherwise plasmid DNA and 1 µl or 3 µl Lipofectamine 2000 reagent (24-well and 6-well plate, respectively) were mixed in Opti-MEM (Invitrogen #11058021) and incubated with cells for 24 h for transfections lasting 24-40 h.

2.5.7 Dual luciferase reporter assay

For transfection reporter assays, 293ET cells were transfected in 24-well plates (see 2.5.6) with a mixture of 20 ng pRLTK, 50 ng reporter plasmid (p4κB or pISRE) and 250 ng ptCMV plasmid. After 24 h cells transfected with the ISRE reporter were stimulated overnight (approximately 17 h) with 1.36x 10^3 U/ml hIFNβ (R&D Systems #11415-1). NF-κB reporter cells were stimulated with 50 ng/ml hTNFα (Sigma #SRP3177), 10 ng/ml hIL-1α (Sigma #I2778), 10 ng/ml hIL-1β (Sigma #I9401) or 4 µg/ml high-molecular-weight (HMW) poly(I:C) (Invitrogen #TLRL-PIC). To mimic LPS stimulation cells were transfected with 300 ng pEAKMMP-AU1-TLR4 (or m6pPAC-FLAG-GFP control) vector in addition to the plasmids described above to auto-activate the NF-κB pathway for 24 h prior to harvesting cell lysates. Luciferase activity was measured using a dual luciferase reporter assay system (Promega) and a Tecan Infinite 200 PRO plate reader. NF-κB-regulated luciferase activity was normalised to Renilla luciferase intensity and the results are presented relative to either wild-type-infected samples, unstimulated, GFP-expressing control samples or each unstimulated control sample.

2.5.8 Lactate dehydrogenase assay

To analyse cell death upon *Salmonella* infection, RAW 264.7 macrophages were infected in a 24-well plate as described in 2.5.2. In short, after 30 min of infection, cells were washed in PBS and extracellular bacteria were killed in 200 µl phenol red-free medium containing 100 µg/ml gentamicin for 1 h. To account for total cell death over the course of infection the medium was then diluted (rather than replaced) to a final concentration of 20 µg/ml gentamicin for the remainder of the infection (2-24 h). To analyse TNF-α-, TRAIL- or FasL-induced cell death, HeLa cells were transfected for 24 h with 250 ng pEGFP-N1 control

or ptCMV-GFP-effector plasmids (24-well plate, see 2.5.6). Cell death was subsequently stimulated with 50 ng/ml hTNF-α (Sigma #SRP3177), 200 ng/ml mTRAIL (Sigma #SRP3237) or 100 ng/ml hFasL (R&D Systems #126-FL) in combination with 10 µg/ml cycloheximide (Sigma #C7698) in phenol red-free medium. After 20 h of drug treatment or infection, the cell supernatant (medium) was collected. To remove cell contamination, samples were centrifuged for 1 min at 3000 x g and the supernatant transferred to a new tube. Extracellular lactate dehydrogenase levels were assayed with the CytoTox 96 nonradioactive cytotoxicity assay kit (Promega #G1780) according to the manufacturer's instructions. Absorbance at 490 nm was measured on a Tecan Infinite 200 Pro plate reader in white, clear bottom 96-well plates. Cell death was calculated relative to that caused by the total cell death control (max) which was achieved by freezing the cells for a minimum of 1 h at -80°C.

2.5.9 Propidium iodide uptake assay

RAW 264.7 macrophages were infected in a 96-well plate as described in 2.5.2 with the following adaptations. After 30 min of infection, cells were washed in PBS and incubated with medium (Opti-MEM, 10% FCS) containing 30 µg/ml gentamicin. Propidium iodide (PI, Life Technologies #P3566) was diluted at 1:1,000 in the medium and uptake was then measured on a Tecan Infinite 200 Pro plate reader (excitation at 530 nm, emission at 617 nm) at 37°C in 5% CO_2 for up to 20 h.p.u.. PI uptake was calculated relative to that of a maximum control obtained by cell lysis with 0.1% triton X-100 and normalised to findings at 2 h.p.u. to account for experimental variation.

2.6 Flow cytometry techniques

2.6.1 Quantification of intracellular replication

RAW 264.7 macrophages were infected with GFP-expressing *Salmonella* strains for 2 h, 16 h, or 20 h (12-well plate, see 2.5.2). At the indicated time cells were washed once with 1 ml of PBS and detached using Accutase (Sigma #A6964) for 15 min at room temperature. Samples were subsequently diluted in Opti-MEM (Invitrogen #11058), and the GFP fluorescence intensity per cell was analyzed using a FACSCalibur flow cytometer (BD

Biosciences). To calculate the fold change in bacterial replication the GFP geometric means (Flowing Software version 2.5.1) at 16 h or 20 h were divided by the 2 h time point value.

2.6.2 Quantification of effector translocation

To assess SseK effector translocation by flow cytometry Raw 264.7 macrophages were infected with different *Salmonella* strains in 6-well plates (see 2.5.2). 16 h after infection, cells were washed in PBS, harvested and fixed in 4% PFA (Sigma #P6148) for 20 min at room temperature. Cells were then washed again in PBS and incubated with primary antibody (Table 2.5) in FACS permeabilisation solution (0.1 % saponin (Fisher #S/0380/48), 2% bovine serum albumin (BSA, Sigma #A4503), PBS) for 30 min at 4°C. Subsequently, cells were washed another two times in permeabilisation solution and incubated with the fluorophore linked secondary antibodies for 30 min at 4°C. Finally cells were washed and resuspended in PBS for analysis on a FACSCalibur flow cytometer (BD Biosciences). The percentage of infected cells positive for HA-effector translocation were analysed using the Flowing Software version 2.5.1.

Table 2.5. **Primary and secondary antibodies used for flow cytometry experiments**

Antibody against	Origin	Manufacturer	Dilution
CSA-1	Goat	BacTrace #01-91-99	1:400
HA (3F10)	Rat	Roche #11867423001	1:200
Goat (Alexa488-linked)	Donkey	Invitrogen #A-11055	1:500
Rat (Alexa555-linked)	Donkey	Abcam #ab150154	1:250

2.6.3 Caspase activity assay

To analyze caspase-3/-7 and caspase-8 activity, RAW 264.7 macrophages were infected with GFP-expressing WT or Δ*sseK1/2/3 Salmonella* for 20 h (6-well plate, see 2.5.2). Caspase activity was assayed using the SR-FLICA Caspase-3/-7 or Caspase-8 assay kit (ImmunoChemistry Technologies # 931, # 9149) according to the manufacturer's instructions. 20 h treatment with 50 µg/ml cycloheximide (Sigma #C7698) and 50 ng/ml TNFα (Sigma #SRP3177) was used to induce caspase activity as a positive control. Data were acquired using a Fortessa flow cytometer (BD Biosciences) and analysed with FlowJo (version 8.8.6). To

account for experimental variation the geometric mean of the SR-FLICA signal intensity in infected (GFP positive) cells was normalised to the geometric mean of uninfected cells in the same sample.

2.7 Microscopy techniques

2.7.1 Immuofluorescence microscopy

For immunofluoresce microscopy 293ET cells were seeded on poly-L-lysine (Sigma #P4707) coated coverslips and were transfected with 250 ng m4pGFP-effector plasmids (see 2.5.6) 24 h prior to use. RAW 264.7 macrophage were infected for 16 h on coverslips in 24-well plates (see 2.5.2). After the desired infection or transfection time cells were washed three times with PBS and fixed with 4% paraformaldehyde (PFA, Sigma #P6148) for 20 min at room temperature. Cells were subsequently washed twice with PBS and the PFA was quenched with 100 mM NH_4Cl (VWR #21236.267) for a minimum of 1 h at 4°C. The cells were labelled with the indicated primary antibodies for 2 h at room temperature, washed three times with PBS and then incubated with the secondary antibodies and 0.5 µg/ml 4-,6-diamidino-2-phenylindole (DAPI, Invitrogen #D3571) for 1 h at room temperature. All antibodies were diluted in PBS, 0.1% (v/v) triton X-100 (or saponin (Fisher # S/0380/48), for the experiment shown in Figure 3.1) and 10% horse serum (Sigma # H1270) and are detailed in Table 2.6. Coverslips were then again washed three times in PBS and mounted using Aqua-Poly/Mount (Polysciences, Inc. #18606) and imaged using an LSM 710 inverted confocal microscope (Zeiss GmbH). For quantitative analysis, at least three independent experiments were performed in technical duplicates, and a minimum of 100 (infected) cells per coverslip were scored on an epifluorescence microscope (BX50; Olympus).

Blind scoring was performed by S. Matthews, T. Thurston and R. Günster to ensure objectivity.

Table 2.6. **Primary and secondary antibodies used for immunofluorescence microscopy**

Antibody against	Origin	Manufacturer	Dilution
Arg-GlcNAc	rabbit	Abcam #ab195033	1:400
CSA-1	goat	BacTrace #01-91-99	1:400
FLAG (M2)	mouse	Sigma #F3165	1:400
GM130	mouse	BD # 610822	1:400
HA (3F10)	rat	Roche #11867423001	1:200
Rab6 (C-19)	rabbit	Santa Cruz #sc-310	1:200
TGN46	rabbit	Life Span #LS-B6874	1:200
Goat (Alexa647-linked)	Donkey	Invitrogen #A-21447	1:500
Mouse (Alexa488-linked)	Donkey	Invitrogen #A-21202	1:500
Mouse (Alexa647-linked)	Donkey	Invitrogen #A-31571	1:500
Rabbit (Alexa488-linked)	Donkey	Invitrogen #A-21206	1:500
Rabbit (Alexa555-linked)	Donkey	Invitrogen #A-31572	1:500
Rat (Alexa555-linked)	Donkey	Abcam #ab150154	1:500

2.7.2 p65 nuclear translocation assay

RAW 264.7 macrophages stably expressing p65-GFP were infected with pFCcGi containing *Salmonella* mutant strains constitutively expressing mCherry (see 2.5.2). After 15 h of infection the cells were further stimulated with 1 µg/ml LPS (Sigma #L6143-1MG) for one hour to synchronise p65 translocation to the nucleus. Cells were then washed with PBS, fixed with 4% PFA (Sigma #P6148) for 20 min at room temperature, washed again and the PFA quenched with 100 mM NH_4Cl (VWR #21236.267) for a minimum of 1 h at 4°C. To stain the nucleus cells were incubated with 0.5 µg/ml DAPI (Invitrogen #D3571) for 5 min at room temperature. After mounting in Aqua-Poly/Mount (Polysciences, Inc. #18606) the coverslips were dried and cells were imaged using an LSM 710 inverted confocal microscope (Zeiss GmbH). For quantitative analysis a minimum of 300 cells per coverslip were blind scored from three independent experiments performed in technical duplicates.

2.8 Protein techniques

2.8.1 Preparation of whole cell lysates and cytoplasmic protein fractions

Mammalian cell lysates were prepared by lysing cells for 30 min in Lumier lysis buffer on ice. If required a whole cell lysate sample was taken after this step. To isolate cytoplasmic proteins the samples were then centrifuged for 30 min at 16,000 x g at 4°C and the postnuclear supernatant (cytoplasmic fraction) was separated from the pellet. Both whole cell lysate and cytoplasmic fraction were analysed by SDS-PAGE and immunoblotting.

Lumiers lysis buffer - 150 mM NaCl (Sigma# S7653), 0.1 or 0.3% triton X-100, 20 mM Tris-Cl pH 7.4 (Sigma # T1503), 5% glycerol, 5 mM EDTA, fresh proteasome inhibitors (1 mM PMSF (Sigma #P7626), 1 mM benzamidine (Sigma # B6506) , 2 µg/ml aprotinin (Sigma # 10820), 5µg/ml leupeptin (Sigma # L0649))

2.8.2 One-dimensional SDS-PAGE

Proteins were separated by SDS-PAGE on 10% polyacrylamide (PAA) gels and gel electrophoresis was carried out for ~1.5 h at 110 V in SDS running buffer. Afterwards, the gel was used for immunoblotting or protein staining.

SDS running buffer - 25 µM Tris base (Sigma # T1503), 250 µM glycine (Sigma #G7126), 0.1% SDS (VWR #442444H)

2.8.3 Western blot

The protein content of the SDS-PAGE gels was transferred onto polyvinylidene difluoride (PVDF) Immobilon-P membranes (Millipore) by electroblotting at constant 15V for 15 to 25 min, using the Trans-Blot Turbo Transfer System (Bio-Rad).

5x Transfer buffer - 29 g Tris base (Sigma # T1503) 14.7 g glycine (Sigma #G7126), 2.88 ml 10% SDS (VWR #442444H) to 1 l with dH_2O

Membranes were blocked in 5% non-fat milk or 5% BSA (Sigma #A4503) in TBST for one hour at room temperature to prevent unspecific antibody binding to the PVDF membrane. Incubation with primary antibodies was performed overnight at 4°C, membranes were then

washed three times for 10 min in TBST and incubated for 2 h with horseradish peroxidase (HRP)-coupled secondary antibodies at room temperature. Again the membrane was washed for 30 min (3x 10 min) in TBST and stained with chemoluminescence detection solution (VWR #RPN2109, Fisher #11517371) to visualise specific protein bands.

All antibodies were diluted in 5% non-fat milk or 5% BSA (Sigma #A4503) in TBST according to the manufacturer's recommendation and are listed in Table 2.7.

Table 2.7. **Primary and secondary antibodies used for western blot analysis**

Antibody against	Origin	Manufacturer	Dilution
actin	Rabbit	Sigma #A2066	1:2000
Arg-GlcNAc	Rabbit	Abcam #ab195033	1:1000
c-myc	Mouse	Roche # 11667149001	1:1000
DnaK (8E2/2)	Mouse	Enzo #ADI-SPA-880-D	1:2000
FLAG	Rabbit	Sigma # F7425	1:2000
FLAG (M2)	Mouse	Sigma #F3165	1:2000
ERK1/2 (p44/p42)	Rabbit	Cell Signaling #9102	1:1000
ERK1/2 (p44/p42) phospho-Thr202/Tyr204	Rabbit	Cell Signaling #4377	1:1000
GFP	Rabbit	Life technologies #G10362	1:2000
GFP (3E1)	Mouse	Gift C. Durkin	1:2000
HA.11	Mouse	Covance #MMS-101P	1:2000
IκBα	Mouse	Cell Signaling #4814	1:1000
IκBα phospho-Ser32	Rabbit	Cell Signaling #2859	1:1000
IKKα	Rabbit	Cell Signaling #2682	1:1000
IKKα/β phospho-Ser176/180	Rabbit	Cell Signaling #2697	1:1000
MLKL	Rabbit	Sigma # SAB1302339	1:1000
MLKL phospho-S345	Rabbit	Abcam #196439	1:1000
MAPK p38	Rabbit	Cell Signaling #9212	1:1000
MAPK p38 phospho-Thr180/Tyr182	Mouse	Cell Signaling #9216	1:1000
SAPK/JNK	Rabbit	Cell Signaling #9252	1:1000

Antibody against	Origin	Manufacturer	Dilution
SAPK/JNK phospho-Thr183/Tyr185	Mouse	Cell Signaling #9255	1:1000
TRIM32	Rabbit	Abcam #ab96612	1:1000
β-tubulin (EPR16774)	Rabbit	Abcam #ab179513	1:2000
Mouse (HRP-linked)	Goat	Dako #P0447	1:5000
Rabbit (HRP-linked)	Goat	Dako #P0448	1:5000
Rabbit (HRP-linked)	Goat	Santa Cruz #sc-2004	1:5000

2.8.4 Coomassie staining

After sample separation by SDS-PAGE (see 2.8.2), proteins were stained in the PAA gel using PageBlue Protein Staining Solution (Thermo Fisher #24620) according to the manufacturer's recommendation.

2.8.5 Protein molecular weight determination

To determine the molecular weight of arginine-GlcNAcylated proteins, cytoplasmic fraction of infected RAW 264.7 macrophages were separated by SDS-PAGE and analysed by immunoblotting. The migration distance of the protein standards (GeneFlow #S6-0024) and the unknown proteins were measured in Icy (de Chaumont et al., 2012) using the software's Ruler Helper plug-in. The relative migration distance (R_f) of each protein was calculated as its migration distance divided by the migration distance of the dye front. The plot between R_f versus log molecular weight of the marker proteins was then used to calculate the approximate molecular weight of the unknown proteins based on their R_f.

2.8.6 *In vitro* protein expression, purification and interaction experiments

To express and purify recombinant proteins, BL21 (DE3) *E. coli* carrying petM plasmids were grown overnight to stationary phase and then diluted 1:200 into 1 l fresh LB medium for 3 h growth at 37°C with 200 rpm shaking. Cultures were subsequently cooled on ice and induced with 0.1 mM IPTG (Merck #420322) for growth over night at 16°C. Bacteria were then collected by centrifugation at (4000 x g, 20 min, 4°C) and the pellet snap frozen in liquid

nitrogen. Bacteria were afterwards resuspended in 25 ml 2x GST protein lysis buffer and lysed by sonication (4x 30 sec, max power) on ice. Lysates were then centrifuged at 16,000 rpm for 45 min at 4°C, supernatants removed to new tubes and stored at -80°C after snap freezing in liquid nitrogen.

For *in vitro* interaction of purified proteins one milliliter lysate (soluble fraction) containing MBP- or GST-tagged proteins was incubated with 25 µl Amylose resin (NEB #E8021S) or 25 µl Glutathione sepharose beads (GE #17-5278-01), respectively, for 2 h at 4°C. Beads were then washed 3 times with protein lysis buffer and MBP-TRIM32 eluted with 10 mM maltose (Sigma # M5885) in 400 µl TBS for 20 min at 4°C. The recovered MBP-TRIM32 was added to the Glutathione sepharose beads bound with GST or GST-SseK for 2 h of incubation at 4°C. Bound proteins were subsequently eluted with 10 mM glutathione (Sigma # G4251) in 50 µl TBS pH 8 for 20 min at room temperature and analysed by SDS-PAGE and coomassie staining.

2x GST protein lysis buffer - 50 mM Tris-Cl pH 7.4, 300 mM NaCl, 2 mM EDTA, 10% glycerol, 2 mM DTT (Sigma # D9779), 2 x cOmplete™ EDTA-free Protease Inhibitor Cocktail tablets (Roche # 11873580001), 1 mg/ml lysozyme (Sigma # L6876)

2.9 Specific biochemical techniques

2.9.1 Protein half-life determination

To determine the half-life of SseK3, 293ET cells were transfected with 500 ng m6pPAC-FLAG plasmids using Lipofectamine 2000 (6-well format, see 2.5.6). After 24 h, protein synthesis was inhibited with 50 µg/ml cycloheximide (Sigma #C7698) and the post nuclear supernatant isolated after 1, 2, 4, 8, 12 and 24 h of drug treatment (see 2.8.1). Samples were analysed by SDS-PAGE and western blot (see 2.8.2 and 2.8.3).

2.9.2 Immunoprecipitation experiments

For transfection immunoprecipitation experiments 293ET cells were seeded in 6-well plates. If not specified otherwise 1 µg m6pPAC-FLAG, 1 µg m4pGFP or 200 ng ptCMV-GFP-SseK2 plasmid were used for Lipofectamine transfection (see 2.5.6) according to the

manufacturer's instructions. After 40 h, cells were harvested and lysed in 400 µl Lumier lysis buffer (containing 0.3% triton X-100), and the cytoplasmic fraction was isolated (see 2.8.1). Proteins were immunoprecipitated using 3-5 µl α-GFP Trap_A beads (ChromoTek #gta-20) or 20 µl α-FLAG M2 affinity gel (Sigma #A2220) for 2 h at 4°C. Beads were subsequently washed 3-4 times in lysis buffer (containing 0.1% triton X-100) and the bound proteins eluted by boiling the beads for 5 min at 95°C in final sample buffer (FSB). Finally samples were analyzed by SDS-PAGE and immunoblotting.

For the transfection-infection immunoprecipitation experiments HeLa cells were first transfected with 1 µg of the indicated m6pPAC-FLAG-GFP or m4pGFP plasmids in a 6-well format (see 2.5.6). After 24 h, cells were infected for 16 h with various *Salmonella* strains (see 2.5.2). GFP-tagged proteins were then isolated, immunoprecipitated and analysed as described above.

For infection α-HA immunoprecipitation experiments, RAW 264.7 cells were infected for 16 h in 15 cm ∅ dishes (see 2.5.2). As a standard, two dishes were used per *Salmonella* infection. Proteins were isolated as described 2.8.1. in 1 ml Lumiers lysis buffer (containing 0.3% triton X-100) and 20 µl of α-HA agarose (Pierce #26181) was used to immunoprecipitate proteins for 2 h at 4°C. Beads were then washed 3-4 times in lysis buffer (containing 0.1% triton X-100). For analysis by SDS-PAGE and immunoblotting bound proteins were eluted from the beads by boiling for 5 min at 95°C in FSB. For mass spectrometry (MS) analysis (see 2.9.3) beads from 6 x 15 cm ∅ dishes were pooled (total 60 µl α-HA agarose) and the protein bound beads sent for analysis in TBS pH 7.4.

For α-arginine-GlcNAc immunoprecipitation experiments 5 mg of α-Arg-GlcNAc antibody (Abcam #ab195033) was bound overnight to 20 µl Protein A UltraLink Resin (Thermo Fisher #53139) in TBS pH 7.4 (per sample analysed). As a standard 2x 15 cm ∅ dishes of RAW 264.7 macrophages were infected per *Salmonella* strain (see 2.5.2). After 16 h of infection proteins were isolated as described in 2.8.1 in 1 ml Lumier lysis buffer (containing 0.3% triton X-100) and subsequently proteins were immunoprecipitated with the prepared α-Arg-GlcNAc resins for 2 h at 4°C. After the incubation, resins were then gently washed 3-4 times in 1 ml lysis buffer (containing 0.1% triton X-100). Proteins were then eluted and analysed by SDS-PAGE and western blot as described above. To increase the protein yield for mass spectrometry analysis (see 2.9.3) lysates were incubated twice with α-Arg-GlcNAc resins as described above.

Beads were pooled (total 10 mg Arg-GlcNAc antibody) and the protein bound beads sent for analysis by mass spectrometry in TBS pH 7.4.

2.9.3 Mass spectrometry analysis

Mass spectrometry (LC-MS-MS) analysis of co-immunoprecipitation samples was performed by the Institute of Biochemistry and Biophysics at the Polish Academy of Sciences in Warsaw, Poland. The analysis procedure included: Reduction and alkylation of protein disulfide bonds, tryptic digestion of the bead bound proteins to obtain a peptide mixture, liquid chromatography separation of the sample followed by MS measurement of peptides and their fragmentation spectra (tandem mass spectrometry). Acquired spectra were compared to a protein sequence database (*S.* Typhimurium 14028s*,* Uniprot; Mus musculus, Swiss-Prot) using the MASCOT search engine.

2.10 *In vivo* experiments

2.10.1 Ethical statement

Animal mouse experiments including ear clips for genotyping, infections and culling were conducted by Izabela Glegola-Madejska in accordance with UK Home Office regulations. The project licence for animal research (70/7768) was approved by the Imperial College Animal Welfare and Ethical Review Body (ICL AWERB) committee.

2.10.2 Mouse lines

Wild-type, female C57BL/6 mice were purchased from Charles River Laboratories. B6;129P2-*Trim32*$^{Gt(BGA355)Byg}$/Mmucd mice were kindly provided by Prof. Jens Schwamborn. The mice were selectively bread to obtain wild-type (*Trim32*$^{+/+}$), heterozygote (*Trim32*$^{+/-}$) and knock-out (*Trim32*$^{-/-}$) mice.

2.10.3 Genotyping of mice

Genomic DNA was isolated from mouse ear clips according to the procedure described by Truett *et al.* 2000. In short, ear clips were boiled in 75 µl Alkaline Lysis Buffer (25 mM NaOH (VWR #301674M), 0.2 mM Na_2EDTA (Sigma # E5134), pH 12) for 30 min at 95°C. The reaction was then cooled for a minimum of 5 min at 4°C and 75 µl Neutralisation Buffer (40 mM Tris-Cl (Sigma #T3253), pH 5) was added.

5 µl of the DNA mixture were subsequently used in a 10 µl PCR (Sigma #D1806) to determine the genetic status of the mice using the primers listed in Table 2.8.

Table 2.8. **PCR primers used for genotyping *Trim32*$^{-/-}$ mice**

Genotyping primers				
Internal ID	**Use**		**Species**	**5' to 3' nucleotide sequence**
RGO-097 F	B-Geo	FW	*Mus musculus*	CAAATGGCGATTACCGTTGA
RGO-098 R	B-Geo	REV	*Mus musculus*	TGCCCAGTCATAGCCGAATA
RGO-099 F	*Tcrd*	FW	*Mus musculus*	CAAATGTTGCTTGTCTGGTG
RGO-100 R	*Tcrd*	REV	*Mus musculus*	GTCAGTCGAGTGCACAGTTT
RGO-101 F	*Trim32*	FW	*Mus musculus*	AGCTTCTCACCTGAACCTGGATGC
RGO-102 R	*Trim32*	REV	*Mus musculus*	AGCCTTATACCTTGCCTGAAGATCCC

2.10.4 Competitive Index infections

Competitive Index (CI) infections were performed using 9 to 10 weeks old, littermate, wild-type and *Trim32*$^{-/-}$ C57BL/6 mice. To prepare the inoculum wild-type and Δ*sseK1/3* or Δ*sseK1/2/3 Salmonella* cultures were grown overnight in LB to stationary phase, washed once in PBS, diluted in PBS and mixed at a 1:1 ratio based on the OD_{600} of the cultures. Mice were inoculated with an equal number of wild-type and mutant *Salmonella* by intraperitonal injection of 3-5x 10^4 CFU/mouse. After two days (WT vs Δ*sseK1/2/3*) or four days (WT vs Δ*sseK1/3*) mice were culled, the spleens isolated and bacteria recovered. To do this the spleens were gently homogenised and lysed in sterile water for 30 min on ice, subsequently serial diluted in PBS and plated in duplicates on LB agar plates for assessing colony forming units per spleen. The Competitive Index was obtained by selective patching of a minimum of

200 bacterial colonies per mouse on antibiotic plates and calculated by the following formula: CI = (mutant/WT) output / (mutant /WT) input.

2.10.5 Infections with GFP-expressing *Salmonella*

Wild-type and *Trim32*$^{-/-}$ C57BL/6 mice, age 8 to 15 weeks, were infected with wild-type *Salmonella* carrying the pFPV25.1 plasmid. To prepare the inoculum bacteria were grown overnight in LB to stationary phase and then diluted 1:100 in fresh LB for 2h growth at 37°C. Bacteria were subsequently washed once in PBS and diluted in PBS for inoculation. Mice were infected by intraperitonal injection with 1.7-2.1 x10^4 CFU/mouse. After two days mice were culled, the spleens isolated, weighed, and colony forming units (CFU) measured by serial dilution. In addition splenic macrophages were isolated for flow cytometry and qPCR analysis.

Isolated spleens from (infected) mice were gently homogenised in HBSS and filtered through a 40 µm nylon mesh. 10% of the cells were then lysed in water for 30 min on ice, subsequently serial diluted in PBS and plated in duplicates on LB agar plates for assessing colony forming units per spleen. The rest of the cells were pelleted (300 x g, 5 min, 4°C) and the red blood cells lysed in 0.85% NH_4Cl (VWR #21236.267) in dH_2O for 10 min at room temperature. The reaction was stopped with HBSS, the cells pelleted, washed once in HBSS and pelleted again. The cells were then resuspended in MACS buffer (900 µl/spleen) and 50 µl MACS CD11b MicroBeads (Miltenyi Biotec #130-049-601) added per spleen. Cells and beads were incubated for 15 min on ice, pelleted, washed once in MACS buffer and then the macrophages isolated by magnetic separation on a MACS LS column according to the manufacturers recommendation. The recovered cells were resuspended in Opti-MEM with 5% FCS and 20 µg/ml gentamicin and half the cells used for analysis by flow cytometer. The percentage of infected cells and the GFP geometric mean per cell were measured on a FACSCalibur flow cytometer (BD Biosciences) and analysed with Flowing Software version 2.5.1. The rest of the cells were used for RNA isolation, cDNA synthesis and quantitative RT-PCR.

HBSS - Ca^{2+} Mg^{2+} free Hank's medium (Invitrogen #14175129) with 2% FCS (Invitrogen), 10 mM Hepes (Sigma #H0887)

MACS buffer – 0.5% BSA (Sigma #A4503), 2 mM EDTA (Sigma #ED) in PBS pH 7.2, degased

2.11 Statistical analysis

All presented values are presented as means ± standard error of the mean (SEM) of results from a minimum of three independent experiments. Statistical analysis was performed using Student's t test (two-tailed, unpaired) to compare two experimental groups. To compare multiple groups, statistical significance levels were calculated using one-way analysis of variance (ANOVA) and a post hoc Dunnett test (*, $P < 0.05$; **, $P < 0.01$; ***, P 0.001).

3 PHENOTYPIC CHARACTERISATION OF THE SSEK FAMILY OF *SALMONELLA* EFFECTORS

One interesting and so far poorly characterised group of SPI-2 T3SS effectors is the SseK protein family including SseK1, SseK2 and SseK3. Even though SseK1 and SseK2 were originally identified more than ten years ago by their high amino acid identity to the *E. coli* effector NleB (Kujat Choy et al., 2004), very little is known about their physiological function.

In contrast, two important publications identified NleB as a N-acetylglucosamine transferase that inhibits host cell signalling by irreversible modification of arginine residues within the death domains of target proteins like FADD and TRADD (Li et al., 2013; Pearson et al., 2013). These proteins are required for the signal transduction from death domain receptors (e.g. TNFR, TRAILR) and mediate the activation of NF-κB and cell death pathways. Arginine-GlcNAcylation of FADD and TRADD by NleB prevents the proteins oligomerisation upon activation and thereby leads to reduced NF-κB pathway activation and impaired caspase-8-dependent host cell death during infection. The divalent cation and/or sugar-coordinating catalytic DxD motif essential for this function is fully conserved in all three of the *S*. Typhimurium SseK effectors and experiments show that ectopically expressed SseK1 and SseK3 can inhibit NF-κB signalling (Li et al., 2013; Yang et al., 2015). However, whether this is of relevance during *Salmonella* infection is unknown.

Several studies showed that the distribution of *Salmonella* SseK effectors varies between different serovars (Brown et al., 2011; Nuccio and Bäumler, 2014) with all the SseK effectors being present in *S.* Typhimurium 14028s but only one or two effectors present in other strains. In combination with their high amino acid conservation, this raises the possibility of phenotypic redundancy between the SseK proteins. Yet, ectopic expression of SseK1 showed that it localises to the host cytoplasm whilst SseK3 colocalises with the Golgi network (Kujat Choy et al., 2004; Yang et al., 2015), suggesting that differences might exist in effector function.

This results chapter addresses the phenotypic characterisation of the SseK effector family. The first aim was to examine the translocation and intracellular localisation of the effectors in macrophages, as well as identifying bacterial factors that determine both these processes. The second aim was to identify and characterise host processes targeted by the SseK proteins,

with particular focus on the NF-κB pathway and cytotoxicity response to *Salmonella* infection. During all experiments, similarities and differences between the SseK effectors were investigated to elucidate potential functional redundancy between them.

3.1 Initial characterisation of SseK effector translocation and localisation

Translocation of the SseK effectors into cells by the SPI-2 T3SS has been shown previously by independent studies (Baisón-Olmo et al., 2015; Brown et al., 2011; Kujat Choy et al., 2004). However, this was studied mainly in epithelial cells and using CyaA-fusion experiments which assesses the translocation of effector-adenylate cyclase fusion proteins by monitoring the cAMP concentration in the host cell. As this work will focus mainly on the effects of *Salmonella* infections on/in macrophages it was first tested if the SseK effectors are translocated by the SPI-2 T3SS into macrophages. Low copy number complementation plasmids (pWSK29) expressing C-terminally HA-tagged SseK effectors under the control of their endogenous promoters were created and RAW 264.7 cells were infected with various *Salmonella* strains carrying the complementation plasmids. Immunofluorescence analysis revealed that all three SseK-HA effectors were translocated into the host cell from their isogenic deletion mutants at 16 h.p.u. (Figure 3.1A). Effector translocation was not detected from the secretion system deficient Δ*ssaV* deletion strain, showing that this process is dependent on the SPI-2 T3SS. Even compensation of the Δ*ssaV* mutant's severe replication deficit by infection with ten times the MOI of wild-type *Salmonella* did not result in detectable SseK effector translocation into the host cell despite clear effector production in bacteria (Figure 3.1D).

Previous publications studying ectopically expressed SseK1 (Kujat Choy et al., 2004) and SseK3 (Yang et al., 2015) showed that they localise to the cytoplasm and Golgi network, respectively. Immunofluorescence microscopy analysis of effector translocation into RAW 264.7 macrophages at 16 h.p.u. revealed a predominantly cytoplasmic localisation of SseK1-HA whilst both SseK2-HA and SseK3-HA colocalised strongly with the Golgi network marker Rab6 in all cells positive for translocated effector (Figure 3.1A). Translocation of the SseK effectors was detected in approximately 60% of all infected macrophages when analysed by immunofluorescence microscopy (Figure 3.1B).

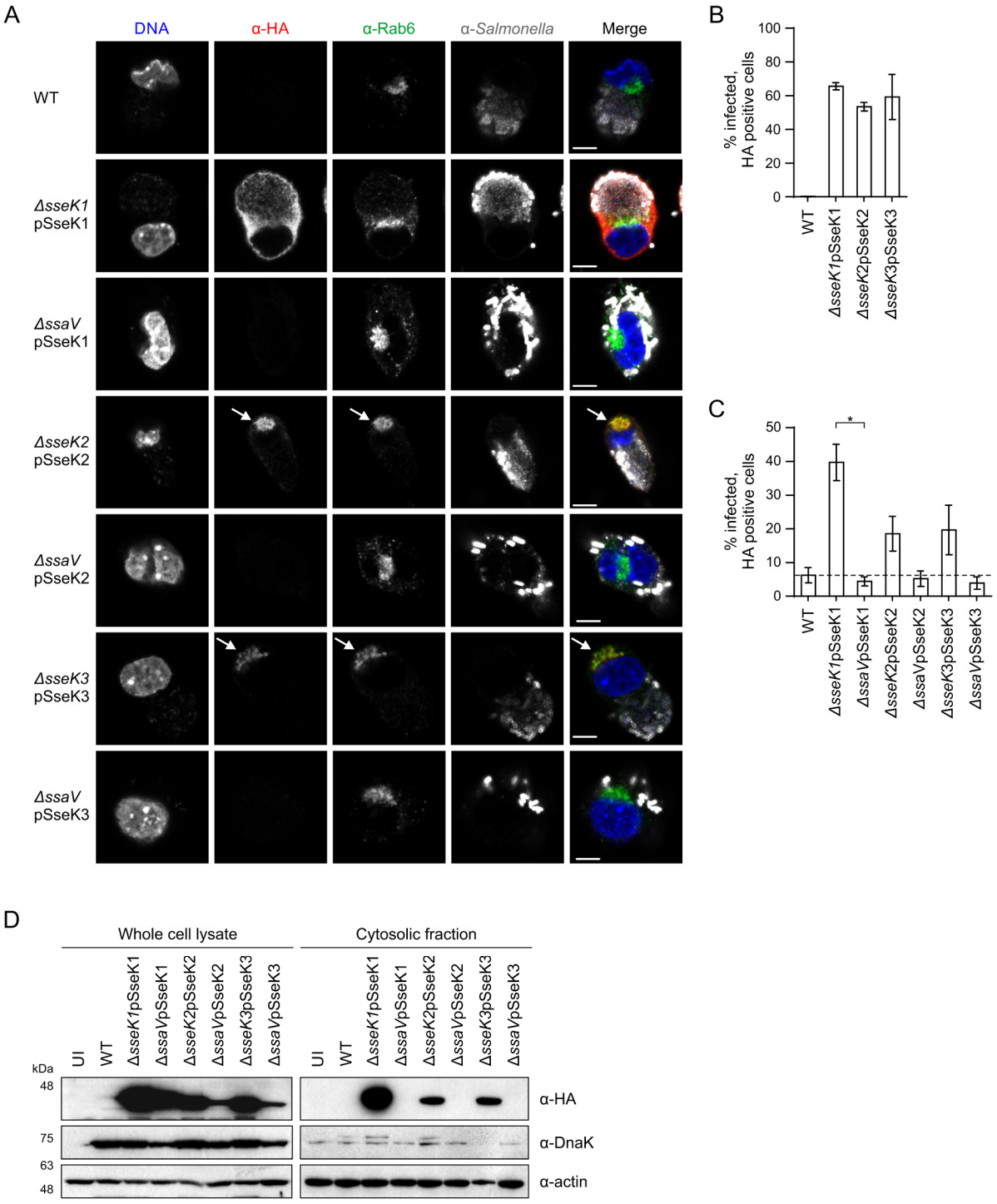

Figure 3.1. **SPI-2-dependent translocation and intracellular localisation of SseK effector proteins**
(A) Representative confocal immunofluorescence microscopy of RAW 264.7 macrophages infected for 16 h with the indicated *Salmonella* strains. The arrows highlight effector localisation to the Golgi network. DNA (DAPI, blue), effectors (α-HA, red), Golgi network (α-Rab6, green) and *Salmonella* (α-CSA-1, grey). Scale bar, 5 µm. (B) Percentage infected cells with translocated HA-tagged SseK effector quantified by immunoflorescence microscopy as in (A). A minimum of 600 infected cells from three independent experiments were blind-scored and are represented as the mean ± SEM. (C) Flow cytometry quantification of infected RAW 264.7 macrophages with translocated HA-tagged effectors at 16 h.p.u. Data are the mean of three independent experiments ± SEM.

The dotted line indicates unspecific background labelling. (D) RAW 264.7 cells were infected with the indicated *Salmonella* strains to asses SPI-2 dependent translocation of SseK effector proteins into macrophages. To compensate for the severe replication deficit of the Δ*ssaV* mutant 10x the wild-type MOI was used. After 16 h cells were lysed and proteins analysed by SDS-PAGE and immunoblotting. Effectors (α-HA), *Salmonella* (α-DnaK) and loading control (α-actin). Data represent results of two independent experiments. UI, uninfected.

To quantify this using a high throughput method, SseK effector translocation was also analysed by flow cytometry (Figure 3.1C). Wild-type bacteria with no HA-tagged effector were used to establish an appropriate gate for cells with unspecific/background HA-labelling (annotated on the figure as a dotted line). After 16 h of RAW 264.7 macrophage infection, SseK1 effector translocation from the Δ*ssaV* deletion mutant was reduced to background levels, strengthening the microscopy and western blot results in Figure 3.1A and D. The percentage of infected cells with translocated SseK2 and SseK3 (from Δ*sseK2*pSseK2 or Δ*sseK3*pSseK3, respectively) was considerably lower when analysed by flow cytometry (~20%) compared to immunofluorescence microscopy (~60%) and was statistically not different from the unspecific background labelling detected in wild-type infected cells (Figure 3.1C). This might be due to sensitivity limitations of the method in detecting poorly expressed, tightly localised effectors. Therefore, immunofluorescence microscopy was used in further experiments for effector translocation and localisation experiments.

Amino acid sequence alignment of the SseK effectors with NleB revealed that the metal coordinating DxD motif required for NleB catalytic function is fully conserved in the SseK proteins (Figure 1.7). For phenotypic studies of the proteins, mutation of this motif to obtain a catalytic SseK mutant is a useful tool. However, it has previously been reported that mutagenesis of bacterial effectors can alter protein translocation and potentially intracellular effector localisation in the host cell (Wong Fok Lung et al., 2016). To test if this is the case for the SseK effector family the putative catalytic DxD motif was replaced by a triple alanine sequence ($SseK_{AAA}$) and effector translocation and localisation analysed. Confocal microscopy analysis of infected RAW 264.7 macrophages showed that at 16 h.p.u. both wild-type and mutant SseK1 were cytosolic whilst SseK2 and SseK3, as well as their DxD mutants, localised to the Golgi network (Figure 3.2A). However, even though no difference in effector localisation was detected, quantification of the percentage infected cells with translocated effector revealed that a significantly lower percentage of cells contained translocated $SseK_{AAA}$

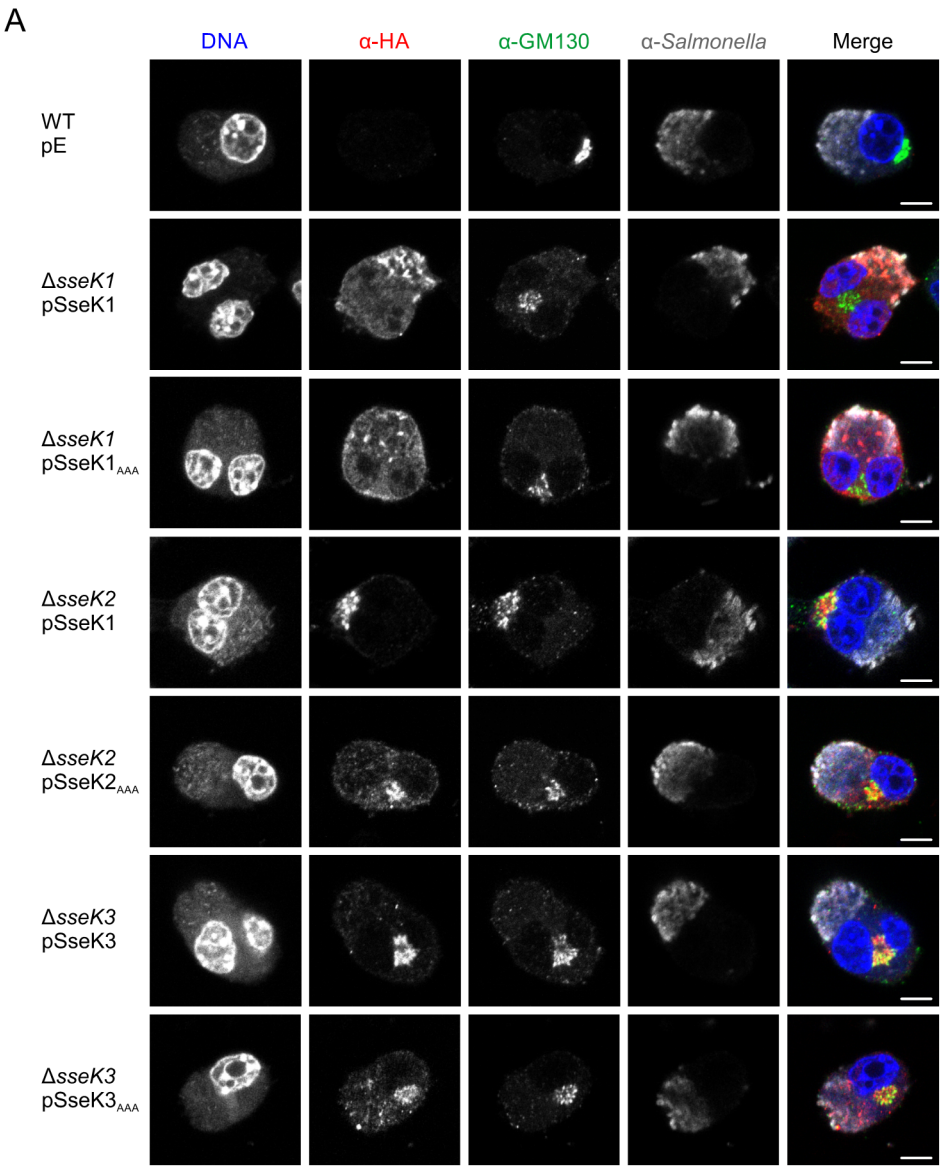
A
DNA
α-HA
α-GM130
α-Salmonella
Merge
WT pE
ΔsseK1 pSseK1
ΔsseK1 pSseK1AAA
ΔsseK2 pSseK1
ΔsseK2 pSseK2AAA
ΔsseK3 pSseK3
ΔsseK3 pSseK3AAA

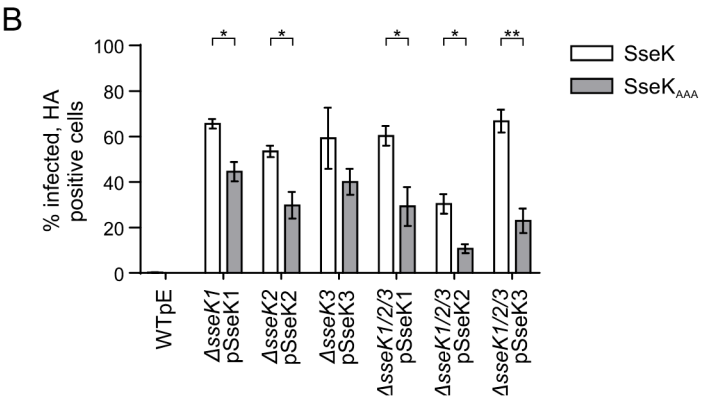
B
% infected, HA positive cells
100
80
60
40
20
0
SseK
SseKAAA
*
*
*
*
**
WTpE
ΔsseK1 pSseK1
ΔsseK2 pSseK2
ΔsseK3 pSseK3
ΔsseK1/2/3 pSseK1
ΔsseK1/2/3 pSseK2
ΔsseK1/2/3 pSseK3

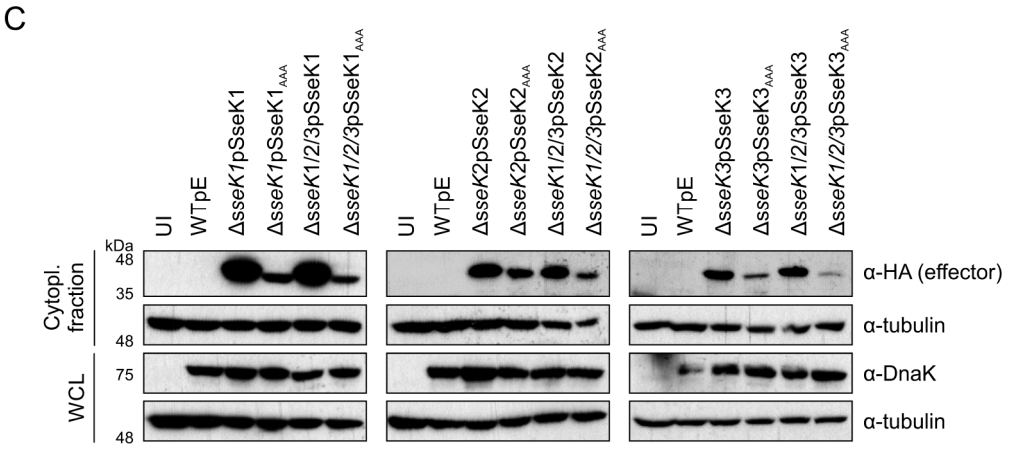

Figure 3.2. **Putative catalytic SseK mutants ($SseK_{AAA}$) are less abundant but show comparable intracellular localisation to their wild-type counterparts**

RAW 264.7 macrophages were infected with *Salmonella* strains expressing HA-tagged wild-type or catalytic mutant (AAA) SseK effectors at 16 h.p.u. (A) Representative confocal immunofluorescence microscopy images. DNA (DAPI, blue), effectors (α-HA, red), Golgi network (α-GM130, green) and *Salmonella* (α-CSA-1, grey). Scale bar, 5 µm. (B) Percentage of infected macrophages with translocated HA-tagged effector quantified by immunofluorescence microscopy. Three independent experiments with minimum of 600 infected cells were blind-scored and are represented as the mean ± SEM. * $P < 0.05$, ** $P < 0.01$. (C) Cells were harvested, lysed and the translocated effector levels analysed by SDS-PAGE and immunoblotting. Effectors (α-HA), *Salmonella* (α-DnaK), and loading control (α-actin). Data are representative of three independent experiments. UI, uninfected. pE, empty plasmid.

mutant proteins compared to the wild-type form (Figure 3.2B). This effect was detected both when the mutant SseK effectors were translocated by their isogenic deletion strains (single deletion mutants) as well as a Δ*sseK1/2/3* triple deletion mutant (Figure 3.2B). Western blot analysis of cytoplasmic proteins from RAW 264.7 macrophages infected with different *Salmonella* strain confirmed that the catalytically inactive $SseK_{AAA}$ effector mutants were less abundant in the host cell at 16 h.p.u. compared to their wild-type counterpart (Figure 3.2C). This means that enzymatic activity is not required for the SseK effector's localisation but mutation of the predicted sugar coordinating DxD motive leads to either inefficient effector translocation or decreased protein stability in the host cell. For this reason, the $SseK_{AAA}$ mutants were not used for further phenotypic infection studies.

Transient expression of GFP-tagged SseK effectors in 293ET cells and analysis by immunofluorescence microscopy revealed that ectopically expressed SseK effectors localise to the same subcellular compartments as translocated effector: the cytoplasm (SseK1) and

Golgi network (SseK2 and SseK3) (Figure 3.3A). Again, localisation of the putative catalytic DxD mutants ($SseK_{AAA}$) was indistinguishable from that of the wild-type proteins.

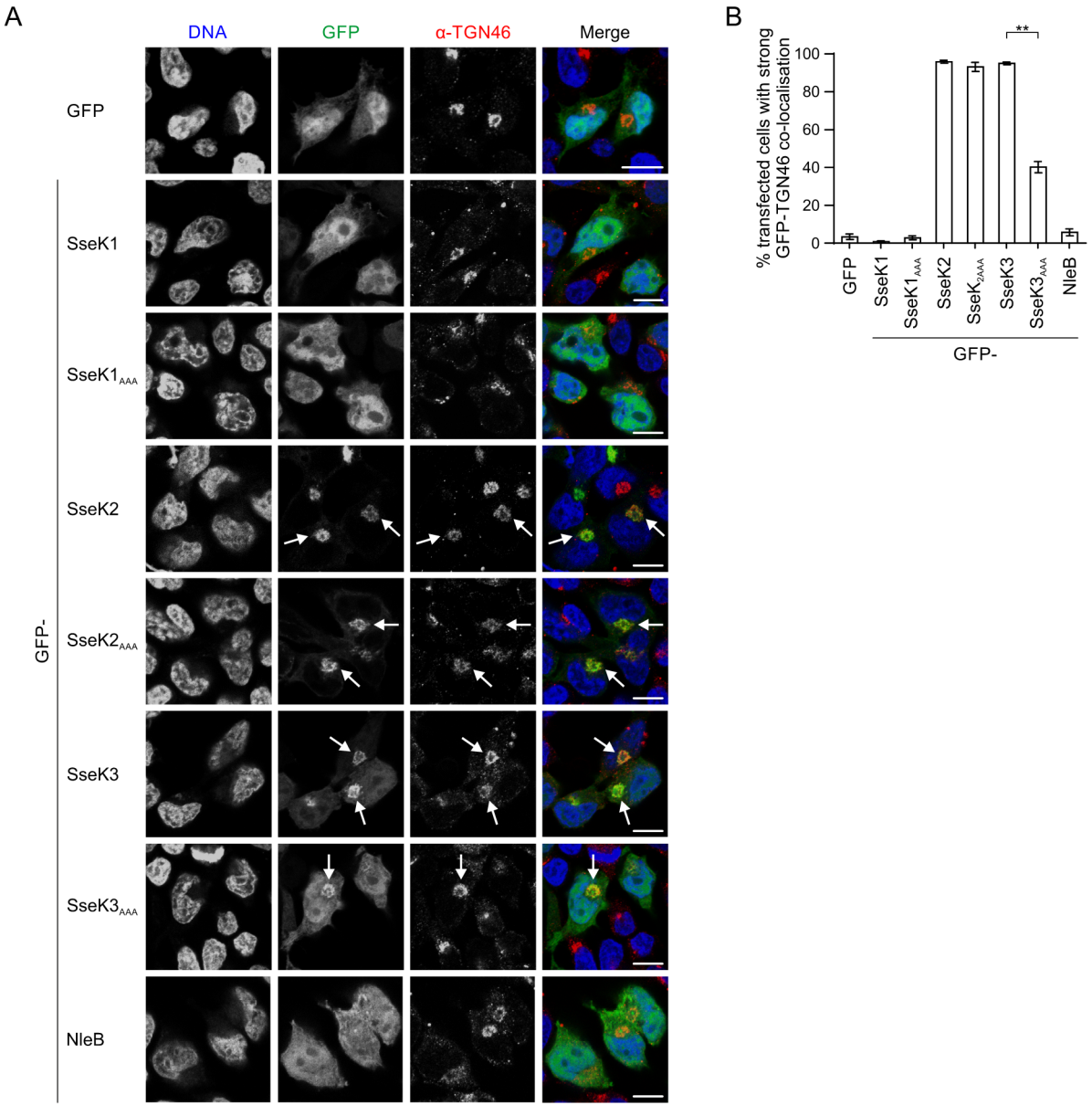

Figure 3.3. **Ectopically expressed SseK proteins localise to the same subcellular structures as the translocated SseK effectors**

(A) Representative confocal microscopy images of the subcellular localisation of ectopically expressed wild-type or mutant GFP-SseK effectors in 293ET cells. The arrows highlight effector localisation to the Golgi network. DNA (DAPI, blue), effectors (GFP, green) and Golgi network (α-TGN46, red). Scale bar, 10 µm. (B) Percentage of transfected cells with strong GFP-TGN46 co-localisation as quantified from (A). Three independent experiments with minimum of 600 cells in total were blind-scored and values represent the mean ± SEM. ** $P < 0.01$.

Interestingly, strong Golgi network localisation of SseK3$_{AAA}$ was significantly reduced compared to wild-type SseK3 (Figure 3.3B). However, western blot analysis of cell lysates from transfected 293ET cells showed that this was not due to overall protein levels as wild-type and mutant forms of all three SseK effectors were similar (Figure 3.8B and Figure 3.12D). As SseK$_{AAA}$ mutants showed similar ectopic expression, these mutants were used for further transfection-based experiments.

Sequence alignment of the SseK effectors revealed that they differ mainly at the N-terminal sequence of the proteins (Figure 1.7). Therefore, I hypothesised that this region might be involved in the differential localisation of the proteins in the host cell. To test this, various N-terminal deletion mutants of SseK3 were created and their localisation assessed after ectopic expression in 293ET cells (Figure 3.4A). SseK3 was chosen as the model effector for this experiment due to its tight, well defined Golgi network localisation. Confocal microscopy showed that deletion of the 13 N-terminal amino acids (ΔN13) was sufficient to significantly reduce Golgi network localisation of SseK3. Deletion of additional amino acids up to amino acid 31 (ΔN31) or 44 (ΔN44) did not further decrease Golgi network localisation (Figure 3.4A and B). Positive charged amino acid regions can meditate protein membrane localisation by electrostatic interaction with the negative charged lipid head groups (Bigay and Antonny, 2012; Mesmin et al., 2004). In the 13 N-terminal amino acids of SseK3 three positively charged residues stand out. To test whether these residues mediated the Golgi network localisation of SseK3 a neutral variant was constructed (R4Q/R6Q/L9Q). This mutant showed an intermediate phenotype ranging between the wild-type SseK3 and ΔN13 deletion mutant with strong Golgi network colocalisation in approximately 50% of the transfected cells (Figure 3.4A and B). To test whether the N-terminal region is sufficient for Golgi network localisation, the 44 N-terminal amino acids were fused to GFP (SseK3$_{N44}$). This small SseK3 peptide-GFP fusion displayed significantly greater localisation with the Golgi network than GFP alone, however not as well as wild-type SseK3 (Figure 3.4A and B). Taken together these data show that the N-terminal region of SseK3 is required but not sufficient for strong Golgi network localisation of the effector.

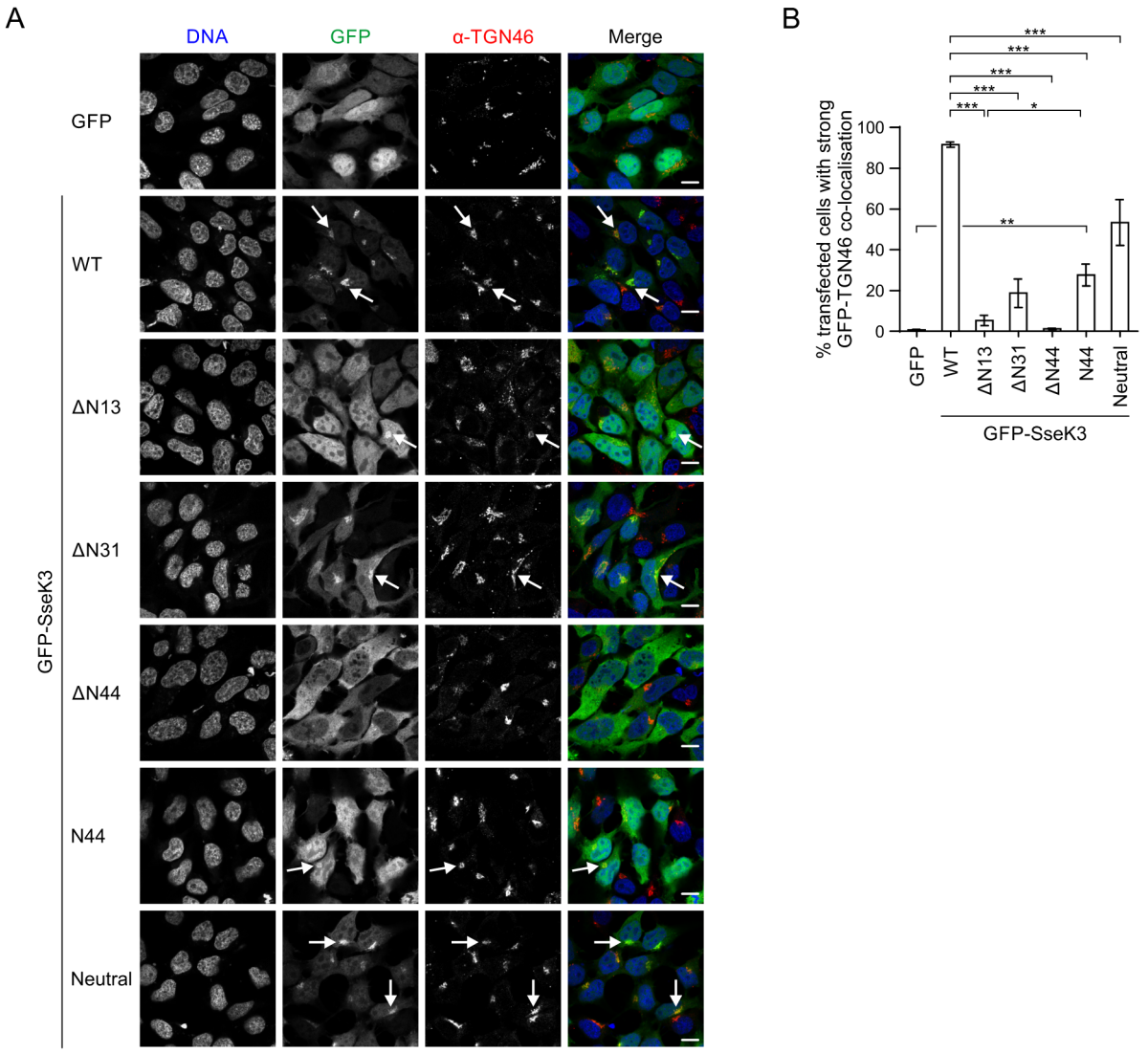

Figure 3.4. **SseK3 N-terminal region is required but not sufficient for strong Golgi network localisation**

(A) Representative confocal images of ectopically expressed wild-type (WT) SseK3, N-terminal SseK3 deletion mutants (ΔN13, ΔN31 and ΔN44), the SseK3 N-terminal region (N44) and a neutral N-terminal variant (R4Q/R6Q/L9Q) of SseK3 in 293ET cells. The arrows highlight effector localisation to the Golgi network. DNA (DAPI), effectors (GFP) and Golgi network (α-TGN46). Scale bar, 10 µm. (B) Strong GFP-TGN46 co-localisation in transfected cells quantified by blind scoring from (A). A minimum of 600 infected cells from three independent experiments was analysed and values represent the mean ± SEM. * $P < 0.05$, ** $P < 0.01$, *** $P < 0.001$.

3.2 Phenotypic characterisation - NF-κB pathway inhibition

To analyse SseK function during macrophage infection I first tested if any of the single, double or triple *sseK* deletion mutants have a replication defect in this cell type. To do this,

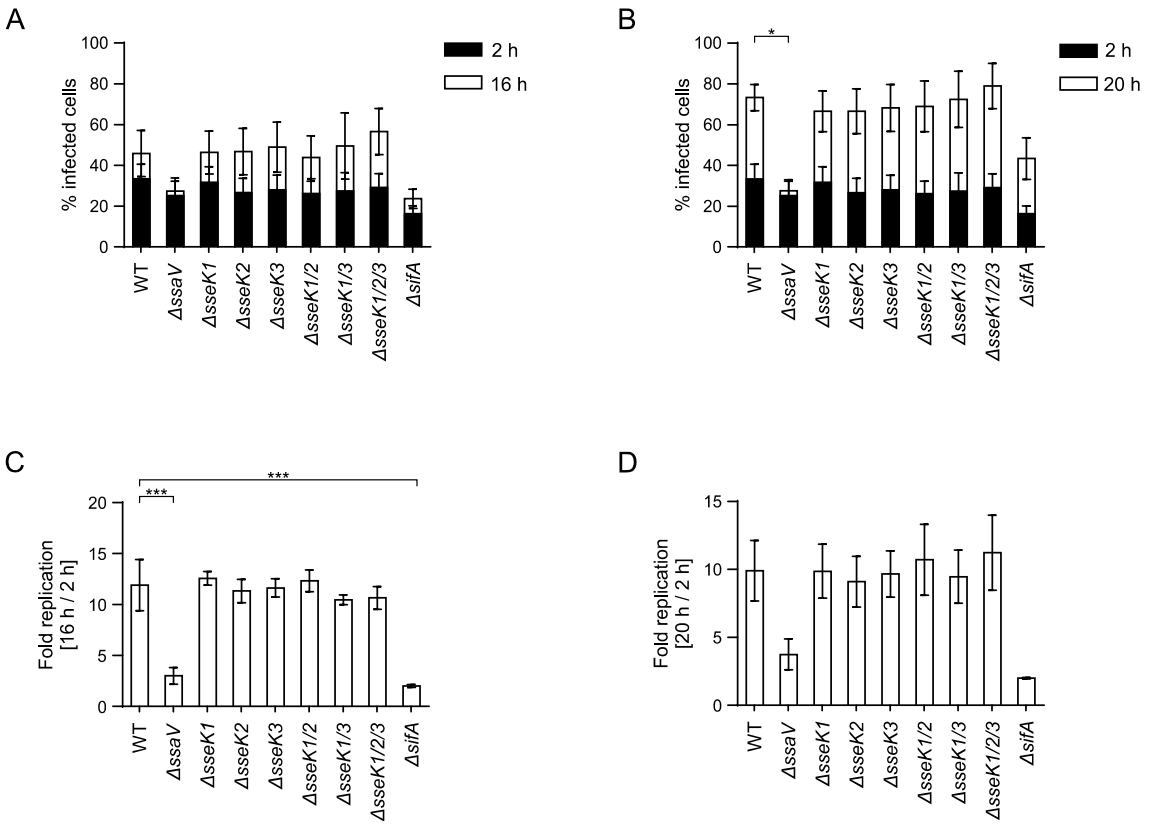

Figure 3.5. **SseK deletion strains do not have a replication defect in macrophages**

RAW 264.7 macrophages were infected with GFP-expressing *Salmonella* strains for 2 h, 16 h and 20 h. The infection rates at 16 h.p.u (A) and 20 h.p.u. (B) were analysed by flow cytometry. Data were acquired during the same experiments and values for 2 h.p.u. are duplicated in both panels for ease of interpretation. The fold geometric mean of 16 h.p.u (C) and 20 h.p.u. (D) relative to 2 h.p.u. were calculated after analysis by flow cytometry. The data represents the mean ± SEM of three independent experiments. * $P < 0.05$, *** $P < 0.001$.

RAW 264.7 macrophages were infected with GFP-expressing mutant *Salmonella* stains and the infection rate and bacterial replication were determined by flow cytometry. The percentage *Salmonella* infected cells at 2, 16 and 20 h.p.u. was not affected by the absence of SseK effectors. However, at late time points the percentage of infected cells was markedly reduced for the SPI-2 T3SS mutant Δ*ssaV* and a control effector mutant Δ*sifA* (Figure 3.5A and B). Importantly, none of the Δ*sseK* deletion mutants showed growth attenuation whereas the expected replication deficit of the Δ*sifA* and Δ*ssaV* mutants (Figueira et al., 2013) were apparent at late infection time points (16 and 20 h.p.u.) (Figure 3.5C and D). The similar replication of Δ*sseK* mutants and wild-type bacteria means that any phenotypic variations identified are unlikely to arise from differences in bacterial burden. This made the mutants suitable for further use in phenotypic infection experiments.

Previous studies using ectopic expression of SseK1 (Li et al., 2013) and SseK3 (Yang et al., 2015) showed, that both effectors inhibit the NF-κB signalling pathway. However, neither study addressed whether the translocated effectors have the same physiological function. To test this, NF-κB reporter macrophages were used. This RAW 264.7 macrophage cell line stably encodes a Firefly Luciferase gene under the control of an NF-κB responsive promoter and additionally constitutively expresses Renilla Luciferase as an internal control for cell numbers (see material and methods for further details). Infection of the reporter cell line with wild-type *Salmonella* resulted in a five-fold increase in NF-κB reporter activation 16 h.p.u. compared to uninfected cells, showing responsiveness of the cell line to infection (Figure 3.6A). As expected from previous studies (Rolhion et al., 2016) the SPI-2 T3SS deficient Δ*ssaV* mutant elicited a statistically significant higher NF-κB response than wild-type *Salmonella*.

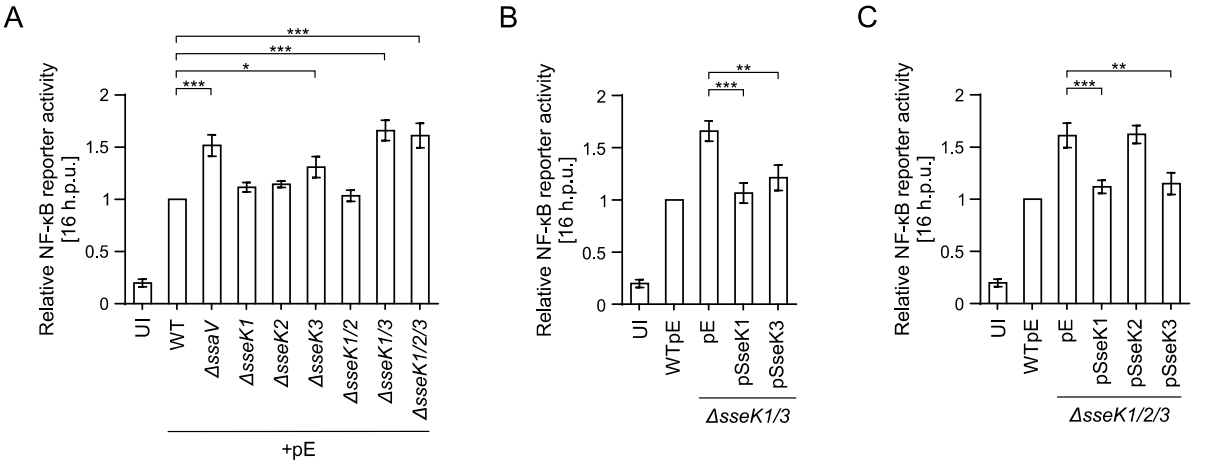

Figure 3.6. **SseK1 and SseK3 inhibit an NF-κB-induced reporter in an additive manner during macrophage infection**

(A-C) NF-κB reporter RAW 264.7 macrophages stably transduced with an NF-κB responsive Firefly Luciferase reporter element and a constitutively expressed Renilla Firefly gene were infected for 16 h with the indicated Salmonella strains. Data represent the mean fold activation relative to wild-type infected cells from five independent experiments ± SEM.* P < 0.05, ** P < 0.01, *** P < 0.001. UI, uninfected. pE, empty plasmid. All data were acquired at the same time. The UI, WTpE, ΔsseK1/3pE, and ΔsseK1/2/3pE data are reproduced in each panel for ease of interpretation.

To investigate if this was due to lack of SseK effector translocation, various single, double and triple Δ*sseK* mutants were analysed. Infection with the Δ*sseK3* mutant but not the Δ*sseK1* or Δ*sseK2* strain significantly increased NF-κB reporter activation compared to wild-type infected cells at 16 h post-uptake (Figure 3.6A). This was further increased by additional deletion of

SseK1 (Δ*sseK1/3*) whilst the Δ*sseK1/2/3* triple deletion mutant showed no additive effect compared to the Δ*sseK1/3* strain. Increased NF-κB reporter activity elicited by the Δ*sseK1/3* or Δ*sseK1/2/3* mutant was complemented by expression of SseK1 or SseK3 (Figure 3.6B and C). However, deletion of SseK2 or expression of SseK2 in the Δ*sseK1/2/3* strain had no discernable effect on NF-κB reporter activity. Taken together these results showed that SseK1 and SseK3 inhibit activation of the NF-κB reporter during macrophage infection in an additive manner.

During *Salmonella* infection various bacterial and host cell factors contribute to the activation of the NF-κB pathway. Even though the initial steps of pathway activation differ between stimuli, the signalling cascades converge at the level of IKK complex activation and share a conserved series of events leading to NF-κB dependent gene expression (Figure 1.2). To narrow down the target of the SseK effectors I next tested if they inhibit a specific or conserved component of the NF-κB pathway. To this end RAW 264.7 macrophages that stably express GFP-tagged p65 were infected with various *Salmonella* mutants constitutively expressing mCherry. During the last hour of the 16 h infection, the cells were additionally stimulated with LPS to synchronise NF-κB signalling and nuclear p65 accumulation, as a marker for pathway activation, was scored by immunofluorescence microscopy (Figure 3.7A and B). Purified LPS induced strong nuclear accumulation of p65 in approximately 60% of naïve, non-infected cells (Figure 3.7B). Fewer cells displayed nuclear p65 when wild-type *Salmonella* infected cells were additionally stimulated with purified LPS, suggesting that bacteria might inhibit LPS-induced accumulation of nuclear p65. Indeed, the SPI-2 Δ*ssaV* null mutant was not able to suppress p65 translocation to the nucleus. However, *Salmonella*-mediated inhibition of LPS-induced nuclear p65 accumulation was not due to the lack of SseK effector translocation, as nuclear p65 levels of cells infected with the single Δ*sseK* deletion mutants were similar to wild-type infected cells (Figure 3.7B). Deletion of all three SseK effectors also did not significantly increase accumulation of nuclear p65 compared to wild-type *Salmonella*-infected cells. Taken together this indicates that the SseK effectors are not sufficient to suppress NF-κB activity induced by a pulse with purified LPS.

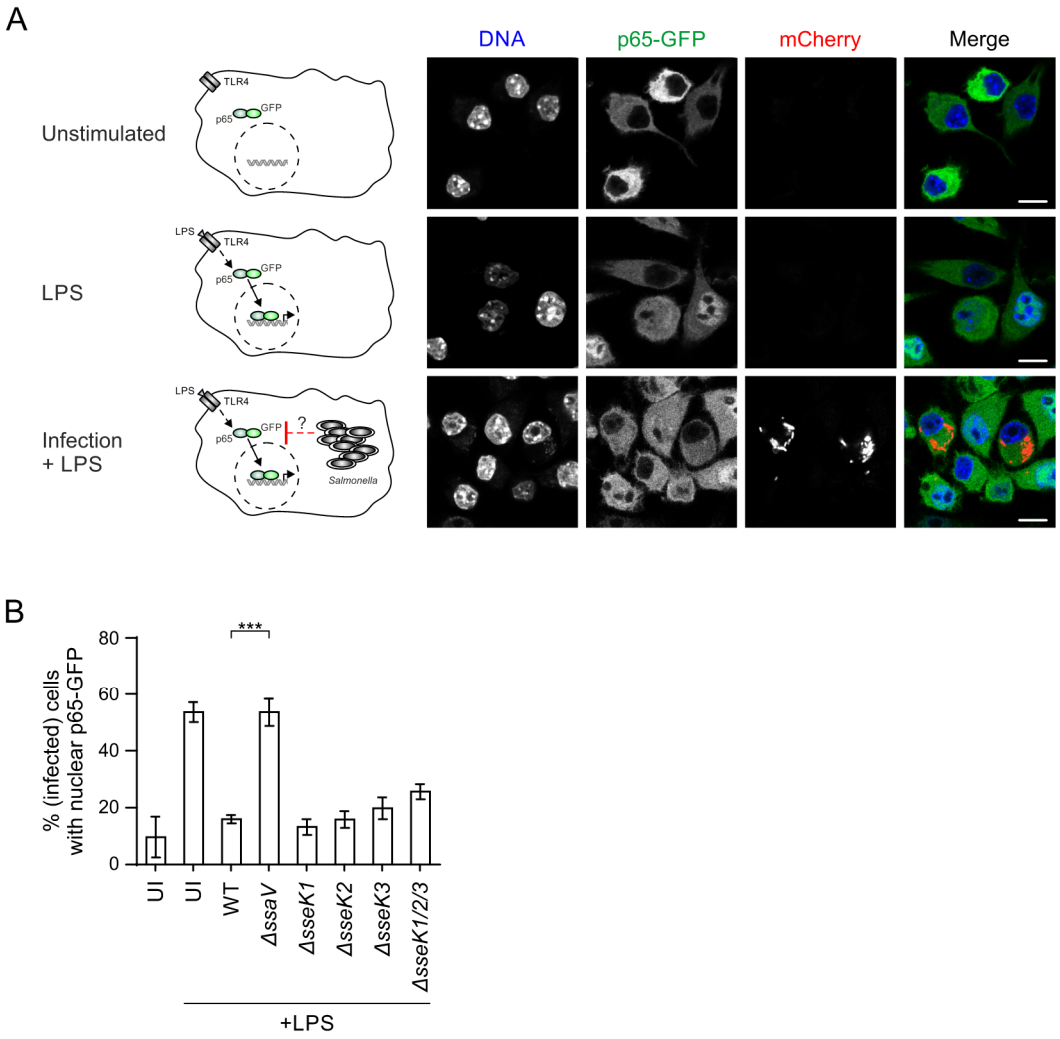

Figure 3.7. **SseK effectors do not inhibit LPS driven p65 translocation to the nucleus**

RAW 264.7 macrophages stably transduced with p65-GFP were infected for 16 h with *Salmonella* strains carrying the pFCcGi plasmid. During the last hour of infection the cells were additionally stimulated with 1 µg/ml LPS.

(A) Schematic representation and representative confocal microscopy images of the experiment. DNA (DAPI, blue), p65-GFP (GFP, green) and *Salmonella* (mCherry, red). Scale bar, 10 µm. (B) Blind scoring of (infected) cells with predominantly nuclear p65-GFP. Approximately 500 cells were scored per biological repeat. Data are the mean of three independent experiments ± SEM. *** $P < 0.001$. UI, uninfected

To test whether the SseK effectors specifically inhibit a different stimulus during macrophage infection a pulse of TNFα was used. However, stimulation of macrophages with TNFα did not result in a strong, well-synchronised activation of the NF-κB pathway and accumulation of

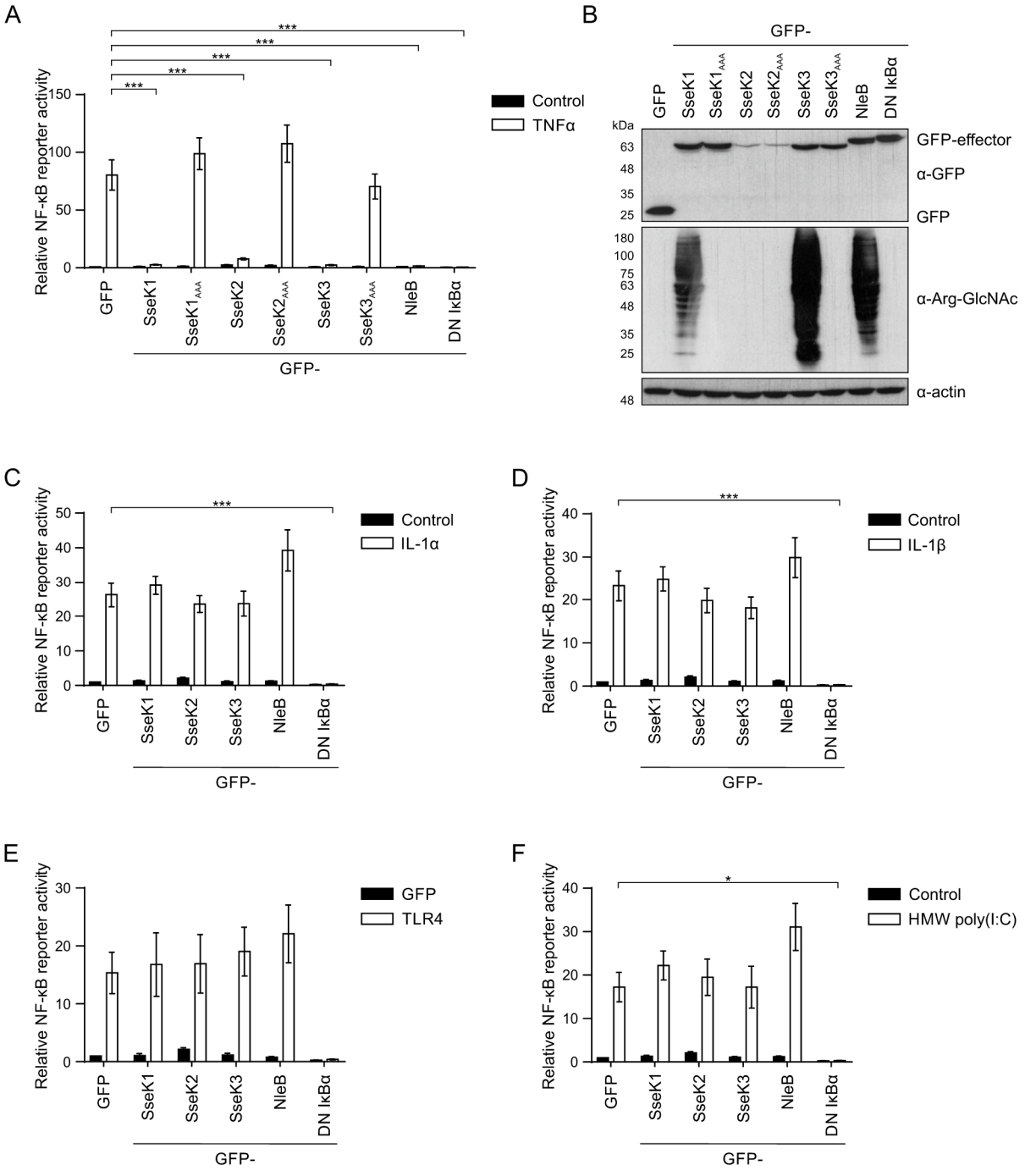

Figure 3.8. ***Salmonella* SseK effectors selectively inhibit TNFα-mediated NF-κB signalling**

(A, C-F) Transfection luciferase reporter assays in 293ET cells transiently co-transfected with an NF-κB -dependent luciferase reporter plasmid, pTK-Renilla luciferase plasmid, and the indicated ptCMV-GFP-effector plasmids. Alternatively dominant-negative (DN) IκBα was used as a positive control. 50 ng/ml TNFα (A), 10 ng/ml IL-1α (C), 10 ng/ml IL-1β (D) or 4 μg/ml high-molecular weight (HMW) poly(I:C) (E) were used to activate the NF-κB pathway overnight. Alternatively the pathway was auto-activated by overexpression of TLR4 (F) to mimic LPS stimulation for 24 h prior to cell lysis and analysis of luciferase activity. Results shown in panels C, D, and E were acquired at the same time and contain the same unstimulated control data. Results are presented as the fold activation relative to activation of unstimulated, GFP-expressing control cells. Data shown are means of 4 to 7

independent experiments ± SEM. *, P < 0.05; ***, P < 0.001. (B) Representative immunoblot of cell lysates as described for (A). Effectors (α-GFP), arginine-GlcNAc (α-Arg-GlcNAc) and loading control (α-actin).

nuclear p65 was too inhomogeneous to quantify (data not shown). Therefore NF-κB inhibition by the SseK effectors was further studied in transfection reporter assays with a defined, single stimulus.

To do this 293ET cells were transiently transfected with an NF-κB reporter plasmid expressing Firefly Luciferase under an NF-κB dependent promoter, a constitutive expressed Renilla Luciferase plasmid and plasmids expressing GFP-tagged effectors. Overnight stimulation with TNFα led to substantial NF-κB pathway activation which was strongly suppressed by the expression of SseK1, SseK2 and SseK3 as well as the positive controls NleB and dominant negative (S32A/S36A) IκBα (Traenckner et al., 1995) (Figure 3.8A). Mutation of the putative catalytic DxD motif to alanines ($SseK_{AAA}$) abolished the SseK effector's ability to inhibit the NF-κB pathway and to GlcNAcylate proteins, despite similar expression levels to the wild-type proteins (Figure 3.8B). Interleukin-1 (IL-1) is a strong host activator of the NF-κB pathway during *Salmonella* infection. However, none of the SseK effectors inhibited NF-κB signalling after IL-1α (Figure 3.8C) or IL-1β (Figure 3.8D) stimulation. As expected from previous work (Newton et al., 2010; Ruchaud-Sparagano et al., 2011), NleB did not suppress IL-1 driven NF-κB signalling whilst dominant-negative (DN) IκBα could. Another major *Salmonella* activator of the NF-κB pathway during infection is bacterial LPS. To mimic LPS stimulation in a more quantitative experimental setup compared to the above mentioned infection assay (Figure 3.7), the LPS receptor (TLR4) was overexpressed in 293ET cells to auto-activate the NF-κB pathway. Neither the SseK effectors nor NleB inhibited TLR4 driven NF-κB signalling whereas the positive control (DN IκBα) inhibited pathway activity (Figure 3.8E). In addition to extracellular NF-κB pathway activation, *Salmonella* RNA can also become cytosolic during infection and thereby activate the NF-κB pathway via RIG-I and MDA5 (Dixit and Kagan, 2013; Schmolke et al., 2014). To mimic this, the cells were stimulated with high molecular weight polyinosinic-polycytidylic acid (HMW poly(I:C)). Again, neither the SseK effectors nor NleB inhibited the NF-κB pathway upon poly(I:C) stimulation whereas DN IκBα could (Figure 3.8F). Taken together this shows that the SseK effectors specifically inhibit TNFα-driven NF-κB signalling in a catalytically dependent manner and do not target a shared component of the NF-κB pathway.

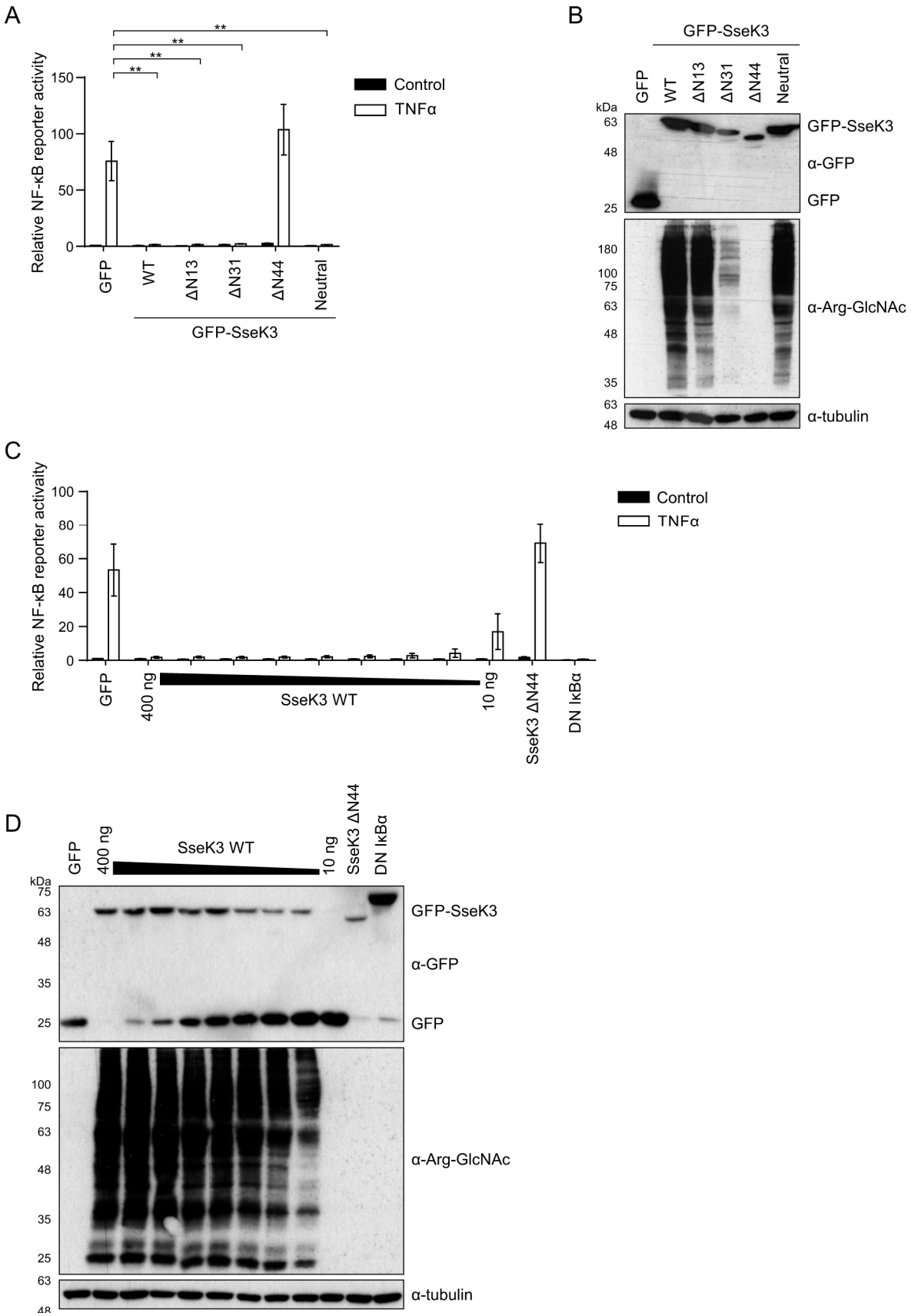

Figure 3.9. **Strong Golgi network localisation of SseK3 is not required for NF-κB pathway inhibition**

(A) 293ET cells were co-transfected with the NF-κB -dependent luciferase reporter plasmid, pTK-Renilla luciferase plasmid, and the indicated ptCMV-GFP-effector plasmids to express wild-type (WT) SseK3 or N-

terminal SseK3 deletion mutants (ΔN13, ΔN31 and ΔN44). After overnight stimulation with 50 ng/ml TNFα cells were lysed and the luciferase activity measured. Data are shown as the fold activation relative to the activity of unstimulated, GFP-expressing control cells. Data represent the mean of four independent experiments ± SEM. **, P < 0.01. Data S. Matthews. (B) Representative immunoblot of cell lysates from (A). Effectors (α-GFP), arginine-GlcNAc (α-Arg-GlcNAc) and loading control (α-tubulin). Data S. Matthews. (C) Transfection reporter assay as described in (A) with the titration of WT SseK3 (400 to 10 ng plasmid DNA) compared to 400 ng of the SseK3 ΔN44 mutant. Total DNA levels were adjusted with the plasmid pEGFP. Data are the mean of three independent experiments ± SEM. (D) Representative immunoblot of cell lysates from (C). Effectors (α-GFP), arginine-GlcNAc (α-Arg-GlcNAc) and loading control (α-tubulin).

Next, it was tested if Golgi network localisation of SseK3 is correlated with its ability to inhibit the NF-κB pathway. To do this, the previously described N-terminal SseK3 deletion mutants (ΔN13, ΔN31, ΔN44) were tested in a transfection NF-κB reporter assay as described above. This assay was chosen over a *Salmonella* infection NF-κB reporter assay to avoid the complication that the N-terminal region of *Salmonella* effectors (including SseK1) is often required for (efficient) effector translocation (Dean, 2011; Kujat Choy et al., 2004; Samudrala et al., 2009). The ΔN13 and ΔN31 SseK3 deletion mutants showed strong inhibition of TNFα driven NF-κB signalling despite the mutant's significant reduction in Golgi network localisation (Figure 3.9A, data obtained in collaboration with S. Matthews). In contrast the ΔN44 SseK3 deletion mutant did not inhibit the NF-κB pathway or arginine-GlcNAcylate proteins (Figure 3.9A and B). However, analysis of the cell lysates from the reporter experiments showed that this mutant was expressed at a markedly lower level compared to wild-type SseK3 or the ΔN13 and ΔN31 SseK3 deletion mutants (Figure 3.9B, data obtained in collaboration with S. Matthews). Therefore, loss of NF-κB pathway inhibition of the ΔN44 mutant could be due to different reasons; amino acids 32-43 are required for catalytic activity of the effector, reduced protein levels that are not sufficient to elicit a detectable phenotype or the protein is unstructured due to the N-terminal deletion. To investigate this further, wild-type SseK3 protein levels were adjusted. Titration of wild-type SseK3 to similar protein expression levels as the ΔN44 mutant showed that the loss of NF-κB pathway inhibition and inability to GlcNAcylate target proteins is an intrinsic property of the ΔN44 deletion mutant and not due to the reduced expression of the protein (Figure 3.9C and D). Taken together, strong Golgi network localisation of SseK3 is not required for NF-κB pathway inhibition but deletion of the N-terminal 44 amino acids abolishes NF-κB pathway inhibition.

3.3 Phenotypic characterisation – Host cell death inhibition

Activation of the TNF receptor leads to both NF-κB signalling and the induction of cell death in macrophages, resulting in a complex balance of pro- and anti- survival signals (Brenner et al., 2015; Vanden Berghe et al., 2015). Therefore it was next investigated if the SseK effectors also inhibit host cell death during macrophage infection.

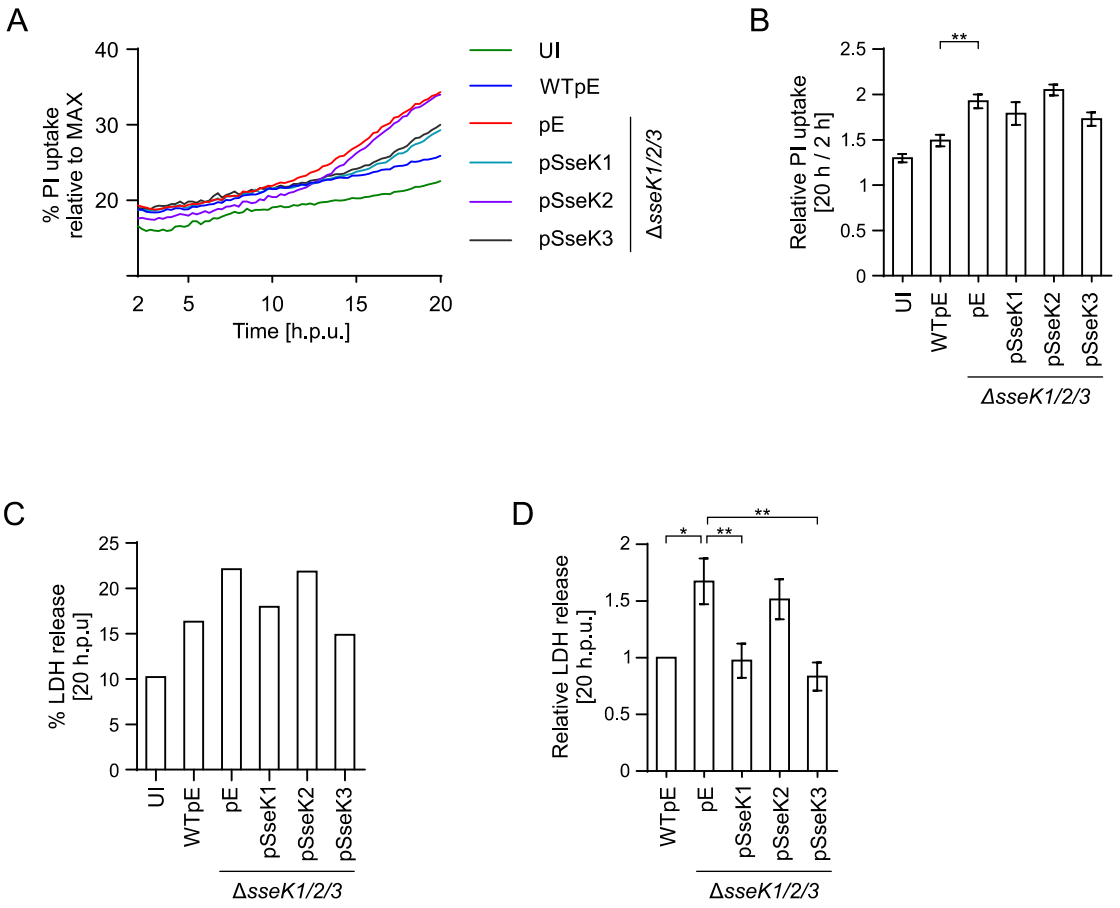

Figure 3.10. **SseK1 and SseK3 inhibit *Salmonella*-induced cell death in macrophages**

(A-B) To analyse *Salmonella*-induced cell death in RAW 264.7 macrophages cells were infected with the indicated *Salmonella* strains and the uptake of propidium iodide (PI) was measured over time. Results were calculated relative to maximum PI uptake (representative experiment (A)) and are presented as the mean fold increase relative to results at 2 h.p.u. from three independent experiments ± SEM (B). *, $P < 0.05$. (C-D) Lactate dehydrogenase (LDH) release from RAW 264.7 macrophages infected with the indicated *Salmonella* strains at 20 h.p.u. Cell death was calculated relative to a maximum control and a representative experiment is shown in (C). Additionally *Salmonella*-induced cell death was calculated and further normalised to that for WT infected cells (D). Data are the means of eight independent experiments, ± SEM. *, $P < 0.05$, **, $P < 0.01$. UI, uninfected. pE, empty plasmid.

To this end RAW 264.7 macrophages were infected with wild-type *Salmonella* or the Δ*sseK1/2/3* deletion mutant carrying a plasmid expressing a single HA-tagged SseK effector. During the course of infection the uptake of propidium iodide (PI), a cell impermeable dye that only enters cells with a compromised plasma membrane, was measured (Figure 3.10A and B). This showed that at 20 h.p.u. a significantly higher proportion of cells infected with the triple *sseK* deletion mutant became PI positive compared to wild-type infected cells (Figure 3.10B). Expression of either SseK1 or SseK3 in the Δ*sseK1/2/3* mutant had no significant effect on PI uptake compared to the triple mutant (Figure 3.10B).

To test this with an additional assay, *Salmonella* cell death was also measured by lactate dehydrogenase (LDH) release into the cell culture medium. Therefore, RAW 264.7 macrophages were infected with the indicated *Salmonella* strains and extracellular LDH levels measured 20 h.p.u. (Figure 3.10C and D). Infection with the Δ*sseK1/2/3* deletion mutant led to significantly more LDH release compared to cells infected with wild-type *Salmonella*. Expression of SseK1 or SseK3 in the triple *sseK* deletion mutant significantly restored cell death inhibition whereas expression of SseK2 was ineffective (Figure 3.10D). This shows that SseK1 and SseK3 inhibit *Salmonella* induced cell death during macrophage infection.

Under most conditions NF-κB signalling leads to the expression of pro-survival genes. However, this depends on the balance with various other immune signalling pathways and can also result in the expression of anti-survival genes (Lawrence et al., 2001; Lin et al., 1999; Perkins and Gilmore, 2006). For this reason it was next addressed if the SseK protein's effect on host cell death is a direct result of NF-κB pathway inhibition. Therefore, NF-κB reporter macrophages were pre-treated for 1 h and infected in the presence of the IKK inhibitor PS-1145 (Hideshima et al., 2002). Drug treatment significantly reduced *Salmonella* infection-induced activation of the NF-κB pathway at 20 h.p.u., without significant effect on bacterial infection and replication rates (Figure 3.11A and B). Even though NF-κB signalling was strongly decreased (Figure 3.11C), infection with the Δ*sseK1/3* deletion mutant still elicited a higher amount of LDH release than infection with wild-type *Salmonella* (Figure 3.11D). This indicates that host cell death inhibition by SseK1 and SseK3 is not a direct consequence of their ability to inhibit the NF-κB pathway.

Next it was investigated if cell death inhibition by SseK1 and SseK3 is also specific to TNFα driven cell death. To investigate this, HeLa cells were transiently transfected with plasmids

expressing GFP-tagged effectors and cell death stimulated by a 20 h treatment with a combination of cycloheximide and TNFα. Overall LDH release was calculated (Figure 3.12, left hand panels) and in addition relative cell death levels per effector (Figure 3.12, right hand panels) calculated to account for variations in basal cell death upon GFP-SseK effector expression.

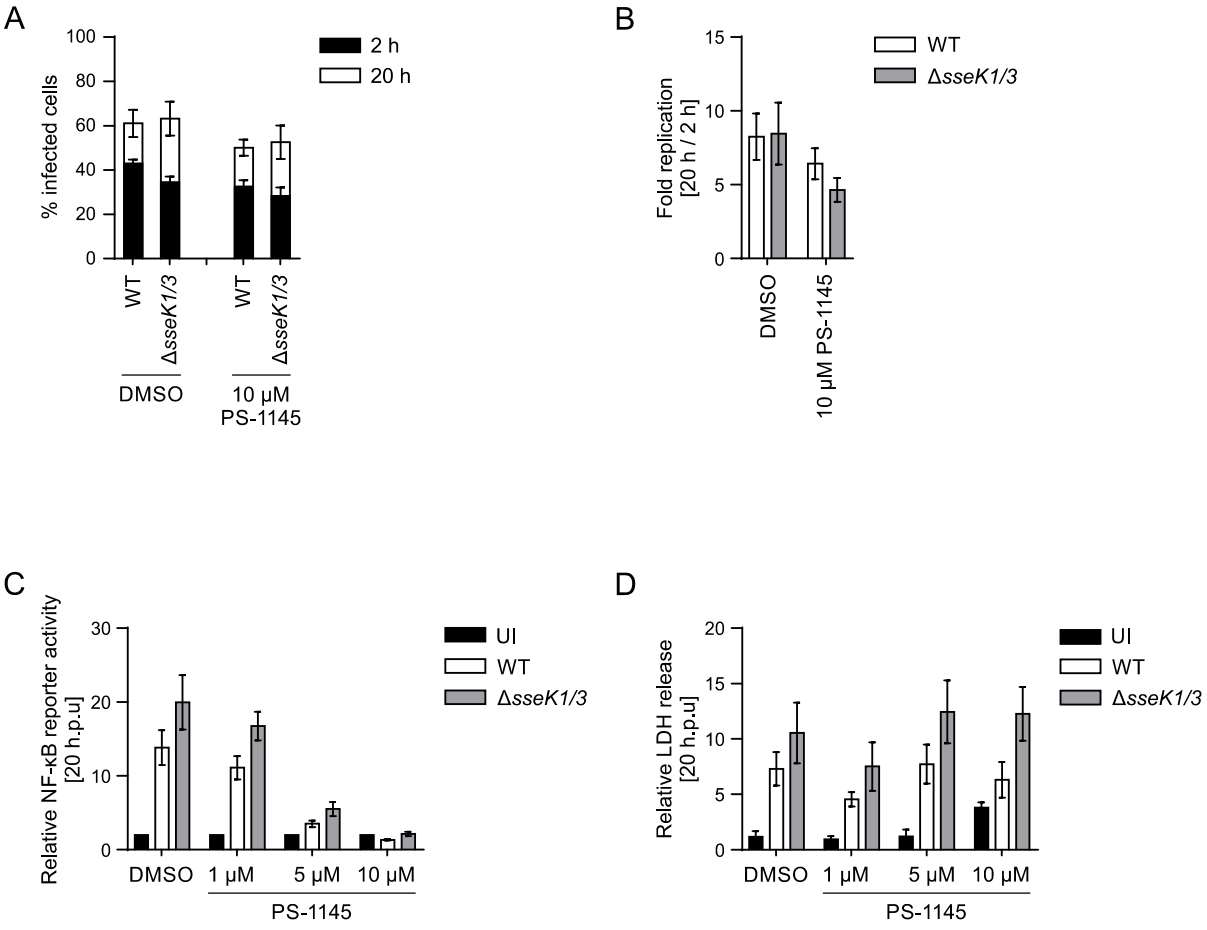

Figure 3.11. **Cell death in Δ*sseK1/3* infected macrophages is not a direct consequence of NF-κB pathway suppression**

To inhibit total NF-κB signalling in RAW 264.7 macrophages cells were pre-treated with 1, 5 or 10 μM PS-1145 or an equal volume of DMSO for 1 h and subsequently infected with *Salmonella* for 2 or 20 h in the presence of the drug. Infection rate (A) and GFP geometric mean (B) were analysed by flow cytometer as both WT and Δ*sseK1/3* mutant *Salmonella* carried the GFP expression plasmid pFPV25.1. (C) NF-κB pathway activity was assessed by infection of NF-κB reporter macrophages for 20 h, followed by lysis of the cells and analysis of luciferase activity levels. Data presented are the mean fold activation relative to uninfected cells per treatment condition from four independent experiments ± SEM. (D) The supernatant of samples from (C) were analysed for lactate dehydrogenase activity (LDH). Total cell death was calculated relative to a maximum control and is presented as them mean from four independent experiments ± SEM.

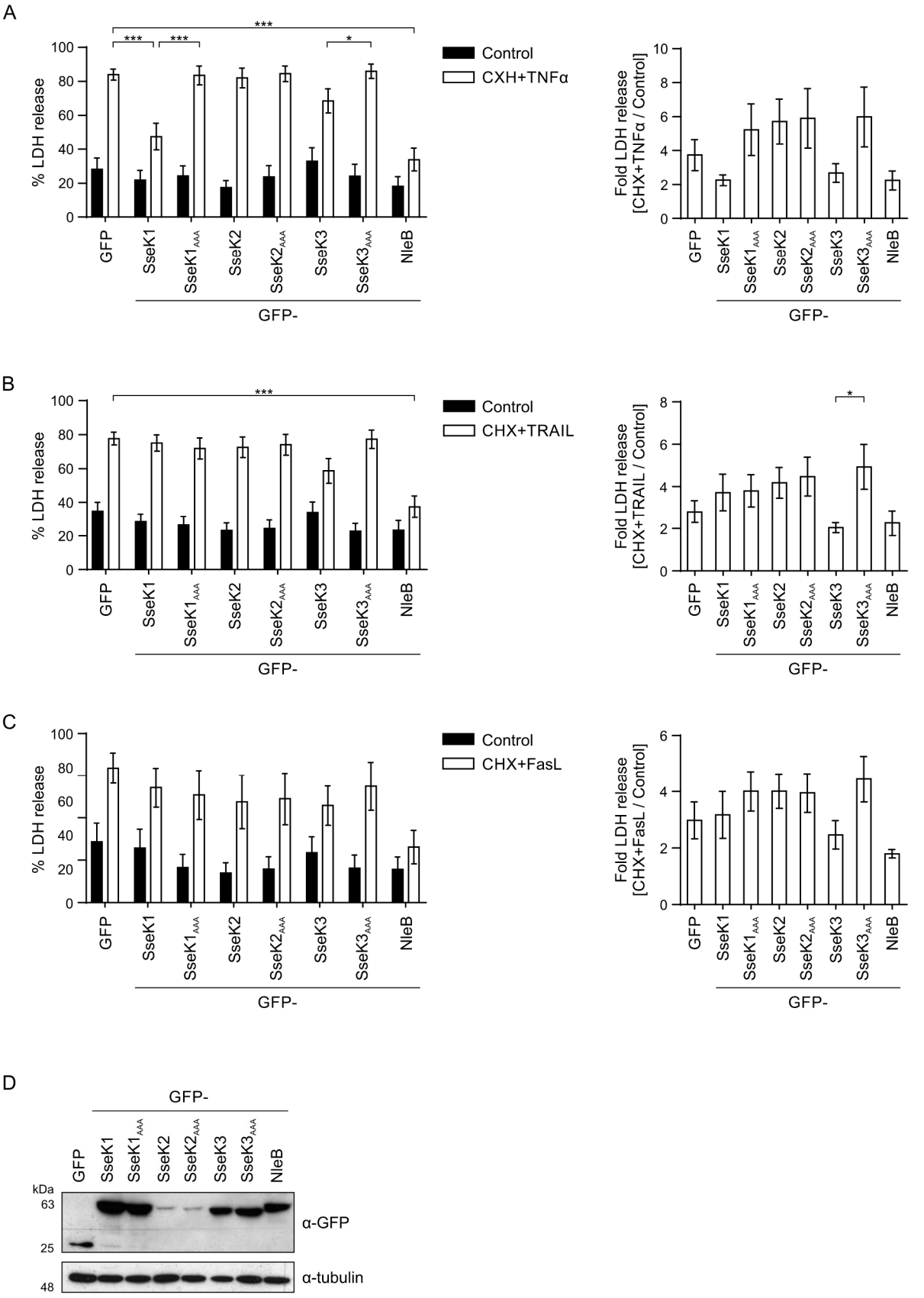

Figure 3.12. **SseK-dependent inhibition of apoptosis in HeLa cells**

Lactate dehydrogenase (LDH) release from transfected HeLa cells expressing GFP-tagged wild-type or catalytic mutant (AAA) SseK effectors. Cell death was stimulated with 10 µg/ml cycloheximide (CHX) together with 50 ng/ml TNF-α (A), 200 ng/ml TRAIL (B) or 100 ng/ml FasL (C) for 20 h. Total levels of cell death were calculated relative to a maximum control (left hand panels) and further normalised to each untreated control sample (right hand panels). Data presented are the mean results of five to nine independent experiments ± SEM. *, $P < 0.05$; ***, $P < 0.001$. Data were acquired with the help of S. Matthews. (D) Representative immunoblot of cell lysates described above. Effectors (α-GFP) and loading control (α-tubulin).

Analysis of extracellular LDH levels, as a measure of cell death, showed that SseK1 and the positive control NleB inhibited TNFα-induced cell death (Figure 3.12A). The inactive SseK1 mutant ($SseK1_{AAA}$) was incapable of cell death suppression despite similar protein expression (Figure 3.12D), indicating that this effect was dependent on the effectors enzymatic activity. Expression of SseK3 only had a minor effect on overall TNFα-driven cell death compared to control cells but this effect was again dependent on the effectors putative catalytic DxD motif (Figure 3.12A). SseK2 had no detectable effect on TNFα driven cell death in HeLa cells.

Various components of the TNFα signalling pathway are shared by the TRAIL and Fas receptors (Wilson et al., 2009) and cell death induction by these proteins is therefore also inhibited by the SseK homologue NleB (Li et al., 2013; Pearson et al., 2013). For this reason it was next investigated, in the same experimental setup as described above, if the SseK proteins inhibit TRAIL and Fas ligand (FasL) driven cell death. Interestingly, only SseK3 and NleB inhibited cycloheximide-TRAIL induced cell death (Figure 3.12B). Even though overall levels of TRAIL-induced cell death were only slightly reduced in SseK3 expressing cells (Figure 3.12B, left hand panel), normalisation to account for the increase levels of basal cell death in those cells revealed that inhibition of TRAIL-induced cell death by SseK3 was dependent on its catalytic activity (Figure 3.12B, right hand panel). In contrast, SseK1 and SseK2 were incapable of inhibiting TRAIL driven cell death in HeLa cells. Cell death induction with combined treatment of cycloheximide and FasL led to very inconsistent levels of overall cell death and the data were therefore inconclusive. (Figure 3.12C). Taken together these data show that SseK1 and SseK3 inhibit TNFα-induced cell death in HeLa cells whereas only SseK3 weakly inhibits TRAIL and potentially FasL driven cell death.

To additionally analyse stimulus specificity of the SseK effectors during the more physiological condition of *Salmonella* infection of macrophage, cell-death agonist inducing conditions were

first tested in a propidium iodide uptake assay. RAW 264.7 macrophages were highly susceptible to treatment with cycloheximide leading to complete cell death during 20 h of drug treatment despite the use of 10 times lower inhibitor concentration compared to the HeLa cell experiments (Figure 3.13). This was even further exaggerated by the addition of LPS to mimic *Salmonella* infection, resulting in 100% cell death in the first 10 h of treatment. Therefore it was not possible to address the effect of the SseK proteins on TNFα-driven cell death by performing the TNFα-cycloheximide experiments during RAW 264.7 macrophage infections.

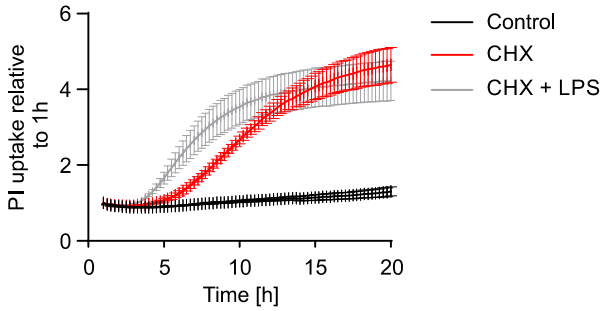

Figure 3.13. **RAW 264.7 macrophage are highly sensitive to cycloheximide**

Propidium iodine (PI) uptake analysis of RAW 264.7 macrophages treated with 1 µg/ml cycloheximide (CHX) and 1 µg/ml LPS. Results from three independent experiments were calculated relative to maximum PI uptake and are presented as the mean fold increase relative to results at 1 h ± SEM.

To circumvent the problem of cycloheximide-induced cell death in macrophages, Enbrel, a competitive TNFα inhibitor (Goffe and Cather, 2003; Gottlieb, 2007; Peppel et al., 1991), was used to test if SseK1 and SseK3 inhibit TNFα-driven cell death during macrophage infection. Overnight treatment of the NF-κB reporter macrophages with TNFα led to a strong activation of the NF-κB signalling pathway in a dose dependent manner (Figure 3.14A). This effect was significantly reduced by the addition of 10 or 50 µg/ml Enbrel to the cell culture medium (Figure 3.14B). In contrast incubation of the reporter macrophages with IL-1β did not lead to an increase in NF-κB pathway activation (Figure 3.14A). Therefore, the IL1R inhibitor Anakinra (Furst, 2004) was only used as an independent antibody control.

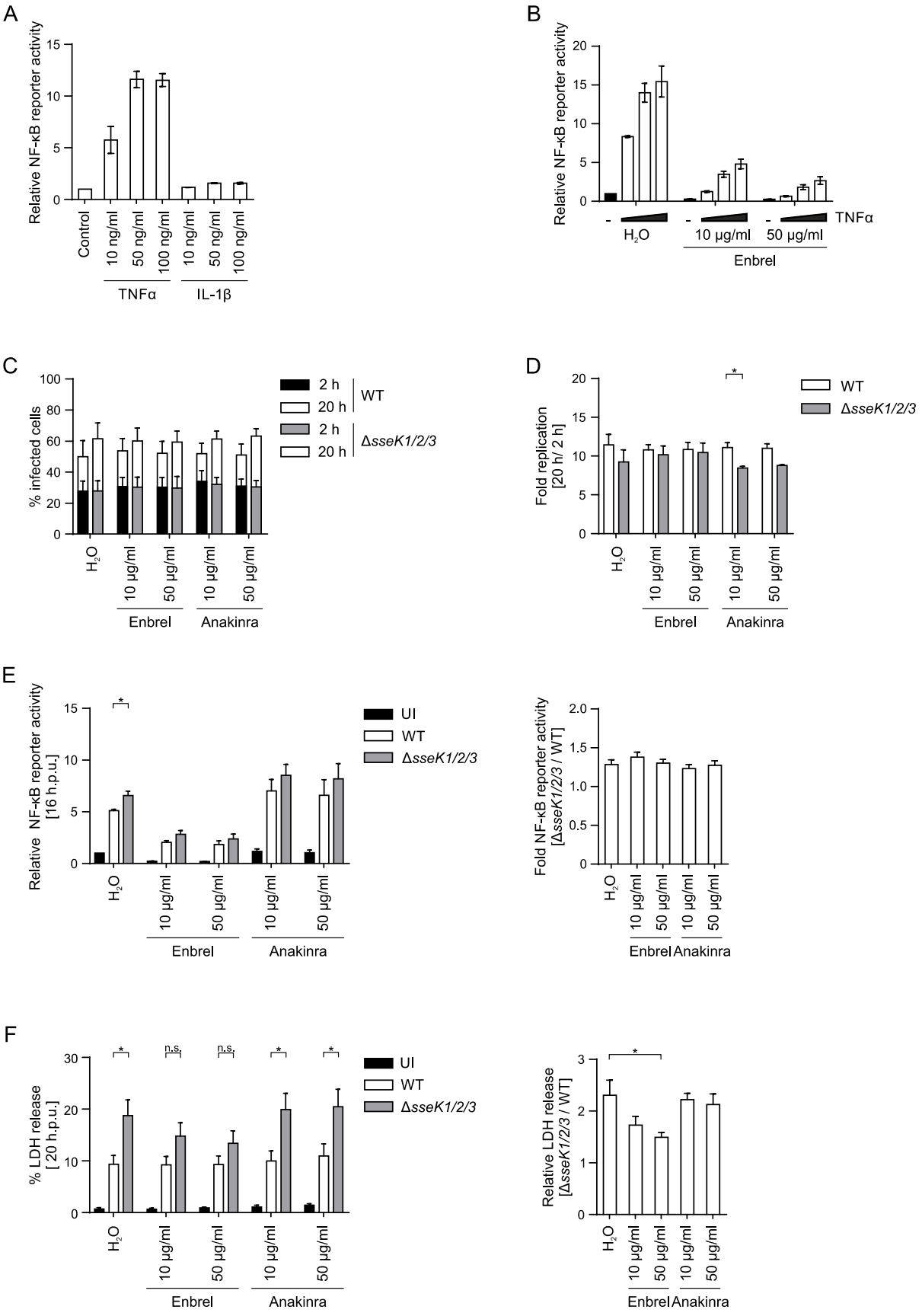

Figure 3.14. **SseK1 and SseK3 inhibit TNFa-driven cell death in macrophages**

(A) NF-κB reporter RAW 264.7 macrophages were stimulated with 10, 50 or 100 ng/ml TNFα or IL-1β for 16 h, lysed and luciferase activity levels were measured. Data are normalised to untreated control samples and represent the mean of three independent experiments ± SEM. (B) 10 or 50 µg/ml Enbrel (Etanercept, Pfizer), a competitive TNFα inhibitor, was used to block 10, 50 or 100 ng/ml TNFα driven NF-κB pathway activity. NF-κB reporter macrophages were pre-incubated for 30 min with Enbrel and the drug maintained during TNFα stimulation for 16 h. Data are normalised to untreated water control cells and represent the mean of three independent experiments ± SEM. (C-H) To inhibit TNFα driven NF-κB signalling reporter macrophages were pre-treated with 10 or 50 µg/ml Enbrel (Etanercept, Pfizer) and then infected with GFP-expressing wild-type or Δ*sseK1/2/3 Salmonella* strains in the presence of the drugs. 10 or 50 µg/ml Anakinra (Kineret, Sobi) served as a control antibody. Infection rates (C) and fold geometric mean (D) at 2 and 20 h.p.u. were analysed by flow cytometry and are the mean of three independent experiments ± SEM. *, $P < 0.05$. (E) NF-κB reporter activity was measured at 16 h.p.u. and values are presented relative to uninfected, water treated control cells (left hand panel) or normalised to each WT infected sample per condition (right hand panel). Both panels contain different normalisations of the same data and are the mean of four independent experiments ± SEM. *, $P < 0.05$. (F) Lactate dehydrogenase (LDH) release was measured at 20 h.p.u. and total cell death levels calculated relative to a maximum control (left hand panel) or each wild-type infected sample precondition (right hand panel). Both panels present different normalisations of the same data and are the mean of six independent experiments ± SEM. UI, uninfected. *, $P < 0.05$. n.s., non-significant.

Treatment of RAW 264.7 macrophages with Enbrel or Anakinra 30 min prior to and during *Salmonella* infection had no effect on bacterial infection and replication rates compared to water treated control cells (Figure 3.14C and D). However, Enbrel significantly reduced NF-κB pathway activity levels during *Salmonella* infection whereas treatment with the control antibody Anakinra was indistinguishable from water-treated cells (Figure 3.14E, left hand panel). As expected from previous experiments, 16 h of macrophage infection with the Δ*ssek1/2/3* deletion mutant resulted in a significantly higher level of NF-κB pathway activation than wild-type *Salmonella* infection in the control, water treated cells. This effect was abolished by treatment with Enbrel (Figure 3.14E, left hand panel). However, Enbrel treatment also decreased basal NF-κB pathway activity levels in uninfected cells. To account for this, the data were also analysed as fold NF-κB pathway activation of Δ*ssek1/2/3* infected compared to wild-type infected cells (Figure 3.14E, right hand panel). This showed no significant difference between water, Enbrel or Anakinra treated samples. As the interpretation of the data differs between the two normalisation methods these findings were considered inconclusive. In contrast, treatment of wild-type *Salmonella* infected macrophages with Enbrel did not alter overall *Salmonella*-induced cell death levels at 20 h.p.u. (Figure 3.14F, left hand panel). However, the increased cell death in Δ*ssek1/2/3* mutant infected control cells was reduced by treatment with Enbrel in a dose dependent manner but

not by incubation with Anakinra. Analysis of the fold cell death ratios between wild-type and mutant *Salmonella* infected cells also showed a significant decrease in cell death in Enbrel treated Δ*ssek1/2/3*infected cells compared to the control samples (Figure 3.14F, right hand panel). Taken together, this revealed that the SseK effectors inhibit TNFα-driven cell death during macrophage infection.

Activation of the TNFα receptor can lead to apoptotic or necroptotic cell death depending on the levels of (active) caspases in the cell (Vanden Berghe et al., 2015; Vercammen et al., 1998). To address which type of cell death SseK1 and SseK3 inhibit during macrophage infection, RAW 264.7 macrophages were infected for 20 h and markers for both types of cell death analysed by flow cytometry. Measurement of cells with positive Annexin-V labelling (which binds phosphatidylserine on the extracellular surface of apoptotic cells (Vermes et al., 1995)) revealed that only a small proportion of *Salmonella* infected cells undergo apoptosis during macrophage infection and this is independent of the SseK effectors (Figure 3.15A, experiments done together with T. Thurston). Additional analysis of caspase-3 and caspase-8 activation, two hallmarks of apoptotic cell death (Elmore, 2007), also showed no difference between wild-type and *sseK1/2/3* infected cells (Figure 3.15B, C and D). However, apoptosis induction by treatment with TNFα and cycloheximide resulted in clearly increased caspase activation levels compared to naïve cells, indicating that the lack of difference between wild-type and Δ*sseK1/2/3* mutant infected macrophages was not due to a technical issue (Figure 3.15D). Next, SseK dependent effects on necroptotic cell death were investigated. RAW 264.7 macrophages were infected for 20 h with either wild-type or different versions of the Δ*sseK1/2/3 Salmonella* mutant. Western blot analysis of the phosphorylation status of MLKL, an essential component of necroptotic cell death (Murphy et al., 2013; Sun et al., 2012; Zhao et al., 2012), revealed that MLKL phosphorylation levels were indistinguishable between uninfected and wild-type *Salmonella* infected macrophages. In contrast, Δ*sseK1/2/3* mutant infected cells had increased MLKL phosphorylation compared to uninfected or wild-type infected macrophages (Figure 3.15E). This effect was complemented by the expression of SseK1 and SseK3 but not SseK2. Importantly, overall levels of MLKL were not affected by *Salmonella* infection, showing that SseK1 and SseK3 only alter the post-translational modification and thereby activation status of this protein. Taken together, these results

indicate that SseK1 and SseK3 specifically inhibit necroptosis during macrophage infection with *Salmonella*.

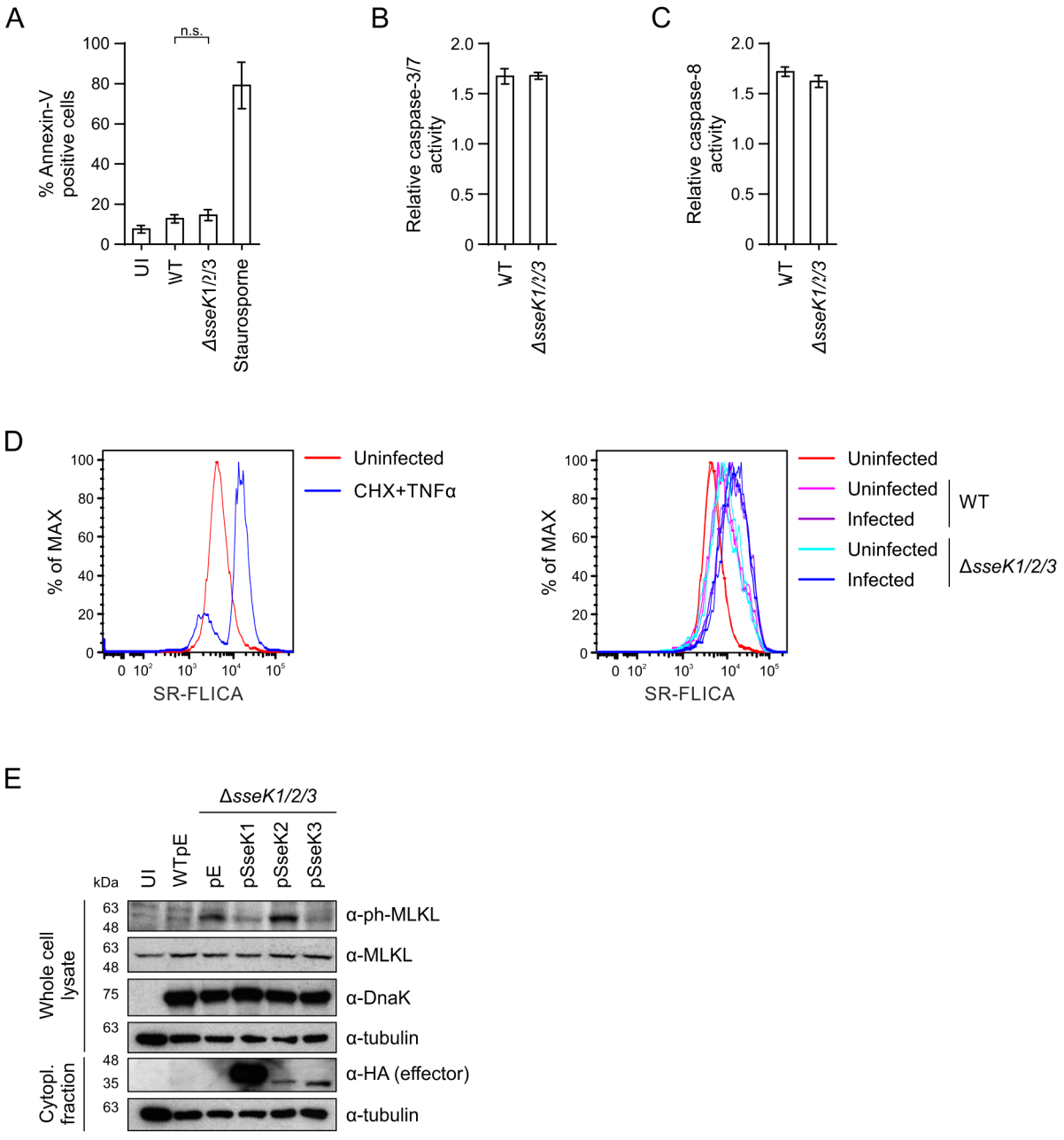

Figure 3.15. **SseK1 and SseK3 inhibit necroptotic macrophage cell death**

(A) Annexin-V labeling of RAW 264.7 macrophages infected for 20 h with the indicated GFP-expressing *Salmonella* strains was analyzed by flow cytometry. Staurosporine (1 µM) was used as a positive control to induce apoptosis. Data are the mean results of three independent experiments, ± SEM. n.s., non-significant. Data T. Thurston. (B-D) Caspase-3/7 and caspase-8 activity were analysed using the SR-DEVD-FMK (B) or FAM-LETD-FMK (C) FLICA probers respectively at 20 h.p.u. in RAW 264.7 macrophages infected with GFP-expressing *Salmonella*. The data were analyzed by flow cytometry and are presented as the fold change in activity of infected versus uninfected cells from the same sample. Values are the mean results ± SEM of three independent

experiments. Treatment with 50 µg/ml cyclohexamide and 50 ng/ml TNFα for 20 h was used as a positive control. (D) Representative histograms of (B). (E) RAW 26.47 macrophages were infected for 20 h with the indicated *Salmonella* strains, lysed and whole cell lysates and cytoplasmic proteins analysed by SDS-PAGE and immunoblotting. Phospho-MLKL (α-ph-MLKL), MLKL (α -MLKL), effectors (α -HA), *Salmonella* (α -DnaK) and loading control (α -tubulin). Data are representative of results from three independent experiments. UI, uninfected; Cytopl., cytoplasmic.

4 CHACTERISATION AND PHYSIOLOGICAL SIGNIFICANCE OF THE SSEK3-TRIM32 INTERACTION

The only published interaction partner for SseK3 is the E3 ubiquitin ligase Tripartite motif-containing protein 32 (TRIM32). Work from both our laboratory and another study (Yang et al., 2015) found that TRIM32 interacts with SseK3 in HEK293 cells. However, whether this interaction occurs during *Salmonella* infection and if it is physiologically relevant for SseK3's function was not further addressed.

The SseK3-TRIM32 interaction could have four different outcomes in the host cell: (i) The interaction is neutral and has no effect on the function of either protein, (ii) SseK3 alters TRIM32 function, (iii) TRIM32 changes SseK3 function or (iv) the interaction alters the function of both proteins.

TRIM32 has previously been reported to activate NF-κB signalling and modulate apoptotic cell death (Albor et al., 2006; Cui et al., 2016; Horn et al., 2004; Ito et al., 2017) and I have shown in Chapter 3 that SseK3 inhibits both NF-κB signalling and host cytotoxicity during *Salmonella* infection. Therefore, I hypothesised that during *Salmonella* infection of macrophages the effects of SseK3 on both NF-κB signalling and host cytotoxicity pathways are dependent on TRIM32.

This chapter summarises my work to characterise the SseK3-TRIM32 interaction and investigates the effects of SseK3 on TRIM32 function. In addition it summarises work addressing the reciprocal effect of TRIM32 on SseK3 function during macrophage infection with focus on the NF-κB pathway and host cell death. In the last section of this chapter the requirement of TRIM32 for short term, systemic *Salmonella* infections in the mouse model was investigated to gain a more comprehensive understanding of TRIM32 physiology.

4.1 Characterisation of the SseK3-TRIM32 interaction

To test if TRIM32 interacts with SseK3 during *Salmonella* infection, RAW 264.7 macrophages were infected for 16 h with *Salmonella* strains expressing HA-tagged SseK effectors. Translocated effector proteins were then immunoprecipitated from the host cell cytoplasm and bound proteins analysed by SDS-PAGE and western blot. TRIM32 bound stably

to translocated SseK3, but not SseK1, SseK2 or the negative control SseL during *Salmonella* infection (Figure 4.1A). This strengthens the hypothesis that the SseK effectors have different host cell targets during macrophage infection.

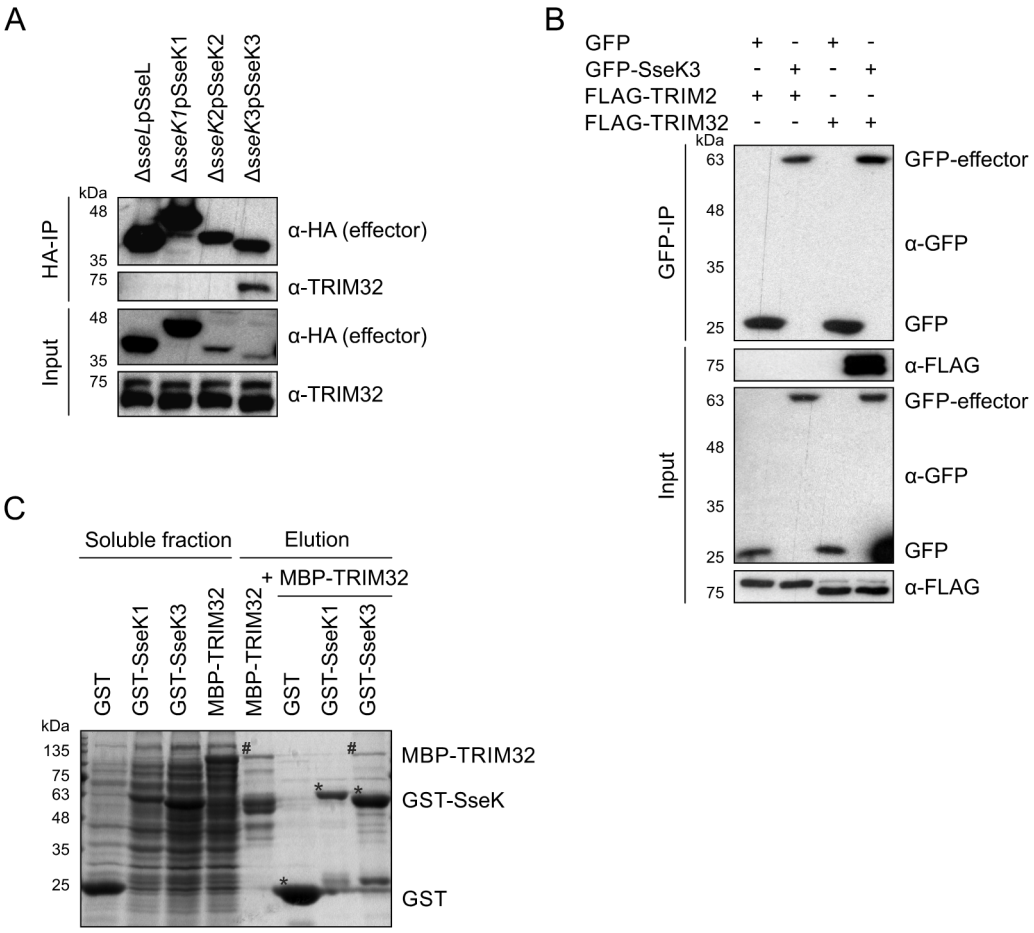

Figure 4.1. **TRIM32 is a direct and specific interaction partner of SseK3**

(A) RAW 264.7 macrophages were infected for 16 h with the indicated Salmonella strains, lysed, proteins α-HA-immunoprecipitated (IP) and analysed by SDS-PAGE and immunoblotting. Effectors (α-HA), TRIM32 (α-TRIM32). (B) 293ET cells were co-transfected with plasmids encoding GFP-(SseK3) and FLAG-tagged TRIM proteins. After 24 h cells were lysed, proteins α-GFP-immunoprecipitated and analysed by SDS-PAGE and immunoblotting. Effectors (α-GFP), TRIMs (α-FLAG), arginine-GlcNAc (α-Arg-GlcNAc) and loading control (α-tubulin). (C) Recombinant MBP-TRIM32 and GFP-tagged effectors were purified, mixed and interaction tested by α-GST-immunoprecipitation. Samples were analysed by SDS-PAGE and visualised by coomassie staining. # indicates full length MBP-TRIM32, * marks full length GST, GST-SseK1 or GST-SseK3. Data shown are representative of two to four independent experiments.

Based on the proteins' domain structure TRIM32 is grouped with TRIM2, TRIM3 and TRIM71 as C-VII TRIM-NHL proteins (Tocchini and Ciosk, 2015). To investigate if SseK3 specifically

interacts with TRIM32 or also other C-VII proteins, binding to TRIM2 was tested. To do this, plasmids encoding GFP-SseK3 and FLAG-tagged TRIM proteins were co-transfected into 293ET cells. Subsequently, proteins were isolated by GFP-immunoprecipitation and analysed by SDS-PAGE and immunoblotting. This revealed that SseK3 selectively interacted with TRIM32 but not the related TRIM2 (Figure 4.1B), whereas GFP alone interacted with neither TRIM protein. This showed specificity of SseK3 to interact with TRIM32 but not TRIM2.

To investigate whether the detected interaction between SseK3 and TRIM32 is direct, *in vitro* binding assays were conducted with recombinant proteins. To this end MBP-TRIM32, GST, GST-SseK1 and GST-SseK3 were expressed in *E. coli* and isolated by affinity purification. Eluted MBP-TRIM32 protein was then incubated with GST or GST-SseK fusion proteins, isolated by sepharose resin precipitation and binding analysed by SDS-PAGE and Coomassie Blue staining. Full length MBP-TRIM32 interacted directly with GST-SseK3 but not with GST alone or GST-SseK1 (Figure 4.1C), indicating that the TRIM32-SseK3 interaction is (a) direct and (b) specific and not due to the GST-tag. Recombinant full-length TRIM32 (Figure 4.1C, indicated by the # symbol) was unstable, resulting in degradation of the protein. Therefore, *in vitro* ubiquitination experiments with purified protein to test if SseK3 is ubiquitinated by TRIM32 were not pursued. Taken together, these results show that SseK effectors bind to different host proteins with SseK3 but not SseK1 or SseK2 interacting with TRIM32 and that SseK3 does not interact with all NHL-containing TRIM proteins but specifically with TRIM32.

TRIM32 localises to cytosolic peri-nuclear speckles (Ichimura et al., 2013; Kawaguchi et al., 2017; Locke et al., 2009) as well as the Golgi network, where it partially co-localises with ectopically expressed SseK3 (Yang et al., 2015). I have shown in chapter 3 that the first 13 amino acids of SseK3 are required for its localisation to the Golgi network (Figure 3.4). To test whether the N-terminal region of SseK3 also mediates the SseK3-TRIM32 interaction, 293ET cells were co-transfected with plasmids encoding FLAG-TRIM32 and various GFP-tagged SseK3 mutants. The ability of TRIM32 to interact with the SseK3 deletion mutants was then analysed by anti-GFP immunoprecipitation and immunoblotting. Wild-type and ΔN13 SseK3 both interacted with TRIM32 (Figure 4.2A), indicating that strong Golgi network localisation of the effector is not required for the SseK3-TRIM32 interaction.

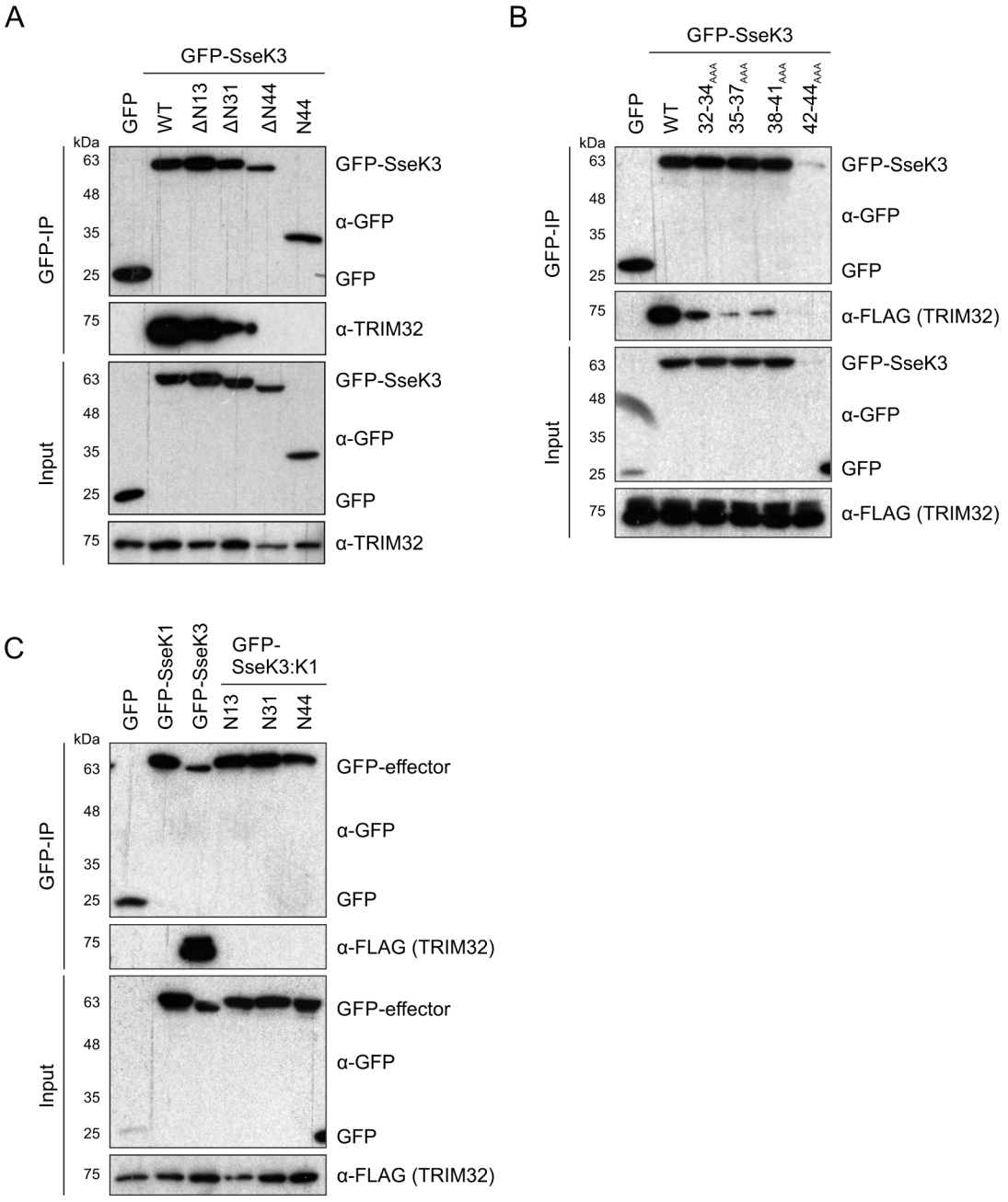

Figure 4.2. **SseK3 N-terminal region (N44) is required but not sufficient for TRIM32 interaction**

293ET cells were transiently transfected with plasmids expressing FLAG-tagged TRIM32 and GFP-tagged SseK variants. Protein-protein interactions were tested by cells lysis, α-GFP immunoprecipitation and samples were analysed by SDS-PAGE and immunoblotting. (A) Analysis of various N-terminal deletion mutants of SseK (ΔN13, ΔN31, ΔN44) and a short N-terminal SseK3 fragment (N44). (B) Analysis of four SseK3 variants with amino acid substitution to alanine between positions 32 to 44. (C) Analysis of chimeric SseK3-SseK1 fusion proteins containing the SseK3 N-terminus and the main portion of SseK1. Effectors (α-GFP) and TRIM32 (α-FLAG). Data shown are representative of two to three independent experiments.

Deletion of the 31 N-terminal amino acids of SseK3 ($SseK3_{\Delta N31}$) reduced TRIM32 binding compared to the wild-type protein and TRIM32 interaction was completely lost when the ΔN44 deletion mutant of SseK3 ($SseK3_{\Delta N44}$) was used (Figure 4.2A). However, the SseK3 N-terminal 44 amino acids alone fused to GFP ($SseK3_{N44}$) were not sufficient for TRIM32 to stably interact with SseK3 (Figure 4.2A). It is important to note that the ΔN44 mutant of SseK3 was poorly expressed and/or unstable and therefore four times the $SseK3_{\Delta N44}$ DNA amount was transfected to achieve similar protein levels to wild-type SseK3 (Figure 4.2A).

To identify which amino acids of SseK3 are required for TRIM32 binding, SseK3 variants with blocks of three to four alanine substitutions between amino acids 32-44 were created and their binding to TRIM32 assessed. TRIM32 binding to $SseK3_{32\text{-}34AAA}$, $SseK3_{35\text{-}37AAA}$ and $SseK3_{38\text{-}41AAA}$ was markedly reduced compared to wild-type SseK3 (Figure 4.2B). However, there was no consistent difference between the mutants that could point to a specific amino acid required for the SseK3-TRIM32 interaction. Substitution of residues 42-44 to alanine in SseK3 ($SseK3_{42\text{-}44AAA}$) resulted in poor expression and it was therefore not possible to determine whether these amino acids are required for SseK3 interaction with TRIM32 (Figure 4.2B).

To circumvent the problem of unstable $SseK3_{\Delta N44}$ expression and to test the protein regions of SseK3 required for interaction with TRIM32 from a different angle, SseK3:SseK1 chimeric proteins were created. This had two advantages: (i) Protein stability was not affected and protein folding was predicted to be maintained due to the high amino acid identity between the SseK effectors. (ii) As the SseK3 N-terminal 44 amino acids were not sufficient for TRIM32 binding, SseK3:K1 chimeras might reveal conserved SseK sequences that are additionally required for the SseK3-TRIM32 interaction. Interaction between ectopically expressed SseK3:K1 chimeras and FLAG-TRIM32 was analysed as described above. Three chimeric proteins were tested; $SseK3_{N13}$:$K1_{\Delta N12}$, $SseK3_{N31}$:$K1_{\Delta N30}$, $SseK3_{N44}$:$K1_{\Delta N43}$. Each showed expression indistinguishable from wild-type SseK1 (Figure 4.2C), cytosolic localisation in the cell (data not shown) and none of the chimeras stably interacted with TRIM32, whereas wild-type SseK3 did (Figure 4.2C). This suggests that binding of SseK3 to TRIM32 requires additional regions of SseK3 than just the N-terminal 44 amino acids. To investigate this further a collaboration with Diego Esposito and Katrin Rittinger (Francis Crick Institute, London) was established to determine the crystal structure of SseK3 (in complex with TRIM32). Taken

together, these data show that amino acids 32-44 of SseK3 might be required for binding to TRIM32, however it cannot be excluded that mutation of these amino acids resulted in the unfolding of the protein. Nevertheless, strong Golgi network localisation, mediated by the first 13 amino acids of SseK3, is clearly not required for TRIM32 interaction.

4.2 Investigation of effects of SseK3 on TRIM32

4.2.1 TRIM32 is not an SseK3 GlcNAcylation target and TRIM32 target binding is not detectably altered by SseK3

Arginine-GlcNAcylation of death domain proteins like FADD or TRADD by NleB prevents the oligomerisation of the proteins, rendering them non-functional. Experiments by Yang and colleagues did not detect GlcNAcylation of TRIM32 by SseK3 when using an *O*-GlcNAc specific detection antibody (Yang et al., 2015). However, this antibody was raised against *O*-linked serine-/threonine-GlcNAc residues and only interacts weakly with the arginine-GlcNAc post translational modification (Pan et al., 2014). Therefore, putative modification of TRIM32 by SseK3 was analysed using the Arg-GlcNAc specific antibody that does not detect endogenous GlcNAc posttranslational modifications (Pan et al., 2014). To do this, FLAG-TRIM32 and GFP-tagged effectors were expressed ectopically in 293ET cells and isolated by anti-FLAG-immunoprecipitation. Immunoblotting showed that SseK3 interacted stably with TRIM32 but no arginine-GlcNAcylation of the E3 ligase was detected upon co-expression with SseK1, SseK2, SseK3 or NleB (Figure 4.3). This confirmed previous findings (Yang et al., 2015), that TRIM32 is not a substrate of SseK3 despite stable interaction occurring between the two proteins.

Several substrates of TRIM32, including STING, XIAP and p53 interact with the C-terminal NHL repeat domain (aa 359-647) of TRIM32 (Liu et al., 2014; Ryu et al., 2011; Zhang et al., 2012). In addition, SseK3 also interacts with the NHL-domain of TRIM32 (T. Thurston, personal communication). Therefore, one hypothesis is that SseK3 might occlude TRIM32 from (directly or indirectly) interacting with and/or modifying other mammalian proteins. To test this, the interaction of TRIM32 with four previously published, immune relevant proteins was analysed (Interleukin-1 receptor-associated kinase 1 (IRAK1) (Li et al., 2011), stimulator of

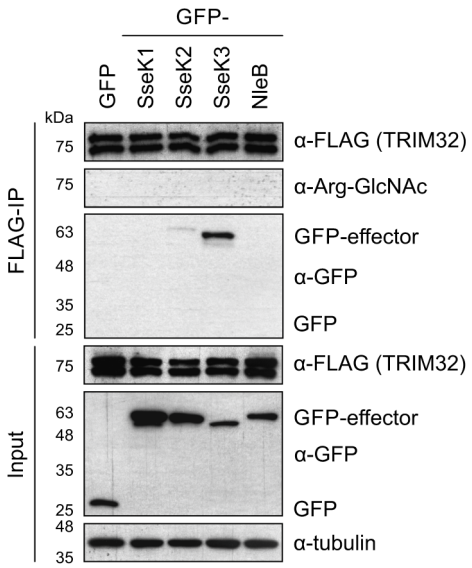

Figure 4.3. **SseK3 does not arginine-GlcNAcylate TRIM32**

293ET cells were co-transfected with plasmids encoding GFP-effectors and FLAG-TRIM32. After 40 h cells were lysed, proteins α-FLAG-immunoprecipitated and analysed by SDS-PAGE and immunoblotting. Effectors (α-GFP), TRIM32 (α-FLAG), arginine-GlcNAc (α-Arg-GlcNAc) and loading control (α-tubulin). Data is representative for three independent experiments.

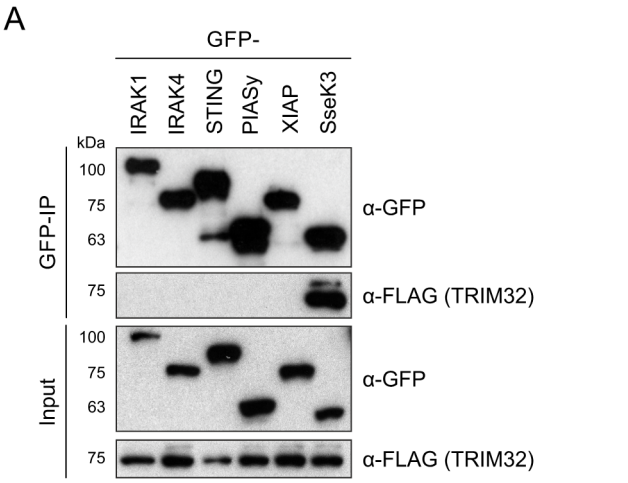

Figure 4.4. **Analysis of TRIM32 interaction partners**

(A) Plasmids encoding FLAG-TRIM32 and GFP-tagged published interaction partners were co-transfected into 293ET cells. TRIM32 interaction with target proteins was analysed by cell lysis, α-GFP immuno-precipitation and proteins were analysed by SDS-PAGE and immuno-blotting. Effectors (α-GFP) and TRIM32 (α-FLAG). The immunoblot shown is representative of two independent experiments. (B) RAW 267.4 macrophages stably expressing GFP-TRIM2 or GFP-TRIM32 were infected with wild-type (WT) or Δ*sseK3 Salmonella*. After 16 h cells were lysed, proteins isolated by α-GFP co-immunoprecipitation and analysed by SDS page and coomassie staining. The presented data is representative for three independent experiments. UI, uninfected.

interferon genes (STING) (Zhang et al., 2012), protein inhibitor of activated STAT protein γ (PIASγ) (Albor et al., 2006) and X-linked inhibitor of apoptosis protein (XIAP) (Ryu et al., 2011)). After co-transfection of plasmids encoding the GFP-tagged target proteins and FLAG-TRIM32 into 293ET cells, followed by anti-GFP immunoprecipitation, no stable interaction of TRIM32 to IRAK1, STING, PIASγ or XIAP was detected under the tested conditions (Figure 4.4A). As expected SseK3 interacted with TRIM32. Therefore, the effect of SseK3 on these specific TRIM32 targets could not be further addressed.

As an alternative approach to analyse TRIM32-interacting proteins, GFP-tagged TRIM32 was immunoprecipitated from uninfected, WT and Δ*sseK3* mutant *Salmonella* infected RAW 264.7 macrophages. After 16 h of infection, GFP-TRIM32 was isolated from the stably transduced RAW 264.7 macrophages and bound proteins analysed by SDS-PAGE and Coomassie Blue staining. No obvious differences in the proteins co-immunoprecipitated with GFP-TRIM32 were detected in cell lysates from uninfected and *Salmonella* infected samples (Figure 4.4B). In addition, the band pattern of TRIM32-bound proteins from WT and Δ*sseK3* infected cell lysates were indistinguishable (Figure 4.4B). Additional silver staining of the gels revealed more proteins, but again no differences between the uninfected, WT and Δ*sseK3* mutant *Salmonella*-infected macrophage lysates were detected (data not shown). Patterns of GFP-TRIM2 bound proteins, analysed as a control, were different from GFP-TRIM32 samples (Figure 4.4B), indicating that at least some detected proteins were specific to TRIM32.

4.2.2 SseK3 does not affect inhibition of IFNβ signalling by TRIM32

The best characterised functions of TRIM32 (e.g. muscle degeneration and neuronal development) have no obviouse relevance during *Salmonella* infection of macrophages where the SseK3 phenotypes were detected. However, TRIM32 has been described to alter NF-κB and ISRE reporter levels when overexpressed or depleted (Uchil et al., 2013; Versteeg et al., 2013; Yang et al., 2015). As the published results on whether TRIM32 is a positive or negative regulator of immunity are contradictory, the effect of TRIM32 overexpression on both pathways was first tested and then any alteration by SseK3 investigated. To do this, 293ET cells were transfected with an NF-κB or ISRE luciferase reporter plasmid, the constitutively expressed Renilla Luciferase plasmid and plasmids encoding the indicated FLAG-tagged TRIM proteins and/or GFP or GFP-SseK3. Then the cells were stimulated

overnight with the indicated agonists and luciferase levels measured and reporter activation calculated relative to unstimulated, GFP expressing control cells (Figure 4.5A, C and E, left side panels). Protein expression was confirmed by immunoblotting (Figure 4.5B and D). Analysis of the NF-κB pathway activity revealed that expression of TRIM32 did not change the amount of TNFα-driven reporter activation compared to the GFP control (Figure 4.5A, left side panel). However, it is important to note that expression of TRIM32 significantly increased basal reporter activity ($P < 0.001$). This was due to a reduction in Renilla Luciferase levels compared to GFP expressing cells. To account for changes in basal NF-κB reporter activation, fold activation for each transfection condition (stimulated/basal activation levels) was additionally calculated (Figure 4.5A, C and E, right side panels). This analysis showed that the fold NF-κB reporter activation was reduced significantly in TRIM32 expressing cells but not upon expression of TRIM2 or TRIM3 (Figure 4.5A, right side panel). Whether this is a genuine effect of TRIM32 or an artefact of the reduced Renilla levels in the TRIM32-expressing cells is currently not clear. Therefore these experiments were not pursued further.

Expression of TRIM32 significantly inhibited IFNβ-induced ISRE reporter activation compared to control GFP samples, whereas TRIM2 and TRIM3 caused a modest but significant increase in reporter activity (Figure 4.5C). This was apparent when comparing overall activation levels of the IFNβ-stimulated ISRE reporter (Figure 4.5C, left side panel) as well as fold activation of the luciferase reporter (Figure 4.5C, right side panel) revealing that TRIM32 overexpression inhibits IFNβ signalling. To test if the TRIM32-mediated inhibition of IFNβ-induced ISRE reporter activation can be altered by SseK3, GFP or GFP-SseK3 were coexpressed with TRIM32 in the transfection ISRE reporter assay. Expression of SseK3 alone had no effect on basal or IFNβ-stimulated ISRE reporter activity (Figure 4.5E). In addition co-expression of SseK3 with TRIM3 or TRIM32 did not alter the E3 ligases' effects on IFNβ signalling. Reduced IFNβ stimulated ISRE reporter activity in TRIM32 expressing cells was similar in control GFP and GFP-SseK3 expressing cells (Figure 4.5E). The lack of an SseK3 effect was not due to lack of protein expression, as western blotting confirmed the presence of GFP-SseK3 (Figure 4.5F).

These data suggest that SseK3 does not counteract TRIM32-mediated inhibition of IFNβ signalling.

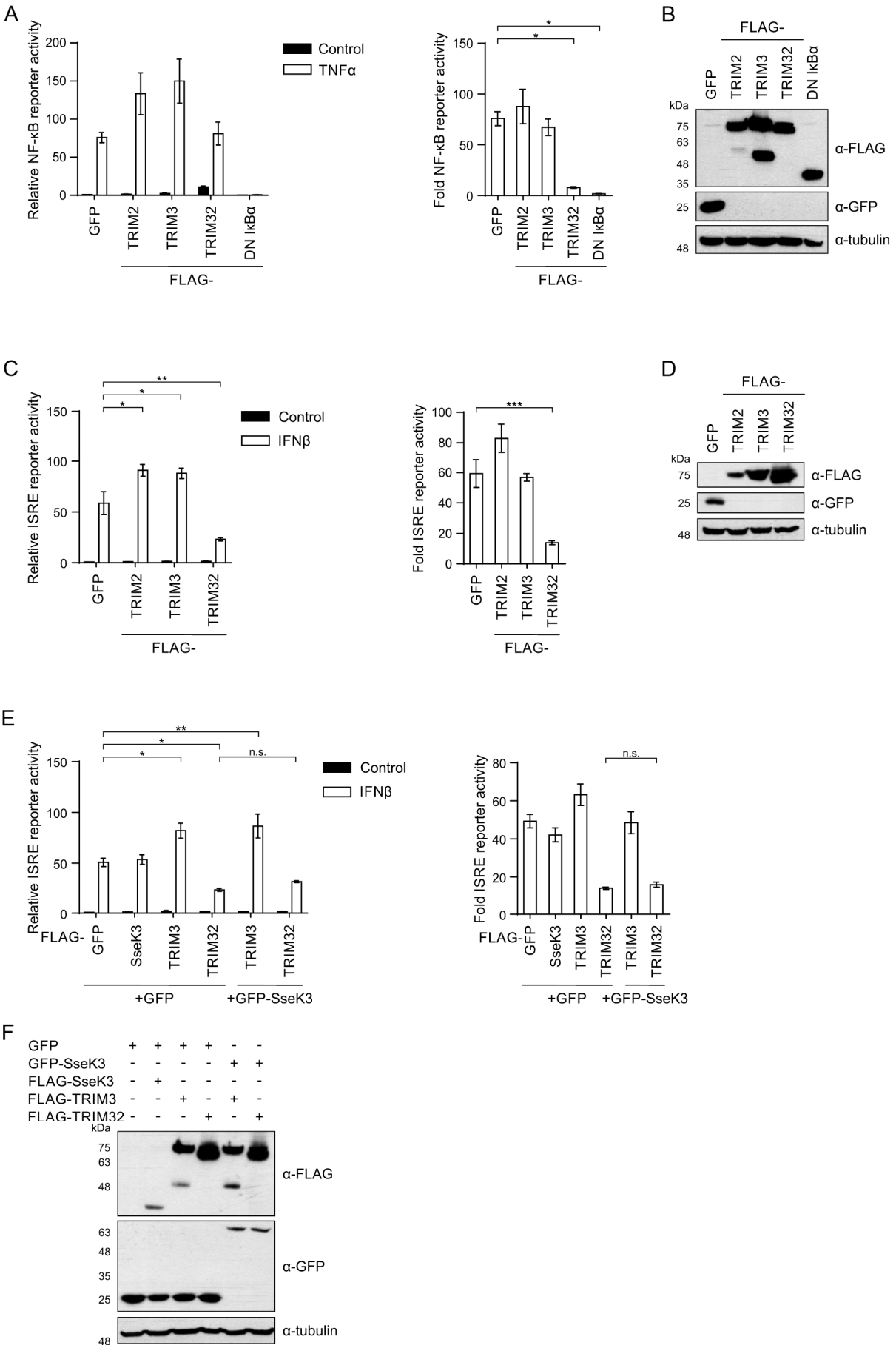
A
Relative NF-κB reporter activity
Control
TNFα
GFP
TRIM2
TRIM3
TRIM32
DN IκBα
FLAG-
Fold NF-κB reporter activity
B
FLAG-
kDa
α-FLAG
α-GFP
α-tubulin
C
Relative ISRE reporter activity
Control
IFNβ
Fold ISRE reporter activity
D
E
n.s.
SseK3
+GFP
+GFP-SseK3
F
GFP-SseK3
FLAG-SseK3
FLAG-TRIM3
FLAG-TRIM32

Figure 4.5. **SseK3 does not counteract TRIM32 inhibition of IFNβ-driven ISRE reporter activity**

293ET cells were cotransfected with the NF-κB (A) or ISRE (C, E) luciferase reporter plasmid, pTK-Renilla luciferase plasmid and ptCMV plasmids expressing the indicated TRIM and SseK proteins. Cells were stimulated overnight with50 ng/ml TNFα or concentration IFNβ, then lysed and luciferase activities assayed. The same data are shown either as the fold activation relative to the activity of unstimulated, GFP-expressing control cells (left hand panels) or as the fold activation relative to the activity of each unstimulated control (right hand panels). All data presented are the mean of four independent experiments ± SEM. (B, D, F) Representative immunoblots of cell lysates from A, C and E, respectively. TRIMs (α-FLAG), SseK3 (α-GFP or α-FLAG) and loading control (α-tubulin).

4.3 Investigation of TRIM32 effects on SseK3 physiology

To test if TRIM32 is required for SseK3 function during *Salmonella* infection, TRIM32 CRISPR knock-out RAW 264.7 macrophages were used (Günster et al., 2017). Initial characterisation of the cells identified the deletion of two cytosine base pairs in the TRIM32 sequence. The resulting frameshift in the protein caused complete loss of detectable TRIM32 (Figure 4.5, Figure 4.6A and B). Bacterial replication in wild-type macrophages, control cells that unsuccessfully underwent the CRISPR procedure (CRISPR control) and TRIM32 KO macrophages was analysed by flow cytometry. No significant differences in the infection rate and replication of wild-type *Salmonella* were detected in any of the three cell types at 16 h.p.u. (Figure 4.6C and D, data T. Thurston). Replication of the Δ*sseK1/2/3* mutant strain was also not affected by the deletion of TRIM32 (Figure 4.6C and D). This made the cell line suitable for comparative *Salmonella* infection studies.

4.3.1 The translocation, localisation and stability of SseK3 in the host cell is independent of TRIM32

Post translational modification and changes to effector specificity mediated by host proteins is an emerging concept in cellular microbiology (Popa et al., 2016). To test whether translocation, localisation and stability of SseK3 requires its TRIM32 interaction, TRIM32 KO cells were analysed. Wild-type and TRIM32 KO macrophages were infected for 16 h with *Salmonella* strains expressing HA-SseK3 and effector translocation was analysed.

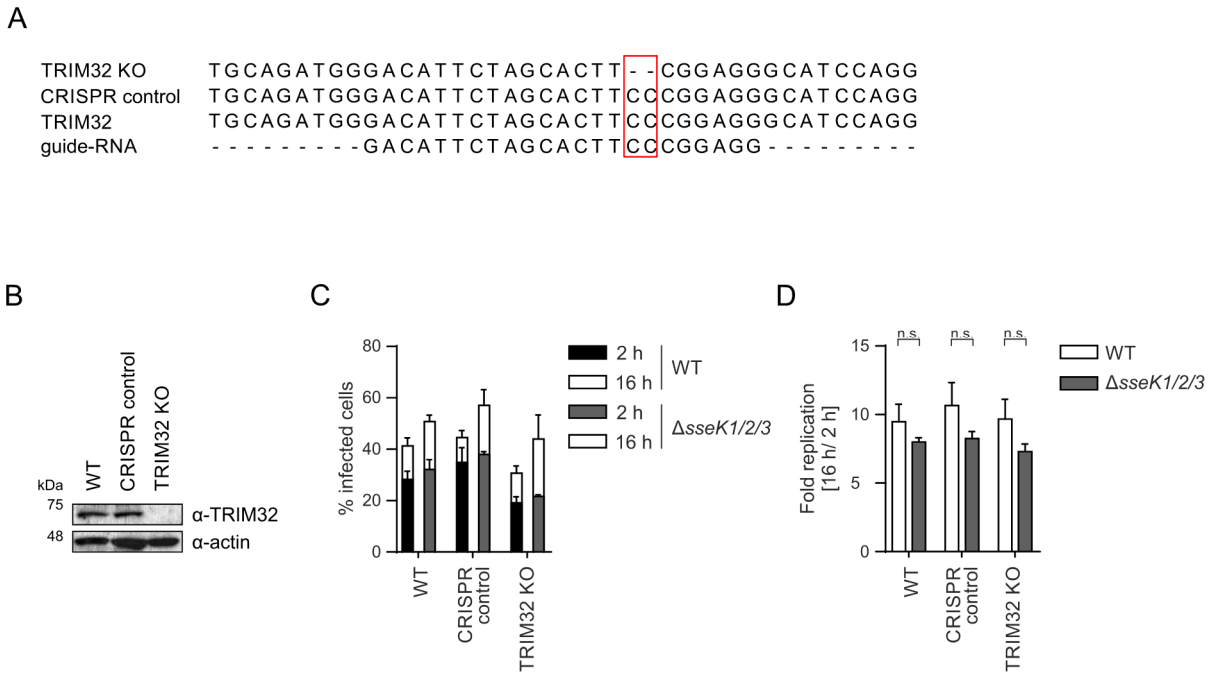

Figure 4.6. **Characterisation of CRISPR generated TRIM32 KO macrophages**

(A) Sequence alignment of *Trim32* in wild-type RAW 264.7 macrophages, CRISPR generated TRIM32 knock-out (KO) cells and the guide-RNA used to generate the KO. A clonal population of macrophages that went through the CRISPR knockout procedure unsuccessfully served as an additional negative control (CRISPR control). The red box highlights the base pair deletion in the TRIM32 KO genome. Alignment generated with Jalview (Waterhouse et al., 2009). (B) Representative immunoblot of whole cell lysates from wild-type, CRISPR control and CRISPR generated TRIM32 KO RAW 264.7 macrophages. TRIM32 (α-TRIM32) and loading control (α-actin). (C, D) Wild-type, CRISPR control or TRIM32 KO RAW 264.7 macrophages were infected with the indicated *Salmonella* strains expressing GFP for 2 and 16 h. At these time points bacterial infection rates (C) and replication assessed by flow cytometry. Fold replication at 16 h.p.u. (D) was calculated relative to 2 h.p.u. and is presented as the mean from three independent experiments ± SEM. n.s., not significant. Data was acquired by T. Thurston.

No difference in amount of translocated SseK3 protein was detected in wild-type and TRIM32 KO cells when SseK3 protein levels were analysed by SDS-PAGE and immunoblotting (Figure 4.7A). Analysis by confocal microscopy revealed that approximately 70% of infected cells contained detectable levels of SseK3 in both wild-type and TRIM32 KO macrophages. Furthermore, SseK3 localisation to the Golgi network was detected in all cells with translocated effector, independent of TRIM32 (Figure 4.7B and C).

TRIM32 is an E3 ubiquitin ligase that targets several of its interaction partners for degradation (Locke et al., 2009; Mokhonova et al., 2015). To test if TRIM32 mediates the degradation of SseK3, the half-life of ectopically expressed Ssek3 in the presence and absence of

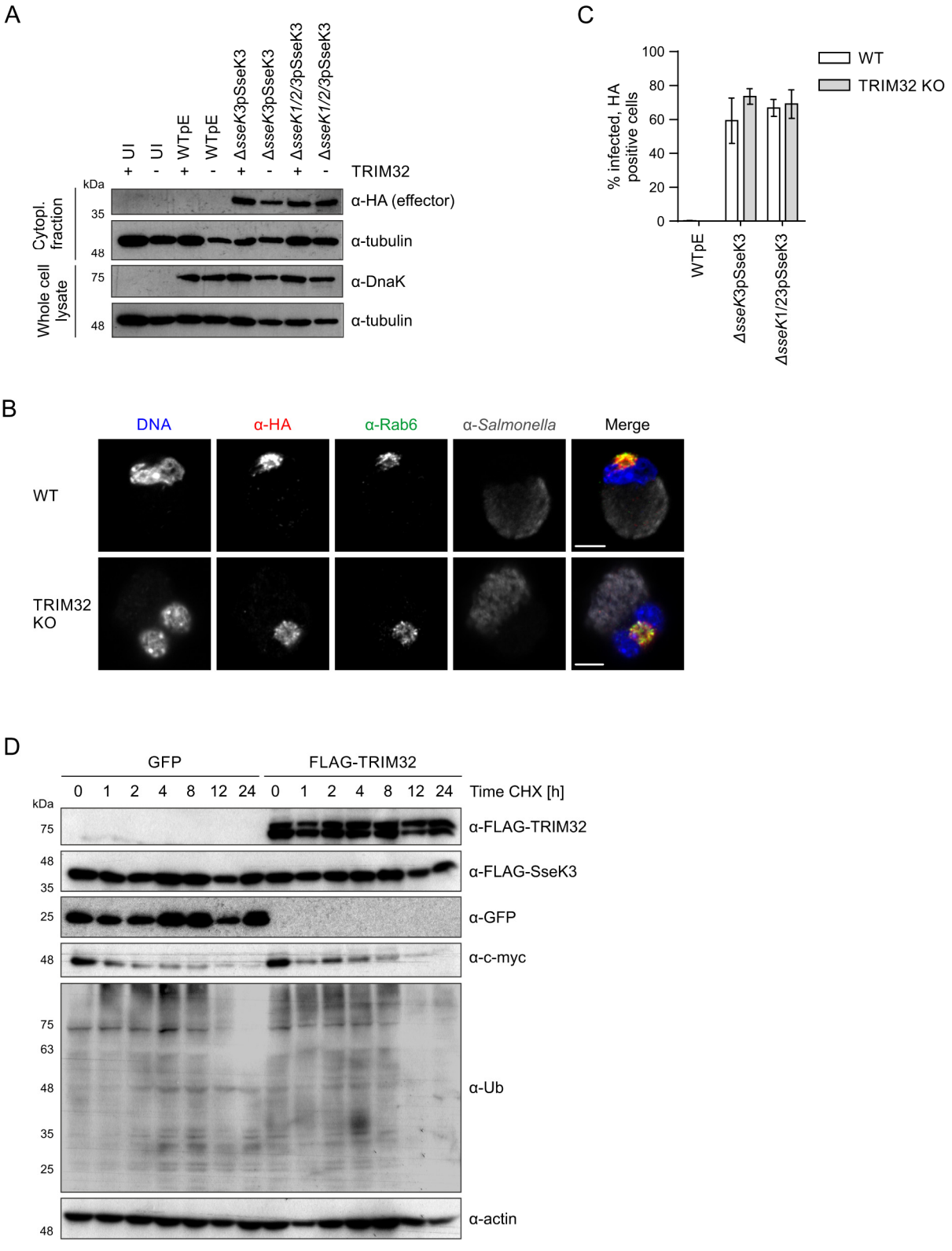

Figure 4.7. **TRIM32 does not affect SseK3 translocation, localisation or protein stability**

(A) Wild-type (WT) and TRIM32 KO RAW 264.7 macrophages were infected with the indicated *Salmonella* strains. 16 h.p.u. cells were lysed and SseK3-HA effector translocation assessed by SDS-PAGE and immunoblotting. SseK3 (α-HA), *Salmonella* (α-DnaK) and loading control (α-tubulin). Data are representative of three independent experiments. (B) Representative confocal immunofluorescence microscopy images of wild-type (WT) or TRIM32

KO RAW 264.7 infected with the Δ*sseK3*pSseK3 strain for 16 h. DNA (DAPI, blue), SseK3 (α-HA, red), Golgi network (α-Rab6, green) and *Salmonella* (α-CSA-1, grey). Scale bar, 5 μm. (C) Percentage of infected cells with translocated SseK3-HA effector, quantified from experiments as in (B). A minimum of 600 infected cells from three independent experiments were blind-scored and are represented as the mean ± SEM. Data was acquired at the same time as Figure 3.2B and the data for wild-type cells are reproduced in this figure for ease of interpretation. (D) 293ET cells were co-transfected with a plasmid encoding FLAG-tagged SseK3 together with plasmids expressing GFP or FLAG-tagged TRIM32. 24 h after transfection cells were treated with 50 mg/ml cycloheximide (CHX) for 1 to 24 h. Cells were then collected, lysed and post nuclear supernatants analysed by SDS-PAGE and immunoblotting. Degradation of c-myc and ubiquitinated proteins served as a positive control for drug treatment. SseK3/TRIM32 (α-FLAG), GFP (α-GFP), c-myc (α-c-myc) ubiquitin (α-Ub) and the loading control (α-actin). Immunoblots are representative of three independent experiments.

co-expressed TRIM32 was tested. Plasmids encoding FLAG-SseK3 and GFP or FLAG-TRIM32 were transiently transfected into 293ET cells. After one day protein translation was inhibited by the addition of cycloheximide to the culture medium and protein levels were then analysed at the indicated time points. As expected, c-myc and ubiquitin, two proteins with a fast cellular turnover rate, deceased over the course of the experiment, indicating that protein synthesis was inhibited by cycloheximide (Figure 4.7D). No difference in TRIM32 protein levels were detected during the 24 h treatment with cycloheximide. SseK3 protein levels did not change detectably over the course of the experiment, even when TRIM32 was overexpressed (Figure 4.7D). Cycloheximide treatment for more than 24 h was cytotoxic, so the half-life of SseK3 could not be determined by this method.

Taken together, these data show that SseK3 translocation and localisation in the host cell is independent of TRIM32 and that the stability of SseK3 is not altered by co-expression of TRIM32 over a 24 h time period.

4.3.2 SseK3-mediated inhibition of NF-κB signalling and cell death is independent of TRIM32

In chapter 3 I showed that SseK3 inhibits NF-κB signalling and host cell cytotoxicity during macrophage infection (Figure 3.6 and Figure 3.10). Therefore, I wanted to test the hypothesis that TRIM32 is required for SseK3-mediated inhibition of NF-κB signalling and cell death during *Salmonella* infection.

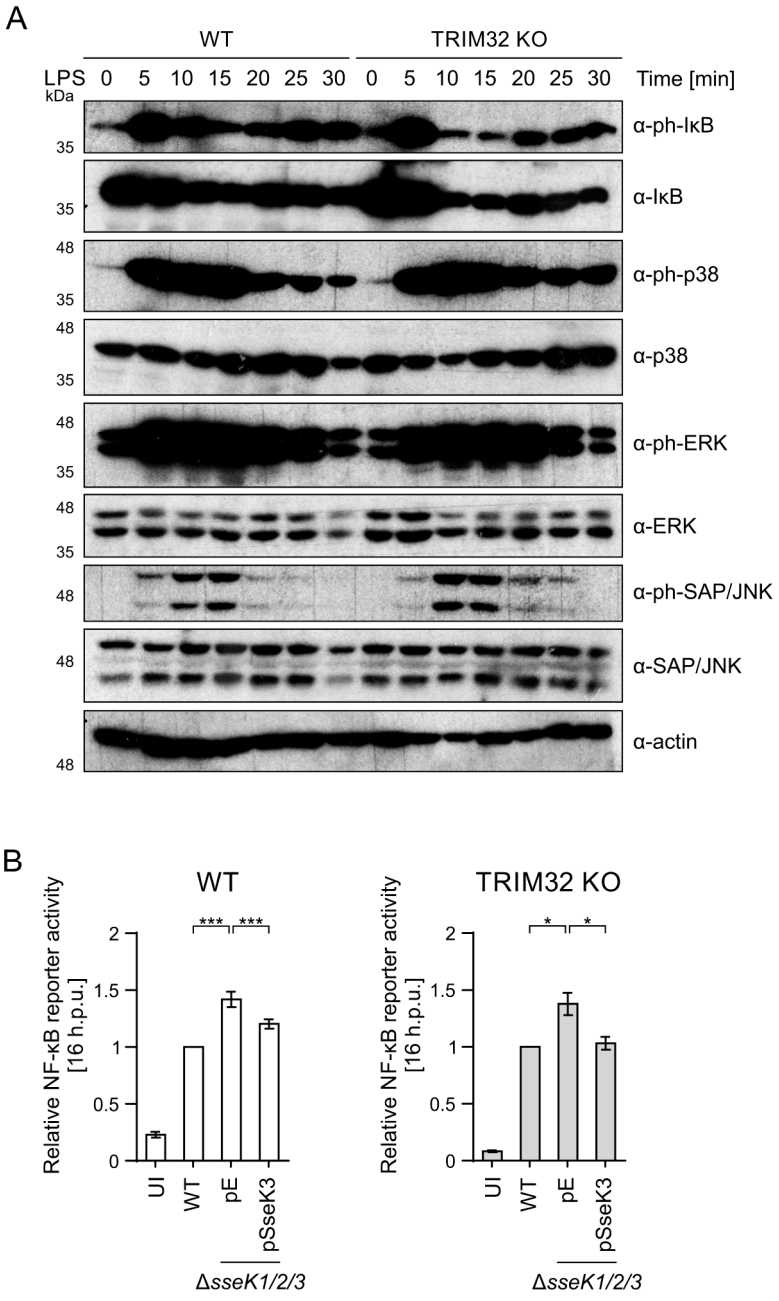

Figure 4.8. **Suppression of NF-κB signalling by SseK3 does not depend on TRIM32**

(A) Wild-type or TRIM32 KO RAW 264.7 macrophages were stimulated with 1 µg/ml LPS for 5 to 30 min, lysed and whole cell lysates analysed by SDS-PAGE and immunoblotting. IκBα phospho-Ser32 (α-ph-IκBα), IκBα (α-IκBα), MAPK p38 phospho-Thr180/Tyr182 (α-ph-p38), MAPK p38 (α-p38), ERK1/2 (p44/p42) phospho-Thr202/Tyr204 (α-ph-ERK), ERK1/2 (p44/p42) (α-ERK), SAP/JNK phospho-Thr183/Tyr185 (α-ph-SAP/JNK), SAP/JNK (α-SAP/JNK) and loading control (α-actin). Immunoblots shown are representative for three independent experiments. (B) Wild-type (WT) or TRIM32 KO RAW 264.7 macrophages stably transduced with a NF-κB Firefly luciferase reporter element and a constitutively expressed Renilla luciferase gene were infected with the indicated *Salmonella* strains. 16 h.p.u. cells were lysed and luciferase activity measured. Data represent the mean fold activation relative to wild-type infected cells from three independent experiments ± SEM.* $P < 0.05$, *** $P < 0.001$. UI, uninfected. pE, empty vector control.

Depletion of TRIM32 by shRNA is reported to impair TNFα-induced NF-κB innate immune signalling (Yang et al., 2015). As LPS represents a major PAMP during *Salmonella* infection, the cellular response of wild-type and TRIM32 KO macrophages to LPS stimulation was tested prior to the phenotypic analysis of SseK3 in the TRIM32 KO cells. Wild-type and TRIM32 KO macrophages were simulated with purified *S.* Typimurium LPS and phosphorylation (and thereby activation) of key innate immune signalling components was analysed by immunoblotting of cell lysates. Activation of the NF-κB (IκBα) and MAPK (p38, ERK, SAP/JNK) pathways were indistinguishable between wild-type and TRIM32 KO macrophages at different times past stimulation (Figure 4.8A). This revealed that TRIM32 KO macrophages responded to LPS like wild-type cells, making them suitable for *Salmonella* infection studies. To analyse next whether TRIM32 is required for SseK3-mediated inhibition of NF-κB signalling during macrophage infection, the NF-κB Firefly Luciferase reporter and control Renilla Luciferase elements were stably introduced into the CRISPR TRIM32 KO macrophages creating a TRIM32 KO NF-κB reporter cell line. Wild-type and TRIM32 KO NF-κB reporter macrophages were then infected for 16 h with different *Salmonella* strains and luciferase levels were measured in cell lysates. In both cell lines the Δ*sseK1/2/3* mutant strain induced significantly higher reporter activation compared to cells infected with wild-type *Salmonella* (Figure 4.8B). This phenotype was complemented by plasmid based expression of SseK3 in the Δ*sseK1/2/3* mutant in both wild-type and TRIM32 KO cells (Figure 4.8B). Therefore, SseK3-mediated inhibition of NF-κB signalling in macrophages is independent of TRIM32.

To test if TRIM32 is required for SseK3-mediated inhibition of macrophage cytotoxicity, wild-type and TRIM32 KO macrophages were infected with the indicated *Salmonella* strains and after 20 h the extracellular LDH levels were measured. As expected, *Salmonella*-induced cell death was significantly higher in cells infected with the *sseK1/2/3*pE stain compared to wild-type infected cells (Figure 4.9). In both wild-type and TRIM32 KO macrophages this difference was complemented by expression of SseK3 from a low copy number plasmid in the Δ*ssek1/2/3* strain (Figure 4.9).

Taken together, these data show that inhibition of the NF-κB pathway and suppression of *Salmonella*-induced cell death by SseK3 are independent of TRIM32.

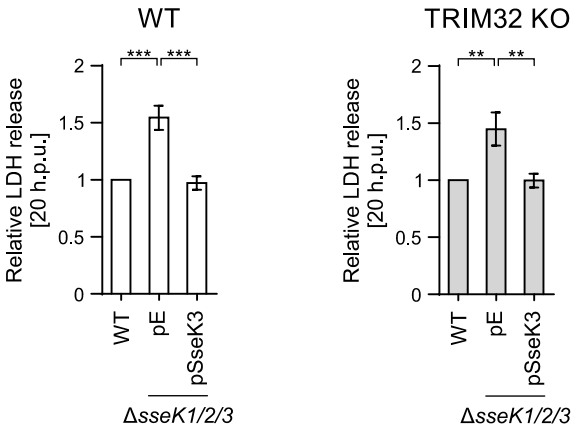

Figure 4.9**. Suppression of host cell cytotoxicity by SseK3 does not depend on TRIM32**

Lactate dehydrogenase (LDH) release from WT or TRIM32 KO RAW 264.7 macrophages infected for 20 h with the indicated *Salmonella* strains. *Salmonella*-induced cell death is presented relative to WT infected cells. Data are the means of three independent experiments, ± SEM.* * P < 0.01, *** P < 0.001. UI, uninfected. pE, empty vector control.

4.4 Infection of TRIM32 deficient mice by *Salmonella*

The experiments described above did not reveal a phenotype for TRIM32 during macrophage infection, neither with respect to *Salmonella* replication nor in relation to SseK3 function. However, this might be due to the targeted approach that focused on specific aspects of *Salmonella* infection or due to the artificial condition in tissue culture-based experiments. To test if TRIM32 is required for the control of bacterial burden and mediates innate immune responses during *Salmonella* infection of a whole animal, *Trim32* deficient mice were obtained (kind gift from J. Schamborn). *Trim32*$^{-/-}$ mice show mild signs of myopathy (Kudryashova et al., 2009) and impaired neurogenesis (Hillje et al., 2015, 2013) but have no described immunodeficiency. Due to the maternal care deficit of homozygous *Trim32*$^{-/-}$ mice only heterozygote females were used for breeding. This necessitated the genotyping of all mice (Figure 4.10A and B) but also allowed the comparison of wild-type and *Trim32*$^{-/-}$ mice from the same litters as mice were bred to heterozygous *Trim32*$^{+/-}$ males.

To investigate the function of TRIM32 in systemic *Salmonella* infection, a total of 9 wild-type and 9 *Trim32*$^{-/-}$ mice were inocculated by intraperitonal injection with 2 x 10^4 CFU wild-type *Salmonella* constitutively expressing GFP. After two days of infection the spleens were isolated and the bacterial burden determined by colony forming unit assay. This revealed similar bacterial loads in spleens from wild-type and *Trim32*$^{-/-}$ mice (Figure 4.10C). However,

this does not exclude differences in the amount of infected cells or the bacterial load per cell. Splenic macrophages are the main replication niche for *Salmonella* in the mouse spleen (Salcedo et al., 2001) and therefore CD11b positive cells, which comprise mainly macrophages, were isolated and further analysed by flow cytometry. No difference was detected in the percentage of infected CD11b positive cells nor in the bacterial load per cell when comparing wild-type and *Trim32*$^{-/-}$ mice (Figure 4.10D and E). Splenic macrophages are also a major source of cytokines during bacterial infection. TRIM32 deficiency has previously been linked to aberrant cytokine expression in psoriasis models (Liu et al., 2010; Yuangang Liu et al., 2017), therefore, cytokine expression in the isolated CD11b cells was analysed. This showed that *Trim32*$^{-/-}$ mice responded to *Salmonella* infection with increased expression of *ifnβ, tnfα, il-6* and *irf7* mRNA, key cytokines of the anti-bacterial immune response (Figure 4.10F), when compared to naïve, uninfected mice. This was indistinguishable from the response in infected wild-type mice (Figure 4.10F). In summary, no difference in bacterial burden and host cell responses were detected in short term intraperitoneal infections of wild-type and *Trim32*$^{-/-}$ mice.

The literature presents conflicting information on whether the SseK effectors contribute to *Salmonella* virulence in mice (Brown et al., 2011; Buckner et al., 2011; Kidwai et al., 2013; Kujat Choy et al., 2004). To address this and at the same time to test if TRIM32 is required for *Salmonella* virulence, competitive infections between wild-type and Δ*sseK* mutant bacteria were done in wild-type and *Trim32*$^{-/-}$ mice. Sets of 4-6 mice were inoculated by intraperitoneal injection with an equal mixture of wild-type and Δ*sseK1/3* or Δ*sseK1/2/3* mutant *Salmonella*. After 2 (WT/ Δ*sseK1/2/3*) or 4 (WT/ Δ*sseK1/3*) days of infection, the spleens were isolated and the competitive index was calculated as the ratio of recovered mutant over wild-type bacteria. A ratio of 1 represents no difference in bacterial fitness, whereas a value below 1 indicates attenuation of the mutant strain compared to wild-type *Salmonella*. Competitive index analysis showed no attenuation of the Δ*sseK1/3* (Figure 4.10G) and Δ*sseK1/2/3* (Figure 4.10H) mutants compared to wild-type bacteria in both wild-type and *Trim32*$^{-/-}$ mice. This indicates that the SseK effectors are not required for short term systemic infection in C57Bl/6 mice and that this is not affected by TRIM32.

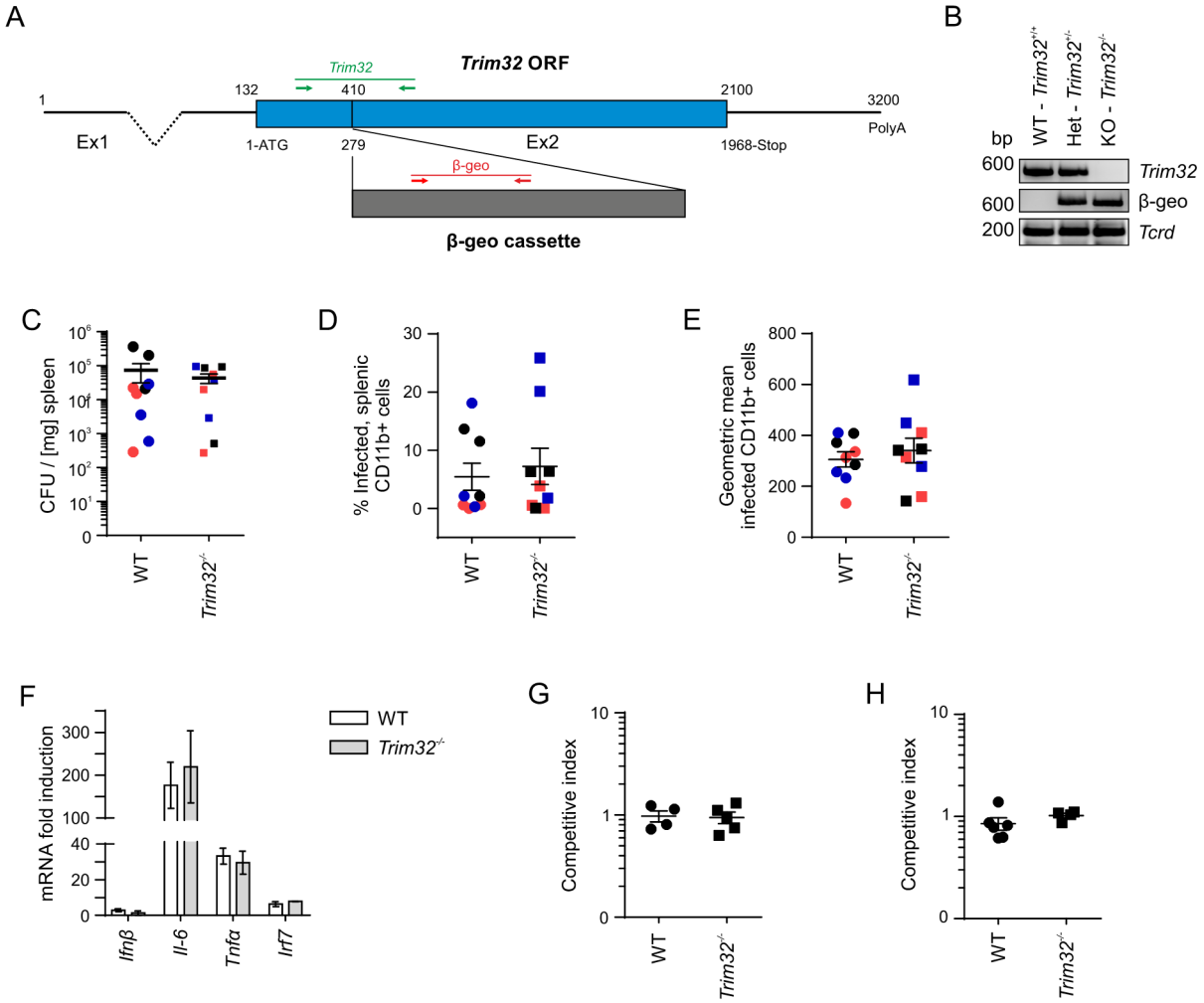

Figure 4.10. ***Trim32*$^{-/-}$ mice respond to *Salmonella* infection similar to WT mice in short term infection**

(A) Schematic of the *Trim32* gene with integrated β-geo cassette in the *Trim32*$^{-/-}$ knock-out (KO) mice. (B) Representative genotyping PCR for the presence of the gene trap and/or the *Trim32* gene using specific genotyping primers (indicated by arrows in A). PCR results were a 625 bp band amplified from the allele with the integrated β -geo cassette (red primers) and/or a 535 bp band from the WT *Trim32* allele (green primers). *Tcrd* (250 bp) served as an independent PCR control. (C-E) Wild-type and *Trim32*$^{-/-}$ mice were infected by intraperetonial injection with approximately 2 x 10^4 CFU of GFP-expressing *Salmonella* per mouse. After two days, spleens were isolated and the number of bacteria per spleen determined by colony forming unit (CFU) assay (C). In addition, splenic CD11b positive cells were isolated and the percentage of *Salmonella* infected cells (D) and the mean GFP fluorescence per cell as a proxy for bacterial load (E) determined by flow cytometry. The scatter plots are values obtained from individual mice from three independent experiments (red, black and blue) and the means ± SEM are indicated. (F) Quantitative RT-PCR analysis of *Ifnβ*, *IL-6, Tnfα* and *Irf7* mRNA levels in splenic CD11b positive cells isolated from mice described in (C-E). mRNA expression was normalised to *Rps9* mRNA and is presented as the fold change relative to uninfected control mice. Results are presented as means from two independent infections (represented in red and black in C-E) ± SEM. (G, H) Wild-type and *Trim32*$^{-/-}$ mice were inoculated with an equal number of wild-type (WT) and Δ*sseK1/3* (G) or Δ*sseK1/2/3* (H) mutant *Salmonella* by intraperitonial injection with 3-5 x 10^4 CFU/mouse for two days. Bacteria were recovered from

infected spleens and the competitive index (CI) values were calculated. The scatter plot are CI values obtained for individual mice and are the means ± SEM.

5 SSEK TARGET IDENTIFICATION AND VALIDATION

As detailed in chapter 3, both SseK1 and SseK3 inhibit host cell NF-κB signalling and cell death during *Salmonella* infection of macrophages. However, the physiological targets required for both these functions are unknown. Phenotypic analysis of SseK3 in TRIM32 knock-out cells showed that both NF-κB pathway and cell death inhibition were independent of the E3 ubiquitin ligase, despite the stable interaction of both proteins (Chapter 4). These findings suggest that SseK3 has at least one, possibly multiple, other physiological target(s) during macrophage infection that mediate these functions. A previous study by Li and collegues (Li et al., 2013) showed that ectopic expression of SseK1 resulted in arginine-GlcNAcylation of TRADD. However, whether this also occurs upon delivery of physiologically relevant amounts of enzyme following translocation into host cells during *Salmonella* infection was unknown.

In this chapter different approaches to identify and characterise novel SseK effector targets are presented, highlighting common and distinct target specificities of the SseK effectors.

5.1 Analysis of arginine-GlcNAcylation patterns during macrophage infection

Functional analysis of SseK1 and SseK3 (Chapter 3) suggest that both effectors have at least one, possibly multiple, physiological target(s) during macrophage infection. To test whether they share a common or distinct target spectrum, RAW 264.7 macrophages were infected with wild-type or Δ*sseK* mutant *Salmonella* strains and host cytosolic arginine-GlcNAcylated proteins were analysed by western blot after 16 h of infection. This revealed numerous arginine-GlcNAcylated proteins, ranging in molecular mass from approximately 30 to 95 kDa, in wild-type *Salmonella*-infected cells (Figure 5.1A). In contrast, lysates of uninfected cells and Δ*sseK1/3* or Δ*sseK1/2/3* deletion mutant infected cells were devoid of arginine-GlcNAcylated proteins, indicating that arginine-GlcNAcylation is a *Salmonella*-induced effect, dependent on both SseK1 and SseK3. Deletion of *sseK2* or expression of the protein in the Δ*sseK1/2/3* strain had no detectable effect on the arginine-GlcNAcylation pattern in host cells (Figure 5.1A and B). Single deletion of *sseK1* resulted in the loss of two distinct arginine-GlcNAcylated proteins of approximately 30 and 40 kDa (Figure 5.1, indicated with the * and ‡, respectively) compared to wild-type infected cells. Interestingly,

overexpression of SseK1 from a low-copy-number plasmid in the Δ*sseK1/2/3* deletion strain restored arginine-GlcNAcylation of two proteins of similar molecular mass, indicating that these proteins are genuine SseK1 targets during macrophage infection (Figure 5.1B). In addition, two proteins of approximately 65 and 95 kDa molecular mass (Figure 5.1B, bands a and b, respectively) became apparent. Infection with the single Δ*ssek3* deletion mutant resulted in the loss of arginine-GlcNAcylation of at least six high molecular weight proteins ranging from 55 to 100 kDa (Figure 5.1A, indicated with the #). Bands of similar molecular mass were restored in Δ*sseK1/2/3*pSseK3-infected cells and additionally three proteins of 32, 35, and 43 kDa (Figure 5.1B, bands c, d, and e) were detected. It is noteworthy that the 9 strong SseK3-dependent bands detected upon plasmid-based expression in the *ΔsseK1/2/3* strain are all of different molecular masses to those detected after expression of SseK1 (Figure 5.1B). This shows that SseK1 and SseK3 exhibit differential substrate specificity.

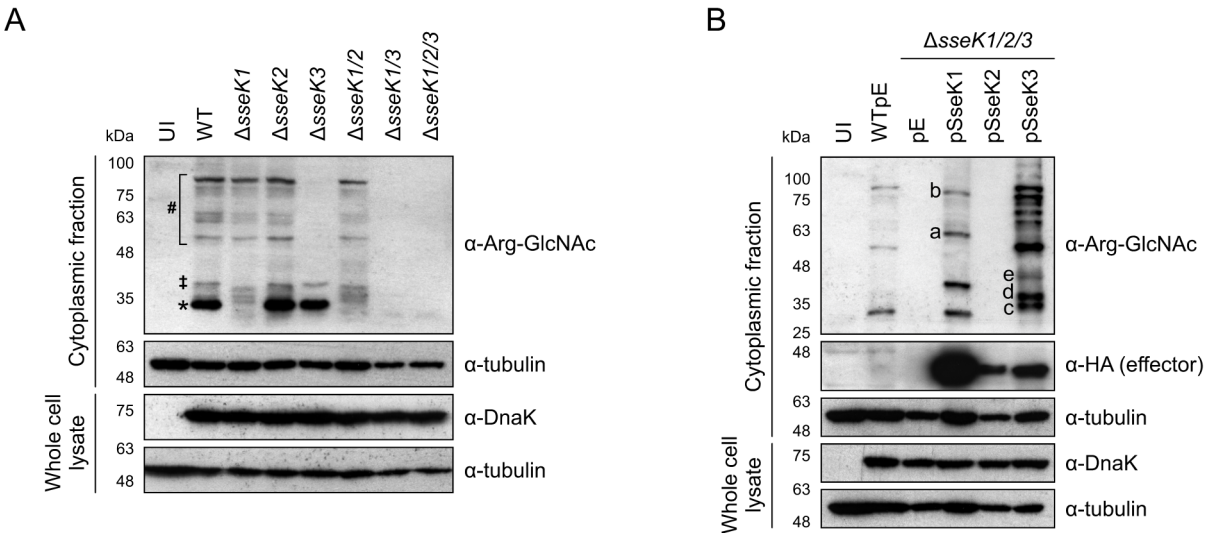

Figure 5.1. **Expression of SseK1 and SseK3 results in different patterns of arginine-GlcNAcylated proteins during infection of macrophages**

(A, B) Representative immunoblots of RAW 264.7 macrophage lysates infected with the indicated *Salmonella* strains. To visualise arginine-GlcNAcylated proteins, cells were lysed 16 h.p.u. and analysed by SDS-PAGE and immunoblotting. Effectors (α-HA), arginine-GlcNAc (α-Arg-GlcNAc), *Salmonella* (α-DnaK) and loading control (α-tubulin). Data are representative of three independent experiments.

SseK1 and SseK3 localise to different subcellular compartments after bacterial translocation into the host cell (Figure 3.1). Therefore, the subcellular localisation of arginine-GlcNAcylated proteins was investigated during macrophage infection. To test this, RAW 264.7 macrophages

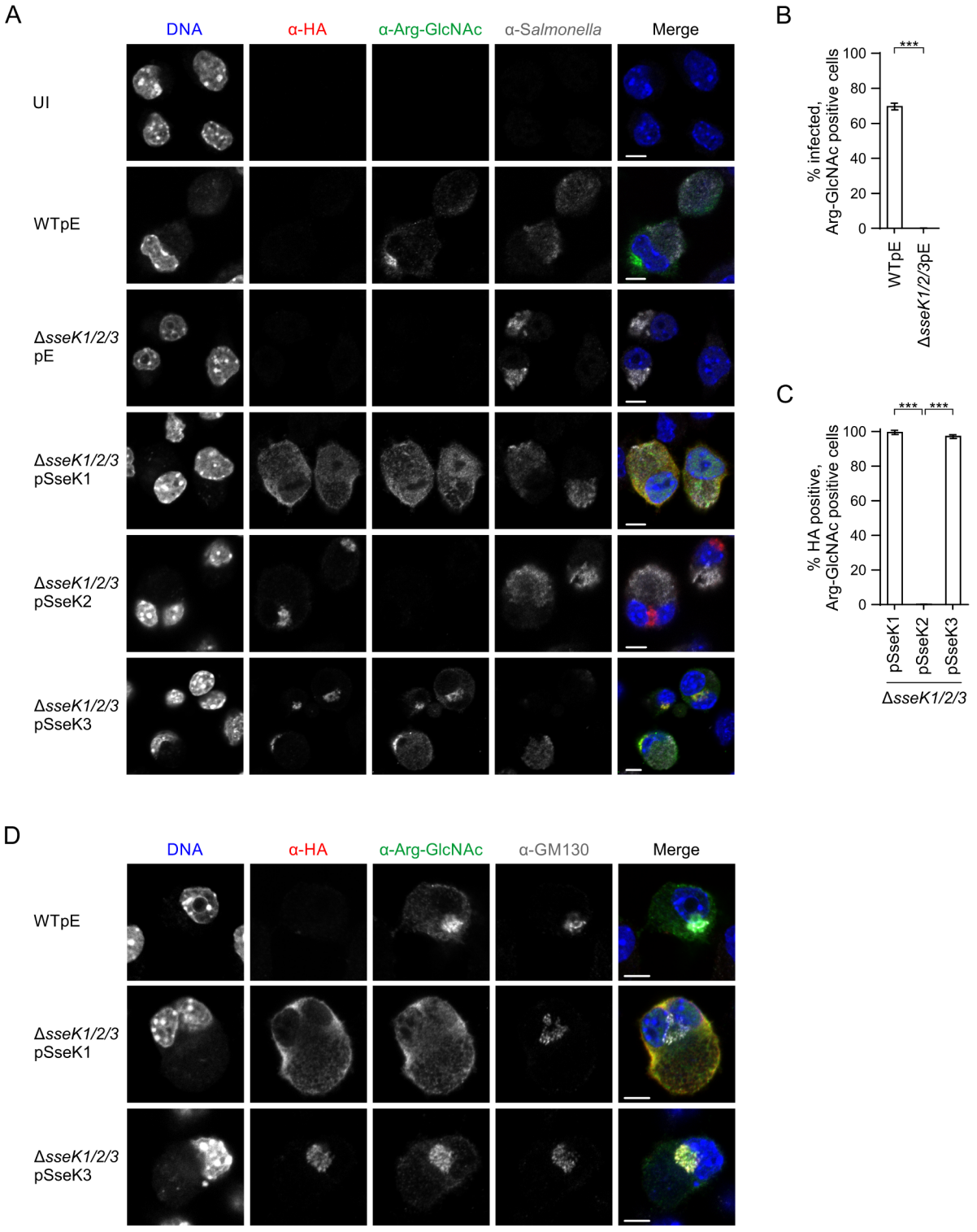

Figure 5.2. **SseK-dependent differential localisation of arginine-GlcNAcylated proteins in infected macrophages**

(A) Representative confocal microscopy images of RAW 264.7 macrophages infected for 16 h with the indicated wild-type or HA-tagged effector expressing *Salmonella* strains. Effectors (α-HA, red), arginine-GlcNAc (α -Arg-GlcNAc, green), *Salmonella* (α-CSA-1, gray) and DNA (DAPI, blue). Scale bar, 5 µm. (B) Percentage of *Salmonella*-infected cells with arginine-GlcNAcylated proteins. (C) Percentage of *Salmonella*-infected cells with translocated HA-tagged effector, showing a positive arginine-GlcNAc signal. Data (B, C) were quantified from experiments as shown (A) and are the mean ± SEM of three independent experiments with at least 600 infected cells counted

in total. ***, P < 0.001. (D) Representative confocal microscopy images of arginine-GlcNAcylation (α-Arg-GlcNAc, green) and Golgi network (α-GM130, gray) colocalisation in RAW 264.7 macrophages at 16 h.p.u. Scale bar, 5 µm. UI, uninfected; pE, empty vector control.

were infected for 16 h with wild-type *Salmonella* or an Δ*sseK1/2/3* deletion strain expressing the indicated low copy number plasmid and arginine-GlcNAcylation was analysed by confocal immunofluorescence microscopy. Wild-type *Salmonella*-infected macrophages showed an arginine-GlcNAcylation signal in the cytosol and at the Golgi network in approximately 70% of the infected cells, whereas arginine-GlcNAcylation was not detected in cells infected with the Δ*sseK1/2/3* mutant (Figure 5.2A and B). Plasmid-based expression of SseK1 in the Δ*sseK1/2/3* strain restored arginine-GlcNAcylation in the cytoplasm, whilst expression of SseK3 resulted in arginine-GlcNAcylation in both the cytoplasm and at the Golgi network (Figure 5.2A and D). Arginine-GlcNAcylation was detected in 100% of all cells with translocated SseK1 or SseK3 effector (Figure 5.2C) but was absent in cells infected with the Δ*sseK1/2/3*pSseK2 strain despite clear translocation of SseK2 (detected via α-HA).

Taken together, these data indicate that SseK1 and SseK3 function as arginine-GlcNAc transferases during macrophage infection with different substrates, some of which have distinct sub-cellular localisations.

5.2 SseK target identification - infection HA-immunoprecipitation

To identify infection relevant interaction partners of the SseK effectors a combination of infection, co-immunoprecipitation and mass spectrometry was used. RAW 264.7 cells were infected with *Salmonella* strains expressing HA-tagged SseK effectors. After 16 h of macrophage infection, the cells were lysed and the effectors, together with any interacting proteins, were isolated by α-HA immunoprecipitation. SseL, a *Salmonella* deubiquitinase was used as an independent control to identify unspecific protein binding to the anti-HA antibody and beads. A pilot experiment identified that elution of the recovered proteins with HA peptide was less efficient than tryptic digest of the proteins on the anti-HA agarose (data not shown); therefore results from this experiment were not included in the analysis.

Samples were analysed by LC-MS/MS in the Institute of Biochemistry and Biophysics at the Polish Academy of Sciences in Warsaw (Poland) and the recovered peptides matched to the

mouse and *S.* Typhimurium 14028s proteome using the Swiss-Prot or Uniprot database, respectively. To identify mammalian proteins specifically bound to single or multiple SseK proteins (or to SseL) the resulting list of proteins was refined using the following criteria: (i) Proteins were absent from the negative control sample Δ*sseL*pSseL and/or were a minimum of 5 fold enriched over the negative control and any other sample. (ii) Only proteins identified in both biological repeats were considered reliable hits. (iii) Proteins with a MASCOT protein score below 100 were excluded from further analysis due to low confidence levels. The combined results of two independent experiments are presented in Figure 5.3, Table 5.1 and Table 5.2. An extended table, including proteins with MASCOT scores below 100, is detailed in the appendix (Table 7.1).

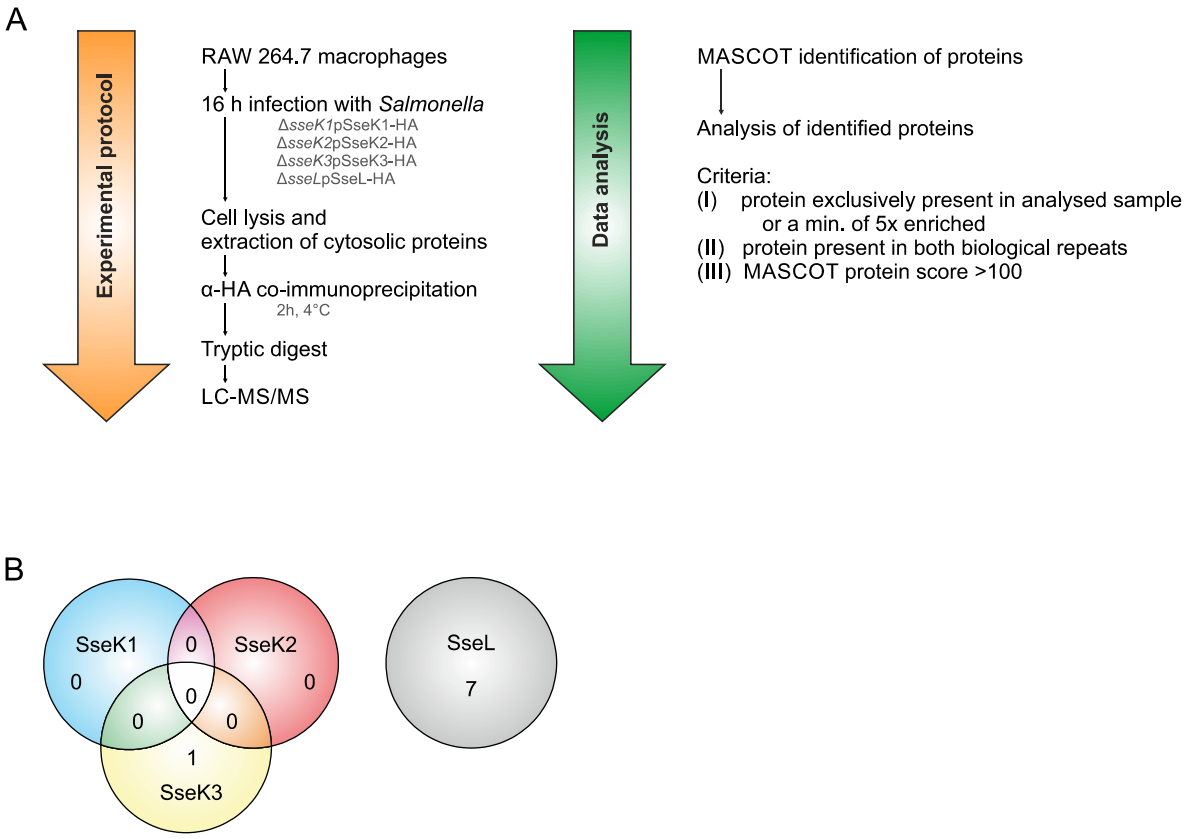

Figure 5.3. **Identification of SseK binding proteins using infection α-HA immunoprecipitation and mass spectrometry**

(A) Schematic representation of the experimental procedure and data analysis criteria used for the infection α-HA co-immunoprecipitation experiments. (B) Venn diagram summarizing results from the infection α-HA co-immunoprecipitation experiments.

As expected, the bait proteins SseK1, SseK2, SseK3 and SseL were the highest scoring *Salmonella* proteins identified in their respective immunoprecipitation samples (Table 5.1). Interestingly no other *Salmonella* proteins were found to interact stably with the SseK effectors.

Table 5.1. **MASCOT protein scores for the used bait proteins of the infection-HA immunoprecipitation experiments**

Accession: UniProt database identifier

Score: Mass spectrometry score obtained through MASCOT analysis

Peptides: Number of significant peptide matches identified by LC-MS/MS MASCOT analysis

Rep_B and Rep_E: Two independent biological repeats

Accession	**Score (peptides)**		**Description**
	Rep_B	Rep_E	
A0A0F6B9Z0	6072 (91)	21209 (415)	Putative cytoplasmic protein (SseK1)
A0A0H3NIW0	1876 (27)	2697 (40)	T3SS effector protein (SseK2)
A0A0F6B2Z0	2941 (44)	2916 (51)	Uncharacterized protein (SseK3)
A0A0F6B423	10213 (105)	11073 (193)	Deubiquitinase (SseL)

Oxysterol-binding protein 1 (OSBP) was previously identified as an SseL interaction partner (Auweter et al., 2011) and was exclusively found in the mass spectrometry analysis of SseL-IP samples, serving as a positive control for the experimental setup (Table 5.2). In addition, six new potential interaction partners of SseL were identified (UBE2C, VAPB, IFITM2, TMEM106A, WBP2 and SLC38A2). However, the validation and characterisation of these targets was not the focus of this work. The only specific and reproducible interaction partner for SseK3 identified was the E3 ubiquitin ligase TRIM32 (Table 5.2). This result is consistent with data presented in Figure 4.1, yet no additional mammalian binding partners for SseK3 were detected. Analysis of the mammalian proteins co-immunoprecipitated with the SseK effectors did not identify stable interaction partners for SseK1 and SseK2. In addition no shared interaction partners between SseK1-SseK2, SseK2-SseK3, SseK1-SseK3 or all three SseK effectors were identified. Relaxing the analysis criteria to include proteins that were present in several samples and at least 5-fold enriched in the analysed SseK immunoprecipitation, did

not reveal any additional, reproducible, binding partners. This indicates that SseK-target binding during macrophage infection is transient or occurs with weak affinity; infection-immunoprecipitation of tagged effectors might therefore not be the best technique to identify new targets and other approaches should be considered.

Table 5.2. **Murine proteins identified by tandem LC-MS/MS analysis as SseK-HA or SseL-HA specific binding partners**

Accession: Swiss-Prot database identifier

Score: Mass spectrometry score obtained through MASCOT analysis

Peptides: Number of significant peptide matches identified by LC-MS/MS MASCOT analysis

Rep_B and Rep_E: Two independent biological repeats

Accession	**Score (Peptides)**		**Description**
	Rep_B	Rep_E	
SseK3-HA specific protein			
Q8CH72	654 (10)	779 (21)	E3 ubiquitin-protein ligase TRIM32 (TRIM32)
SseL-HA specific proteins			
Q3B7Z2	2420 (43)	2301 (51)	Oxysterol-binding protein 1 (OSBP)
Q9QY76	283 (7)	487 (11)	Vesicle-associated membrane protein-associated protein B (VAPB)
Q9D1C1	191 (3)	230 (5)	Ubiquitin-conjugating enzyme E2 C (UBE2C)
Q8VC04	238 (5)	160 (3)	Transmembrane protein 106A (TMEM106A)
Q99J93	194 (2)	146 (4)	Interferon-induced transmembrane protein 2 (IFITM2)
Q8CFE6	104 (1)	198 (6)	Sodium-coupled neutral amino acid transporter 2 (SLC38A2)
P97765	110 (3)	124 (5)	WW domain-binding protein 2 (WBP2)

5.3 Targeted approach to identify SseK arginine-GlcNAcylation substrates

As the infection-immunoprecipitation experiments did not result in the identification of new SseK effector interaction partners, a targeted approach was used next. NleB stably binds to and arginine-GlcNAcylates death domain containing proteins including FADD and TRADD (Li et al., 2013; Pearson et al., 2013). Li and colleges also showed arginine-GlcNAcylation of TRADD by ectopically expressed SseK1 (Li et al., 2013). Therefore, it was hypothesised that all SseK effectors modify death domain containing proteins similar to NleB. To test this 293ET cells were transiently transfected with plasmids encoding FLAG-tagged FADD and GFP-tagged effectors. After approximately 40 h of transfection cells were lysed, FADD isolated by anti-FLAG immunoprecipitation and arginine-GlcNAcylation of immunoprecipitates was analysed by SDS-PAGE and western blot. Expression of NleB served as a positive control that stably bound and modified FADD as expected from previously published work (Pearson et al., 2013) (Figure 5.4A). In contrast, none of the SseK effectors stably interacted with FADD. Nevertheless, strong arginine-GlcNAcylation of FADD was detected when SseK1 was co-expressed (Figure 5.4A). Mutation of the effectors cation and/or sugar-coordinating motif DxD ($SseK1_{AAA}$) abolished FADD modification, indicating that catalytic function of SseK1 is required for arginine-GlcNAcylation of FADD (Figure 5.4B). Expression of neither SseK2 nor SseK3 resulted in arginine-GlcNAcylation of FADD (Figure 5.4A), strengthening the hypothesis of target specificity between the effectors. NleB GlcNAcylates arginine 117 in the death domain of FADD, preventing oligomerisation of the protein and thereby rendering it inactive (Pearson et al., 2013). To test whether SseK1 induces modification of the same residue, a FADD R117A mutant was analysed by the same experimental setup as described above. Expression of both SseK1 and NleB resulted in strong arginine-GlcNAcylation of wild-type but not R117A mutant FADD (Figure 5.4C). These data show that ectopically expressed *Salmonella* SseK1 can modify FADD at residue R117, functioning similar to NleB.

Next, post-translational modification of TRADD by the SseK effectors was analysed in a similar experimental setup as described for the analysis of FADD arginine-GlcNAcylation. 293ET cells were transfected with plasmids expressing FLAG-TRADD and GFP-tagged effectors, TRADD

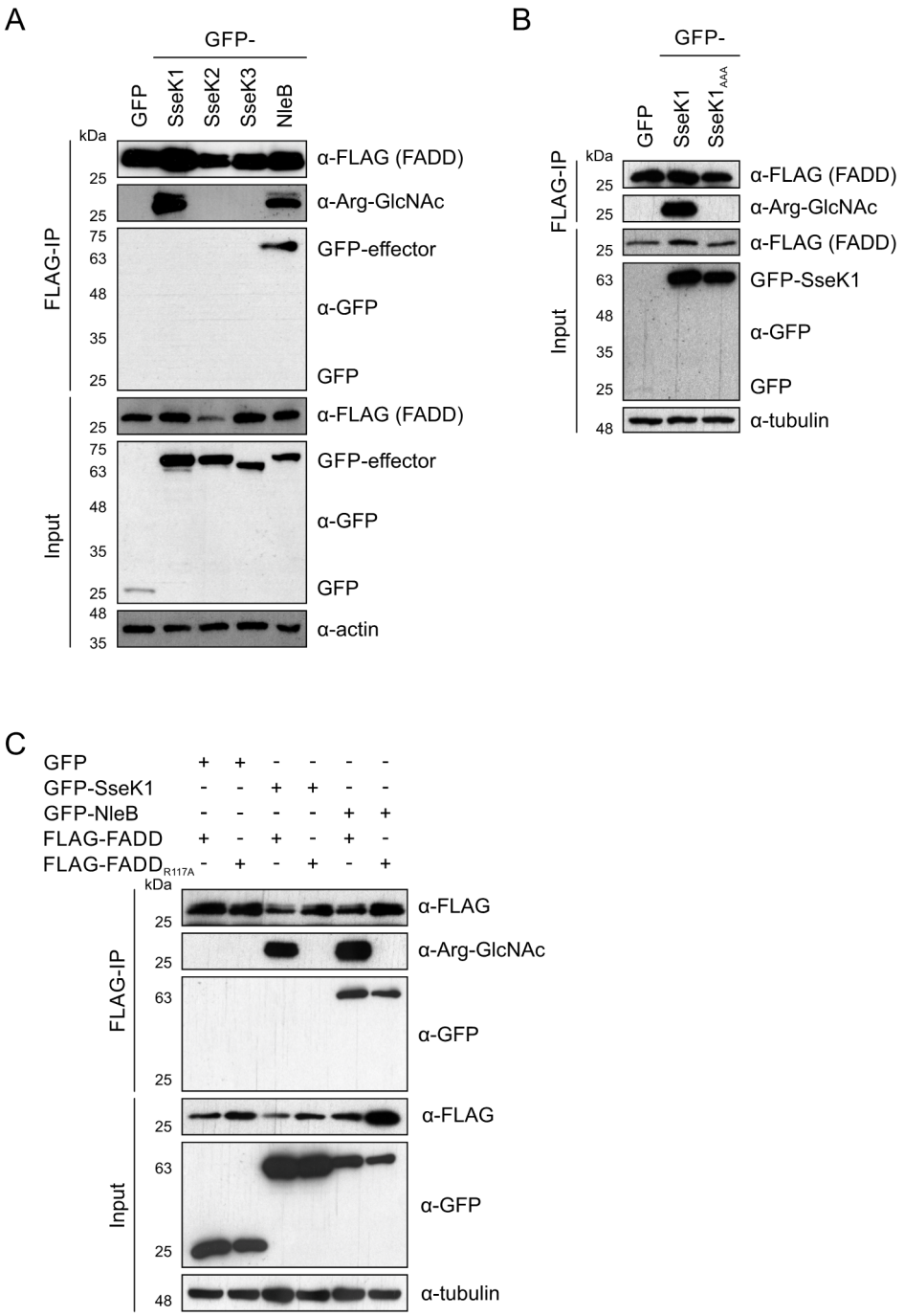

Figure 5.4. **SseK1 arginine-GlcNAcylates arginine 117 in FADD**

(A - C) 293ET cells were transfected with plasmids expressing wild-type or mutant FLAG-tagged FADD and various GFP-tagged effectors to determine the arginine-GlcNAcylation status of FADD. 40 h after transfection, cells were lysed and proteins isolated by α-FLAG immunoprecipitation. Samples were analysed by SDS-PAGE and immunoblotting against the effectors (α-GFP), FADD (α-FLAG), arginine-GlcNAc (α-Arg-GlcNAc) and the loading control (α-tubulin). All data are representative of three independent experiments.

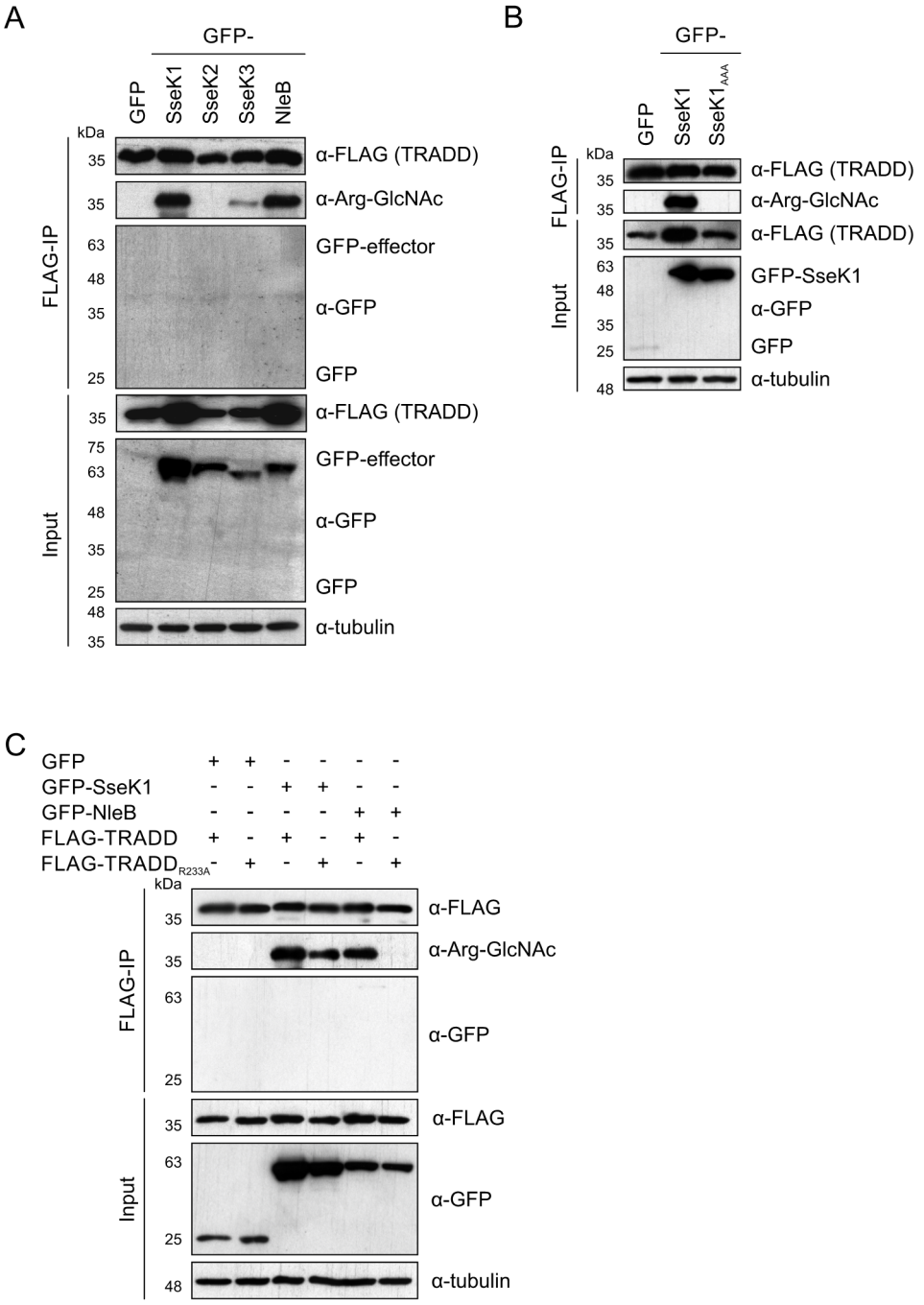

Figure 5.5. **Arginine-GlcNAcylation of TRADD upon SseK1 and SseK3 expression**

(A-C) Plasmids harbouring wild-type or mutant GFP-tagged effectors and FLAG-tagged TRADD were cotransfected into 293ET cells. 40 h after transfection, cells were lysed, proteins isolated by α-FLAG immunoprecipitation and samples analysed by SDS-PAGE and immunoblotting. Effectors (α-GFP), TRADD (α-FLAG), arginine-GlcNAc (α-Arg-GlcNAc) and the loading control (α-tubulin). Data are representative of three independent experiments.

was isolated by immunoprecipitation and arginine-GlcNAcylation analysed by SDS-PAGE and western blot. Even though no stable interaction between TRADD and the SseK effector or

NleB was detected, arginine-GlcNAcylation of TRADD was detected when SseK1, SseK3 or NleB were co-expressed (Figure 5.5A). In contrast, expression of the catalytically inactive mutant SseK1$_{AAA}$ did not result in arginine-GlcNAcylation of TRADD (Figure 5.5B). Expression of SseK2 had no detectable effect. SseK1 and NleB modify FADD at the same amino acid residue within the death domain (Figure 5.4C); this arginine is conserved in the death domain of TRADD and is modified by NleB (Li et al., 2013; Pearson et al., 2013). To test if SseK1 results in modification of the same arginine residue, post-translational modification of TRADD R233A was analysed. NleB strongly arginine-GlcNAcylated wild-type TRADD but not the R233A mutant as expected from previously published work (Li et al., 2013) (Figure 5.5C). In contrast, SseK1 modified both wild-type and R233A mutant TRADD (Figure 5.5C).

Together, this shows that ectopically expressed SseK1 and SseK3 arginine-GlcNAcylate TRADD, SseK1 in a catalytically dependent manner. However, SseK1-mediated arginine-GlcNAcylation of TRADD occurs either on different or on multiple arginine residues compared to NleB, which specifically modifies R233.

Next it was investigated whether translocated SseK effectors also modify FADD and TRADD during *Salmonella* infection, following natural delivery of bacterial effectors. Antibodies tested for the analysis of endogenous FADD or TRADD in macrophages were inadequate. In addition, transfection of RAW 264.7 macrophages led to an unacceptable level of cell death. Therefore, GFP-tagged FADD or TRADD were transiently expressed in HeLa cells and the cells subsequently infected with various *Salmonella* strains. After 16 hours of infection, proteins were isolated by anti-GFP immunoprecipitation and analysed with anti-arginine-GlcNAc antibody. Infection with wild-type *Salmonella* resulted in arginine-GlcNAcylation of both FADD and TRADD but this was not the case when the cells were infected with the Δ*sseK1/2/3* mutant (Figure 5.6, middle and right hand panel). In contrast, GFP alone was not modified under any tested infection conditions (Figure 5.6, left hand panel) indicating that arginine-GlcNAcylation of FADD and TRADD was specific. Plasmid-based expression of SseK1 in the Δ*sseK1/2/3* mutant restored arginine-GlcNAcylation of FADD and TRADD and bacterial expression of SseK3 in the Δ*sseK1/2/3* mutant led to weak modification of TRADD but not FADD (Figure 5.6, middle and right hand panel). Translocated SseK2 had no detectable effect on FADD or TRADD, which was in line with the transfection based experiments.

Taken together, this showed that during *Salmonella* infection, FADD arginine-GlcNAcylation is dependent on SseK1 and SseK1 and/or SseK3 mediate TRADD modification.

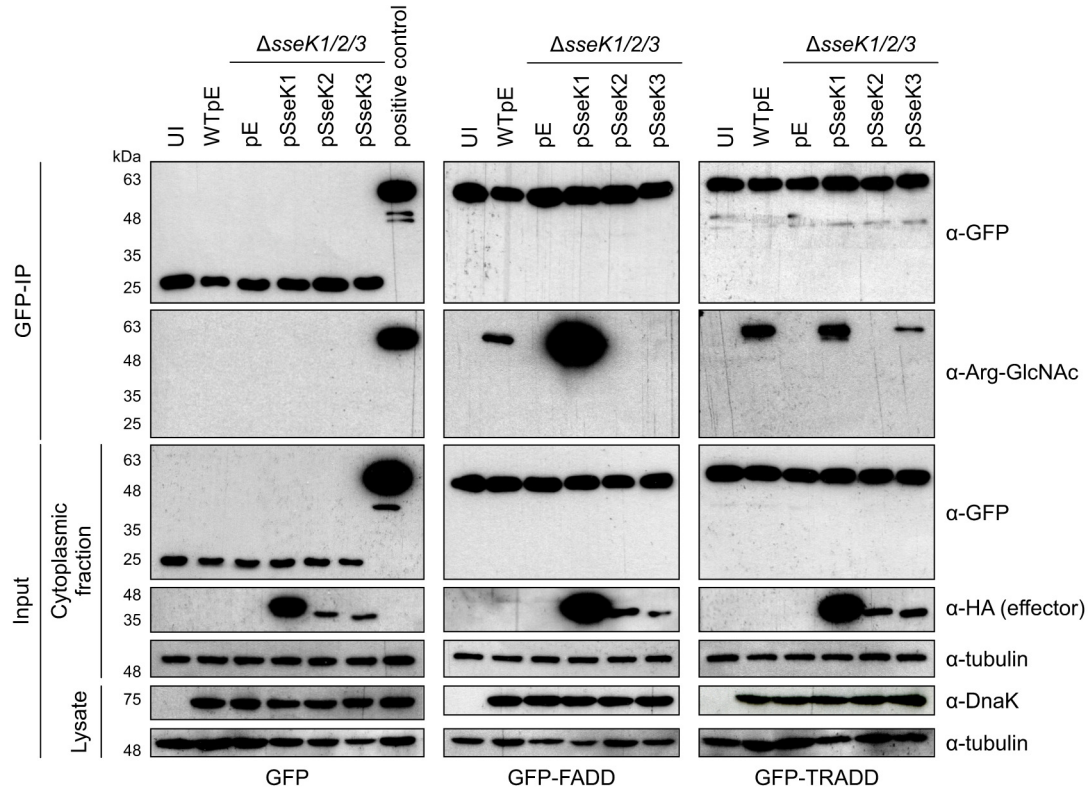

Figure 5.6. **FADD and TRADD are arginine-GlcNAcylated during HeLa cell infection**

HeLa cells were transiently transfected with plasmids expressing GFP (left panel), GFP-FADD (middle panel) or GFP-TRADD (right panel). After 24 h cells were additionally infected with the indicated *Salmonella* strains. 16 h.p.u. cells were lysed, proteins isolated by α-GFP immunoprecipitation and analysed by SDS-PAGE and immunoblotting. Effectors (α-HA), GFP/TRADD/FADD (α-GFP), arginine-GlcNAc (α-Arg-GlcNAc), *Salmonella* (α-DnaK) and the loading control (α-tubulin). The positive control in the left hand panel is GFP-TRADD-transfected cells infected with WTpE *Salmonella*, as in the right panel. Data were acquired with the help of S. Matthews and T. Thurston and are representative of three independent experiments.

When analysing TRIM32 arginine-GlcNAcylation no modification of the E3 ubiquitin ligase was detected (Figure 4.3). However, on the arginine-GlcNAc immunoblot a weak band was detected for immunoprecipitation samples where TRIM32 and SseK3 were co-expressed. This band did not correspond to the molecular mass of TRIM32 but possibly to TRIM32 bound, GFP-tagged SseK3. Therefore I hypothesised that SseK3 might be auto-GlcNAcylated. To test this, 293ET cells were transfected with plasmids encoding GFP-tagged effectors. After 40 h of

transfection, proteins were isolated by anti-GFP immunoprecipitation and analysed by SDS-PAGE and western blot. This showed that ectopically expressed SseK1 and SseK3 were strongly arginine-GlcNAcylated (Figure 5.7). In contrast, no modification was detected for NleB or the catalytically inactive mutants of SseK1 and SseK3 ($SseK1_{AAA}$ and $SseK3_{AAA}$, respectively). After long overexposure of the immunoblot, weak GlcNAcylation of SseK2 was detected (Figure 5.7).

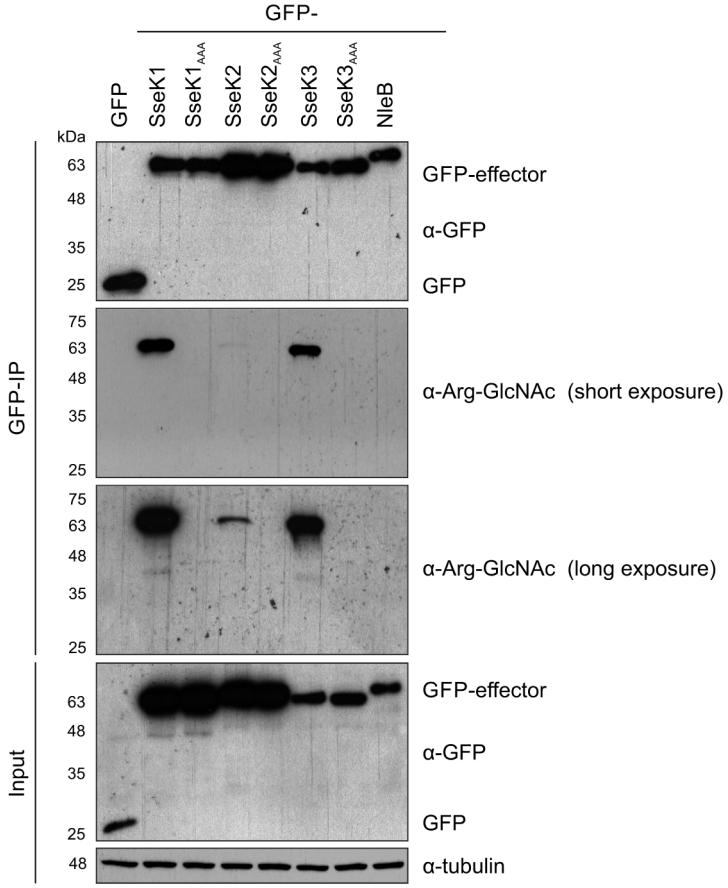

Figure 5.7. **Auto-GlcNAcylation of ectopically expressed SseK effectors**

Plasmids encoding GFP-tagged effectors were transiently transfected into 293ET cells. 40 h after transfection cells were lysed, the effectors isolated by α-GFP immunoprecipitation and analysed by SDS-PAGE and immunoblotting. Effectors (α-GFP), arginine-GlcNAc (α-Arg-GlcNAc) and loading control (α-tubulin). Data are representative of three independent experiments.

Next, to determine whether auto-arginine-GlcNAcylation was an artefact of ectopic overexpression of the proteins or if this also occurs during *Salmonella* infection, translocated effectors were analysed. RAW 264.7 macrophages were infected with HA-tagged effector

expressing *Salmonella* strains and after 16 h translocated effector was isolated by anti-HA immunoprecipitation. Anti-arginine-GlcNAc immunoblotting revealed one modified protein in each of the immunoprecipitated samples containing SseK1 and SseK3 but none in the SseK2 sample or the negative control, SseL. The detected proteins corresponded in molecular mass to SseK1 and SseK3, respectively, indicating auto-GlcNAcylation of SseK1 and SseK3 during macrophage infection (Figure 5.8A).

To analyse auto-GlcNAcylation of SseK1 and SseK3 with an additional method, the reciprocal immunoprecipitation using the anti-arginine-GlcNAc antibody was done. To do this, RAW 264.7 macrophages were infected for 16 h with *Salmonella* strains expressing HA-tagged effectors and subsequently proteins were isolated by anti-arginine-GlcNAc immunoprecipitation. SseK1-HA and SseK3-HA were specifically detected after immunoprecipitation with the anti-arginine-GlcNAc antibody but not in the control IgG antibody samples (Figure 5.8B). HA-tagged SseK2 and SseL were not enriched in the anti-arginine-GlcNAc immunoprecipitations over the IgG controls.

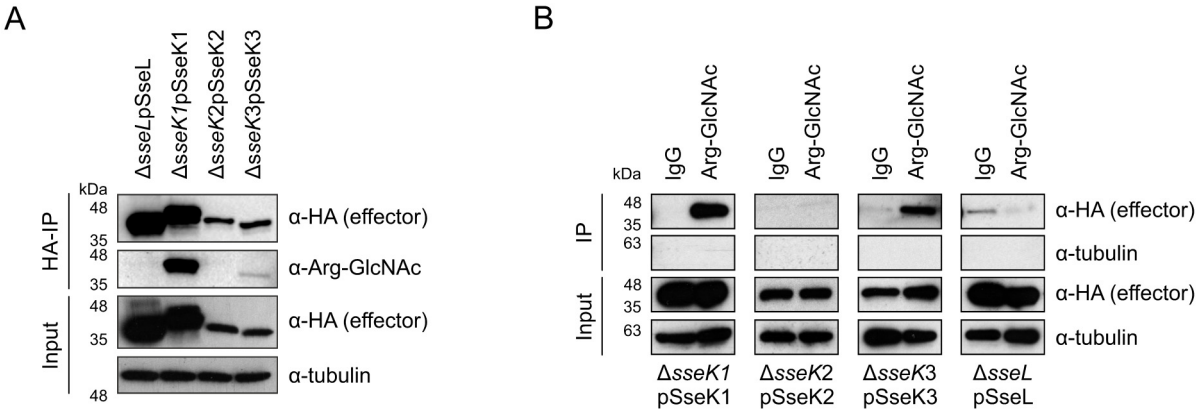

Figure 5.8. **Auto-GlcNAcylation of SseK1 and SseK3 occurs during macrophage infection**

RAW 264.7 macrophages were infected for 16 h with the indicated *Salmonella* strains. Cells were then lysed and proteins isolated by α-HA immunoprecipitation (A) or α-arginine-GlcNAc immunoprecipitation (B). IgG isotype control immunoprecipitation served as a negative control. Sample were analysed by SDS-PAGE and immunoblotting against the effectors (α-HA), arginine-GlcNAc (α-Arg-GlcNAc), *Salmonella* (α-DnaK) and the loading control (α-tubulin). Data is representative of three (A) or two (SseK2, SseL) to three (SseK1, SseK3) (B) independent experiments.

Taken together, these data show that SseK1 and SseK3 become auto-GlcNAcylated after ectopic expression or translocation, highlighting additional differences between the SseK effectors and NleB.

5.4 SseK target identification using infection arginine-GlcNAc-immunoprecipitation

The Arg-GlcNAc antibody (Pan et al., 2014) used for the detection of the SseK and NleB specific arginine-GlcNAc post translational modification (PTM) is a powerful tool to study the effectors' functions and target spectrum. As it can be used to detect the arginine-GlcNAc PTM during immunofluorescence I hypothesised that it could be used for immunoprecipitation of non-denatured proteins. However, depletion of host cell lysates using anti-arginine-GlcNAc immunoprecipitation could not be achieved despite the high specificity of the antibody to the arginine-GlcNAc PTM. This might be due to low affinity resulting from the small epitope detected. Variation of the lysis and immunoprecipitation conditions including detergent, detergent concentration, salt concentration, antibody-bead ratio, antibody-bead conjugation and incubation time did also not result in full depletion of the sample (data not shown). Yet, detection of auto-GlcNAcylated SseK1 and SseK3 using anti-arginine-GlcNAc immunoprecipitation showed that this method is nevertheless useful to isolate arginine-GlcNAcylated proteins for analysis by sensitive detection methods. Therefore, anti-arginine-GlcNAc immunoprecipitation in combination with mass spectrometry analysis was used to identify novel SseK target proteins during *Salmonella* infection of macrophages.

To do this, RAW 264.7 macrophages were infected with the Δ*sseK1/2/3* mutant strain expressing plasmid encoded HA-tagged effectors or carrying the empty vector control plasmid. Infection with the Δ*sseK1/2/3*pE strain was chosen as a negative control to identify unspecific protein binding to the anti-arginine-GlcNAc antibody and beads as previous experiments established that this strain does not cause arginine-GlcNAcylation of host proteins (Figure 5.1A and Figure 5.2A). In addition, expression of single SseK effectors in the Δ*sseK1/2/3* strain was used to identify specific SseK effector targets, which was preferred over wild-type *Salmonella* infections which result in a mixture of arginine-GlcNAcylated proteins from multiple SseKs. After 16 h of infection the macrophages were lysed, proteins isolated by anti-arginine-GlcNAc immunoprecipitation and analysed by LC-MS/MS in the Institute of Biochemistry and Biophysics at the Polish Academy of Sciences in Warsaw

(Poland). Detected peptides were matched to the mouse and *S.* Typhimurium 14028s proteomes using the MASCOT software and the Swissprot and Uniprot databases, respectively. The identified proteins were further analysed and considered a specific hit when fulfilling the following criteria: (i) Proteins were absent from the negative control sample Δ*sseK1/2/3*pE and/or were a minimum of 5-fold enriched over any other sample. (ii) Identified proteins were present in all three biological repeats and (iii) had a minimum MASCOT protein score of 100 to increase confidence. The experimental outline and results of the anti-arginine-GlcNAc immunoprecipitation are summarised in Figure 5.9 and Table 5.3. An extended list of all proteins that were detected in a minimum of two repeats, independent of the MASCOT score is available in the appendix, Table 7.2.

Anti-arginine-GlcNAc immunoprecipitation from cells infected with the Δ*sseK1/2/3*pSseK2 strain did not lead to the detection of any specific and reproducible proteins. In addition, SseK2 itself was not found amongst the recovered proteins which is in line with results presented in Figure 5.8. These data strengthen the hypothesis that SseK2 does not function as an arginine-GlcNAc transferase in macrophages.

Five proteins were specifically identified in cells infected with the Δ*sseK1/2/3*pSseK1 strain; murine TXNDC9 as well as four *Salmonella* proteins ArcA, SseK1, OmpR and RbfA (Table 5.3). The identification of SseK1 is consistent with auto-GlcNAcylation results presented in Figure 5.7 and 5.8 whereas the new potential SseK1 targets need to be confirmed with further experiments.

TRADD as well as RAN and IFIT1 were identified in both pSseK1 and pSseK3 samples (Table 5.3) suggesting an at least partially overlapping target spectrum for SseK1 and SseK3 during macrophage infection.

Anti-arginine-GlcNAc immunoprecipitation from cells infected with Δ*sseK1/2/3*pSseK3 strain identified 20 putative murine substrates specifically identified upon the expression of SseK3, as well as SseK3 itself (Table 5.3). Except for auto-GlcNAcylation of SseK3, which is in line with my results presented in Figures 5.7 and 5.8, none of the identified potential SseK3 targets have previously been linked to the effector or any of its described functions. To gain further insight into the physiological processes the identified proteins are involved in, gene ontology analysis using the DAVID annotation tool was used (Huang et al., 2009a, 2009b). This revealed a significant correlation of the proteins with the Golgi network as well as Golgi related protein

transport processes (Figure 5.9C and D). Further work is necessary to validate the potential targets but the data suggest that SseK3 might have additional, so far uncharacterised functions in the host cell linked to Golgi network organisation or vesicle transport.

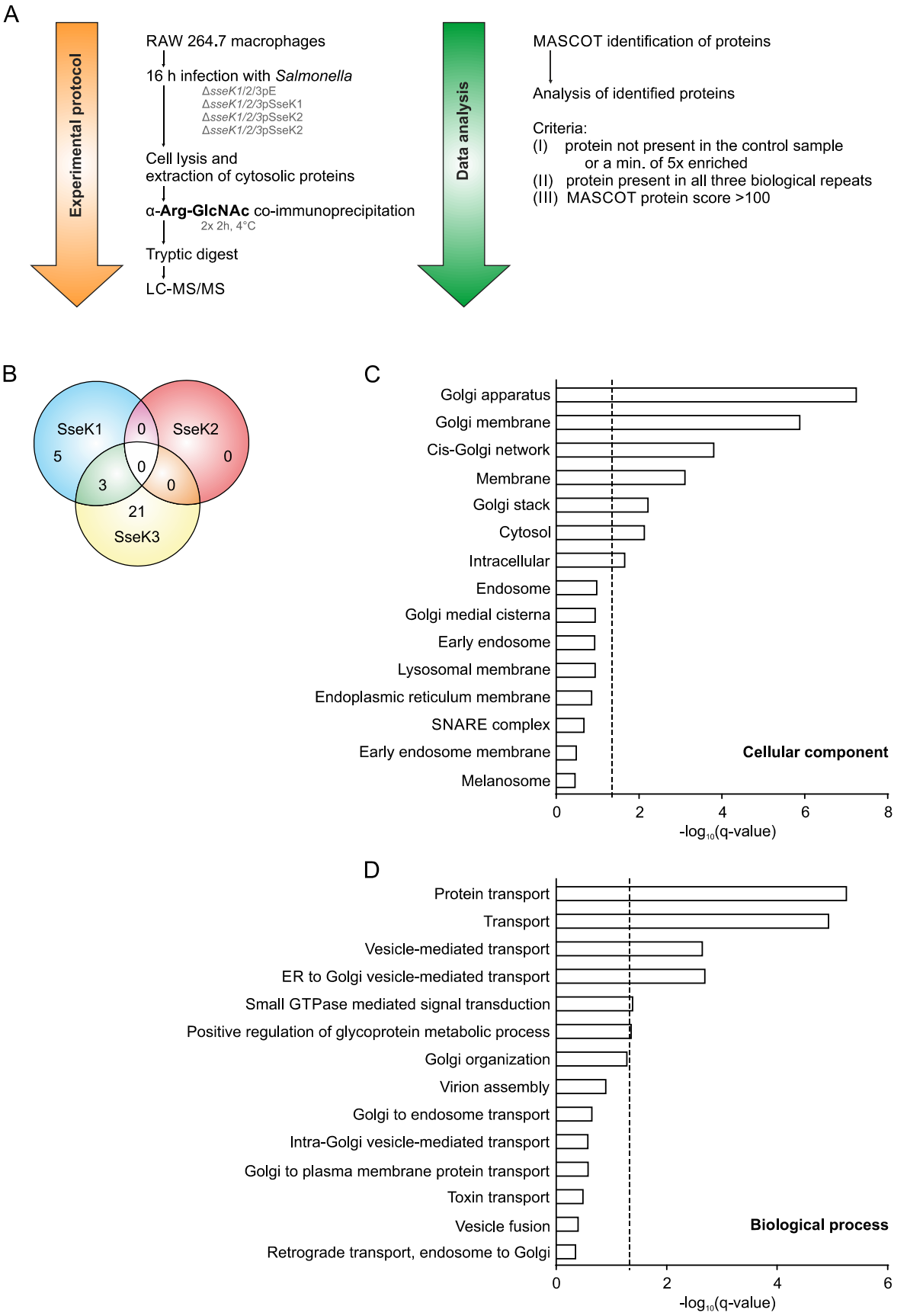

Figure 5.9. **SseK effector target identification using Arg-GlcNAc immunoprecipitation**

(A) Schematic representation of the experimental procedure and data analysis criteria used for immunoprecipitation of putative arginine-GlcNAcylated proteins from *Salmonella*-infected macrophages. (B) Venn diagram summarizing results from α-arginine-GlcNAc immunoprecipitations of *Salmonella*-infected macrophages. (C-D) Gene enrichment analysis using the DAVID functional annotation tool (Huang et al., 2009a, 2009b) of the SseK3 specific, murine proteins identified by LC-MS/MS analysis. The dotted line indicates a q value of 0.05.

Table 5.3. **Proteins identified by tandem LC-MS/MS analysis after arginine-GlcNAc immunoprecipitation** from RAW 264.7 macrophage infection with ΔsseK1/2/3pE, ΔsseK1/2/3pSseK1, ΔsseK1/2/3pSsek2 or ΔsseK1/2/3pSseK3 for 16 h.

Accession: SwissProt database identifier (Mus musculus)

UniProt database identifier (*S.* Typhimurium 14028s) highlighted in light blue.

Score: Mass spectrometry score obtained through MASCOT analysis

Peptides: Number of significant peptide matches identified by LC-MS/MS MASCOT analysis

Rep_1, Rep_2 and Rep_3: Three independent biological repeats

Accession	**Score (Peptides)**			**Description [molecular weight]**
	Rep_1	Rep_2	Rep_3	
pSseK1 specific proteins				
Q9CQ79	361 (7)	612 (12)	325 (4)	Thioredoxin domain-containing protein 9 (TXNDC9) [26.3 kDa]
A0A0F6BBE4	1035 (21)	2149 (27)	1799 (22)	Two-component response regulator (ArcA) [27.3 kDa]
A0A0F6B9Z0	537 (9)	2278 (31)	1044 (14)	Putative cytoplasmic protein (SseK1) [38.8 kDa]
A0A0F6B7V9	374 (6)	703 (10)	344 (7)	Osmolarity response regulator (OmpR) [27.4 kDa]
A0A0F6B770	143 (3)	163 (2)	429 (6)	Ribosome-binding factor A (RbfA) [15.2 kDa]
pSseK3 specific proteins				
Q99K01	1145 (26)	3960 (58)	1789 (28)	Pyridoxal-dependent decarboxylase domain-containing protein 1 (PDXDC1) [87.3 kDa]
Q91V41	631 (11)	1760 (30)	1565 (22)	Ras-related protein Rab-14 (RAB14) [23.9 kDa]
Q9D1G1	801 (16)	1879 (31)	1228 (20)	Ras-related protein Rab-1B (RAB1B) [22.2 kDa]
P62821	681 (13)	1483 (27)	1070 (16)	Ras-related protein Rab-1A (RAB1A) [22.7 kDa]

Accession	Score (Peptides)			Description [molecular weight]
	Rep_1	Rep_2	Rep_3	
O88630	853 (16)	1379 (29)	867 (11)	Golgi SNAP receptor complex member 1 (GOSR1) [28.5 kDa]
Q9QYE6	546 (11)	1288 (19)	1089 (17)	Golgin subfamily A member 5 (GOLGA5) [82.4 kDa]
Q8BMP6	434 (9)	1248 (17)	803 (12)	Golgi resident protein GCP60 (ACBD3) [60.2 kDa]
P35278	537 (9)	1310 (22)	271 (6)	Ras-related protein Rab-5C (RAB5C) [23.4 kDa]
Q8K1T1	206 (5)	907 (13)	469 (6)	Leucine-rich repeat-containing protein 25 (LRRC25) [32.7 kDa]
Q8BRF7	678 (12)	572 (7)	326 (7)	Sec1 family domain-containing protein 1 (SCFD1) [72.3 kDa]
P46460	134 (4)	616 (18)	560 (14)	Vesicle-fusing ATPase (NSF) [82.6 kDa]
Q6NZC7	371 (8)	300 (8)	424 (10)	SEC23-interacting protein (SEC23IP) [110.9 kDa]
Q8BVW3	120 (3)	266 (6)	399 (9)	Tripartite motif-containing protein 14 (TRIM14) [49.6 kDa]
O35153	117 (1)	206 (3)	297 (3)	BET1-like protein (BET1L) [12.4 kDa]
P52332	124 (3)	301 (6)	179 (4)	Tyrosine-protein kinase JAK1 (JAK1) [133.4 kDa]
Q8BJM5	106 (2)	176 (2)	283 (6)	Zinc transporter 6 (SLC30A6) [51.0 kDa]
Q3B7Z2	131 (2)	281 (5)	145 (5)	Oxysterol-binding protein 1 (OSBP) [88.8 kDa]
Q8VDV3	163 (2)	214 (3)	156 (2)	Guanine nucleotide exchange factor for Rab-3A (RAB3IL1) [42.7 kDa]

Accession	Score (Peptides)			Description [molecular weight]
	Rep_1	Rep_2	Rep_3	
Q8CGY8	144 (5)	211 (5)	153 (4)	UDP-N-acetylglucosamine—peptide N-acetylglucosaminyl transferase 110 kDa subunit (OGT) [116.9 kDa]
O70480	197 (2)	120 (1)	173 (2)	Vesicle-associated membrane protein 4 (VAMP4) [16.4 kDa]
A0A0F6B2Z0	163 (2)	216 (4)	136 (3)	Uncharacterized protein (SseK3) [37.9 kDa]
pSseK1 and pSseK3 specific proteins				
Q3U0V2				Tumor necrosis factor receptor type 1-associated DEATH domain protein (TRADD) [34.6 kDa]
SseK1	3183 (61)	5351 (104)	2924 (46)	
SseK3	556 (13)	430 (8)		
P62827				GTP-binding nuclear protein Ran (RAN) [24.4 kDa]
SseK1		341 (7)	140 (3)	
SseK3	300 (6)	905 (14)	615 (12)	
Q64282				Interferon-induced protein with tetratricopeptide repeats 1 (IFIT1) [53.7 kDa]
SseK1	184 (6)	4902 (69)	4231 (56)	
SseK3	52 (1)	1487 (26)	1092 (17)	

6 DISCUSSION

During infection *Salmonella* faces a large variety of host defences that need to be overcome in order for successful colonisation of the host. In this respect, recognition of PAMPs by host cells and the subsequent activation of innate immune signalling and host cell death, which results in inflammatory recruitment of immune cells to clear pathogens, represents one of the major obstacles for *Salmonella*. In response to this host immune response, *Salmonella* has evolved sophisticated mechanisms to interfere with host cell function to achieve bacterial survival and replication. Several SPI-2 T3SS effector proteins specifically target / interfere with host innate immunity, including GtgA, GogB, SpvC, SpvD and SspH1. In addition, the SseK family of effectors, SseK1, SseK2 and SseK3, have been implicated in inhibition of NF-κB signalling due to their homology to the *E. coli* translocated effector, NleB, a potent suppressor of host immune signalling. However, mechanistic insight and the physiological function of the SseK effector family during *Salmonella* infection of macrophages remained to be investigated prior to this thesis work.

6.1 Key findings

Work presented in this thesis revealed that SseK1 and SseK3 inhibit NF-κB activation and necroptosis during *Salmonella* infection of macrophages. This inhibition is specific for TNFα-induced immune signalling and required a DxD motif, which in SseK1 and SseK3 is essential for arginine-GlcNAcylation of target proteins. Expression of either SseK1 or SseK3 induces GlcNAcylation of TRADD which is most likely the cause for the inhibitory effect on host cell innate immunity. Despite stable interaction of SseK3 with the E3 ubiquitin ligase TRIM32, SseK3-mediated inhibition of NF-κB signalling and host cytotoxicity does not require TRIM32. During macrophage infection, SseK1 and SseK3 cause arginine-GlcNAcylation of a diverse range of distinct bacterial and host proteins, suggesting additional effector functions during *Salmonella* infection.

6.2 SseK effector translocation during infection

At first glance, one might hypothesise that the SseK effectors are interchangeable. All three proteins share a high level of amino acid identity (60-75%), are translocated by the SPI-

2 T3SS and when ectopically expressed in mammalian cells inhibit TNFα driven NF-κB signalling. However, when various mutant and complemented mutant strains were investigated during infection, it became apparent that the SseK proteins differ in (i) their expression level (ii) their subcellular localisation, (iii) their host protein target spectrum and (iv) their physiological function.

Initial analysis of the SseK proteins revealed that levels of expressed and translocated SseK1 were much greater than the levels of SseK2 and SseK3, with the lowest protein levels detected for SseK2. This is consistent with a previous study that was unable to detect SseK2 translocation due to low protein levels (Kujat Choy et al., 2004). Differences in protein levels were apparent both during *in vitro* expression of the effectors in SPI-2 inducing minimal medium (data not shown) as well as during host cell infection and independent of the analysis method (western blot, mass spectrometry analysis of isolated protein, immunofluorescence microscopy). In addition, this variation in the detected SseK protein levels correlated with reported RNA expression levels of the effectors (Colgan et al., 2016; Srikumar et al., 2015). However, ectopic expression of SseK proteins from plasmids transfected into 293ET cells resulted in a similar pattern of protein expression levels (SseK1 > SseK3 > SseK2) as that detected during endogenous translocation of SseK proteins from bacteria, suggesting additional levels of regulation. Therefore, it is currently unclear whether the observed differences arise from differential expression and stability of the RNA, translation or protein turnover but nevertheless these findings suggest a sophisticated fine-tuning of SseK effector levels during *Salmonella* infection.

All three SseK effectors are translocated into macrophages and epithelial cells via the SPI-2 T3SS, yet inside the host cell these proteins have distinct sub-cellular localisations. Microscopy experiments using HA-tagged effector delivered into host cells during infection have confirmed previous findings from ectopic expression in HeLa cells that SseK1 is uniformly distributed throughout the cytoplasm (Kujat Choy et al., 2004). In stark contrast, SseK2 and SseK3 were observed in tight peri-nuclear accumulations that co-localised with Golgi network markers in infected macrophages. Currently the mechanism(s) of how SseK2 and SseK3 are targeted to and maintained at the Golgi apparatus are not fully understood. Predominant Golgi network association of SseK2 and SseK3 also occurred in transfected 293ET cells, showing that effector subcellular localisation does not require the context of infection or

cooperation between the effectors. Neither SseK2 nor SseK3 have any predicted trans-membrane helices suggesting that the proteins' Golgi network association is indirect, possibly via protein-protein or protein-lipid interaction(s) and/or posttranslational modification(s). Analysis of SseK3 deletion mutants revealed that the N-terminal region, which is diverse in sequence between the SseK family members, is required but not sufficient for strong Golgi network localisation of SseK3. In addition, positive charge of the N-terminal region, as well as catalytic activity, contribute to SseK3 Golgi network association. Whether this is due to an interaction with host protein(s), auto-GlcNAcylation of SseK3 or interaction with Golgi membrane lipids requires further investigation. Out of the 13 N-terminal amino acids required for Ssek3 Golgi network localisation 9 are conserved in SseK2, whilst only the initiator methionine is conserved between SseK3 and SseK1. This suggests that the mechanism(s) mediating SseK2 and SseK3 Golgi network association are similar. Currently there are no data suggesting that SseK2 and SseK3 share a host target spectrum and SseK2 is not detectably auto-GlcNAcylated. Therefore, to identify the molecular determinants of how SseK2 and SseK3 associate with the Golgi network, interaction studies of recombinant SseK2 and SseK3 (and mutants thereof) with liposomes of varying size and lipid composition might be the most promising futur direction of research. Interestingly, SseK3-SseK1 chimeric proteins ($SseK3_{N44}$-$SseK1_{\Delta 43}$) did not localise to the Golgi network whereas the SseK3 N-terminal region fused to GFP ($SseK3_{N44}$) partially did. This suggests that an inherent property of SseK1 keeps the protein in the cytosol, presumably by interaction with host proteins. To further investigate the properties that mediate differential localisation of SseK3 and SseK1, studies of additional SseK3-SseK1 chimeras as well as SseK2-SseK1 chimeras might be useful. This, together with the analysis of point mutants and liposome assays (mentioned above), will hopefully enable the identification of additional effector regions required for the differential localisation of the SseK proteins.

6.3 SseK1 and SseK3 induce arginine-GlcNAcylation of host cell proteins

Based on the SseK's sequence identity to NleB and the effectors predicted secondary structure, they were hypothesised to be glycosyltransferases. Indeed, Li and colleagues (2013) found that overexpression of SseK1 leads to arginine-GlcNAcylation of TRADD. The catalytic DxD motif of NleB is fully conserved in the SseK proteins and essential for SseK3-mediated

inhibition of TNFa signalling following ectopic expression (Yang et al., 2015). In my assays the putative catalytic DxD motif of SseK1 and SseK3 were required for the induction of a large number of arginine-GlcNAcylated proteins in the host cell, including the effectors themselves. This strongly suggests that the effectors are bona fide functional enzymes. In addition, no arginine-GlcNAcylated proteins were detected in cells infected with the Δ*sseK1/2/3* mutant suggesting that this post translational modification is not a reaction of the mammalian cell to *Salmonella* infection but an active process mediated by the SseK effectors. However, further experiments with purified SseK proteins are required to irrevocably demonstrate that SseK1 and SseK3 are arginine-GlcNAc transferases.

Sugar modification of arginine residues is not present in mammalian cells under physiological conditions but in recent years it has become clear that this atypical mono-glycosylation is present in other organisms. Arginine-glucosylation as a PTM was already described in 1995, mediated by the sweet corn protein β-glucosylarginine (Singh et al., 1995). Interestingly, this protein auto-glucosylates itself (Singh et al., 1995), yet whether this is of physiological relevance was not determined. During the course of this thesis, arginine-rhamnosylation by the EarP glycosyltransferase from *E. coli* was discovered (Lassak et al., 2015). Structural analysis of EarP showed that it belongs to the GT-B family of glycosyltransferases (Krafczyk et al., 2017) and is therefore distinct from NleB and the SseK effectors (which are classified as GT-A glycosyltransferases), suggesting that the proteins developed arginine-glycosyltansferase activity independently. The crystal structure of SseK3 has recently been solved and revealed that the effector adopts a GT-A fold that shares the highest structural similarity with the PaToxG glycosyltransferase from entomopathogenic *Photorhabdus asymbiotica* (D. Esposito and K. Rittinger, unpublished personal communication). PaTox mono-O-glycosylates a tyrosine residue of eukaryotic Rho GTPases using UDP-GlcNAc as a substrate (Jank et al., 2013). As there is no significant sequence similarity between SseK3 and PaTox it is currently not possible to predict other bacterial (arginine-) GlcNAc transferase without structural information. Yet, the increasing number of atypical glycosyltransferases discovered in the last years suggest that mono-glycosylation on residues besides serine and threonine is more prevalent than originally assumed.

Infection of macrophages with a Δ*sseK1/2/3* deletion mutant differs from wild-type infected cells in at least three aspects: (i) absence of arginine-GlcNAcylated host proteins (ii) increased

host NF-κB pathway activation and (iii) increased host cell death. Each of these phenotypes could be complemented by plasmid-based expression of SseK1 or SseK3 in the Δ*sseK1/2/3* strain, suggesting a functional correlation between the phenotypes and the effectors catalytic activity. Transfection based experiments using putative catalytic DxD mutants of the effectors, strengthened the link between arginine-GlcNAcylation and inhibition of host cell immunity. Unfortunately, as the DxD SseK mutants were poorly translocated from bacteria into the host cell, it was not possible to study this in the physiological context of *Salmonella* infection. It was previously reported that mutagenesis of NleB, at numerous residues, results in decreased translocation of the effector (Wong Fok Lung et al., 2016), however whether this is the case for the catalytic DxD mutant was not investigated. Two additional amino acids in NleB (E253A and Y219A), required for catalytic function of NleB were also identified in the study (Wong Fok Lung et al., 2016), which are fully conserved in the SseK proteins. Both amino acids are in close proximity to the catalytic DxD motive in the crystal structure of SseK3 and are predicted to be involved in the coordination of the sugar donor or required for the catalytic nucleophilic attack (unpublished, D. Esposito and K. Rittinger). Mutagenesis of these amino acids in the *Salmonella* effectors might provide an appropriate tool to study catalytic effector mutants during *Salmonella* infection.

6.4 SseK1 and SseK3 inhibit TNFα-driven NF-κB activation and host cell death

Inhibition of NF-κB signalling by SseK1 and SseK3 was previously described (Li et al., 2013; Yang et al., 2015) but the mechanism and relevance during *Salmonella* infection was not understood. Using a RAW 264.7 macrophage NF-κB-reporter cell line I showed that both SseK1 and SseK3 function additively to inhibit NF-κB activation during infection. As infection with the Δ*sseK1/3* double or Δ*sseK1/2/3* triple mutants yielded a similar degree of enhanced NF-κB reporter induction as the SPI-2 defective *ssaV* mutant strain it is tempting to speculate that these effectors are the only ones to modulate NF-κB activity during macrophage infection. However, this is unlikely to be the case. First, the *ssaV* mutant has a severe replication defect at the 16 h time points assayed and so is likely to elicit reduced induction of the reporter. Second, the SPI-2 dependent effector SpvD has been reported to inhibit NF-κB induction (Grabe et al., 2016; Rolhion et al., 2016) with a role for SseL being more controversial (Le Negrate et al., 2008; Mesquita et al., 2013). Whether there is a SPI-2- as well

as SPI-1-dependent role for GtgA/PipA and GogA requires further investigation (Sun et al., 2016). It is likely that multiple effectors inhibiting NF-κB induction enable *Salmonella* to fine-tune host immune responses, potentially in a cell-type and temporal manner that awaits further investigation. RNA sequencing of wild-type and mutant *Salmonella* infected host cells at various time points post uptake could help to investigate specific host gene expression profiles and immune responses modulated by the effectors. In addition, investigation of the host immune response when challenged with combined deletion mutant strains might clarify if the currently known NF-κB pathway modulating effectors (SseK1, SseK3, GtgA, PipA, GogA and SpvD) have distinct or redundant function during *Salmonella* infection.

Neither in this work, nor in previous studies (Buckner et al., 2011; Kidwai et al., 2013), did deletion of individual or all three SseK effectors cause attenuation of the *Salmonella* mutant in mice. This was independent of the inoculation route (oral gavage or intraperitoneal injection) and the duration of infection, with tested conditions ranging from between 2 to 14 days. The commonly used competitive index infection assay has the disadvantage that the co-inoculated wild-type stain might cross-complement (subtle) defects of the investigated mutant and differences in virulence might therefore not be apparent. Therefore, it cannot be excluded that effects of the SseK effectors on *Salmonella* fitness were missed. Due to the additive effect of SseK1 and SseK3 on innate immune signalling, analysis of cytokine expression and host cell recruitment to immunological sites might give more insight into whether inhibition of NF-κB signalling by the SseK effectors modulates the host immune response during *Salmonella* infection.

Many different stimuli contribute to the activation of the NF-κB signalling cascade during *Salmonella* infection (Lawrence, 2009). Interestingly, all three SseK effectors were able to inhibit TNFα-driven NF-κB pathway signalling when ectopically expressed. Therefore, the effectors are sufficient for signalling modulation and can function individually and independently of the context of *Salmonella* infection. However, neither the SseK effectors nor their *E.coli* homologue NleB inhibited overall pathway activity after IL-1α, IL-1β, HMW poly(I:C) stimulation or auto-activation by TLR4 overexpression. These data indicate that the SseK proteins do not inhibit a component of the classical, conserved NF-κB pathway but a TNFα agonist-specific component of the cascade prior to IKK complex phosphorylation. This is in contrast to other SPI-2 T3SS effectors including GtgA, GogB and SpvD, which target

proteins common to numerous agonists (Pilar et al., 2012; Rolhion et al., 2016; Sun et al., 2016). It is important to verify the specific effect of SseK1 and SseK3 on TNFα-driven NF-κB signalling during macrophage infection, however attempts to address this using Enbrel, a TNFα antagonist, were inconclusive. Treatment with this competitive inhibitor drastically reduced overall activation of an NF-κB reporter during *Salmonella* infection, suggesting that at late infection time points NF-κB pathway activation in macrophages is mainly driven by TNFα. However, due to the minimal activation levels of the NF-κB reporter it was not possible to conclusively determine if differences in NF-κB signalling activity between wild-type and Δ*sseK1/2/3 Salmonella* infected macrophages depended on TNFα. Analysis of NF-κB signalling and NF-κB-regulated cytokines in *Tnfα*$^{-/-}$ or *Tnfr*$^{-/-}$ mice (or associated cell lines) upon wild-type and Δ*sseK1/2/3 Salmonella* infection would therefore help to further understand the stimulus-specific effects(s) of SseK1 and SseK3 on NF-κB pathway activity.

NF-κB signalling and cell death are tightly linked innate immune responses to bacterial infection and are both regulated by TNFα signalling. Similar to their effect on NF-κB signalling both SseK1 and SseK3 inhibit host cell death during macrophage infection. Dependent on the cellular context, both effectors can inhibit apoptosis or necroptosis. During macrophage infection *Salmonella* causes necroptotic cell death (Robinson et al., 2012), which is inhibited by SseK1 and SseK3, whereas levels of apoptosis are low in this cell type. Treatment with the TNFα inhibitor Enbrel mitigated enhanced cell death induced by the Δ*sseK1/2/3* mutant compared to wild-type *Salmonella* infection, showing that SseK1 and SseK3 specifically inhibit TNFα-induced necroptosis in macrophages. Interestingly, cytotoxicity of wild-type *Salmonella* infected macrophages was unaffected by Enbrel treatment, suggesting that the SseK effectors are potent inhibitors of TNFα-induced cell death during macrophage infection. Necroptotic cell death is highly inflammatory and required for the control of bacterial infection in mice (e.g. *Yersinia pestis* (Weng et al., 2014)*, Staphylococcus aureus* (Kitur et al., 2016). On the other hand, necroptosis-deficient mice (Rip3$^{-/-}$) infected with *Salmonella* display less macrophage death and enhanced control of *S*. Typhimurium *in vivo* without any substantial difference detected in animal survival (Robinson et al., 2012). This paradoxical observation requires further investigation but suggests that a tight control of necroptotic cell death (by the SseK effectors) is required for *Salmonella* pathogenesis. To clarify this, investigation of *Salmonella* infection in MLKL deficient mice is required. This is preferred over further studies

in RIPK deficient mice as MLKL is the ultimate component of necroptosis signaling, whereas RIPK3 is involved in the balance between apoptotic and necroptotic cell death (Newton et al., 2014) and therefore phenotypic outcomes observed in *Ripk3*$^{-/-}$ mice are more complex. In addition, analysis of *Salmonella* infection in *Mlkl*$^{-/-}$ mice over a longer timeframe, as well as comparing the outcome of infection after inoculation of mice with sseK deletion strains, will help to understand the role of necroptosis and the SseK effectors during *Salmonella* infection.

NleB achieves specificity towards inhibiting TNFα-driven cell signalling due to the modification of death domain containing proteins, including FADD and TRADD. Targeted analysis of these proteins as putative SseK substrates revealed that SseK1 induces GlcNAcylation of overexpressed FADD during transfection and infection of HeLa cells without stable interaction between the proteins. SseK1-induced Arginine-GlcNAcylation of FADD occurred on R117, the same amino acid targeted by NleB (Pearson et al., 2013). This suggests that SseK1 prevents FADD oligomerisation and downstream signalling in a comparable mechanism to NleB. However, FADD was not detected when SseK1-specific arginine-GlcNAcylated proteins were analysed during *Salmonella* infection of macrophages, suggesting that FADD is a cell type or context specific target of SseK1. In contrast, both SseK1 and SseK3 expression induced arginine-GlcNAcylation of TRADD when ectopically overexpressed as well as during macrophage infection. Interestingly, mutation of the arginine residue modified by NleB (R233) was insufficient to prevent SseK1-induced arginine-GlcNAcylation of TRADD. Evidently, SseK1 modifies either different or multiple arginine residue(s) in TRADD. Mass spectrometry-based identification of the precise amino acid modified is required to fully understand the impact of the PTM on TRADD function. It is however likely that similar to NleB-mediated modification of TRADD, SseK-mediated modification prevents oligomerisation of the TRADD death domain and thereby inhibits TNFR1-TRADD, TRADD-FADD and TRADD-RIPK1 interactions (Park et al., 2014), resulting in loss of protein function. Alternatively, arginine-GlcNAcylation in the N-terminal domain of TRADD might alter TRAF2 interaction (Park et al., 2000) and impede immune signaling. In addition, the amino acid modified by SseK3 has not been investigated and it is possible that both effectors arginine-GlcNAcylate different residues in TRADD to achieve cooperative or differential physiological outcomes.

Modification of TRADD might be sufficient to explain the specificity of SseK1 and SseK3 to TNFα-driven NF-κB pathway inhibition in contrast to other (secondary) stimuli as this death

domain protein is essential for functional TNFR signalling (Pobezinskaya et al., 2008). In contrast, neither LPS- nor IL-1-induced NF-κB signalling in macrophages require TRADD (Ermolaeva et al., 2008; Pobezinskaya et al., 2008), making them immune to the SseK effectors. In contrast, intracellular detection of cytosolic RNA (or poly(I:C)) by RLRs and subsequent activation of NF-κB signalling requires FADD and TRADD (Balachandran et al., 2004; Kawai et al., 2005; Michallet et al., 2008; Takahashi et al., 2006). Therefore it is surprising that this signalling cascade is not inhibited by SseK1, SseK3 and NleB. It is possible, that this is due to the differential localisation of the death domain-containing proteins in the host cell, protein complex composition or inaccessibility of the target amino acid in the complex. Identification of the precise amino acid(s) GlcNAcylated in TRADD by SseK1 and SseK3 will help to gain insight into this puzzle.

Similarly, cell death inhibition by SseK1 and SseK3 following TNFα-stimulation of cells can be explained by arginine-GlcNAcylation of death domain containing proteins as both FADD and TRADD are crucial for this process (Lin et al., 2004; Pobezinskaya et al., 2008) In contrast, only FADD is required for TRAIL-induced cell death (Sprick et al., 2000) whereas TRADD negatively regulates this process (Cao et al., 2011), probably due to competitive interaction with the TRAIL receptor. Interestingly, despite GlcNAcylation of both FADD and TRADD by SseK1, no effect on TRAIL-induced apoptosis by overexpressed SseK1 was detected. Higher modification levels of TRADD compared to FADD by SseK1 might account for this phenotype, yet whether this is due to differential affinity of SseK1 activity towards the death domain proteins or protein abundance in the host cell is currently unknown. Again, this revealed differences between the effectors as SseK3 inhibited both TNFα-and TRAIL-driven cell death in a catalytically dependent manner. This suggests that in addition to TRADD, SseK3 has further host cell targets involved in death-domain receptor signalling. To date, these additional targets remain unknown, as mass spectrometry analysis of SseK3-dependent arginine-GlcNAcylated proteins did not detect proteins involved in host cell death besides TRADD. To address this more directly future work should analyse (SseK3-dependent) arginine-GlcNAcylated proteins specifically after engagement of the TRAIL-receptor. Interestingly, when challenged with *S.* Typhimurium, survival of TRAIL receptor deficient mice are comparable to wild-type animals (Diehl et al., 2004), suggesting that either TRAIL signaling is not required for the control of *Salmonella* infection or that *Salmonella* successfully suppresses

any TRAIL-mediated effects, possible by SseK3 function. Overall, neither of the *Salmonella* SseK proteins inhibited cell death in response to all three death-inducing agonists, TNFα, TRAIL or FasL as potently as NleB. Substrate diversification of SseK proteins (beyond death-domain containing protein) may mean they are enzymatically less effective / potent towards particular substrates. This might be the reason for the retention of more than one SseK effector in several strains of *Salmonella*.

6.5 The physiological function of SseK2 remains unknown

Due to the homology to the *E. coli* effector NleB (Brown et al., 2011), I hypothesised that all three SseK effectors are arginine-GlcNAc transfers that inhibit NF-κB signalling and host cell death in a redundant manner. However, analysis of these phenotypes revealed interesting and unexpected differences between the effectors. In respect to its physiological relevance, SseK2 seems to be distinct from both SseK1 and SseK3, and its function during *Salmonella* infection remains enigmatic. SseK2 overexpression did inhibit TNFα-induced NF-κB activation upon transfection of 293ET cells. This was dependent on its putative catalytic DxD motif, suggesting that SseK2 is a functional enzyme. This is further supported by weak auto-GlcNAcylation of SseK2 and the detection of weak arginine-GlcNAcylated proteins when SseK2 was ectopically expressed (Günster et al., 2017). However, these phenotypes were only apparent when SseK2 was highly overexpressed and not detectable during macrophage infection, suggesting that both phenotypes might be non-physiological. Nonetheless, it remains possible that any effects of SseK2 on the NF-κB pathway and host cell death during *Salmonella* infection were below the detection limit or occur in a different cell type or time point than assayed here. Despite the fact that SseK2 was translocated into macrophages in a SPI-2 T3SS dependent manner, no arginine-GlcNAcylated proteins were detected by immunofluorescence or western blot for the *sseK1/2/3* mutant strain expressing SseK2. Low expression levels of SseK2 (compared to SseK1 or SseK3) from the complementing plasmid might account for this observation. Yet, all detectable GlcNAcylated signal was absent in cell lysates from *sseK1/3* mutant infected cells, when compared to wild-type *Salmonella* infected cell lysates. In addition, no SseK2-specific arginine-GlcNAcylated proteins were identified by mass spectrometry of infected RAW 264.7 macrophages, suggesting that SseK2 does not function as an arginine-GlcNAc transferase under the tested conditions. However, the

predicted structure of SseK2 and its requirement of the DxD motif to inhibit NF-κB signalling when overexpressed suggest that SseK2 is a functional enzyme, likely a GT-A glycosyltransferase. It is possible that SseK2 has evolved to preferentially catalyse the GlcNAcylation of different amino acid residue(s) or to transfer a different saccharide moiety that is not detected by the arginine-GlcNAc-specific antibody used in this study. To date, the primary amino acid sequence of bacterial GTs is not sufficient to predict the sugar donor substrate utilised by the enzyme (Brockhausen, 2014; Schmid et al., 2016). Therefore, measurement of the binding affinity of SseK2 to a large variety of sugar donors as well as extensive structural analysis of SseK2 will be required to determine the enzymatic function of the effector. Any validated substrates might then indicate the function of SseK2 during infection. Alternatively, it is possible that rather than enzymatic diversification, SseK2 is on its way to becoming "dead" as sseK2 is disrupted in a large number of *Salmonella enterica* serovars including *S.* Enteritidis, *S.* Paratyphi A and *S.* Typhi (Nuccio and Bäumler, 2014).

6.6 TRIM32 - the enigma

Mass spectrometry analysis of SseK3 binding partners during macrophage infection identified a single protein, TRIM32. Work by Yang and colleagues (2015) previously showed specific binding of SseK3 to this E3-Ubiquitin ligase when SseK3 was ectopically expressed. Yet whether this interaction occurs during *Salmonella* infection was previously unknown. SseK3, not SseK1 and SseK2, specifically and directly binds to TRIM32. This sets this protein family apart from other SPI-2 T3SS effectors like the GtgA/GogA/PipA families where all three effectors bind to and cleave the same substrates, the NF-κB transcription factors RelA and RelB (Sun et al., 2016).

SseK3-TRIM32 binding occurs in the NHL domain of TRIM32 (T. Thurston, unpublished) and was completely abolished when using an N-terminal deletion mutant of SseK3 ($SseK3_{\Delta N44}$). However, analysis of the SseK3 crystal structure (D. Esposito and K. Rittinger) suggests that this deletion unfolds the protein, making the inability of the $SseK3_{\Delta N44}$ mutant to bind TRIM32 a probable artifact. Attempts to co-crystallise SseK3 and TRIM32 to gain further insight into the structural details of the protein interaction were unsuccessful due to the insolubility of full-length TRIM32 or the TRIM32 NHL-domain on its own (D. Esposito and K. Rittinger, personal communication). Analysis of a larger range of SseK3-SseK1 chimera proteins might

be required to further characterise the SseK3 regions involved in TRIM32 binding. Interestingly, even though TRIM32 and SseK3 co-localise at the Golgi network, this is not required for the proteins interaction but might be needed for independent functions of the two proteins. Post translational modification and changes to effector specificity mediated by host proteins is an emerging concept in microbiology (Popa et al., 2016). For a large number of proteins binding to the TRIM32 NHL domain results in ubiquitination and degradation of the proteins (Horn et al., 2004; Kano et al., 2008; Liu et al., 2014). In contrast, there was no change in molecular mass of SseK3 when co-expressed with TRIM32 that could indicate ubiquitination of the effector and translocation, intracellular localisation and protein stability of SseK3 were independent of TRIM32. This suggests that SseK3 is not a direct TRIM32 ubiquitination target but it cannot be excluded that the interaction facilitates other posttranslational modifications of the effector. Sensitive mass spectrometry analysis of purified SseK3 might help to further elucidate this.

Even though TRIM32's involvement in muscle development and disease (Lazzari and Meroni, 2016) is characterised best, several studies link the E3 ligase to innate immunity (Albor et al., 2006; Horn et al., 2004; Ryu et al., 2011). Overexpression of TRIM32 positively regulates NF-κB signalling activity (Albor et al., 2006; Uchil et al., 2013) whereas knock-down of the E3 ligase prevented NF-κB reporter activation (Yang et al., 2015). This is in partial contrast to my data as TRIM32 KO macrophages responded similarly to wild-type cells when stimulated with LPS and no differences in cytokine levels were detected in macrophages from infected wild-type or *Trim32*$^{-/-}$ mice. However, this might be due to adaptation and compensation of the cells due to the long-term absence of TRIM32. Overall, many TRIM proteins have different phenotypes depending on the cell type analysed and tight regulation of protein levels seems to be crucial (Uchil et al., 2013). In a recent study investigating TRIM32 function it was found that low and high levels of TRIM32 overexpression result in opposing phenotypes that are additionally cell type dependent (Pavlou et al., 2016) suggesting that the opposing (published) phenotypes might be due to different experimental conditions and not necessarily contradictory. Reintroduction of TRIM32 into the *Trim32*$^{-/-}$ cells and subsequent analysis of innate immune signaling was hampered as retroviral transduction resulted in significantly higher levels of TRIM32 protein than wild-type cells (data not shown).

The published links to immune signalling made TRIM32 a likely target for GlcNAcylation by SseK3 to mediate the effectors NF-κB suppressive phenotype. However, no modification of TRIM32 by SseK3 was detected (Figure 4.3, (Yang et al., 2015)) and inhibition of IFNβ-induced ISRE reporter activation by TRIM32 was unaffected by coexpression of SseK3. This is similar to the SPI-2 T3SS effector SseL which stably interacts with oxysterol-binding protein-1 (OSBP) (Auweter et al., 2011), yet does not seem to deubiquitinate OSBP (Auweter et al., 2012). Currently, for both interactions, the physiological relevance is unknown and it is therefore possible that the interactions are neutral and without consequence for the function of either interaction partner. TRIM32 self-associates into a tetramer (Koliopoulos et al., 2016) and could therefore function as a structural scaffold for SseK3 function rather than being a direct effector target. However, TRIM32 was not required for SseK3-mediated inhibition of NF-κB signalling or host cell death. Therefore, the physiological significance of the SseK3-TRIM32 interaction remains enigmatic. Analysis of arginine-GlcNAcylated proteins revealed a large number of potentially new SseK3 targets and phenotypes, including the arginine-GlcNAcylation of SseK3 itself. Investigation into whether these proteins are arginine-GlcNAcylated in the TRIM32 KO macrophages might shed light onto the physiological relevance of the TRIM32-SseK3 interaction. In addition, quantitative mass spectrometry analysis of TRIM32-bound proteins in uninfected and *Salmonella*-infected cells might help to elucidate the role of TRIM32 during *Salmonella* infection.

Short-term infection of *Trim32*$^{-/-}$ mice was indistinguishable from wild-type mice in the overall bacterial load as well as amount of *Salmonella*-infected splenic macrophages, suggesting that TRIM32 is not required for the control of *Salmonella* infection. Subsequent to this work, a study showed that loss of TRIM32 leads to an enhanced TH2 response in a mouse dermatitis model (Yuangang Liu et al., 2017). This is due to a reduction in TH17 cytokines (IL-17, CCL20) and increased expression of TH2 cytokines (IL-4, IL-5), resulting in enhanced recruitment of TH2 cells, mast cells and eosinophil's to psoriatic lesions (Yuangang Liu et al., 2017). During *Salmonella* infection of mice, differences in immune cell recruitment to immunological organs like the mesenteric lymph nodes and the spleen only become apparent during long-term infection (> 2 weeks, (Mittrücker et al., 2002; Pie et al., 1997)). Therefore, it would be interesting to analyse the cytokine pattern and T-cell response of wild-type and *Trim32*$^{-/-}$ mice

during long-term and persistent *Salmonella* infections in mice to gain further understanding of TRIM32 function during *Salmonella* infection.

6.7 Revealing target specificities between SseK1 and SseK3

After macrophage infection wth wild-type *Salmonella*, multiple proteins of different molecular mass were arginine-GlcNAcylated. Analysis of arginine-GlcNAc patterns induced by various sseK mutant strains revealed that SseK1 and SseK3 have different host cell targets during *Salmonella* infection.

To determine the identity of these proteins I used different approaches. The most common un-biased approach to identify effector binding proteins is isolation of the bacterial protein from transfected or infected cells followed by mass spectrometry analysis of the co-purified proteins (Auweter et al., 2011; Sontag et al., 2016). Using this approach for translocated SseK effectors isolated from macrophages did not identify any new SseK interaction partners. This was probably due to the catalytic activity of the enzymes, resulting in highly transient interactions with target proteins. This is different to NleB which does form a stable interaction with death domain containing proteins (Li et al., 2013; Pearson et al., 2013), which might reflect greater affinity of NleB to its substrates. Lack of stable SseK-host protein binding was also observed during transfection experiments, where target protein arginine-GlcNAcylation was observed but no stable protein-protein interactions were detected. To circumvent this problem, catalytically inactive trapping mutants can be used (López-Otín and Overall, 2002), however the SseK DxD mutants are poorly translocated and can therefore not be used during *Salmonella* infection. The only protein that formed a stable interaction with any SseK effector was TRIM32 to SseK3, yet this protein was not GlcNAcylated by the effector and was not required for SseK3-mediated NF-κB and cell death inhibition.

In a second unbiased approach, arginine-GlcNAcylated proteins from infected macrophages were isolated by anti-Arg-GlcNAc immunoprecipitation and analysed by mass spectrometry. This revealed a vastly different putative target spectrum for SseK1 and SseK3 but was unable to identify SseK2-dependent arginine-GlcNAcylated host proteins. Due to the low affinity of the anti-Arg-GlcNAc antibody, it is likely that the recovered proteins only represent the most abundant or highly modified proteins during macrophage infection and additional SseK

targets (below the detection limit) might exist. For all the identified SseK-dependent arginine-GlcNAcylated proteins additional verification is required, ideally using an *in vitro* GlcNAcylation assay, which has the added benefit that identification of the modified amino acid residue(s) by subsequent mass spectrometry is possible. In addition however, it will important to verify these putative substrates following infection of cells with bacteria. However, as all the identified proteins were highly specific (absent from controls) and reproducible, it is tempting to speculate on additional functions for SseK1 and SseK3.

Interestingly, both by a targeted approach as well as unbiased mass spectrometry, auto-GlcNAcylation of SseK1 and SseK3 was detected. This is in clear contrast to NleB, which is not arginine-GlcNAcylated but is similar to auto-arginine-glucosylation of the sweet corn protein β-glucosylarginine (Singh et al., 2005). Currently it is unknown whether auto-GlcNAcylation occurs in a cis-or trans-fashion and if it is required for the effectors catalytic function, substrate specificity or subcellular localisation. Identification of the modified arginine residue(s) in SseK1 and SseK3 will allow further insight into the functional difference between SseK1, SseK3 and NleB.

In addition to SseK1 itself, only a few proteins were modified in an SseK1-dependent manner as identified by anti-Arg-GlcNAc immunoprecipitation and mass spectrometry from *S.* Typhimurium infected macrophages. The largest number of identified peptides corresponded to TRADD, confirming results from the targeted approach using overexpressed protein and suggesting that TRADD is the main SseK1 target during macrophage infection. Additionally, the Thioredoxin Domain Containing protein 9 (TXNDC9, also named PHLP3) was identified. The exact function of TXNDC9 is currently unknown but it has a function in establishing a functional cytoskeleton (Stirling et al., 2006). Therefore, actin and tubulin disturbance by SseK1 might be possible and should be investigated. Unexpectedly, three SseK1-dependent arginine-GlcNAcylated *Salmonella* proteins were also detected. OmpR and ArcA are transcriptional response regulators (Evans et al., 2011; Lee et al., 2000), whilst RbfA is a ribosome binding factor. None of these *Salmonella* proteins are reported to be translocated into the host cell and were likely in the analysed cytoplasmic fraction due to the cell lysis conditions used (0.3 % triton X-100) or bacterial cell death. Nevertheless, it is possible that SseK1 has dual functions, modifying proteins inside *Salmonella* as well as in the host cell. Analysis of arginine-GlcNAcylated proteins from bacteria grown in SPI-2 inducing minimal

medium is likely to clarify this. During macrophage infection several proteins of different molecular weight were GlcNAcylated in an SseK1-dependent manner. One arginine-GlcNAcylated protein of approximately 38 kDa present in wild-type *Salmonella* infected cells (Figure 5.1, highlighted by the ‡ symbol) could represent SseK1 itself (38.8 kDa) as this protein was absent during infections with the *ΔsseK1* deletion stain. Instead an additional protein of approximately 41 kDa was present during infection with the *ΔsseK1/2/3*pSseK1 strain, which could represent 2xHA-tagged SseK1. Additional arginine-GlcNAcylated proteins with a similar molecular weight to TRADD and TXNDC9 were detected in macrophage lysates. But which (if any) of these represent TRADD or TXNDC9 remains to be established. Analysis of the arginine-GlcNAcylation protein pattern in respective knock down or knock out cells would be required for this.

Anti-Arg-GlcNAc immunoprecipitation and mass spectrometry analysis from macrophages infected with *Salmonella* expressing SseK3 revealed a large number of putative host cell targets of SseK3. Gene ontology analyses showed that the majority of these proteins localise to host cell membranes, mainly at the Golgi network (e.g. BET1L, RAB14, RAB1A, RAB1B, SCFD1, ACBD3, GOSR1, GOLGA5, OSBP, PDXDC1, SLC30A6, VAMP4). This correlates with the subcellular localisation of SseK3-dependent arginine-GlcNAcylated proteins detected by immunofluorescence as well as SseK3's localisation in the host cell. Currently it is not known whether the differences in SseK1 and SseK3-dependent modified proteins is solely due to the differential subcellular localisation of the proteins in the host cell. Redirection or tethering of SseK1 to the Golgi network for example with nanobody traps (Harmansa et al., 2017) might resolve this question. In addition, *in vitro* target glycosylation assays as well as the structure-based identification and subsequent mutation of the SseK-target interface will help to further elucidate SseK1 and SseK3 target specificity.

In addition to their Golgi network localisation, several of the SseK3-dependent identified proteins are involved in (vesicle-mediated) protein transport to and from the Golgi network (e.g. BET1L, NSF, RAB14, RAB1A, RAB1B, RAB3IL1, RAB5C, SCFD1, GOSR1). Manipulation of intracellular protein transport and host cell organelles is a common defence mechanism of a large number of bacterial pathogens (Escoll et al., 2015). Of the SPI-2 T3SS effectors, SifA, SseG and SseF have been shown to redirect exocytic post-Golgi vesicles to the vicinity of the SCV (Kuhle et al., 2006), however whether SseK3 contributes to this process was not

addressed in the study and requires further investigation. Interestingly, both SseF and SseG interact with the Golgi protein ACBD3 (Yu et al., 2016), which was also identified as a putative SseK3 target. Currently there is no evidence of cooperation or antagonism between SseK3 and SseF-SseG. SseK3 alone is sufficient to inhibit NF-κB signalling and cell death, yet analysis of Golgi network associated functions of the effector in differential deletion mutants might further our understanding of SPI-2 T3SS effector coordination. In addition, SopB, PipB2 and SspH2 block host cell exocytosis (Perrett and Zhou, 2013). Yet, in the same study no effect of SseK3 on exocytosis was detected (Perrett and Zhou, 2013) suggesting that any effect on protein transport is limited to intracellular trafficking. Golgi network localisation of SseK3 was not required for the effectors inhibition of NF-κB signalling but might be essential for effects on protein redistribution in the host cell and therefore requires further investigation. Besides the Golgi network associated proteins, several other potential SseK3 targets stand out. TRADD and JAK1 are both involved in innate immune signalling. While TRADD is likely to be the SseK3 target responsible for NF-κB signalling inhibition, no effect of SseK3 on JAK1-mediated IFNβ signalling was detected. Nevertheless, it is possible that JAK1 modification by SseK3 might affect IL-6 or IFNγ signalling. Unexpectedly, the mammalian *O*-GlcNAc transferase (OGT) was also identified in the anti-Arg-GlcNAc immunoprecipitation mass spectrometry. Whether this is due to unspecific binding of the antibody or if OGT is a true SseK3 target is currently unknown but presents an intriguing line of future research. Overall, verification of the identified putative SseK3 arginine-GlcNAcylation targets might reveal a target “motif” as recently suggested for NleB (El qaidi et al., 2017) and also open up a large number of research avenues with potentially interesting new Ssek3 functions during *Salmonella* infection of macrophages.

In summary, the work presented in this thesis revealed intriguing similarities and differences between the SseK effectors. Both SseK1 and SseK3 inhibit NF-κB activation and necroptosis during *Salmonella* infection of macrophages but this is not the case for SseK2. SseK function requires a DxD motif, which in SseK1 and SseK3 is essential for protein arginine-GlcNAcylation. Inhibition of immune signaling and host cell death by the SseK effectors is specific for TNFα-induced inflammation and probably due to the arginine-GlcNAcylation of TRADD by SseK1 and SseK3. Interestingly, SseK3 function was found to be independent of

TRIM32, despite stable interaction of the proteins during *Salmonella* infection. In addition, SseK1 and SseK3 caused GlcNAcylation of different proteins in infected macrophages revealing that these effectors have distinct substrate specificities and additional, yet-to-be validated functions during *Salmonella* infection.

7 APPENDIX

Table 7.1. **Murine proteins identified by tandem LC-MS/MS analysis as SseK-HA or SseL-HA specific binging partners**

Accession: Swiss-Prot database identifier

Score: Mass spectrometry score obtained through MASCOT analysis

Peptides: Number of significant peptide matches identified by LC-MS/MS MASCOT analysis

Rep_B and Rep_E: Two independent biological repeats

Accession	**Score (Peptides)**		**Description**
	Rep_B	Rep_E	
SseK1-HA specific proteins			
Q7TMX5	52 (1)	124 (3)	Protein SHQ1 homolog
Q8BH35	99 (1)	48 (1)	Complement component C8 beta chain
Q64261	42 (2)	28 (2)	Cyclin-dependent kinase 6
D3YZP9	37 (2)	24 (1)	Coiled-coil domain-containing protein 6
Q56A10	31 (2)	29 (2)	Zinc finger protein 608 1
Q6ZWX6	37 (1)	23 (1)	Eukaryotic translation initiation factor 2 subunit 1
Q9QZ05	31 (1)	26 (2)	Eukaryotic translation initiation factor 2-alpha kinase 4
SseK2-HA specific proteins			
Q6ZWR6	43 (2)	44 (4)	Nesprin-1
P48428	34 (1)	27 (1)	Tubulin-specific chaperone A
SseK3-HA specific proteins			
Q8CH72	654 (10)	779 (21)	E3 ubiquitin-protein ligase TRIM32
Q7TPR4	54 (1)	85 (2)	Alpha-actinin-1
Q9CQI6	49 (2)	38 (1)	Coactosin-like protein
E9Q414	31 (1)	48 (2)	Apolipoprotein B-100
A2AQ25	35 (1)	41 (2)	Sickle tail protein
P56394	42 (1)	29 (1)	Cytochrome c oxidase copper chaperone
Q8BZQ7	25 (1)	29 (1)	Anaphase-promoting complex subunit 2
Q7TQG0	25 (1)	16 (1)	Zinc finger and BTB domain-containing protein 5
SseL-HA specific proteins			
Q3B7Z2	2420 (43)	2301 (51)	Oxysterol-binding protein 1

Q9QY76	283 (7)	487 (11)	Vesicle-associated membrane protein-associated protein B
Q9D1C1	191 (3)	230 (5)	Ubiquitin-conjugating enzyme E2 C
Q80X71	317 (6)	96 (2)	Transmembrane protein 106B
Q8VC04	238 (5)	160 (3)	Transmembrane protein 106A
Q99J93	194 (2)	146 (4)	Interferon-induced transmembrane protein
Q8CFE6	104 (1)	198 (6)	Sodium-coupled neutral amino acid transporter 2
P27601	95 (2)	181 (4)	Guanine nucleotide-binding protein subunit alpha-13
P97765	110 (3)	124 (5)	WW domain-binding protein 2
O70404	85 (1)	141 (6)	Vesicle-associated membrane protein 8
P61028	59(3)	132 (3)	Ras-related protein Rab-8B
O35609	77 (1)	112 (1)	Secretory carrier-associated membrane protein 3
Q9ER00	58 (1)	125 (2)	Syntaxin-12
P35295	68 (1)	100 (2)	Ras-related protein Rab-20
Q61542	87 (1)	73 (1)	StAR-related lipid transfer protein
Q9JKK1	102 (1)	52 (1)	Syntaxin-6
O88384	28 (2)	109 (2)	Vesicle transport through interaction with t-SNAREs homolog 1B
Q2TBE6	77 (1)	57 (1)	Phosphatidylinositol 4-kinase type 2-alpha
P20934	34 (1)	89 (1)	Protein EVI2A
Q9D4H8	82 (3)	38 (2)	Cullin-2
Q9D6M3	43 (1)	67 (1)	Mitochondrial glutamate carrier 1
Q5Y5T1	50 (1)	52 (1)	Probable palmitoyltransferase ZDHHC20
O54965	47 (1)	52 (1)	E3 ubiquitin-protein ligase RNF13
Q9QXK3	78 (2)	19 (1)	Coatomer subunit gamma-2
Q9JLJ0	55 (1)	42 (1)	Lipopolysaccharide-induced tumor necrosis factor-alpha factor homolog
P70398	36 (2)	35 (2)	Probable ubiquitin carboxyl-terminal hydrolase FAF-X
Q60972	35 (1)	36 (1)	Histone-binding protein RBBP4
Q9D799	33 (2)	24 (1)	Methionyl-tRNA formyltransferase, mitochondrial
Q9Z0P4	25 (1)	28 (1)	Paralemmin-1
Q8BS95	28 (1)	19 (1)	Golgi pH regulator

SseK1-HA and SseK3-HA specific proteins			
A2ARI4			Leucine-rich repeat-containing G-protein coupled receptor 4
SseK1	23 (1)	28 (1)	
SseK3	24 (1)	21 (1)	
O35737			Heterogeneous nuclear ribonucleoprotein H
SseK1	138 (2)	136 (4)	
SseK3	84 (1)	103 (3)	
SseK2-A and SseK3-HA specific proteins			
Q8BV66			Interferon-induced protein 44
SseK2	72 (2)	53 (1)	
SseK3	69 (1)	32 (1)	
SseK1-HA, SseK2-HA and SseK3-HA specific proteins			
P04945			Ig kappa chain V-VI region NQ2-6.1
SseK1	129 (1)	66 (1)	
SseK2	138 (1)	89 (1)	
SseK3	342 (3)	205 (2)	
P47757			F-actin-capping protein subunit beta
SseK1	299 (5)	74 (2)	
SseK2	131 (4)	42 (1)	
SseK3	80 (3)	55 (2)	
P26443			Glutamate dehydrogenase 1, mitochondrial
SseK1	64 (1)	29 (1)	
SseK2	45 (1)	68 (1)	
SseK3	46 (1)	59 (1)	

Table 7.2. **Proteins identified by tandem LC-MS/MS analysis after arginine-GlcNAc immunoprecipitation** from RAW 264.7 macrophage infection for 16 h with ΔsseK1/2/3pE, ΔsseK1/2/3pSseK1, ΔsseK1/2/3pSsek2 or ΔsseK1/2/3pSseK3.

Accession: SwissProt database identifier (Mus musculus)

UniProt database identifier (*S.* Typhimurium 14028s) highlighted in light blue.

Score: Mass spectrometry score obtained through MASCOT analysis

Peptides: Number of significant peptide matches identified by LC-MS/MS MASCOT analysis

Rep_1, Rep_2 and Rep_3: Three independent biological repeats

Accession	**Score (Peptides)**			**Description**
	Rep_1	Rep_2	Rep_3	
pSseK1 specific proteins				
Q9CQ79	361 (7)	612 (12)	325 (4)	Thioredoxin domain-containing protein 9
Q64112		464 (8)	324 (6)	Interferon-induced protein with tetratricopeptide repeats 2
Q99PN3	83 (2)	46 (1)	322 (4)	Tripartite motif-containing protein 26
Q99NB9		117 (2)	213 (2)	Splicing factor 3B subunit 1
Q8QZY1	36 (1)	152 (3)	127 (2)	Eukaryotic translation initiation factor 3 subunit L
Q8R1S0		162 (16)	125 (13)	Ubiquinone biosynthesis monooxygenase COQ6, mitochondrial
O70469		114 (2)	162 (3)	Docking protein 2
Q61210		161 (17)	112 (14)	Rho guanine nucleotide exchange factor 1
Q9DCH4	24 (1)	92 (1)	134 (1)	Eukaryotic translation initiation factor 3 subunit F
P70460	47 (1)	170 (4)		Vasodilator-stimulated phosphoprotein
P63001		119 (2)	96 (3)	Ras-related C3 botulinum toxin substrate 1
Q9CZ44		175 (3)	36 (1)	NSFL1 cofactor p47
P62814		90 (2)	110 (1)	V-type proton ATPase subunit B, brain isoform 1
Q3U0V1		43 (1)	150 (3)	Far upstream element-binding protein 2

Accession	**Score (Peptides)**			**Description**
	Rep_1	Rep_2	Rep_3	
Q6NZJ6		102 (2)	89 (2)	Eukaryotic translation initiation factor 4 gamma 1
Q9DBR1		115 (2)	54 (1)	5’-3’ exoribonuclease 2
Q60875		61 (2)	70 (1)	Rho guanine nucleotide exchange factor 2
Q9D0L8		74 (1)	35 (2)	mRNA cap guanine-N7 methyltransferase
P05555		45 (1)	62 (2)	Integrin alpha-M
P60229		34 (1)	64 (2)	Eukaryotic translation initiation factor 3 subunit E
Q3UZ39		59 (1)	38 (1)	Leucine-rich repeat flightless-interacting protein 1 2
P23116		34 (1)	47 (1)	Eukaryotic translation initiation factor 3 subunit A
Q9Z0P5		23 (1)	37 (1)	Twinfilin-2
A2AAY5		25 (1)	15 (1)	SH3 and PX domain-containing protein 2B
A0A0F6BBE4	1035 (21)	2149 (27)	1799 (22)	Two-component response regulator
A0A0F6B9Z0	537 (9)	2278 (31)	1044 (14)	Putative cytoplasmic protein (SseK1)
A0A0F6B7V9	374 (6)	703 (10)	344 (7)	Osmolarity response regulator
A0A0F6B770	143 (3)	163 (2)	429 (6)	Ribosome-binding factor A
A0A0F6B9X6	53 (1)	401 (5)		Elongation factor Tu
D0ZV90		180 (2)	198 (2)	Virulence transcriptional regulatory protein PhoP
A0A0F6B6M4		117 (3)	162 (3)	Putative acetyl-CoA
A0A0F6B0S7		149 (4)	43 (1)	Phenylalanine—tRNA ligase beta subunit
pSseK2 specific proteins				
O70133		73 (1)	71 (1)	ATP-dependent RNA helicase A

Accession	**Score (Peptides)**			**Description**
	Rep_1	Rep_2	Rep_3	
Q9CQ65		100 (1)	25 (1)	S-methyl-5’-thioadenosine phosphorylase
Q9CX86		63 (1)	38 (1)	Heterogeneous nuclear ribonucleoprotein A0
Q8BKC5		45 (1)	32 (1)	Importin-5 OS=Mus musculus
P35550	32 (1)	33 (2)		rRNA 2'-O-methyltransferase fibrillarin
Q3TZ89	21 (1)	28 (1)		Protein transport protein Sec31B
pSseK3 specific proteins				
Q99K01	1145 (26)	3960 (58)	1789 (28)	Pyridoxal-dependent decarboxylase domain-containing protein 1
Q91V41	631 (11)	1760 (30)	1565 (22)	Ras-related protein Rab-14
Q9D1G1	801 (16)	1879 (31)	1228 (20)	Ras-related protein Rab-1B
P62821	681 (13)	1483 (27)	1070 (16)	Ras-related protein Rab-1A
O88630	853 (16)	1379 (29)	867 (11)	Golgi SNAP receptor complex member 1
Q9QYE6	546 (11)	1288 (19)	1089 (17)	Golgin subfamily A member 5
7Q8BMP6	434 (9)	1248 (17)	803 (12)	Golgi resident protein GCP60
P35278	537 (9)	1310 (22)	271 (6)	Ras-related protein Rab-5C
Q9D662	386 (6)	1330 (17)		Protein transport protein Sec23B
Q8K1T1	206 (5)	907 (13)	469 (6)	Leucine-rich repeat-containing protein 25
Q8BRF7	678 (12)	572 (7)	326 (7)	Sec1 family domain-containing protein 1

Accession	Score (Peptides)			Description
	Rep_1	Rep_2	Rep_3	
Q6PHN9		694 (10)	820 (11)	Ras-related protein Rab-35
Q922F4		680 (16)	799 (19)	Tubulin beta-6 chain
P46460	134 (4)	616 (18)	560 (14)	Vesicle-fusing ATPase
Q8CG50	99 (2)	618 (10)	483 (7)	Ras-related protein Rab-43
Q6NZC7	371 (8)	300 (8)	424 (10)	SEC23-interacting protein
O08547	243 (6)	731 (12)		Vesicle-trafficking protein SEC22b
Q921M4	273 (5)	518 (9)	80 (3)	Golgin subfamily A member 2
Q8K1E0	42 (1)	438 (9)	382 (6)	Syntaxin-5
P53564	190 (5)	576 (10)	46 (2)	Homeobox protein cut-like 1
Q8BVW3	120 (3)	266 (6)	399 (9)	Tripartite motif-containing protein 14
Q8CIE6	80 (3)	359 (9)	236 (6)	Coatomer subunit alpha
P70403		617 (11)	122 (3)	Protein CASP
P27601		304 (5)	398 (6)	Guanine nucleotide-binding protein subunit alpha-13
Q9Z1Q5	98(1)	494 (7)		Chloride intracellular channel protein 1
P53994	279 (4)	330 (4)	63 (1)	Ras-related protein Rab-2A
Q9DCD5	63 (1)	227 (7)	376 (4)	Tight junction-associated protein
P60843	30 (1)	620 (11)		Eukaryotic initiation factor 4A-I
Q9WUH1	36 (1)	334 (5)	279 (3)	Transmembrane protein 115
Q8CD26	29 (1)	527 (10)	86 (3)	Solute carrier family 35 member E1
O35153	117 (1)	206 (3)	297 (3)	BET1-like protein
P52332	124 (3)	301 (6)	179 (4)	Tyrosine-protein kinase JAK1
Q9EQC5	68 (1)	388 (7)	126 (3)	N-terminal kinase-like protein
Q99J93		186 (3)	330 (5)	Interferon-induced transmembrane protein 2
Q8CCB4		274 (7)	304 (6)	Vacuolar protein sorting-associated protein 53 homolog
Q8BJM5	106 (2)	176 (2)	283 (6)	Zinc transporter 6
Q3B7Z2	131 (2)	281 (5)	145 (5)	Oxysterol-binding protein 1

Accession	Score (Peptides)			Description
	Rep_1	Rep_2	Rep_3	
Q9DB05		326 (4)	213 (3)	Alpha-soluble NSF attachment protein
Q8VDV3	163 (2)	214 (3)	156 (2)	Guanine nucleotide exchange factor for Rab-3A
Q8CGY8	144 (5)	211 (5)	153 (4)	UDP-N-acetylglucosamine--peptide N-acetylglucosaminyltransferase 110 kDa subunit
O70480	197 (2)	120 (1)	173 (2)	Vesicle-associated membrane protein 4
E9Q3L2		329 (6)	144 (3)	Phosphatidylinositol 4-kinase alpha
Q60766		194 (4)	239 (3)	Immunity-related GTPase family M protein 1
Q8BH60	47 (1)	248 (5)	133 (3)	Golgi-associated PDZ and coiled-coil motif-containing protein
Q9DB43	45 (1)	266 (6)	116 (2)	Zinc finger protein-like 1
P55937	56 (1)	265 (7)	91 (2)	Golgin subfamily A member 3
Q3UM29		315 (8)	82 (1)	Conserved oligomeric Golgi complex subunit 7
Q8BRM2	52 (1)	221 (4)	108 (1)	RAB6-interacting golgin
Q8C0L8		323 (5)	57 (1)	Conserved oligomeric Golgi complex subunit 5
P35282		248 (3)	125 (1)	Ras-related protein Rab-21
Q9EQH3	117 (3)	250 (5)		Vacuolar protein sorting-associated protein 35
Q921L5	96 (1)	241 (6)		Conserved oligomeric Golgi complex subunit 2
Q9CWU2	294 (5)		39 (1)	Palmitoyltransferase ZDHHC13
Q9JIF7		266 (5)	59 (1)	Coatomer subunit beta
P61982		195 (5)	94 (1)	14-3-3 protein gamma
A2A5R2	26 (1)	179 (5)	107 (2)	Brefeldin A-inhibited guanine nucleotide-exchange protein 2

Accession	Score (Peptides)			Description
	Rep_1	Rep_2	Rep_3	
Q3UVL4	34 (2)	273 (4)		Vacuolar protein sorting-associated protein 51 homolog
Q78PY7		138 (4)	161 (2)	Staphylococcal nuclease domain-containing protein 1
Q6ZPE2	85 (2)	200 (4)	151 (2)	Myotubularin-related protein 5
Q99JX3		189 (4)	93 (1)	Golgi reassembly-stacking protein 2
O54774	36 (1)	113 (2)	120 (2)	AP-3 complex subunit delta-1
Q7TMB8		190 (5)	78 (1)	Cytoplasmic FMR1-interacting protein 1
Q9JKB3		190 (3)	74 (1)	Y-box-binding protein 3
Q9Z160		152 (2)	112 (3)	Conserved oligomeric Golgi complex subunit 1
Q8C129		159 (4)	103 (3)	Leucyl-cystinyl aminopeptidase
Q920I9		169 (3)	87 (1)	WD repeat-containing protein 7
Q9EQG9		185 (4)	64 (1)	Collagen type IV alpha-3-binding protein
Q8C754	22 (1)	160 (6)	62 (1)	Vacuolar protein sorting-associated protein 52 homolog 1
Q8R1N4	118 (1)	124 (1)		NudC domain-containing protein 3
Q9JKK1	23 (1)	74 (1)	136 (3)	Syntaxin-6
Q8CI04		167 (4	62 (1)	Conserved oligomeric Golgi complex subunit 3
O55143	49 (2)	170 (2)		Sarcoplasmic/endoplasmic reticulum calcium ATPase 2
Q99P88		182 (5)	34 (2)	Nuclear pore complex protein Nup155
P48962		105 (2)	104 (2)	ADP/ATP translocase 1
Q5XJY5	29 (1)	127 (3)	48 (1)	Coatomer subunit delta
Q9Z1Z0	68 (1)	32 (1)	98 (2)	General vesicular transport factor p115
O35382		133 (2)	61 (1)	Exocyst complex component 4
G3X9K3		112 (5)	81 (1)	Brefeldin A-inhibited guanine nucleotide-exchange protein 1

Accession	Score (Peptides)			Description
	Rep_1	Rep_2	Rep_3	
P98078		40 (1)	127 (2)	Disabled homolog 2
P59016	35 (1)	119 (2)	100 (2)	Vacuolar protein sorting-associated protein 33B
P62874		90 (2)	55 (2)	Guanine nucleotide-binding protein G(I)/G(S)/G(T) subunit beta-1
Q8BFR5		76 (1)	68 (1)	Elongation factor Tu, mitochondrial
Q9DBQ7		49 (1)	95 (1)	Protein-associating with the carboxyl-terminal domain of ezrin
Q9JM52		59 (3)	80 (5)	Misshapen-like kinase 1
O88685		81 (3)	56 (1)	26S protease regulatory subunit 6A
Q9D5V5	56 (1)		81 (2)	Cullin-5 3
Q9QYJ0		83 (1)	50 (1)	DnaJ homolog subfamily A member 2
O09005		35 (1)	92 (1)	Sphingolipid delta(4)-desaturase DES1
O08579		39 (1)	87 (1)	Emerin
Q8BLR5		54 (1)	72 (1)	PH and SEC7 domain-containing protein 4
Q8R4H9	82 (2)	43 (1)		Zinc transporter 5
Q8BGB2		62 (1)	61 (1)	Tetratricopeptide repeat protein 7A
Q8BMS1		60 (1)	63 (1)	Trifunctional enzyme subunit alpha, mitochondrial
Q9D4H2	55 (1)	60 (1)		GRIP and coiled-coil domain-containing protein 1
Q9CX30		71 (1)	37 (1)	Protein YIF1B
E9PVA8		73 (3)	34 (1)	eIF-2-alpha kinase activator GCN1
Q64151	68 (2)	37 (1)		Semaphorin-4C
Q9Z2D1		58 (1)	41 (1)	Myotubularin-related protein 2
Q9WUA3		44 (1)	54 (2)	ATP-dependent 6-phosphofructokinase, platelet type
O55029		27 (1)	70 (2)	Coatomer subunit beta'

Accession	Score (Peptides)			Description
	Rep_1	Rep_2	Rep_3	
P17809	25 (1)	64 (1)		Solute carrier family 2, facilitated glucose transporter member 1
Q8BH43		44 (1)	43 (1)	Wiskott-Aldrich syndrome protein family member 2
Q8JZR0		26 (1)	58 (2)	Long-chain-fatty-acid--CoA ligase 5
Q99KN9		54 (1)	27 (2)	Clathrin interactor 1
B2RQE8		42 (3)	37 (2)	Rho GTPase-activating protein 42
Q80U72		55 (2)	24 (1)	Protein scribble homolog
Q99KG5		29 (1)	45 (1)	Lipolysis-stimulated lipoprotein receptor
Q9WTL7		21 (1)	46 (1)	Acyl-protein thioesterase 2
P27046	25 (1)		32 (1)	Alpha-mannosidase 2
Q8BP86		26 (1)	29 (1)	snRNA-activating protein complex subunit 4
Q8K441		23 (1)	29 (1)	ATP-binding cassette sub-family A member 6
Q9D172		20 (1)	20 (1)	ES1 protein homolog, mitochondrial
A0A0F6B2Z0	163 (2)	216 (4)	136 (3)	Uncharacterized protein (SseK3)
A0A0F6B1A9		58 (1)	39 (1)	Putative dehydratase
A0A0F6B247		31 (1)	51 (2)	Regulator of RpoS
pSseK1 and pSseK3 specific proteins				
Q3U0V2				Tumor necrosis factor receptor type 1-associated DEATH domain protein
SseK1	3183 (61)	5351 (104)	2924 (46)	
SseK3	556 (13)	430 (8)		
P62827				GTP-binding nuclear protein Ran
SseK1		341 (7)	140 (3)	
SseK3	300 (6)	905 (14)	615 (12)	
Q64282				Interferon-induced protein with

Accession	Score (Peptides)			Description
	Rep_1	Rep_2	Rep_3	
SseK1	184 (6)	4902 (69)	4231 (56)	tetratricopeptide repeats 1
SseK3	52 (1)	1487 (26)	1092 (17)	
P17742				Peptidyl-prolyl cis-trans isomerase A
SseK1	368 (6)		1320 (25)	
SseK3	393 (6)		697 (16)	
P26039				Talin-1
SseK1		330 (5)	270 (5)	
SseK3	51 (1)	390 (8)	395 (7)	
Q99LF4				tRNA-splicing ligase RtcB homolog
SseK1		106 (4)	151 (6)	
SseK3		57 (3)	63 (2)	
Q9D967				Magnesium-dependent phosphatase 1
SseK1		42 (1)	51 (1)	
SseK3		136 (3)	126 (1)	
P10852				4F2 cell-surface antigen heavy chain
SseK1		115 (1)	115 (1)	
SseK3		54 (1)	69 (1)	
Q62448				Eukaryotic translation initiation factor 4
SseK1		76 (2)	132 (3)	gamma 2
SseK3		94 (4)	39 (1)	
Q9DCN2				NADH-cytochrome b5 reductase 3
SseK1	44 (1)	74 (2)		
SseK3	67 (1)	150 (2)		
Q91VH6				Protein MEMO1
SseK1		153 (2)	92 (1)	
SseK3	30 (1)	64 (2)	25 (1)	

Accession	Score (Peptides)			Description
	Rep_1	Rep_2	Rep_3	
P30999				Catenin delta-1
SseK1		52 (1)	48 (1)	
SseK3		183 (3)	28 (1)	
P49813				Tropomodulin-1
SseK1		48 (1)	45 (1)	
SseK3		62 (2)	122 (2)	
D0ZIB5				Secreted effector kinase SteC
SseK1		57 (1)	102 (2)	
SseK3		132 (2)	70 (2)	
pSseK1, pSseK2 and pSseK3 specific proteins				
P0C0S6				Histone H2A.Z
SseK1	272 (8)		451 (13)	
SseK2	481 (11)		392 (11)	
SseK3	405 (9)		627 (15)	
Q9WVA4				Transgelin-2
SseK1		199 (4)	216 (2)	
SseK2		23 (1)	104 (1)	
SseK3	129 (2)	155 (2)	64 (1)	
P80315				T-complex protein 1 subunit delta
SseK1	36 (1)	151 (4)	186 (5)	
SseK2		43 (1)	35 (2)	
SseK3		38 (1)	38 (1)	

8 REFERENCES

Aachoui, Y., Leaf, I.A., Hagar, J.A., Fontana, M.F., Campos, C.G., Zak, D.E., Tan, M.H., Cotter, P.A., Vance, R.E., Aderem, A., Miao, E.A., 2013. Caspase-11 Protects Against Bacteria That Escape the Vacuole. Science 339, 975–978.

Aglietti, R.A., Estevez, A., Gupta, A., Ramirez, M.G., Liu, P.S., Kayagaki, N., Ciferri, C., Dixit, V.M., Dueber, E.C., 2016. GsdmD p30 elicited by caspase-11 during pyroptosis forms pores in membranes. Proc. Natl. Acad. Sci. 113, 7858–7863.

Albor, A., El-Hizawi, S., Horn, E.J., Laederich, M., Frosk, P., Wrogemann, K., Kulesz-Martin, M., 2006. The interaction of Piasy with Trim32, an E3-ubiquitin ligase mutated in limb-girdle muscular dystrophy type 2H, promotes Piasy degradation and regulates UVB-induced keratinocyte apoptosis through NF-κB. J. Biol. Chem. 281, 25850–25866.

Ao, T.T., Feasey, N.A., Gordon, M.A., Keddy, K.H., Angulo, F.J., Crump, J.A., 2015. Global Burden of Invasive Nontyphoidal *Salmonella* Disease, 2010. Emerg. Infect. Dis. 21, 941–949.

Apweiler, R., Hermjakob, H., Sharon, N., 1999. On the frequency of protein glycosylation, as deduced from analysis of the SWISS-PROT database. Biochim. Biophys. Acta 1473, 4–8.

Arthur, J.S.C., Ley, S.C., 2013. Mitogen-activated protein kinases in innate immunity. Nat. Rev. Immunol. 13, 679–692.

Auweter, S.D., Bhavsar, A.P., De Hoog, C.L., Li, Y., Chan, Y.A., Van Der Heijden, J., Lowden, M.J., Coombes, B.K., Rogers, L.D., Stoynov, N., Foster, L.J., Finlay, B.B., 2011. Quantitative Mass Spectrometry Catalogues *Salmonella* Pathogenicity Island-2 effectors and Identifies Their Cognate Host Binding Partners. J. Biol. Chem. 286, 24023–24035.

Auweter, S.D., Yu, H.B., Arena, E.T., Guttman, J.A., Finlay, B.B., 2012. Oxysterol-binding protein (OSBP) enhances replication of intracellular Salmonella and binds the *Salmonella* SPI-2 effector SseL via its N-terminus. Microbes Infect. 14, 148–154.

Azmatullah, A., Qamar, F.N., Thaver, D., Zaidi, A.K., Bhutta, Z.A., 2015. Systematic review of the global epidemiology, clinical and laboratory profile of enteric fever. J. Glob. Health 5, 20407.

Bader, M.W., Sanowar, S., Daley, M.E., Schneider, A.R., Cho, U., Xu, W., Klevit, R.E., Le Moual, H., Miller, S.I., 2005. Recognition of antimicrobial peptides by a bacterial sensor kinase. Cell 122, 461–472.

Baeuerle, P.A., Baltimore, D., 1988. IkB: A Specific Inhibitor of the NF-kB Transcription Factor. Science 242, 540–546.

Baisón-Olmo, F., Galindo-Moreno, M., Ramos-Morales, F., 2015. Host cell type-dependent translocation and PhoP-mediated positive regulation of the effector SseK1 of *Salmonella enterica*. Front. Microbiol. 6, 396.

Balachandran, S., Thomas, E., Barber, G.N., 2004. A FADD-dependent innate immune mechanism in mammalian cells. Nature 432, 401–405.

Bao, S., Beagley, K.W., France, M.P., Shen, J., Husband, A.J., 2000. Interferon-gamma plays a critical role in intestinal immunity against Salmonella typhimurium infection. Immunology 99, 464–472.

Barthel, M., Hapfelmeier, S., Kremer, M., Rohde, M., Hogardt, M., Pfeffer, K., Rüssmann, H., Hardt, W.-D., Barthel, M., Hapfelmeier, S., Quintanilla-Martínez, L., Kremer, M., Rohde, M., Hogardt, M., Pfeffer, K., Ru, H., 2003. Pretreatment of Mice with Streptomycin Provides a *Salmonella enterica* Serovar Typhimurium Colitis Model That Allows Analysis of Both Pathogen and Host. Infect. Immun. 71, 2839–2858.

Bayer-Santos, E., Durkin, C.H., Rigano, L.A., Kupz, A., Alix, E., Cerny, O., Jennings, E., Liu, M., Ryan, A.S., Lapaque, N., Kaufmann, S.H.E., Holden, D.W., 2016. The *Salmonella* Effector SteD Mediates MARCH8-Dependent Ubiquitination of MHC II Molecules and Inhibits T Cell Activation. Cell Host Microbe 20, 584–595.

Bergsbaken, T., Fink, S.L., Cookson, B.T., 2009. Pyroptosis: host cell death and inflammation. Nat. Rev. Microbiol. 7, 99–109.

Bernal-Bayard, J., Cardenal-Muñoz, E., Ramos-Morales, F., 2010. The *Salmonella* Type III Secretion Effector, *Salmonella* Leucine-rich Repeat Protein (SlrP), Targets the Human Chaperone ERdj3. J. Biol. Chem. 285, 16360–16368.

Bernal-Bayard, J., Ramos-Morales, F., 2009. *Salmonella* Type III Secretion Effector SlrP is an E3 ubiquitin Ligase for Mammalian Thioredoxin. J. Biol. Chem. 284, 27587–27595.

Beuzón, C.R., Méresse, S., Unsworth, K.E., Ruíz-Albert, J., Garvis, S., Waterman, S.R., Ryder, T.A., Boucrot, E., Holden, D.W., 2000. *Salmonella* maintains the integrity of its intracellular vacuole through the action of SifA. EMBO J. 19, 3235–3249.

Bhavsar, A.P., Brown, N.F., Stoepel, J., Wiermer, M., Martin, D.D.O., Hsu, K.J., Imami, K., Ross, C.J., Hayden, M.R., Foster, L.J., Li, X., Hieter, P., Finlay, B.B., 2013. The *Salmonella* Type III Effector SspH2 Specifically Exploits the NLR Co-chaperone Activity of SGT1 to Subvert

Immunity. PLoS Pathog. 9, 1–12.

Bigay, J., Antonny, B., 2012. Curvature, Lipid Packing, and Electrostatics of Membrane Organelles: Defining Cellular Territories in Determining Specificity. Dev. Cell 23, 886–895.

Birmingham, C.L., Smith, A.C., Bakowski, M.A., Yoshimori, T., Brumell, J.H., 2006. Autophagy controls *Salmonella* Infection in Response to Damage to the Salmonella-containing vacuole. J. Biol. Chem. 281, 11374–11383.

Bogoyevitch, M.A., Ngoei, K.R.W., Zhao, T.T., Yeap, Y.Y.C., Ng, D.C.H., 2010. c-Jun N-terminal kinase (JNK) signaling: Recent advances and challenges. Biochim. Biophys. Acta 1804, 463–475.

Borden, K.L., 1998. RING fingers and B-boxes: zinc-binding protein-protein interaction domains. Biochem. Cell Biol. 76, 351–358.

Borg, K., Stucka, R., Locke, M., Melin, E., Åhlberg, G., Klutzny, U., von der Hagen, M., Huebner, A., Lochmüller, H., Wrogemann, K., Thornell, L.E., Blake, D.J., Schoser, B., 2009. Intragenic deletion of TRIM32 in compound heterozygotes with sarcotubular myopathy/LGMD2H. Hum. Mutat. 30, E831–E844.

Brenner, D., Blaser, H., Mak, T.W., 2015. Regulation of tumour necrosis factor signalling: live or let die. Nat. Rev. Immunol. 15, 362–374.

Brinkmann, V., Reichard, U., Goosmann, C., Fauler, B., Uhlemann, Y., Weiss, D.S., Weinrauch, Y., Zychlinsky, A., 2004. Neutrophil Extracellular Traps Kill Bacteria. Science 303, 1532–1535.

Brockhausen, I., 2014. Crossroads between bacterial and mammalian glycosyltransferases. Front. Immunol. 5, 1–21.

Brown, N.F., Coombes, B.K., Bishop, J.L., Wickham, M.E., Lowden, M.J., Gal-Mor, O., Goode, D.L., Boyle, E.C., Sanderson, K.L., Finlay, B.B., 2011. *Salmonella* phage ST64B encodes a member of the SseK/NleB effector family. PLoS One 6, e17824.

Browne, S.H., Hasegawa, P., Okamoto, S., Fierer, J., Guiney, D.G., 2008. Identification of *Salmonella* SPI-2 secretion system components required for SpvB-mediated cytotoxicity in macrophages and virulence in mice. FEMS Immunol. Med. Microbiol. 52, 194–201.

Broz, P., Dixit, V.M., 2016. Inflammasomes: mechanism of assembly, regulation and signalling. Nat. Rev. Immunol. 16, 407–420.

Bruno, V.M., Hannemann, S., Lara-Tejero, M., Flavell, R.A., Kleinstein, S.H., Galan, J.E., 2009. *Salmonella* typhimurium type III secretion effectors stimulate innate immune responses

in cultured epithelial cells. PLoS Pathog. 5, e1000538.

Buckle, G.C., Walker, C.L.F., Black, R.E., 2012. Typhoid fever and paratyphoid fever: Systematic review to estimate global morbidity and mortality for 2010. J. Glob. Health 2, 10401.

Buckner, M.M.C., Croxen, M.A., Arena, E.T., Finlay, B.B., 2011. A comprehensive study of the contribution of *Salmonella enterica* serovar Typhimurium SPI2 effectors to bacterial colonization, survival, and replication in typhoid fever, macrophage, and epithelial cell infection models. Virulence 2, 208–216.

Byndloss, M.X., Rivera-Chavez, F., Tsolis, R.M., Baumler, A.J., 2016. How bacterial pathogens use type III and type IV secretion systems to facilitate their transmission. Curr. Opin. Microbiol. 35, 1–7.

Cao, X., Pobezinskaya, Y.L., Morgan, M.J., Liu, Z., 2011. The role of TRADD in TRAIL-induced apoptosis and signaling. FASEB J. 25, 1353–1358.

Carter, P.B., Collins, F.M., 1974. The route of enteric infection in normal mice. J. Exp. Med. 139, 1189–1203.

CDC, 2016. National *Salmonella* Surveillance Annual Report, 2013. Centers for Disease Control and Prevention 1–89.

Chae, J.J., Wood, G., Richard, K., Jaffe, H., Colburn, N.T., Masters, S.L., Gumucio, D.L., Shoham, N.G., Kastner, D.L., 2008. The familial Mediterranean fever protein, pyrin, is cleaved by caspase-1 and activates NF-kB through its N-terminal fragment. Immunobiology 112, 1794–1803.

Chen, H.M., Wang, Y., Su, L.H., Chiu, C.H., 2013. Nontyphoid *Salmonella* infection: Microbiology, clinical features, and antimicrobial therapy. Pediatr. Neonatol. 54, 147–152.

Chen, Z., Hagler, J., Palombella, V.J., Melandri, F., Seherer, D., Ballard, D., Maniatis, T., 1995. Phosphorylation targets IkBa to the ubiquitin-proteasome pathway. Genes Dev. 9, 1586–1598.

Chiang, A.P., Beck, J.S., Yen, H., Tayeh, M.K., Scheetz, T.E., Swiderski, R.E., Nishimura, D.Y., Braun, T.A., Kim, K.A., Huang, J., Elbedour, K., Carmi, R., Slusarski, D.C., Casavant, T.L., Stone, E.M., Sheffield, V.C., 2006. Homozygosity mapping with SNP arrays identifies TRIM32 , an E3 ubiquitin ligase , as a Bardet – Biedl syndrome gene (BBS11). Proc. Natl. Acad. Sci. 103, 6287–6292.

Cirillo, D.M., Valdivia, R.H., Monack, D.M., Falkow, S., 1998. Macrophage-dependent

induction of the *Salmonella* pathogenicity island 2 type III secretion system and its role in intracellular survival. Mol. Microbiol. 30, 175–188.

Cohen, S., Zhai, B., Gygi, S.P., Goldberg, A.L., 2012. Ubiquitylation by Trim32 causes coupled loss of desmin, Z-bands, and thin filaments in muscle atrophy. J. Cell Biol. 198, 575–589.

Colgan, A.M., Kröger, C., Diard, M., Hardt, W.D., Puente, J.L., Sivasankaran, S.K., Hokamp, K., Hinton, J.C.D., 2016. The Impact of 18 Ancestral and Horizontally-Acquired Regulatory Proteins upon the Transcriptome and sRNA Landscape of *Salmonella enterica* serovar Typhimurium. PLoS Genet. 12, 1–42.

Cossée, M., Lagier-Tourenne, C., Seguela, C., Mohr, M., Leturcq, F., Gundesli, H., Chelly, J., Tranchant, C., Koenig, M., Mandel, J.L., 2009. Use of SNP array analysis to identify a novel TRIM32 mutation in limb-girdle muscular dystrophy type 2H. Neuromuscul. Disord. 19, 255–260.

Costa, L.F., Paixão, T.A., Tsolis, R.M., Bäumler, A.J., Santos, R.L., 2012. Salmonellosis in cattle: Advantages of being an experimental model. Res. Vet. Sci. 93, 1–6.

Crump, J.A., Luby, S.P., Mintz, E.D., 2004. The global burden of typhoid fever. World Health Organisation 82, 346–353.

Cui, X., Lin, Z., Chen, Y., Mao, X., Ni, W., Liu, J., Zhou, H., Shan, X., Chen, L., Lv, J., Shen, Z., Duan, C., Hu, B., Ni, R., 2016. Upregulated TRIM32 correlates with enhanced cell proliferation and poor prognosis in hepatocellular carcinoma. Mol. Cell. Biochem. 421, 127–137.

D'Costa, V.M., Braun, V., Landekic, M., Shi, R., Proteau, A., McDonald, L., Cygler, M., Grinstein, S., Brumell, J.H., 2015. *Salmonella* Disrupts Host Endocytic Trafficking by SopD2-Mediated Inhibition of Rab7. Cell Rep. 12, 1508–1518.

de Chaumont, F., Dallongeville, S., Chenouard, N., Hervé, N., Pop, S., Provoost, T., Meas-Yedid, V., Pankajakshan, P., Lecomte, T., Le Montagner, Y., Lagache, T., Dufour, A., Olivo-Marin, J.-C., 2012. Icy: an open bioimage informatics platform for extended reproducible research. Nat. Methods 9, 690–696.

Dean, P., 2011. Functional domains and motifs of bacterial type III effector proteins and their roles in infection. FEMS Microbiol. Rev. 35, 1100–1125.

Deiwick, J., Nikolaus, T., Shea, J.E., Holden, D.W., Hensel, M., Deiwick, R.G., Gleeson, C., 1998. Mutations in *Salmonella* Pathogenicity Island 2 (SPI2) Genes Affecting Transcription of SPI1 Genes and Resistance to Antimicrobial Agents. J. Bacteriol. 180, 4775–4780.

Desai, P.T., Porwollik, S., Long, F., Cheng, P., Wollam, A., Clifton, S.W., Weinstock, G.M., 2013. Evolutionary Genomics of *Salmonella enterica* Subspecies. mBio 4, 1–13.

Diehl, G.E., Yue, H.H., Hsieh, K., Kuang, A.A., Ho, M., Morici, L.A., Lenz, L.L., Cado, D., Riley, L.W., Winoto, A., 2004. TRAIL-R as a negative regulator of innate immune cell responses. Immunity 21, 877–889.

Ding, J., Wang, K., Liu, W., She, Y., Sun, Q., Shi, J., Sun, H., Wang, D., Shao, F., 2016. Pore-forming activity and structural autoinhibition of the gasdermin family. Nature 535, 111–116.

Dixit, E., Kagan, J.C., 2013. Intracellular Pathogen Detection by RIG-I-Like Receptors. Adv. Immunol. 117, 99–125.

Domingues, L., Holden, D.W., Mota, L.J., 2014. The *Salmonella* effector SteA contributes to the control of membrane dynamics of Salmonella-containing vacuoles. Infect. Immun. 82, 2923–2934.

Dorman, C.J., Chatfield, S., Higgins, C.F., Hayward, C., Dougan, G., 1989. Characterization of porin and ompR mutants of a virulent strain of *Salmonella* typhimurium: ompR mutants are attenuated in vivo. Infect. Immun. 57, 2136–2140.

Dougan, G., Baker, S., 2014. *Salmonella enterica* Serovar Typhi and the Pathogenesis of Typhoid Fever. Annu. Rev. Microbiol. 68, 317–336.

Edsall, G., Gaines, S., Landy, M., Tigertt, W.D., Sprinz, H., Trapani, R.J., Mandel, A.D., Beneson, A.S., 1960. Studies on infection and immunity in experimental typhoid fever. I. Typhoid fever in chimpanzees orally infected with *Salmonella* typhosa. J. Exp. Med. 112, 143–166.

El qaidi, S., Chen, K., Halim, A., Siukstaite, L., Rueter, C., Hurtado-Guerrero, R., Clausen, H., Hardwidge, P.R., 2017. NleB/SseK effectors from *Citrobacter rodentium*, *Escherichia coli*, and *Salmonella enterica* display distinct differences in host substrate specificity. J. Biol. Chem. 292, 11423–11430.

Elmore, S., 2007. Apoptosis: a review of programmed cell death. Toxicol. Pathol. 35, 495–516.

Ermolaeva, M.A., Michallet, M.C., Papadopoulou, N., Utermohlen, O., Kranidioti, K., Kollias, G., Tschopp, J., Pasparakis, M., 2008. Function of TRADD in tumor necrosis factor receptor 1 signaling and in TRIF-dependent inflammatory responses. Nat. Immunol. 9, 1037–1046.

Escoll, P., Mondino, S., Rolando, M., Buchrieser, C., 2015. Targeting of host organelles by pathogenic bacteria: a sophisticated subversion strategy. Nat. Rev. Microbiol. 14, 5–19.

Evans, M.R., Fink, R.C., Vazquez-Torres, A., Porwollik, S., Jones-Carson, J., McClelland, M., Hassan, H.M., 2011. Analysis of the ArcA regulon in anaerobically grown *Salmonella*. BMC Microbiol. 11, 58.

Farache, J., Koren, I., Milo, I., Gurevich, I., Kim, K., Zigmond, E., Furtado, G.C., Lira, S.A., Shakhar, G., 2013. Luminal Bacteria Recruit CD103+ Dendritic Cells into the Intestinal Epithelium to Sample Bacterial Antigens for Presentation. Immunity 38, 581–595.

Feasey, N.A., Dougan, G., Kingsley, R.A., Heyderman, R.S., Gordon, M.A., 2012. Invasive non-typhoidal salmonella disease: An emerging and neglected tropical disease in Africa. Lancet 379, 2489–2499.

Figueira, R., Holden, D.W., 2012. Functions of the *Salmonella* pathogenicity island 2 (SPI-2) type III secretion system effectors. Microbiology 158, 1147–1161.

Figueira, R., Watson, K.G., Holden, D.W., Helaine, S., 2013. Identification of *Salmonella* Pathogenicity Island-2 Type III Secretion System Effectors Involved in Intramacrophage Replication of *S. enterica* Serovar Typhimurium: Implications for Rational Vaccine Design. mBio 4, 1–10.

Fiskin, E., Bhogaraju, S., Herhaus, L., Kalayil, S., Hahn, M., Dikic, I., 2017. Structural basis for the recognition and degradation of host TRIM proteins by *Salmonella* effector SopA. Nat. Commun. 8, 14004.

Fiskin, E., Bionda, T., Dikic, I., Behrends, C., 2016. Global Analysis of Host and Bacterial Ubiquitinome in Response to *Salmonella* Typhimurium Infection. Mol. Cell 62, 967–981.

Fitzgerald, K. a, McWhirter, S.M., Faia, K.L., Rowe, D.C., Latz, E., Golenbock, D.T., Coyle, A.J., Liao, S.-M., Maniatis, T., 2003. IKKepsilon and TBK1 are essential components of the IRF3 signaling pathway. Nat. Immunol. 4, 491–496.

Fookes, M., Schroeder, G.N., Langridge, G.C., Blondel, C.J., Mammina, C., Connor, T.R., Seth-Smith, H., Vernikos, G.S., Robinson, K.S., Sanders, M., Petty, N.K., Kingsley, R.A., Baumler, A.J., Nuccio, S.P., Contreras, I., Santiviago, C.A., Maskell, D., Barrow, P., Humphrey, T., Nastasi, A., Roberts, M., Frankel, G., Parkhill, J., Dougan, G., Thomson, N.R., 2011. *Salmonella bongori* provides insights into the evolution of the salmonellae. PLoS Pathog. 7, e1002191.

Fridell, R.A., Harding, L.S., Bogerd, H.P., Cullen, B.R., 1995. Identification of a novel human zinc finger protein that specifically interacts with the activation domain of lentiviral Tat proteins. Virology 209, 347-357.

Frosk, P., Weiler, T., Nylen, E., Sudha, T., Greenberg, C.R., Morgan, K., Fujiwara, T.M., Wrogemann, K., 2002. Limb-Girdle Muscular Dystrophy Type 2H Associated with Mutation in TRIM32 , a Putative E3-Ubiquitin-Ligase Gene. Am. J. Hum. Genet. 70, 663–672.

Fu, B., Wang, L., Ding, H., Schwamborn, J.C., Li, S., Dorf, M.E., 2015. TRIM32 Senses and Restricts Influenza A Virus by Ubiquitination of PB1 Polymerase. PLOS Pathog. 11, e1004960.

Fu, Q., Zou, M., Zhu, J., Zhang, Y., Chen, W., 2017. TRIM32 affects the recovery of motor function following spinal cord injury through regulating proliferation of glia. Oncotarget 8, 45380–45390.

Fu, Y., Galán, J.E., 1999. A *Salmonella* protein antagonizes Rac-1 and Cdc42 to mediate host-cell recovery after bacterial invasion. Nature 401, 293–297.

Furst, D.E., 2004. Anakinra: review of recombinant human interleukin-1 receptor antagonist in the treatment of rheumatoid arthritis. Clin. Ther. 26, 1960–1975.

Gack, M.U., Albrecht, R.A., Urano, T., Inn, K.S., Huang, I.C., Carnero, E., Farzan, M., Inoue, S., Jung, J.U., García-Sastre, A., 2009. Influenza A Virus NS1 Targets the Ubiquitin Ligase TRIM25 to Evade Recognition by the Host Viral RNA Sensor RIG-I. Cell Host Microbe 5, 439–449.

Gack, M.U., Shin, Y.C., Joo, C.-H., Urano, T., Liang, C., Sun, L., Takeuchi, O., Akira, S., Chen, Z., Inoue, S., Jung, J.U., 2007. TRIM25 RING-finger E3 ubiquitin ligase is essential for RIG-I-mediated antiviral activity. Nature 446, 916–920.

Galán, J.E., 2001. *Salmonella* interactions with host cells: type III secretion at work. Annu. Rev. Cell Dev. Biol. 17, 53–86.

Galán, J.E., Curtiss, R., 1989a. Cloning and molecular characterization of genes whose products allow *Salmonella* typhimurium to penetrate tissue culture cells. Proc. Natl. Acad. Sci. 86, 6383–6387.

Galán, J.E., Curtiss, R., 1989b. Virulence and vaccine potential of phoP mutants of *Salmonella* typhimurium. Microb. Pathog. 6, 433–443.

Gao, X., Pham, T.H., Feuerbacher, L.A., Chen, K., Hays, M.P., Singh, G., Rueter, C., Guerrero, R.H., Hardwidge, P.R., 2016. *Citrobacter rodentium* NleB inhibits tumor necrosis factor (TNF) receptor-associated factor 3 (TRAF3) ubiquitination to reduce host type I interferon production. J. Biol. Chem. 291, 18232–18238.

Gao, X., Wang, X., Pham, T.H., Feuerbacher, L.A., Lubos, M.L., Huang, M., Olsen, R., Mushegian, A., Slawson, C., Hardwidge, P.R., 2013. NleB, a bacterial effector with glycosyltransferase activity, targets GADPH function to inhibit NF-κB activation. Cell Host Microbe 13, 87–99.

Goffe, B., Cather, J.C., 2003. Etanercept: An overview. J. Am. Acad. Dermatol. 49, 105–111.

Gonzalez-Cano, L., Hillje, A.-L., Fuertes-Alvarez, S., Marques, M.M., Blanch, A., Ian, R.W., Irwin, M.S., Schwamborn, J.C., Marín, M.C., 2013. Regulatory feedback loop between TP73 and TRIM32. Cell Death Dis. 4, e704.

Gonzalez-Escobedo, G., Marshall, J.M., Gunn, J.S., 2011. Chronic and acute infection of the gall bladder by *Salmonella* Typhi: understanding the carrier state. Nat. Rev. Microbiol. 9, 9–14.

Gottlieb, A.B., 2007. Tumor necrosis factor blockade: mechanism of action. J. Investig. Dermatol. Symp. Proc. 12, 1–4.

Govoni, G., Vidal, S., Gauthier, S., Skamene, E., Malo, D., Gros, P., 1996. The Bcg/Ity/Lsh locus: Genetic transfer of resistance to infections in C57BL/6J mice transgenic for the Nramp1(Gly169) allele. Infect. Immun. 64, 2923–2929.

Grabe, G.J., Zhang, Y., Przydacz, M., Rolhion, N., Yang, Y., Pruneda, J.N., Komander, D., Holden, D.W., Hare, S.A., 2016. The *Salmonella* effector SpvD is a cysteine hydrolase with a serovar-specific polymorphism influencing catalytic activity, suppression of immune responses, and bacterial virulence. J. Biol. Chem. 291, 25853–25863.

Grandvaux, N., Servant, M.J., tenOever, B., Sen, G.C., Balachandran, S., Barber, G.N., Lin, R., Hiscott, J., 2002. Transcriptional profiling of interferon regulatory factor 3 target genes: direct involvement in the regulation of interferon-stimulated genes. J. Virol. 76, 5532–5539.

Grimont, P., Weill, F., 2007. Antigenic Formulae Of The *Salmonella* Serovarse. World Health Organisation 1–166.

Grütter, M.G., Luban, J., 2012. TRIM5 structure, HIV-1 capsid recognition, and innate immune signaling. Curr. Opin. Virol. 2, 142–150.

Guicciardi, M.E., Gores, G.J., 2009. Life and death by death receptors. FASEB J. 23, 1625–1637.

Günster, R.A., Matthews, S.A., Holden, D.W., Thurston, T.L.M., 2017. SseK1 and SseK3 Type III Secretion System Effectors Inhibit NF-κB Signaling and Necroptotic Cell Death in *Salmonella*-Infected Macrophages. Infect. Immun. 85, e00010-17.

Häcker, G., 2000. The morphology of apoptosis. Cell Tissue Res. 301, 5–17.

Haiko, J., Westerlund-Wikström, B., 2013. The Role of the Bacterial Flagellum in Adhesion and Virulence. Biology 2, 1242–1267.

Haneda, T., Ishii, Y., Shimizu, H., Ohshima, K., Iida, N., Danbara, H., Okada, N., 2012. *Salmonella* type III effector SpvC, a phosphothreonine lyase, contributes to reduction in inflammatory response during intestinal phase of infection. Cell. Microbiol. 14, 485–499.

Haraga, A., Miller, S.I., 2003. A *Salmonella enterica* Serovar Typhimurium Translocated Leucine-Rich Repeat Effector Protein Inhibits NF-kB-Dependent Gene Expression. Infect. Immun. 71, 4052–4058.

Harmansa, S., Alborelli, I., Bieli, D., Caussinus, E., Affolter, M., 2017. A nanobody-based toolset to investigate the role of protein localization and dispersal in Drosophila. eLife 6, e22549.

Hart, G.W., Akimoto, Y., 2009. The O-GlcNAc Modification. In: Varki, A., Cummings, R., Esko, J. (Eds.), Essentials of Glycobiology. Cold Spring Harbor Laboratory Press, Cold Spring Harbor (NY), pp. 1–16.

Hart, G.W., Copeland, R.J., 2010. Glycomics hits the big time. Cell 143, 672–676.

Hatakeyama, S., 2011. TRIM proteins and cancer. Nat. Rev. Cancer 11, 792–804.

Hatakeyama, S., 2017. TRIM Family Proteins: Roles in Autophagy, Immunity, and Carcinogenesis. Trends Biochem. Sci. 42, 297–311.

Hayward, R.D., Koronakis, V., 1999. Direct nucleation and bundling of actin by the SipC protein of invasive *Salmonella*. EMBO J. 18, 4926–4934.

Helaine, S., Thompson, J.A., Watson, K.G., Liu, M., Boyle, C., Holden, D.W., 2010. Dynamics of intracellular bacterial replication at the single cell level. Proc. Natl. Acad. Sci. 107, 3746–3751.

Henry, T., Couillault, C., Rockenfeller, P., Boucrot, E., Dumont, A., Schroeder, N., Hermant, A., Knodler, L.A., Lecine, P., Steele-Mortimer, O., Borg, J.-P., Gorvel, J.-P., Méresse, S., 2006. The *Salmonella* effector protein PipB2 is a linker for kinesin-1. Proc. Natl. Acad. Sci. 103, 13497–13502.

Hensel, M., Shea, J.E., Gleeson, C., Jones, M.D., Dalton, E., Holden, D.W., 1995. Simultaneous identification of bacterial virulence genes by negative selection. Science 269, 400–403.

Hersh, D., Monack, D.M., Smith, M.R., Ghori, N., Falkow, S., Zychlinsky, A., 1999. The *Salmonella* invasin SipB induces macrophage apoptosis by binding to caspase-1. Proc. Natl. Acad. Sci. 96, 2396–2401.

Hideshima, T., Chauhan, D., Richardson, P., Mitsiades, C., Mitsiades, N., Hayashi, T., Munshi, N., Dang, L., Castro, A., Palombella, V., Adams, J., Anderson, K.C., 2002. NF-κB as a therapeutic target in multiple myeloma. J. Biol. Chem. 277, 16639–16647.

Higginson, E.E., Simon, R., Tennant, S.M., 2016. Animal models for salmonellosis: Applications in vaccine research. Clin. Vaccine Immunol. 23, 746–756.

Higuchi, R., Krummel, B., Saiki, R.K., 1988. A general method of in vitro preparation and specific mutagenesis of DNA fragments: study of protein and DNA interactions. Nucleic Acids Res. 16, 7351–7367.

Hillje, A.-L., Beckmann, E., Pavlou, M. a S., Jaeger, C., Pacheco, M.P., Sauter, T., Schwamborn, J.C., Lewejohann, L., 2015. The neural stem cell fate determinant TRIM32 regulates complex behavioral traits. Front. Cell. Neurosci. 9, 75.

Hillje, A.-L., Pavlou, M.A.S., Beckmann, E., Worlitzer, M.M.A., Bahnassawy, L., Lewejohann, L., Palm, T., Schwamborn, J.C., 2013. TRIM32-dependent transcription in adult neural progenitor cells regulates neuronal differentiation. Cell Death Dis. 4, e976.

Hillje, A.-L., Worlitzer, M.M.A., Palm, T., Schwamborn, J.C., 2011. Neural stem cells maintain their stemness through protein kinase C ζ-mediated inhibition of TRIM32. Stem Cells 29, 1437–1447.

Hochmann, H., Pust, S., Von Figura, G., Aktories, K., Barth, H., 2006. *Salmonella* enterica SpvB ADP-ribosylates actin at position arginine-177 - Characterization of the catalytic domain within the SpvB protein and a comparison to binary clostridial actin-ABP-ribosylating toxins. Biochemistry 45, 1271–1277.

Hoffmann, A., Leung, T.H., Baltimore, D., 2003. Genetic analysis of NF- B/Rel transcription factors defines functional specificities. EMBO J. 22, 5530–5539.

Hoffmann, A., Natoli, G., Ghosh, G., 2006. Transcriptional regulation via the NF-kappaB signaling module. Oncogene 25, 6706–6716.

Honda, K., Taniguchi, T., 2006. IRFs: master regulators of signalling by Toll-like receptors and cytosolic pattern-recognition receptors. Nat. Rev. Immunol. 6, 644–658.

Horn, E.J., Albor, A., Liu, Y., El-Hizawi, S., Vanderbeek, G.E., Babcock, M., Bowden, G.T., Hennings, H., Lozano, G., Weinberg, W.C., Kulesz-Martin, M., 2004. RING protein Trim32 associated with skin carcinogenesis has anti-apoptotic and E3-ubiquitin ligase properties. Carcinogenesis 25, 157–167.

Hsu, H., Huang, J., Shu, H.B., Baichwal, V., Goeddel, D. V., 1996a. TNF-dependent recruitment

of the protein kinase RIP to the TNF receptor-1 signaling complex. Immunity 4, 387–396.

Hsu, H., Shu, H.B., Pan, M.G., Goeddel, D. V., 1996b. TRADD-TRAF2 and TRADD-FADD interactions define two distinct TNF receptor 1 signal transduction pathways. Cell 84, 299–308.

Hsu, H., Xiong, J., Goeddel, D. V., 1995. The TNF receptor 1-associated protein TRADD signals cell death and NF-κB activation. Cell 81, 495–504.

Hu, M.-M., Xie, X.-Q., Yang, Q., Liao, C.-Y., Ye, W., Lin, H., Shu, H.-B., 2015. TRIM38 Negatively Regulates TLR3/4-Mediated Innate Immune and Inflammatory Responses by Two Sequential and Distinct Mechanisms. J. Immunol. 195, 4415–4425.

Huang, D.W., Sherman, B.T., Lempicki, R.A., 2009a. Bioinformatics enrichment tools: Paths toward the comprehensive functional analysis of large gene lists. Nucleic Acids Res. 37, 1–13.

Huang, D.W., Sherman, B.T., Lempicki, R.A., 2009b. Systematic and integrative analysis of large gene lists using DAVID bioinformatics resources. Nat. Protoc. 4, 44–57.

Humphries, A.D., Townsend, S.M., Kingsley, R.A., Nicholson, T.L., Tsolis, M., Ba, A.J., 2001. Role of fimbriae as antigens and intestinal colonization factors of *Salmonella* serovars. FEMS Microbiol. Lett. 201, 121–125.

Hurtado-Guerrero, R., Davies, G.J., 2012. Recent structural and mechanistic insights into post-translational enzymatic glycosylation. Curr. Opin. Chem. Biol. 16, 479–487.

Ichimura, T., Taoka, M., Shoji, I., Kato, H., Sato, T., Hatakeyama, S., Isobe, T., Hachiya, N., 2013. 14-3-3 proteins sequester a pool of soluble TRIM32 ubiquitin ligase to repress autoubiquitylation and cytoplasmic body formation. J. Cell Sci. 126, 2014–2026.

Ito, M., Migita, K., Matsumoto, S., Wakatsuki, K., Tanaka, T., Kunishige, T., Nakade, H., Nakatani, M., Nakajima, Y., 2017. Overexpression of E3 ubiquitin ligase tripartite motif 32 correlates with a poor prognosis in patients with gastric cancer. Oncol. Lett. 13, 3131–3138.

Izumi, H., Kaneko, Y., 2014. Trim32 facilitates degradation of MYCN on spindle poles and induces asymmetric cell division in human neuroblastoma cells. Cancer Res. 74, 5620–5630.

Jank, T., Bogdanović, X., Wirth, C., Haaf, E., Spoerner, M., Böhmer, K.E., Steinemann, M., Orth, J.H.C., Kalbitzer, H.R., Warscheid, B., Hunte, C., Aktories, K., 2013. A bacterial toxin catalyzing tyrosine glycosylation of Rho and deamidation of Gq and Gi proteins. Nat.

Struct. Mol. Biol. 20, 1273–1280.

Jefferies, C., Wynne, C., Higgs, R., 2011. Antiviral TRIMs: friend or foe in autoimmune and autoinflammatory disease? Nat. Rev. Immunol. 11, 617–625.

Jennings, E., Thurston, T.L.M., Holden, D.W., 2017. *Salmonella* SPI-2 Type III Secretion System Effectors: Molecular Mechanisms And Physiological Consequences. Cell Host Microbe 22, 217–231.

Jones, B.D., 1994. *Salmonella* typhimurium initiates murine infection by penetrating and destroying the specialized epithelial M cells of the Peyer's patches. J. Exp. Med. 180, 15–23.

Jones, R.M., Wu, H., Wentworth, C., Luo, L., Collier-Hyams, L., Neish, A.S., 2008. *Salmonella* AvrA Coordinates Suppression of Host Immune and Apoptotic Defenses via JNK Pathway Blockade. Cell Host Microbe 3, 233–244.

Jorgensen, I., Miao, E.A., 2015. Pyroptotic cell death defends against intracellular pathogens. Immunol. Rev. 265, 130–142.

Jorgensen, I., Rayamajhi, M., Miao, E.A., 2017. Programmed cell death as a defence against infection. Nat. Rev. Immunol. 17, 151–164.

Jorgensen, I., Zhang, Y., Krantz, B.A., Miao, E.A., 2016. Pyroptosis triggers pore-induced intracellular traps (PITs) that capture bacteria and lead to their clearance by efferocytosis. J. Exp. Med. 213, 2113–2128.

Kaiser, P., Diard, M., Stecher, B., Hardt, W.D., 2012. The streptomycin mouse model for *Salmonella* diarrhea: Functional analysis of the microbiota, the pathogen's virulence factors, and the host's mucosal immune response. Immunol. Rev. 245, 56–83.

Kaisho, T., Akira, S., 2006. Toll-like receptor function and signaling. J. Allergy Clin. Immunol. 117, 979–987.

Kalliolias, G.D., Ivashkiv, L.B., 2015. TNF biology, pathogenic mechanisms and emerging therapeutic strategies. Nat. Rev. Rheumatol. 12, 49–62.

Kamanova, J., Sun, H., Lara-Tejero, M., Galan, J.E., 2016. The *Salmonella* Effector Protein SopA Modulates Innate Immune Responses by Targeting TRIM E3 Ligase Family Members. PLoS Pathog 12, e1005552.

Kano, S., Miyajima, N., Fukuda, S., Hatakeyama, S., 2008. Tripartite motif protein 32 facilitates cell growth and migration via degradation of Abl-interactor 2. Cancer Res. 68, 5572–5580.

Kawaguchi, Y., Taoka, M., Takekiyo, T., Uekita, T., Shoji, I., Hachiya, N., Ichimura, T., 2017. TRIM32-Cytoplasmic-Body Formation Is an ATP-Consuming Process Stimulated by HSP70 in Cells. PLoS One 12, e0169436.

Kawai, T., Akira, S., 2009. The roles of TLRs, RLRs and NLRs in pathogen recognition. Int. Immunol. 21, 317–337.

Kawai, T., Akira, S., 2011. Toll-like Receptors and Their Crosstalk with Other Innate Receptors in Infection and Immunity. Immunity 34, 637–650.

Kawai, T., Takahashi, K., Sato, S., Coban, C., Kumar, H., Kato, H., Ishii, K.J., Takeuchi, O., Akira, S., 2005. IPS-1, an adaptor triggering RIG-I- and Mda5-mediated type I interferon induction. Nat. Immunol. 6, 981–988.

Kelly, M., Hart, E., Mundy, R., Marche, O., Wiles, S., Badea, L., Luck, S., Tauschek, M., Frankel, G., Robins-Browne, R.M., Hartland, E.L., 2006. Essential Role of the Type III Secretion System Effector NleB in Colonization of Mice by *Citrobacter rodentium*. Society 74, 2328–2337.

Kent, T.H., Formal, S.B., Labrec, E.H., 1966. *Salmonella* gastroenteritis in rhesus monkeys. Arch. Pathol. 82, 272–279.

Keszei, A.F.A., Tang, X., McCormick, C., Zeqiraj, E., Rohde, J.R., Tyers, M., Sicheri, F., 2014. Structure of an SspH1-PKN1 Complex Reveals the Basis for Host Substrate Recognition and Mechanism of Activation for a Bacterial E3 Ubiquitin Ligase. Mol. Cell. Biol. 34, 362–373.

Kidwai, A.S., Mushamiri, I., Niemann, G.S., Brown, R.N., Adkins, J.N., Heffron, F., 2013. Diverse secreted effectors are required for *Salmonella* persistence in a mouse infection model. PLoS One 8, e70753.

Kitur, K., Wachtel, S., Brown, A., Wickersham, M., Paulino, F., Penaloza, H.F., Soong, G., Bueno, S., Parker, D., Prince, A., 2016. Necroptosis Promotes *Staphylococcus aureus* Clearance by Inhibiting Excessive Inflammatory Signaling. Cell Rep. 16, 2219–2230.

Knodler, L.A., Ibarra, J.A., Pérez-Rueda, E., Yip, C.K., Steele-Mortimer, O., 2011. Coiled-coil domains enhance the membrane association of *Salmonella* type III effectors. Cell. Microbiol. 13, 1497–1517.

Knodler, L.A., Vallance, B.A., Celli, J., Winfree, S., Hansen, B., Montero, M., Steele-Mortimer, O., 2010. Dissemination of invasive *Salmonella* via bacterial-induced extrusion of mucosal epithelia. Proc. Natl. Acad. Sci. 107, 17733–17738.

Koliopoulos, M.G., Esposito, D., Christodoulou, E., Taylor, I.A., Rittinger, K., 2016. Functional role of TRIM E 3 ligase oligomerization and regulation of catalytic activity. EMBO J. 35, 1204–1218.

Komander, D., Rape, M., 2012. The Ubiquitin Code. Annu. Rev. Biochem. 81, 203–229.

Krafczyk, R., Macošek, J., Gast, D., Wunder, S., Kumar, P., Jagtap, A., 2017. Structural basis for EarP-mediated arginine glycosylation of translation elongation factor EF-P. BioRxiv.

Kröger, C., Colgan, A., Srikumar, S., Händler, K., Sivasankaran, S.K., Hammarlöf, D.L., Canals, R., Grissom, J.E., Conway, T., Hokamp, K., Hinton, J.C.D., 2013. An infection-relevant transcriptomic compendium for *Salmonella enterica* Serovar Typhimurium. Cell Host Microbe 14, 683–695.

Kudryashova, E., Kramerova, I., Spencer, M.J., 2012. Satellite cell senescence underlies myopathy in a mouse model of limb-girdle muscular dystrophy 2H. J. Clin. Invest. 122, 1764–1776.

Kudryashova, E., Kudryashov, D., Kramerova, I., Spencer, M.J., 2005. Trim32 is a ubiquitin ligase mutated in limb girdle muscular dystrophy type 2H that binds to skeletal muscle myosin and ubiquitinates actin. J. Mol. Biol. 354, 413–424.

Kudryashova, E., Wu, J., Havton, L. A, Spencer, M.J., 2009. Deficiency of the E3 ubiquitin ligase TRIM32 in mice leads to a myopathy with a neurogenic component. Hum. Mol. Genet. 18, 1353–1367.

Kuhle, V., Abrahams, G.L., Hensel, M., 2006. Intracellular *Salmonella* enterica redirect exocytic transport processes in a Salmonella pathogenicity island 2-dependent manner. Traffic 7, 716–730.

Kujat Choy, S.L., Boyle, E.C., Gal-mor, O., David, L., Valdez, Y., Vallance, B.A., Finlay, B.B., Goode, D.L., 2004. SseK1 and SseK2 Are Novel Translocated Proteins of *Salmonella enterica* Serovar Typhimurium. Infect. Immun. 72, 5115–5125.

Lairson, L.L., Henrissat, B., Davies, G.J., Withers, S.G., 2008. Glycosyltransferases: structures, functions, and mechanisms. Annu. Rev. Biochem. 77, 521–555.

LaRock, D.L., Chaudhary, A., Miller, S.I., 2015. Salmonellae interactions with host processes. Nat. Rev. Microbiol. 13, 191–205.

Lassak, J., Keilhauer, E.C., Fürst, M., Wuichet, K., Gödeke, J., Starosta, A.L., Chen, J.-M., Søgaard-Andersen, L., Rohr, J., Wilson, D.N., Häussler, S., Mann, M., Jung, K., 2015. Arginine-rhamnosylation as new strategy to activate translation elongation factor P. Nat.

Chem. Biol. 11, 266–270.

Lawley, T.D., Chan, K., Thompson, L.J., Kim, C.C., Govoni, G.R., Monack, D.M., 2006. Genome-wide screen for *Salmonella* genes required for long-term systemic infection of the mouse. PLoS Pathog. 2, e11.

Lawrence, T., 2009. The nuclear factor NF-κB pathway in inflammation. Cold Spring Harb Perspect Biol. 1, a001651.

Lawrence, T., Gilroy, D.W., Colville-Nash, P.R., Willoughby, D.A., 2001. Possible new role for NF-κB in the resolution of inflammation. Nat. Med. 7, 1291–1297.

Lazzari, E., Meroni, G., 2016. TRIM32 ubiquitin E3 ligase, one enzyme for several pathologies: From muscular dystrophy to tumours. Int. J. Biochem. Cell Biol. 79, 469–477.

Le Negrate, G., Faustin, B., Welsh, K., Loeffler, M., Krajewska, M., Hasegawa, P., Mukherjee, S., Orth, K., Krajewski, S., Godzik, A., Guiney, D.G., Reed, J.C., 2008. *Salmonella* Secreted Factor L Deubiquitinase of *Salmonella* -typhimurium Inhibits NF-kB, Suppresses IkB Ubiquitination and Modulates Innate Immune Responses. J. Immunol. 180, 5045–5056.

Lee, A.K., Detweiler, C.S., Falkow, S., 2000. OmpR regulates the two-component system SsrA-SsrB in *Salmonella* pathogenicity island 2. J. Bacteriol. 182, 771–781.

Lee, Y., Song, B., Park, C., Kwon, K.S., 2013. TRIM11 Negatively Regulates IFNβ Production and Antiviral Activity by Targeting TBK1. PLoS One 8, 1–12.

Legler, D.F., Micheau, O., Doucey, M.A., Tschopp, J., Bron, C., 2003. Recruitment of TNF receptor 1 to lipid rafts is essential for TNFα-mediated NF-κB activation. Immunity 18, 655–664.

Lesnick, M.L., Reiner, N.E., Fierer, J., Guiney, D.G., 2001. The *Salmonella* spvB virulence gene encodes an enzyme that ADP-ribosylates actin and destabilizes the cytoskeleton of eukaryotic cells. Mol. Microbiol. 39, 1464–1470.

Levine, M.M., Black, R.E., Lanata, C., 1982. Precise estimation of the numbers of chronic carriers of *Salmonella* typhi in Santiago, Chile, an endemic area. J. Infect. Dis. 146, 724–726.

Li, J., McQuade, T., Siemer, A.B., Napetschnig, J., Moriwaki, K., Hsiao, Y.S., Damko, E., Moquin, D., Walz, T., McDermott, A., Chan, F.K.M., Wu, H., 2012. The RIP1/RIP3 necrosome forms a functional amyloid signaling complex required for programmed necrosis. Cell 150, 339–350.

Li, S., Wang, L., Berman, M., Kong, Y.-Y., Dorf, M.E., 2011. Mapping a dynamic innate immunity

protein interaction network regulating type I interferon production. Immunity 35, 426–440.

Li, S., Zhang, L., Yao, Q., Li, L., Dong, N., Rong, J., Gao, W., Ding, X., Sun, L., Chen, X., Chen, S., Shao, F., 2013. Pathogen blocks host death receptor signalling by arginine GlcNAcylation of death domains. Nature 501, 242–246.

Liang, Q., Deng, H., Li, X., Wu, X., Tang, Q., Chang, T.-H., Peng, H., Rauscher, F.J., Ozato, K., Zhu, F., 2011. Tripartite Motif-Containing Protein 28 Is a Small Ubiquitin-Related Modifier E3 Ligase and Negative Regulator of IFN Regulatory Factor 7. J. Immunol. 187, 4754–4763.

Lin, B., Williams-Skipp, C., Tao, Y., Schleicher, M.S., Cano, L.L., Duke, R.C., Scheinman, R.I., 1999. NF-κB functions as both a proapoptotic and antiapoptotic regulatory factor within a single cell type. Cell Death Differ. 6, 570–582.

Lin, S.L., Le, T.X., Cowen, D.S., 2003. SptP, a *Salmonella* typhimurium type III-secreted protein, inhibits the mitogen-activated protein kinase pathway by inhibiting Raf activation. Cell. Microbiol. 5, 267–275.

Lin, Y., Choksi, S., Shen, H.M., Yang, Q.F., Hur, G.M., Kim, Y.S., Tran, J.H., Nedospasov, S.A., Liu, Z.G., 2004. Tumor Necrosis Factor-induced Nonapoptotic Cell Death Requires Receptor-interacting Protein-mediated Cellular Reactive Oxygen Species Accumulation. J. Biol. Chem. 279, 10822–10828.

Lionel, A.C., Crosbie, J., Barbosa, N., Goodale, T., Thiruvahindrapuram, B., Rickaby, J., Gazzellone, M., Carson, A.R., Howe, J.L., Wang, Z., Wei, J., Stewart, A.F.R., Roberts, R., McPherson, R., Fiebig, A., Franke, A., Schreiber, S., Zwaigenbaum, L., Fernandez, B.A., Roberts, W., Arnold, P.D., Szatmari, P., Marshall, C.R., Schachar, R., Scherer, S.W., 2011. Rare copy number variation discovery and cross-disorder comparisons identify risk genes for ADHD. Sci. Transl. Med. 3, 95ra75.

Lionel, A.C., Tammimies, K., Vaags, A.K., Rosenfeld, J. A, Ahn, J.W., Merico, D., Noor, A., Runke, C.K., Pillalamarri, V.K., Carter, M.T., Gazzellone, M.J., Thiruvahindrapuram, B., Fagerberg, C., Laulund, L.W., Pellecchia, G., Lamoureux, S., Deshpande, C., Clayton-Smith, J., White, A.C., Leather, S., Trounce, J., Melanie Bedford, H., Hatchwell, E., Eis, P.S., Yuen, R.K.C., Walker, S., Uddin, M., Geraghty, M.T., Nikkel, S.M., Tomiak, E.M., Fernandez, B. A, Soreni, N., Crosbie, J., Arnold, P.D., Schachar, R.J., Roberts, W., Paterson, A.D., So, J., Szatmari, P., Chrysler, C., Woodbury-Smith, M., Brian Lowry, R., Zwaigenbaum, L., Mandyam, D.,

Wei, J., Macdonald, J.R., Howe, J.L., Nalpathamkalam, T., Wang, Z., Tolson, D., Cobb, D.S., Wilks, T.M., Sorensen, M.J., Bader, P.I., An, Y., Wu, B.-L., Musumeci, S.A., Romano, C., Postorivo, D., Nardone, A.M., Monica, M. Della, Scarano, G., Zoccante, L., Novara, F., Zuffardi, O., Ciccone, R., Antona, V., Carella, M., Zelante, L., Cavalli, P., Poggiani, C., Cavallari, U., Argiropoulos, B., Chernos, J., Brasch-Andersen, C., Speevak, M., Fichera, M., Ogilvie, C.M., Shen, Y., Hodge, J.C., Talkowski, M.E., Stavropoulos, D.J., Marshall, C.R., Scherer, S.W., 2014. Disruption of the ASTN2/TRIM32 locus at 9q33.1 is a risk factor in males for autism spectrum disorders, ADHD and other neurodevelopmental phenotypes. Hum. Mol. Genet. 23, 2752–2768.

Lipscomb, M.F., Masten, B.J., 2002. Dendritic Cells: Immune Regulators in Health and Disease. Physiol Rev 82, 97–130.

Liss, V., Swart, A.L., Kehl, A., Hermanns, N., Zhang, Y., Chikkaballi, D., Bohles, N., Deiwick, J., Hensel, M., 2017. *Salmonella enterica* Remodels the Host Cell Endosomal System for Efficient Intravacuolar Nutrition. Cell Host Microbe 21, 390–402.

Liu, J., Zhang, C., Wang, X.L., Ly, P., Belyi, V., Xu-Monette, Z.Y., Young, K.H., Hu, W., Feng, Z., 2014. E3 ubiquitin ligase TRIM32 negatively regulates tumor suppressor p53 to promote tumorigenesis. Cell Death Differ. 21, 1792–1804.

Liu, X., Zhang, Z., Ruan, J., Pan, Y., Magupalli, V.G., Wu, H., Lieberman, J., 2016. Inflammasome-activated gasdermin D causes pyroptosis by forming membrane pores. Nature 535, 153–158.

Liu, Y., Lagowski, J.P., Gao, S., Raymond, J.H., White, C.R., Kulesz-Martin, M.F., 2010. Regulation of the psoriatic chemokine CCL20 by E3 ligases Trim32 and Piasy in keratinocytes. J. Invest. Dermatol. 130, 1384–1390.

Liu, Y., Wang, Z., De La Torre, R., Barling, A., Tsujikawa, T., Hornick, N., Hanifin, J., Simpson, E., Wang, Y., Swanzey, E., Wortham, A., Ding, H., Coussens, L.M., Kulesz-Martin, M., 2017. Trim32 Deficiency Enhances Th2 Immunity and Predisposes to Features of Atopic Dermatitis. J. Invest. Dermatol. 137, 359–366.

Liu, Y., Wu, W., Yang, H., Zhou, Z., Zhu, X., Sun, C., Liu, Y., Yu, Z., Chen, Y., Wang, Y., 2017. Upregulated Expression of TRIM32 Is Involved in Schwann Cell Differentiation, Migration and Neurite Outgrowth After Sciatic Nerve Crush. Neurochem. Res. 42, 1084–1095.

Locke, M., Tinsley, C.L., Benson, M.A., Blake, D.J., 2009. TRIM32 is an E3 ubiquitin ligase for dysbindin. Hum. Mol. Genet. 18, 2344–2358.

López-Otín, C., Overall, C.M., 2002. Protease degradomics: a new challenge for proteomics. Nat. Rev. Mol. Cell Biol. 3, 509–519.

Ma, J., Hart, G.W., 2013. Protein O-GlcNAcylation in diabetes and diabetic complications. Expert Rev. Proteomics 10, 365–380.

MacLennan, C.A., Levine, M.M., 2013. Invasive nontyphoidal *Salmonella* disease in Africa: current status. Expert Rev. Anti. Infect. Ther. 11, 443–446.

Majowicz, S.E., Musto, J., Scallan, E., Angulo, F.J., Kirk, M., O'Brien, S.J., Jones, T.F., Fazil, A., Hoekstra, R.M., 2010. The global burden of nontyphoidal *Salmonella* gastroenteritis. Clin. Infect. Dis. 50, 882–889.

Malorny, B., Hauser, E., Dieckmann, R., 2011. New approaches in subspecies-level *Salmonella* classification. In: Porwollik, S. (Ed.), Salmonella: From Genome to Function. Caister Academic Press, Norfolk, UK, pp. 1–23.

Mandell, M.A., Jain, A., Arko-Mensah, J., Chauhan, S., Kimura, T., Dinkins, C., Silvestri, G., Munch, J., Kirchhoff, F., Simonsen, A., Wei, Y., Levine, B., Johansen, T., Deretic, V., 2014. TRIM Proteins Regulate Autophagy and Can Target Autophagic Substrates by Direct Recognition. Dev. Cell 30, 394–409.

Marcus, S.L., Brumell, J.H., Pfeifer, C.G., Finlay, B.B., 2000. *Salmonella* pathogenicity islands: big virulence in small packages. Microbes Infect. 2, 145–156.

Mastroeni, P., Bryant, C., 2013. Cytokines in Salmonellosis. EcoSal Plus 8.8.5.

Mazurkiewicz, P., Thomas, J., Thompson, J.A., Liu, M., Arbibe, L., Sansonetti, P., Holden, D.W., 2008. SpvC is a *Salmonella* effector with phosphothreonine lyase activity on host mitogen-activated protein kinases. Mol. Microbiol. 67, 1371–1383.

McEwan, W.A., Tam, J.C.H., Watkinson, R.E., Bidgood, S.R., Mallery, D.L., James, L.C., 2013. Intracellular antibody-bound pathogens stimulate immune signaling via the Fc receptor TRIM21. Nat. Immunol. 14, 327–336.

McGourty, K., Thurston, T.L., Matthews, S.A., Pinaud, L., Mota, L.J., Holden, D.W., 2012. *Salmonella* Inhibits Retrograde Trafficking of Mannose-6-Phosphate Receptors and Lysosome Function. Science 338, 963–967.

McIlwain, D.R., Berger, T., Mak, T.W., 2015. Caspase Functions in Cell Death and Disease. Cold Spring Harb. Perspect. Biol. 7, a026716.

McLaughlin, L.M., Govoni, G.R., Gerke, C., Gopinath, S., Peng, K., Laidlaw, G., Chien, Y.H., Jeong, H.W., Li, Z., Brown, M.D., Sacks, D.B., Monack, D., 2009. The *Salmonella* SPI2

effector SseI mediates long-term systemic infection by modulating host cell migration. PLoS Pathog. 5, e1000671.

McNab, F.W., Rajsbaum, R., Stoye, J.P., O'Garra, A., 2011. Tripartite-motif proteins and innate immune regulation. Curr. Opin. Immunol. 23, 46–56.

Medzhitov, R., 2007. Recognition of microorganisms and activation of the immune response. Nature 449, 819–826.

Méresse, S., Unsworth, K.E., Habermann, A., Griffiths, G., Fang, F., Martínez-Lorenzo, M.J., Waterman, S.R., Gorvel, J.P., Holden, D.W., 2001. Remodelling of the actin cytoskeleton is essential for replication of intravacuolar *Salmonella*. Cell. Microbiol. 3, 567–577.

Meroni, G., Diez-Roux, G., 2005. TRIM/RBCC, a novel class of "single protein RING finger" E3 ubiquitin ligases. BioEssays 27, 1147–1157.

Mesmin, B., Robbe, K., Geny, B., Luton, F., Brandolin, G., Popoff, M.R., Antonny, B., 2004. A phosphatidylserine-binding site in the cytosolic fragment of *Clostridium sordellii* lethal toxin facilitates glucosylation of membrane-bound Rac and is required for cytotoxicity. J. Biol. Chem. 279, 49876–49882.

Mesquita, F.S., Holden, D.W., Rolhion, N., 2013. Lack of Effect of the *Salmonella* Deubiquitinase SseL on the NF-κB Pathway. PLoS One 8, 1–9.

Miao, E.A., Alpuche-Aranda, C.M., Dors, M., Clark, A.E., Bader, M.W., Miller, S.I., Aderem, A.A., 2006. Cytoplasmic flagellin activates caspase-1 and secretion of interleukin-1β via Ipaf. Nat. Immunol. 7, 569–575.

Miao, E.A., Brittnacher, M., Haraga, A., Jeng, R.L., Welch, M.D., Miller, S.I., 2003. *Salmonella* effectors translocated across the vacuolar membrane interact with the actin cytoskeleton. Mol. Microbiol. 48, 401–415.

Miao, E.A., Mao, D.P., Yudkovsky, N., Bonneau, R., Lorang, C.G., Warren, S.E., Leaf, I.A., Aderem, A., 2010. Innate immune detection of the type III secretion apparatus through the NLRC4 inflammasome. Proc. Natl. Acad. Sci. 107, 3076–3080.

Michallet, M.C., Meylan, E., Ermolaeva, M.A., Vazquez, J., Rebsamen, M., Curran, J., Poeck, H., Bscheider, M., Hartmann, G., König, M., Kalinke, U., Pasparakis, M., Tschopp, J., 2008. TRADD Protein Is an Essential Component of the RIG-like Helicase Antiviral Pathway. Immunity 28, 651–661.

Micheau, O., Tschopp, J., 2003. Induction of TNF Receptor I-Mediated Apoptosis via Two Sequential Signaling Complexes. Cell 114, 181–190.

Miller, S.I., Kukral, A.M., Mekalanos, J.J., 1989. A two-component regulatory system (phoP phoQ) controls *Salmonella* typhimurium virulence. Proc. Natl. Acad. Sci. 86, 5054–5058.

Mittrücker, H.-W., Köhler, A., Kaufmann, S.H.E., 2002. Characterization of the murine T-lymphocyte response to *Salmonella enterica* serovar Typhimurium infection. Infect. Immun. 70, 199–203.

Mogensen, T.H., 2009. Pathogen recognition and inflammatory signaling in innate immune defenses. Clin. Microbiol. Rev. 22, 240–273.

Mokhonova, E.I., Avliyakulov, N.K., Kramerova, I., Kudryashova, E., Haykinson, M.J., Spencer, M.J., 2015. The E3 ubiquitin ligase TRIM32 regulates myoblast proliferation by controlling turnover of NDRG2. Hum. Mol. Genet. 24, 2873–2883.

Monack, D.M., Bouley, D.M., Falkow, S., 2004. *Salmonella* typhimurium Persists within Macrophages in the Mesenteric Lymph Nodes of Chronically Infected Nramp1+/+ Mice and Can Be Reactivated by IFNγ Neutralization. J. Exp. Med. 199, 231–241.

Moremen, K.W., Tiemeyer, M., Nairn, A. V, 2014. Vertebrate protein glycosylation: diversity, synthesis and function. Nat. Rev. Mol. Cell Biol. 13, 448–462.

Mueller, C.A., Broz, P., Cornelis, G.R., 2008. The type III secretion system tip complex and translocon. Mol. Microbiol. 68, 1085–1095.

Müller, A.J., Hoffmann, C., Galle, M., Van Den Broeke, A., Heikenwalder, M., Falter, L., Misselwitz, B., Kremer, M., Beyaert, R., Hardt, W.D., 2009. The *S.* Typhimurium Effector SopE Induces Caspase-1 Activation in Stromal Cells to Initiate Gut Inflammation. Cell Host Microbe 6, 125–136.

Murphy, J.M., Czabotar, P.E., Hildebrand, J.M., Lucet, I.S., Zhang, J.G., Alvarez-Diaz, S., Lewis, R., Lalaoui, N., Metcalf, D., Webb, A.I., Young, S.N., Varghese, L.N., Tannahill, G.M., Hatchell, E.C., Majewski, I.J., Okamoto, T., Dobson, R.C.J., Hilton, D.J., Babon, J.J., Nicola, N.A., Strasser, A., Silke, J., Alexander, W.S., 2013. The pseudokinase MLKL mediates necroptosis via a molecular switch mechanism. Immunity 39, 443–453.

Nadler, C., Baruch, K., Kobi, S., Mills, E., Haviv, G., Farago, M., Alkalay, I., Bartfeld, S., Meyer, T.F., Ben-Neriah, Y., Rosenshine, I., 2010. The type III secretion effector NleE inhibits NF-κB activation. PLoS Pathog. 6, e1000743.

Nairz, M., Fritsche, G., Crouch, M.L. V, Barton, H.C., Fang, F.C., Weiss, G., 2009. Slc11a1 limits intracellular growth of *Salmonella enterica* sv. Typhimurium by promoting macrophage immune effector functions and impairing bacterial iron acquisition. Cell. Microbiol. 11,

1365–1381.

Napetschnig, J., Wu, H., 2013. Molecular Basis of NF-κB Signaling. Annu. Rev. Biophys. 6, 443–468.

Napolitano, L.M., Jaffray, E.G., Hay, R.T., Meroni, G., 2011. Functional interactions between ubiquitin E2 enzymes and TRIM proteins. Biochem. J. 434, 309–319.

Nectoux, J., de Cid, R., Baulande, S., Leturcq, F., Urtizberea, J.A., Penisson-Besnier, I., Nadaj-Pakleza, A., Roudaut, C., Criqui, A., Orhant, L., Peyroulan, D., Ben Yaou, R., Nelson, I., Cobo, A.M., Arné-Bes, M.-C., Uro-Coste, E., Nitschke, P., Claustres, M., Bonne, G., Lévy, N., Chelly, J., Richard, I., Cossée, M., 2014. Detection of TRIM32 deletions in LGMD patients analyzed by a combined strategy of CGH array and massively parallel sequencing. Eur. J. Hum. Genet. 23, 929–934.

Neri, M., Selvatici, R., Scotton, C., Trabanelli, C., Armaroli, A., De Grandis, D., Levy, N., Gualandi, F., Ferlini, A., 2013. A patient with limb girdle muscular dystrophy carries a TRIM32 deletion, detected by a novel CGH array, in compound heterozygosis with a nonsense mutation. Neuromuscul. Disord. 23, 478–482.

Newton, H.J., Pearson, J.S., Badea, L., Kelly, M., Lucas, M., Holloway, G., Wagstaff, K.M., Dunstone, M.A., Sloan, J., Whisstock, J.C., Kaper, J.B., Robins-Browne, R.M., Jans, D.A., Frankel, G., Phillips, A.D., Coulson, B.S., Hartland, E.L., 2010. The type III effectors NleE and NleB from enteropathogenic *E. coli* and OspZ from *Shigella* block nuclear translocation of NF-κB p65. PLoS Pathog. 6, e1000898.

Newton, K., Dugger, D.L., Wickliffe, K.E., Kapoor, N., de Almagro, M.C., Vucic, D., Komuves, L., Ferrando, R.E., French, D.M., Webster, J., Roose-Girma, M., Warming, S., Dixit, V.M., 2014. Activity of protein kinase RIPK3 determines whether cells die by necroptosis or apoptosis. Science 343, 1357–1360.

Nicklas, S., Okawa, S., Hillje, A.-L., González-Cano, L., Del Sol, A., Schwamborn, J.C., 2015. The RNA helicase DDX6 regulates cell-fate specification in neural stem cells via miRNAs. Nucleic Acids Res. 43, 2638–2654.

Nicklas, S., Otto, A., Wu, X., Miller, P., Stelzer, S., Wen, Y., Kuang, S., Wrogemann, K., Patel, K., Ding, H., Schwamborn, J.C., 2012. TRIM32 regulates skeletal muscle stem cell differentiation and is necessary for normal adult muscle regeneration. PLoS One 7, e30445.

Niemann, G.S., Brown, R.N., Gustin, J.K., Stufkens, A., Shaikh-Kidwai, A.S., Li, J., McDermott,

J.E., Brewer, H.M., Schepmoes, A., Smith, R.D., Adkins, J.N., Heffron, F., 2011. Discovery of novel secreted virulence factors from *Salmonella enterica* serovar Typhimurium by proteomic analysis of culture supernatants. Infect. Immun. 79, 33–43.

Nuccio, S.P., Bäumler, A.J., 2014. Comparative analysis of *Salmonella* genomes identifies a metabolic network for escalating growth in the inflamed gut. mBio 5, 1–8.

Ochman, H., Soncini, F.C., Solomon, F., Groisman, E.A., 1996. Identification of a pathogenicity island required for *Salmonella* survival in host cells. Proc. Natl. Acad. Sci. 93, 7800–7804.

Odendall, C., Rolhion, N., Förster, A., Poh, J., Lamont, D.J., Liu, M., Freemont, P.S., Catling, A.D., Holden, D.W., 2012. The *Salmonella* kinase SteC targets the MAP kinase MEK to regulate the host actin cytoskeleton. Cell Host Microbe 12, 657–668.

Oeckinghaus, A., Ghosh, S., 2009. The NF-kB family of transcription factors and its regulation. Cold Spring Harb Perspect Biol. 1, a000034.

Oeckinghaus, A., Hayden, M.S., Ghosh, S., 2011. Crosstalk in NF-κB signaling pathways. Nat. Immunol. 12, 695–708.

Pan, M., Li, S., Li, X., Shao, F., Liu, L., Hu, H.-G., 2014. Synthesis of and Specific Antibody Generation for Glycopeptides with Arginine N-GlcNAcylation. Angew. Chemie Int. Ed. 53, 14517–14521.

Park, Y.C., Ye, H., Hsia, C., Segal, D., Rich, R.L., Liou, H.C., Myszka, D.G., Wu, H., 2000. A novel mechanism of TRAF signaling revealed by structural and functional analyses of the TRADD-TRAF2 interaction. Cell 101, 777–787.

Park, Y.H., Jeong, M.S., Jang, S.B., 2014. Death domain complex of the TNFR-1, TRADD, and RIP1 proteins for death-inducing signaling. Biochem. Biophys. Res. Commun. 443, 1155–1161.

Pasparakis, M., Vandenabeele, P., 2015. Necroptosis and its role in inflammation. Nature 517, 311–320.

Patel, J.C., Galán, J.E., 2005. Manipulation of the host actin cytoskeleton by *Salmonella* - All in the name of entry. Curr. Opin. Microbiol. 8, 10–15.

Patel, J.C., Galán, J.E., 2006. Differential activation and function of Rho GTPases during Salmonella-host cell interactions. J. Cell Biol. 175, 453–463.

Pavlou, M.A.S., Colombo, N., Fuertes-Alvarez, S., Nicklas, S., Cano, L.G., Marín, M.C., Goncalves, J., Schwamborn, J.C., 2016. Expression of the Parkinson's Disease-Associated Gene Alpha-Synuclein is Regulated by the Neuronal Cell Fate Determinant TRIM32. Mol.

Neurobiol. 54, 4257–4270.

Pearson, J.S., Giogha, C., Ong, S.Y., Kennedy, C.L., Kelly, M., Robinson, K.S., Lung, T.W.F., Mansell, A., Riedmaier, P., Oates, C.V.L., Zaid, A., Mühlen, S., Crepin, V.F., Marches, O., Ang, C.-S., Williamson, N.A., O'Reilly, L. A, Bankovacki, A., Nachbur, U., Infusini, G., Webb, A.I., Silke, J., Strasser, A., Frankel, G., Hartland, E.L., 2013. A type III effector antagonizes death receptor signalling during bacterial gut infection. Nature 501, 247–251.

Peppel, K., Crawford, D., Beutler, B., 1991. A tumor necrosis factor (TNF) receptor-IgG heavy chain chimeric protein as a bivalent antagonist of TNF activity. J. Exp. Med. 174, 1483–1489.

Perkins, D.J., Rajaiah, R., Tennant, S.M., Ramachandran, G., Higginson, E.E., Dyson, T.N., Vogel, S.N., 2015. Salmonella Typhimurium Co-Opts the Host Type I IFN System To Restrict Macrophage Innate Immune Transcriptional Responses Selectively. J. Immunol. 195, 2461–2471.

Perkins, N.D., Gilmore, T.D., 2006. Good cop, bad cop: the different faces of NF-κB. Cell Death Differ. 13, 759–772.

Perrett, C.A., Zhou, D., 2013. *Salmonella* type III effector SopB modulates host cell exocytosis. Emerg. Microbes Infect. 2, e32.

Pie, S., Truffa-Bachi, P., Pla, M., Nauciel, C., 1997. Th1 Response in *Salmonella* typhimurium - Infected Mice with a High or Low Rate of Bacterial Clearance. Infect. Immun. 65, 4509–4514.

Pilar, A.V.C., Reid-Yu, S.A., Cooper, C.A., Mulder, D.T., Coombes, B.K., 2012. GogB is an anti-inflammatory effector that limits tissue damage during *Salmonella* infection through interaction with human FBXO22 and Skp1. PLoS Pathog. 8, e1002773.

Platanias, L.C., 2005. Mechanisms of type-I- and type-II-interferon-mediated signalling. Nat. Rev. Immunol. 5, 375–386.

Plotnikov, A., Zehorai, E., Procaccia, S., Seger, R., 2011. The MAPK cascades: Signaling components, nuclear roles and mechanisms of nuclear translocation. Biochim. Biophys. Acta - Mol. Cell Res. 1813, 1619–1633.

Pobezinskaya, Y.L., Kim, Y.S., Choksi, S., Morgan, M.J., Li, T., Liu, C., Liu, Z., 2008. The function of TRADD in signaling through tumor necrosis factor receptor 1 and TRIF-dependent Toll-like receptors. Nat. Immunol. 9, 1047–1054.

Poh, J., Odendall, C., Spanos, A., Boyle, C., Liu, M., Freemont, P., Holden, D.W., 2008. SteC is

a *Salmonella* kinase required for SPI-2-dependent F-actin remodelling. Cell. Microbiol. 10, 20–30.

Popa, C.M., Tabuchi, M., Valls, M., 2016. Modification of Bacterial Effector Proteins Inside Eukaryotic Host Cells. Front. Cell. Infect. Microbiol. 6, 1–13.

Porwollik, S., McClelland, M., 2003. Lateral gene transfer in *Salmonella*. Microbes Infect. 5, 977–989.

Pruneda, J.N., Durkin, C.H., Geurink, P.P., Ovaa, H., Santhanam, B., Holden, D.W., Correspondence, D.K., Komander, D., 2016. The Molecular Basis for Ubiquitin and Ubiquitin-like Specificities in Bacterial Effector Proteases. Mol. Cell 63, 1–16.

Quezada, C.M., Hicks, S.W., Galan, J.E., Stebbins, C.E., 2009. A family of *Salmonella* virulence factors functions as a distinct class of autoregulated E3 ubiquitin ligases. Proc. Natl. Acad. Sci. 106, 4864–4869.

Rajashekar, R., Liebl, D., Chikkaballi, D., Liss, V., Hensel, M., 2014. Live Cell imaging reveals novel functions of *Salmonella enterica* SPI2-T3SS effector proteins in remodeling of the host cell endosomal system. PLoS One 9, 1–29.

Rajsbaum, R., García-Sastre, A., Versteeg, G.A., 2014a. TRIMmunity: the roles of the TRIM E3-ubiquitin ligase family in innate antiviral immunity. J. Mol. Biol. 426, 1265–1284.

Rajsbaum, R., Versteeg, G.A., Schmid, S., Maestre, A.M., Belicha-Villanueva, A., Martínez-Romero, C., Patel, J.R., Morrison, J., Pisanelli, G., Miorin, L., Laurent-Rolle, M., Moulton, H.M., Stein, D.A., Fernandez-Sesma, A., tenOever, B.R., García-Sastre, A., 2014b. Unanchored K48-Linked Polyubiquitin Synthesized by the E3-Ubiquitin Ligase TRIM6 Stimulates the Interferon-IKKε Kinase-Mediated Antiviral Response. Immunity 40, 880–895.

Rakebrandt, N., Lentes, S., Neumann, H., James, L.C., Neumann-Staubitz, P., 2014. Antibody- and TRIM21-dependent intracellular restriction of *Salmonella enterica*. Pathog. Dis. 2, 131–137.

Ramos-Morales, F., 2012. Impact of *Salmonella enterica* Type III Secretion System Effectors on the Eukaryotic Host Cell. ISRN Cell Biol. 2012, 1–36.

Randow, F., Sale, J.E., 2006. Retroviral transduction of DT40. Subcell. Biochem. 40, 383–386.

Rao, S., Schieber, A.M.P., O'Connor, C.P., Leblanc, M., Michel, D., Ayres, J.S., 2017. Pathogen-Mediated Inhibition of Anorexia Promotes Host Survival and Transmission. Cell 168, 503–516.

Remijsen, Q., Kuijpers, T.W., Wirawan, E., Lippens, S., Vandenabeele, P., Vanden Berghe, T., 2011. Dying for a cause: NETosis, mechanisms behind an antimicrobial cell death modality. Cell Death Differ. 18, 581–588.

Reymond, A., Meroni, G., Fantozzi, A., Merla, G., Cairo, S., Luzi, L., Riganelli, D., Zanaria, E., Messali, S., Cainarca, S., Guffanti, A., Minucci, S., Pelicci, P.G., Ballabio, A., 2001. The tripartite motif family identifies cell compartments. EMBO J. 20, 2140–2151.

Robinson, N., McComb, S., Mulligan, R., Dudani, R., Krishnan, L., Sad, S., 2012. Type I interferon induces necroptosis in macrophages during infection with *Salmonella enterica* serovar Typhimurium. Nat. Immunol. 13, 954–962.

Rolhion, N., Furniss, R.C.D., Grabe, G., Ryan, A., Liu, M., Matthews, S.A., Holden, D.W., 2016. Inhibition of Nuclear Transport of NF-κB p65 by the *Salmonella* Type III Secretion System Effector SpvD. PLoS Pathog. 12, e1005653.

Roskoski, R., 2012. ERK1/2 MAP kinases: Structure, function, and regulation. Pharmacol. Res. 66, 105–143.

Ruan, C.-S., Wang, S.-F., Shen, Y.-J., Guo, Y., Yang, C.-R., Zhou, F.H., Tan, L.-T., Zhou, L., Liu, J.-J., Wang, W.-Y., Xiao, Z.-C., Zhou, X.-F., 2014. Deletion of TRIM32 protects mice from anxiety- and depression-like behaviors under mild stress. Eur. J. Neurosci. 40, 2680–2690.

Ruchaud-Sparagano, M.H., Mühlen, S., Dean, P., Kenny, B., 2011. The enteropathogenic E. coli (EPEC) Tir effector inhibits NF-κB activity by targeting TNFα receptor-associated factors. PLoS Pathog. 7, e1002414.

Ruckdeschel, K., Pfaffinger, G., Haase, R., Sing, A., Weighardt, H., Häcker, G., Holzmann, B., Heesemann, J., 2004. Signaling of apoptosis through TLRs critically involves toll/IL-1 receptor domain-containing adapter inducing IFN-beta, but not MyD88, in bacteria-infected murine macrophages. J. Immunol. 173, 3320–3328.

Ruelas, D.S., Chan, J.K., Oh, E., Heidersbach, A.J., Hebbeler, A.M., Chavez, L., Verdin, E., Rape, M., Greene, W.C., 2015. MicroRNA-155 reinforces HIV latency. J. Biol. Chem. 290, 13736–13748.

Ruiz-Albert, J., Yu, X.J., Beuzón, C.R., Blakey, A.N., Galyov, E.E., Holden, D.W., 2002. Complementary activities of SseJ and SifA regulate dynamics of the *Salmonella* typhimuriumvacuolar membrane. Mol. Microbiol. 44, 645–661.

Rytkönen, A., Poh, J., Garmendia, J., Boyle, C., Thompson, A., Liu, M., Freemont, P., Hinton,

J.C.D., Holden, D.W., 2007. SseL, a *Salmonella* deubiquitinase required for macrophage killing and virulence. Proc. Natl. Acad. Sci. 104, 3502–3507.

Ryu, Y.S., Lee, Y., Lee, K.W., Hwang, C.Y., Maeng, J.S., Kim, J.H., Seo, Y.S., You, K.H., Song, B., Kwon, K.S., 2011. TRIM32 protein sensitizes cells to Tumor Necrosis Factor (TNFα)-induced Apoptosis via its RING domain-dependent E3 ligase activity against X-linked Inhibitor of Apoptosis (XIAP). J. Biol. Chem. 286, 25729–25738.

Sabbagh, S.C., Forest, C.G., Lepage, C., Leclerc, J.M., Daigle, F., 2010. So similar, yet so different: Uncovering distinctive features in the genomes of *Salmonella enterica* serovars Typhimurium and Typhi. FEMS Microbiol. Lett. 305, 1–13.

Saccone, V., Palmieri, M., Passamano, L., Piluso, G., Meroni, G., Politano, L., Nigro, V., 2008. Mutations That Impair Interaction Properties of TRIM32 Associated With Limb-Girdle Muscular Dystrophy 2H. Hum. Mutat. 29, 240–247.

Salcedo, S.P., Holden, D.W., 2003. SseG, a virulence protein that targets *Salmonella* to the Golgi network. EMBO J. 22, 5003–5014.

Salcedo, S.P., Noursadeghi, M., Cohen, J., Holden, D.W., 2001. Intracellular replication of *Salmonella* typhimurium strains in specific subsets of splenic macrophages *in vivo*. Cell. Microbiol. 3, 587–597.

Samudrala, R., Heffron, F., McDermott, J.E., 2009. Accurate Prediction of Secreted Substrates and Identification of a Conserved Putative Secretion Signal for Type III Secretion Systems. PLoS Pathog. 5, e1000375.

Sato, T., Okumura, F., Kano, S., Kondo, T., Ariga, T., Hatakeyama, S., 2011. TRIM32 promotes neural differentiation through retinoic acid receptor-mediated transcription. J. Cell Sci. 124, 3492–3502.

Schmid, J., Heider, D., Wendel, N.J., Sperl, N., Sieber, V., 2016. Bacterial glycosyltransferases: Challenges and Opportunities of a Highly Diverse Enzyme Class Toward Tailoring Natural Products. Front. Microbiol. 7, 1–7.

Schmitt, C.K., Ikeda, J.S., Darnell, S.C., Watson, P.R., Bispham, J., Wallis, T.S., Weinstein, D.L., Metcalf, E.S., O'Brien, A.D., 2001. Absence of all components of the flagellar export and synthesis machinery differentially alters virulence of *Salmonella enterica* serovar typhimurium in models of typhoid fever, survival in macrophages, tissue culture invasiveness, and calf enterocolitis. Infect. Immun. 69, 5619–5625.

Schmolke, M., Patel, J.R., de Castro, E., Sánchez, M.T.A., Uccellini, M.B., Miller, J.C.,

Manicassamy, B., Satoh, T., Kawai, T., Akira, S., Merad, M., García-Sastre, A., 2014. RIG-I Detects mRNA of Intracellular *Salmonella enterica* Serovar Typhimurium during Bacterial Infection. mBio 5, 1–9.

Schroeder, N., Henry, T., de Chastellier, C., Zhao, W., Guilhon, A.-A., Gorvel, J.-P., Méresse, S., 2010. The virulence protein SopD2 regulates membrane dynamics of *Salmonella*-containing vacuoles. PLoS Pathog. 6, e1001002.

Schroeder, N., Mota, L.J., Méresse, S., 2011. *Salmonella*-induced tubular networks. Trends Microbiol. 19, 268–277.

Schwamborn, J.C., Berezikov, E., Knoblich, J.A., 2009. The TRIM-NHL protein TRIM32 activates microRNAs and prevents self-renewal in mouse neural progenitors. Cell 136, 913–925.

Seth-Smith, H.M.B., 2008. SPI-7: *Salmonella's* Vi-Encoding Pathogenicity Island. J. Infect. Dev. Ctries. 2, 267–271.

Sharma, S., tenOever, B.R., Grandvaux, N., Zhou, G.P., Lin, R., Hiscott, J., 2003. Triggering the interferon antiviral response through an IKK-related pathway. Science 300, 1148–1151.

Shi, J., Zhao, Y., Wang, Y., Gao, W., Ding, J., Li, P., Hu, L., Shao, F., 2014. Inflammatory caspases are innate immune receptors for intracellular LPS. Nature 514, 187–192.

Shi, M., Cho, H., Inn, K.-S., Yang, A., Zhao, Z., Liang, Q., Versteeg, G.A., Amini-Bavil-Olyaee, S., Wong, L.-Y., Zlokovic, B. V., Park, H.-S., García-Sastre, A., Jung, J.U., 2014. Negative regulation of NF-κB activity by brain-specific TRIpartite Motif protein 9. Nat. Commun. 5, 4820.

Shi, M., Deng, W., Bi, E., Mao, K., Ji, Y., Lin, G., Wu, X., Tao, Z., Li, Z., Cai, X., Sun, S., Xiang, C., Sun, B., 2008. TRIM30α negatively regulates TLR-mediated NF-κB activation by targeting TAB2 and TAB3 for degradation. Nat. Immunol. 9, 369–377.

Shu, H.B., Takeuchi, M., Goeddel, D. V, 1996. The tumor necrosis factor receptor 2 signal transducers TRAF2 and c-IAP1 are components of the tumor necrosis factor receptor 1 signaling complex. Proc. Natl. Acad. Sci. 93, 13973–13978.

Singh, D.G., Lomako, J., Lomako, W.M., Whelan, W.J., Meyer, H.E., Serwe, M., Metzger, J.W., 1995. B-Glucosylarginine—a New Glucose Protein Bond in a Self-Glucosylating Protein From Sweet Corn. FEBS Lett. 376, 61–64.

Singh, S., Phillips, G.N., Thorson, J.S., 2005. The Structural Biology of Enzymes Involved in Natural Product Glycosylation. Biophys. Chem. 257, 2432–2437.

Slawson, C., Hart, G.W., 2011. O-GlcNAc signalling: implications for cancer cell biology. Nat.

Rev. Cancer 11, 678–684.

Sontag, R.L., Nakayasu, E.S., Brown, R.N., Niemann, G.S., Sydor, M.A., Sanchez, O., Ansong, C., Lu, S.-Y., Choi, H., Valleau, D., Weitz, K.K., Savchenko, A., Cambronne, E.D., Adkins, J.N., 2016. Identification of Novel Host Interactors of Effectors Secreted by *Salmonella* and *Citrobacter*. mSystems 1, e00032-15.

Spanò, S., 2016. Mechanisms of *Salmonella* Typhi Host Restriction. In: Leake, M.C. (Ed.), Biophysics of Infection. Springer International Publishing, pp. 283–294.

Spanò, S., Gao, X., Hannemann, S., Lara-Tejero, M., Galan, J.E., 2016. A Bacterial Pathogen Targets a Host Rab-Family GTPase Defense Pathway with a GAP. Cell Host Microbe 19, 216–226.

Sprick, M.R., Weigand, M.A., Rieser, E., Rauch, C.T., Juo, P., Blenis, J., Krammer, P.H., Walczak, H., 2000. FADD/MORT1 and caspase-8 are recruited to TRAIL receptors 1 and 2 and are essential for apoptosis mediated by TRAIL receptor 2. Immunity 12, 599–609.

Srikumar, S., Kröger, C., Hébrard, M., Colgan, A., Owen, S. V., Sivasankaran, S.K., Cameron, A.D.S., Hokamp, K., Hinton, J.C.D., 2015. RNA-seq Brings New Insights to the Intra-Macrophage Transcriptome of *Salmonella* Typhimurium. PLoS Pathog. 11, 1–26.

Steimle, V., Siegrist, C.A., Mottet, A., Lisowska-Grospierre, B., Mach, B., 1994. Regulation of MHC class II expression by interferon-gamma mediated by the transactivator gene CIITA. Science 265, 106–109.

Stirling, P.C., Cuéllar, J., Alfaro, G.A., El Khadali, F., Beh, C.T., Valpuesta, J.M., Melki, R., Leroux, M.R., 2006. PhLP3 modulates CCT-mediated actin and tubulin folding via ternary complexes with substrates. J. Biol. Chem. 281, 7012–7021.

Sun, H., Kamanova, J., Lara-Tejero, M., Galán, J.E., 2016. A Family of *Salmonella* Type III Secretion Effector Proteins Selectively Targets the NF-κB Signaling Pathway to Preserve Host Homeostasis. PLOS Pathog. 12, e1005484.

Sun, L., Wang, H., Wang, Z., He, S., Chen, S., Liao, D., Wang, L., Yan, J., Liu, W., Lei, X., Wang, X., 2012. Mixed lineage kinase domain-like protein mediates necrosis signaling downstream of RIP3 kinase. Cell 148, 213–227.

Sun, S.-C., 2011. Non-canonical NF-κB signaling pathway. Cell Res. 21, 71–85.

Takahashi, K., Kawai, T., Kumar, H., Sato, S., Yonehara, S., Akira, S., 2006. Roles of caspase-8 and caspase-10 in innate immune responses to double-stranded RNA. J. Immunol. 176, 4520–4524.

Tam, W.F., Sen, R., 2001. IkB Family Members Function by Different Mechanisms. J. Biol. Chem. 276, 7701–7704.

Thurston, T.L.M., Matthews, S.A., Jennings, E., Alix, E., Shao, F., Shenoy, A.R., Birrell, M.A., Holden, D.W., 2016. Growth inhibition of cytosolic *Salmonella* by caspase-1 and caspase-11 precedes host cell death. Nat. Commun. 7, 13292.

Tocchini, C., Ciosk, R., 2015. TRIM-NHL proteins in development and disease. Semin. Cell Dev. Biol. 47–48, 52–59.

Tomar, D., Singh, R., 2015. TRIM family proteins: Emerging class of RING E3 ligases as regulator of NF-kB pathway. Biol. Cell 107, 22–40.

Tomar, D., Sripada, L., Prajapati, P., Singh, R., Singh, A.K., Singh, R., 2012. Nucleo-Cytoplasmic Trafficking of TRIM8, a Novel Oncogene, Is Involved in Positive Regulation of TNF Induced NF-κB Pathway. PLoS One 7, e48662.

Traenckner, E.B., Pahl, H.L., Henkel, T., Schmidt, K.N., Wilk, S., Baeuerle, P.A., 1995. Phosphorylation of human IKB-ox on serines 32 and 36 controls IKB-a proteolysis and NF-KB activation in response to diverse stimuli. EMBO J. 14, 2876–2883.

Tran, Q.T., Gomez, G., Khare, S., Lawhon, S.D., Raffatellu, M., Bäumler, A.J., Ajithdoss, D., Dhavala, S., Adams, L.G., 2010. The *Salmonella enterica* serotype Typhi Vi capsular antigen is expressed after the bacterium enters the ileal mucosa. Infect. Immun. 78, 527–535.

Uche, I.V., MacLennan, C.A., Saul, A., 2017. A Systematic Review of the Incidence, Risk Factors and Case Fatality Rates of Invasive Nontyphoidal *Salmonella* (iNTS) Disease in Africa (1966 to 2014). PLoS Negl. Trop. Dis. 11, 1–28.

Uchil, P.D., Hinz, A., Siegel, S., Coenen-Stass, A., Pertel, T., Luban, J., Mothes, W., 2013. TRIM Protein-Mediated Regulation of Inflammatory and Innate Immune Signaling and Its Association with Antiretroviral Activity. J. Virol. 87, 257–272.

Uchil, P.D., Quinlan, B.D., Chan, W.T., Luna, J.M., Mothes, W., 2008. TRIM E3 ligases interfere with early and late stages of the retroviral life cycle. PLoS Pathog. 4, e16.

Valdivia, R.H., Falkow, S., 1996. Bacterial genetics by flow cytometry: rapid isolation of *Salmonella* typhimurium acid-inducible promoters by differential fluorescence induction. Mol. Microbiol. 22, 367–378.

van der Velden, A.W.M., Bäumler, A.J., Renée, M., Heffron, F., 1998. Multiple Fimbrial Adhesins Are Required for Full Virulence of *Salmonella* typhimurium in Mice. Infect.

Immun. 66, 2803–2808.

Vanden Berghe, T., Kaiser, W.J., Bertrand, M.J., Vandenabeele, P., 2015. Molecular crosstalk between apoptosis, necroptosis, and survival signaling. Mol. Cell. Oncol. 2, e975093.

Vercammen, D., Beyaert, R., Denecker, G., Goossens, V., Van Loo, G., Declercq, W., Grooten, J., Fiers, W., Vandenabeele, P., 1998. Inhibition of caspases increases the sensitivity of L929 cells to necrosis mediated by tumor necrosis factor. J. Exp. Med. 187, 1477–1485.

Vermes, I., Haanen, C., Steffens-Nakken, H., Reutelingsperger, C., 1995. A novel assay for apoptosis. Flow cytometric detection of phosphatidylserine expression on early apoptotic cells using fluorescein labelled Annexin V. J. Immunol. Methods 184, 39–51.

Versteeg, G.A., Rajsbaum, R., Sanchez-Aparicio, M.T., Maestre, A.M., Valdiviezo, J., Shi, M., Inn, K.S., Fernandez-Sesma, A., Jung, J., Garcia-Sastre, A., 2013. The E3-Ligase TRIM Family of Proteins Regulates Signaling Pathways Triggered by Innate Immune Pattern-Recognition Receptors. Immunity 38, 384–398.

Voedisch, S., Koenecke, C., David, S., Herbrand, H., Förster, R., Rhen, M., Pabst, O., 2009. Mesenteric lymph nodes confine dendritic cell-mediated dissemination of *Salmonella enterica* serovar typhimurium and limit systemic disease in mice. Infect. Immun. 77, 3170–3180.

Walczak, H., 2013. Death receptor-ligand systems in cancer, cell death, and inflammation. Cold Spring Harb. Perspect. Biol. 5, a008698.

Wang, C., Deng, L., Hong, M., Akkaraju, G.R., Inoue, J., Chen, Z.J., 2001. TAK1 is a ubiquitin-dependent kinase of MKK and IKK. Nature 412, 346–351.

Wang, H., Sun, L., Su, L., Rizo, J., Liu, L., Wang, L.F., Wang, F.S., Wang, X., 2014. Mixed Lineage Kinase Domain-like Protein MLKL Causes Necrotic Membrane Disruption upon Phosphorylation by RIP3. Mol. Cell 54, 133–146.

Wang, R.F., Kushner, S.R., 1991. Construction of versatile low-copy-number vectors for cloning, sequencing and gene expression in Escherichia coli. Gene 100, 195–199.

Waterhouse, A.M., Procter, J.B., Martin, D.M.A., Clamp, M., Barton, G.J., 2009. Jalview Version 2-A multiple sequence alignment editor and analysis workbench. Bioinformatics 25, 1189–1191.

Weng, D., Marty-Roix, R., Ganesan, S., Proulx, M.K., Vladimer, G.I., Kaiser, W.J., Mocarski, E.S., Pouliot, K., Chan, F.K.-M., Kelliher, M.A., Harris, P.A., Bertin, J., Gough, P.J., Shayakhmetov, D.M., Goguen, J.D., Fitzgerald, K.A., Silverman, N., Lien, E., 2014.

Caspase-8 and RIP kinases regulate bacteria-induced innate immune responses and cell death. Proc. Natl. Acad. Sci. 111, 7391–7396.

Weston, C.R., Davis, R.J., 2002. The JNK signal transduction pathway. Curr. Opin. Genet. Dev. 12, 14–21.

WHO, 2017. Global Priority List of Antibiotic-Resistant Bacteria To Guide Research, Discovery, and Development of New Antibiotics. World Health Organisation.

Wilson, N.S., Dixit, V., Ashkenazi, A., 2009. Death receptor signal transducers: nodes of coordination in immune signaling networks. Nat. Immunol. 10, 348–355.

Wong Fok Lung, T., Giogha, C., Creuzburg, K., Ong, S.Y., Pollock, G.L., Zhang, Y., Fung, K.Y., Pearson, J.S., Hartland, E.L., 2016. Mutagenesis and functional analysis of the bacterial arginine glycosyltransferase effector NleB1 from enteropathogenic *Escherichia coli*. Infect. Immun. 84, 1346–1360.

Woodsmith, J., Jenn, R.C., Sanderson, C.M., 2012. Systematic analysis of dimeric E3-RING interactions reveals increased combinatorial complexity in human ubiquitination networks. Mol. Cell. Proteomics 11, M111.016162.

Xia, B., Fang, S., Chen, X., Hu, H., Chen, P., Wang, H., Gao, Z., 2016. MLKL forms cation channels. Cell Res. 26, 517–528.

Yang, X., Ongusaha, P.P., Miles, P.D., Havstad, J.C., Zhang, F., So, W.V., Kudlow, J.E., Michell, R.H., Olefsky, J.M., Field, S.J., Evans, R.M., 2008. Phosphoinositide signalling links O-GlcNAc transferase to insulin resistance. Nature 451, 964–969.

Yang, Z., Soderholm, A., Lung, T.W.F., Giogha, C., Hill, M.M., Brown, N.F., Hartland, E., Teasdale, R.D., 2015. SseK3 Is a Salmonella Effector That Binds TRIM32 and Modulates the Host's NF-κB Signalling Activity. PLoS One 10, e0138529.

Yi, W., Clark, P.M., Mason, D.E., Keenan, M.C., Hill, C., Goddard III, W.A., Peters, E.C., Driggers, E.M., Hsieh-Wilson, L.C., 2013. PFK1 Glycosylation Is a Key Regulator of Cancer Cell Growth and Central Metabolic Pathways. Science 337, 975–980.

Yokota, T., Mishra, M., Akatsu, H., Tani, Y., Miyauchi, T., Yamamoto, T., Kosaka, K., Nagai, Y., Sawada, T., Heese, K., 2006. Brain site-specific gene expression analysis in Alzheimer's disease patients. Eur. J. Clin. Invest. 36, 820–830.

Yoon, H., McDermott, J.E., Porwollik, S., McClelland, M., Heffron, F., 2009. Coordinated regulation of virulence during systemic infection of *Salmonella enterica* serovar Typhimurium. PLoS Pathog. 5, e1000306.

Yu, X.-J., Liu, M., Holden, D.W., 2016. *Salmonella* Effectors SseF and SseG Interact with Mammalian Protein ACBD3 (GCP60) To Anchor *Salmonella* -Containing Vacuoles at the Golgi Network. mBio 7, e00474-16.

Yuzwa, S.A., Shan, X., Macauley, M.S., Clark, T., Skorobogatko, Y., Vosseller, K., Vocadlo, D.J., 2012. Increasing O-GlcNAc slows neurodegeneration and stabilizes tau against aggregation. Nat. Chem. Biol. 8, 393–399.

Zandi, E., Rothwarf, D.M., Delhase, M., Hayakawa, M., Karin, M., 1997. The IkB Kinase Complex (IKK) Contains Two Kinase Subunits, IKKb1; and IKKb2;, Necessary for IkB Phosphorylation and NFkB Activation. Cell 91, 243–252.

Zhang, D.W., Shao, J., Lin, J., Zhang, N., Lu, B.J., Lin, S.C., Dong, M.Q., Han, J., 2009. RIP3, an energy metabolism regulator that switches TNF-induced cell death from apoptosis to necrosis. Science 325, 332–336.

Zhang, J., Hu, M.-M., Wang, Y.-Y., Shu, H.-B., 2012. TRIM32 protein modulates type I interferon induction and cellular antiviral response by targeting MITA/STING protein for K63-linked ubiquitination. J. Biol. Chem. 287, 28646–28655.

Zhang, S., Kingsley, R.A., Santos, R.L., Andrews-Polymenis, H., Raffatellu, M., Figueiredo, J., Nunes, J., Tsolis, R.M., Adams, L.G., Baumler, A.J., 2003. Molecular Pathogenesis of *Salmonella enterica* Serotype Typhimurium-Induced Diarrhea. Infect. Immun. 71, 1–12.

Zhao, J., Jitkaew, S., Cai, Z., Choksi, S., Li, Q., Luo, J., Liu, Z.-G., 2012. Mixed lineage kinase domain-like is a key receptor interacting protein 3 downstream component of TNF-induced necrosis. Proc. Natl. Acad. Sci. 109, 5322–5327.

Zhou, D., Galán, J., 2001. *Salmonella* entry into host cells: The work in concert of type III secreted effector proteins. Microbes Infect. 3, 1293–1298.

Zhou, D., Mooseker, M.S., Galán, J.E., Zhou, D., Mooseker, M.S., Galin, J.E., 1999. Role of the *S.* typhimurium Actin-Binding Protein SipA in Bacterial Internalization. Science 283, 2092–2095.

Zhu, Y., Shan, X., Yuzwa, S.A., Vocadlo, D.J., 2014. The emerging link between O-GlcNAc and Alzheimer disease. J. Biol. Chem. 289, 34472–34481.